

# **Transboundary Aquifers of the Del Rio/Ciudad Acuña – Laredo/Nuevo Laredo Region**

*Prepared By*

Texas Water Development Board



---

*In Cooperation With*

Comisión Internacional de Límites y Aguas  
International Boundary and Water Commission  
Comisión Nacional del Agua

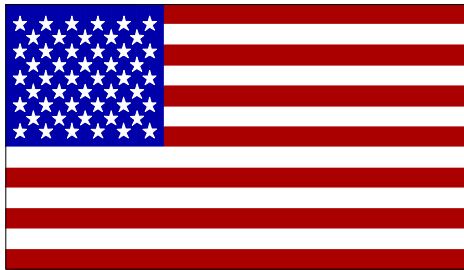
*Prepared For*

U.S. Environmental Protection Agency, Region 6

July, 2002



# Transboundary Aquifers of the Del Rio/Ciudad Acuña – Laredo/Nuevo Laredo Region



---

*Prepared By*

Radu Boghici, Principal Investigator

*GIS Support*

Christy-Ann M. Archuleta, Erika M. Boghici, Wan-Joo Choi,  
Mark E. Hayes, and Miguel A. Pavón

*Technical Assistance*

Douglas B. Coker, John A. Derton, Stephen B. Gifford,  
Stephen W. Moore, and Susan N. Williams

## **Final Report**

*Contract report prepared by the Texas Water Development Board for the U.S. Environmental Protection Agency, Region 6 under interagency contract number X 996343-01-0.*



## **EXECUTIVE SUMMARY**

At the request of the U.S. Environmental Protection Agency, the Texas Water Development Board undertook this study to characterize binational aquifers in parts of southern Texas and the northeastern Mexican States of Coahuila, Nuevo Leon, and Tamaulipas. The study area lies along a corridor connecting the Del Rio/Ciudad Acuña and Laredo/Nuevo Laredo sister city pairs and extends 50 - 100 km on either side of the international border. Assessments were made of the Edwards-Trinity aquifer system, Allende-Piedras Negras Valley aquifer, and Carrizo-Wilcox aquifer. Comisión Nacional del Agua, International Boundary and Water Commission, and Comisión Internacional de Limites y Aguas provided technical and administrative assistance and data.

Many of the surface and groundwater resources along the transboundary corridor are shared between the two nations, yet no binational study of these resources has been undertaken. Solutions to water-related problems can be derived only when a better understanding of transboundary water resources is attained. This study is an important step toward attaining a better understanding of these binational resources.

To complete this study, data from several sources had to be combined into one database. Geographic Information Systems (GIS) coverages of groundwater, surface water, and land use attributes were developed from the new database. Study results for each aquifer are as follows:

## Edwards-Trinity Aquifer System

- The segment of the Edwards-Trinity aquifer system discussed in this report underlies an area of 31,050 km<sup>2</sup>, of which 16,000 km<sup>2</sup> are located in Mexico. The limits of the study region at the northeast, northwest, and southwest are also the aquifer system limits. The eastern boundary of the system in the study region is a hydrogeologic one: the "bad-water line", namely the 1,000 mg/l line of total dissolved solids (TDS) concentration. The "bad water line" has been traced south into Mexico and bounds the aquifer system to the east of Serranía del Burro and Peyotes anticline in Mexico.
- Cretaceous carbonates of the Trinity, Fredericksburg, and Washita groups host the Edwards – Trinity aquifer system, which, in the study area, is composed of two aquifers and the associated confining units. The aquifers are named the Edwards in the Balcones Fault Zone and the Edwards – Trinity (Plateau) in the Edwards Plateau. The Edwards – Trinity (Plateau) aquifer rocks outcrop over most of the study area. Due to their hydraulic interconnectedness these individual aquifers are discussed together, and referred to as the Edwards – Trinity aquifer throughout this report. The Edwards –Trinity aquifer is predominantly made of limestone and dolomite in its upper part and sand in its lower part. The aquifer includes all the Trinity and Fredericksburg strata, plus all the Washita rocks below the Del Rio Clay or Buda Limestone (where the Del Rio is missing) or land surface.
- In the Edwards Plateau, transmissivity ranges from 0.15 to 25,100 m<sup>2</sup>/day and hydraulic conductivity ranges from 0.0009 to 221 m/day, with median values of 38 m<sup>2</sup>/day and 0.7 m/day, respectively. In the Balcones Fault Zone, transmissivity

ranges from 7 to 97,300 m<sup>2</sup>/day and hydraulic conductivity ranges from 0.2 to 2,400 m/day, with mean values of 1,935 m<sup>2</sup>/day and 36 m/day, respectively. Most of the wells in the study area have transmissivities of up to 20,000 m<sup>2</sup>/day. Well yields in the Coahuila part of the Edwards-Trinity aquifer vary greatly. Well yields of 0.5 to 16 l/s are reported in the Serranía del Burro and on mountain flanks where the aquifer is predominantly unconfined. Well yields range from 20 to 400 l/s to in the confined area of the aquifer.

- Groundwater moves generally from the highlands in Coahuila and Texas towards Amistad Reservoir or Rio Grande where hydraulic heads range from 270 m to 340 m above sea level. Hydraulic heads exceed 715 m in the Burro area and 540 m in the Edward Plateau and define areas of groundwater recharge. Hydraulic gradients of 0.016 in the uplands of Serranía del Burro and 0.006 along the Edwards Plateau escarpment have been measured. The hydraulic gradient is very flat (~0.0001) immediately south of Amistad Reservoir and in Val Verde County west of Devils River, and becomes steeper (0.003) in the Del Rio – Ciudad Acuña area.
- Recharge to the Edwards-Trinity aquifer is mostly by direct infiltration of precipitation and streamflow in the aquifer outcrop. A small amount of recharge may occur along faults and fractures and by cross-formational flow through semiconfining beds. The long-term recharge for Edwards, Kinney, and Real Counties was estimated to be 50.8 mm/year. The yearly recharge rate in Val Verde County is estimated to be approximately 38.1 mm. Recharge to the Coahuila part of the Edwards-Trinity aquifer occurs both inside and outside the study area by infiltration of rainwater on the aquifer outcrop and by seepage along various streambeds. The recharge zone of

the Trinity portion of the aquifer corresponds with the extensive Glen Rose outcrops throughout Serranía del Burro and with the arroyos and deep canyons incised in the mountain.

- Groundwater discharges from the Edwards-Trinity aquifer as springs and seeps, as baseflow to gaining streams, and through well withdrawals. Locally, where the water table is shallow, some discharge may take place by evapotranspiration. Among the largest springs on the Texas side are San Felipe, Goodenough, and Las Moras Springs. Their flow ranges from 0.6 m<sup>3</sup>/s to 3.9 m<sup>3</sup>/s. In Coahuila, there are no less than 13 major springs near the cities of Zaragoza, Morelos, Nava, Allende, and Villa Union. Their flow ranges from 0.06 m<sup>3</sup>/s to 1.7 m<sup>3</sup>/s. From 1980 through 1997, an average of 155.92 hm<sup>3</sup> per year of groundwater from the Edwards-Trinity aquifer was used to meet the needs in Val Verde, Edwards, Kinney, and Uvalde counties. More water was used for irrigation than for any other purpose in the study area. From 1980 to 1997, irrigation pumpage was on average 137.74 hm<sup>3</sup>/year or 88.3 percent of the total amount of Edwards-Trinity groundwater that was used.
- Groundwater in both Coahuila and Texas is predominantly fresh with total dissolved solids (TDS) concentrations below 1,000 mg/l). Several wells drilled near the downdip limit of the aquifer (the “bad water zone”) in both Texas and Coahuila had higher TDS concentrations of up to 2,970 mg/l. Low-TDS groundwaters are associated with active recharge areas in the Edwards Plateau and in Serranía del Burro and Lomerio Peyotes. Dissolved solids concentrations increase downgradient as groundwater dissolves aquifer minerals along its flowpath towards the downdip limit of the aquifer. A number of samples with TDS concentrations in the 1,000 mg/l



to 3,000 mg/l range are located near Nava, Allende, Villa Union, and San Carlos, Coahuila, and north of Camp Wood, Texas. The presence of the sulfate and, in subsidiary, chloride ions suggests that the dissolution of evaporite minerals may have contributed to these samples' chemical composition. Of 212 samples analyzed for major and minor ions, 16 samples showed sulfate and nitrate (as  $\text{NO}_3^-$ ) concentrations exceeding the national standards. Carbonate dissolution/precipitation and gypsum dissolution are the main chemical processes responsible for the Edwards-Trinity groundwater chemistry.

### **Allende-Piedras Negras Valley Aquifer**

- The Allende-Piedras Negras Valley aquifer underlies an area of 5,368 km<sup>2</sup> in the northeast part of the state of Coahuila and extends north into Texas where it covers 1,498 km<sup>2</sup>. The aquifer lies within the Río Bravo-Conchos hydrologic region of Coahuila (the Rio Grande basin in Texas) and comprises the sub-basins of the Río Escondido-Río San Antonio, and Castaños Arroyo. The aquifer limits follow the geologic contacts between the unconsolidated deposits of the Piedras Negras Valley and the surrounding Cretaceous and Eocene outcrops.
- The Allende-Piedras Negras Valley aquifer is made of thin alluvial terraces, alluvial bolsons, conglomerates, and floodplain deposits such as clays, silt, sands, and gravels. These unconsolidated sedimentary deposits are the result of erosion and transport of carbonaceous rocks that constitute the higher topographic elevations. In large part, the geology of the area is represented by Upper Cretaceous marine carbonates overlain by Quaternary terrigenous sequences.

- On the Texas side, the majority of the wells yield water from the alluvium in the Quemado Valley, a portion of the Rio Grande floodplain in northwestern Maverick County, Texas. Estimates of aquifer transmissivity range from 1,800 to 3,000 m<sup>2</sup>/day in the Holocene alluvium adjacent to the Rio Grande and average 1,200 m<sup>2</sup>/day in the less permeable Pleistocene terrace deposits away from the river. Hydraulic conductivity values for the aquifer in the Quemado Valley range from 160 to 430 m/day. Well yields in the Coahuila part of the Allende-Piedras Negras Valley aquifer vary between 0.5 l/s and 60 l/s with a median yield of 2 l/s. In 1999, the majority of the wells in the area pumped 5 l/s or less.
- The 1999 potentiometric surface slopes towards the Rio Grande with hydraulic gradients as steep as 0.015 across Lomerio Peyotes just west of Allende. The gradient flattens to 0.003 between Morelos and Nava and becomes very flat (~0.0001) between Nava and the Rio Grande near Santo Domingo. Hydraulic heads in excess of 400 m in the Peyotes area define areas of groundwater recharge. The flat hydraulic gradient in the Rio Grande floodplain between Santo Domingo and Guerrero suggests that the aquifer there is very transmissive, and large amounts of groundwater may flow through it and discharge into the Rio Grande.
- It is estimated that the total amount of water stored in the Allende-Piedras Negras Valley aquifer is about 24,500 hm<sup>3</sup>. Of this amount, 900 hm<sup>3</sup> are stored in the Texas part of the aquifer and 23,600 hm<sup>3</sup> are stored in the Mexican part of the basin. These figures do not include water stored in the Cretaceous bedrock. The distribution of saturated thickness and well yields suggest that the best potential for groundwater development is in Coahuila, particularly between Rio Grande and the Villa Union

parallel. It is estimated that during wet years the aquifer in the Quemado Valley would have about 100 hm<sup>3</sup> of groundwater in storage available for development, of which 75 hm<sup>3</sup> are physically recoverable by wells. During drought, approximately 75 hm<sup>3</sup> of water would be in total storage with 56 hm<sup>3</sup> available for extraction by wells.

- The Allende-Piedras Negras Valley aquifer is recharged in part by direct infiltration of precipitation on the valley floor. The high annual potential evapotranspiration in Piedras Negras Valley suggests that direct percolation of rainwater through the basin floor may take place only following sustained rain events. Additional precipitation recharge to the basin occurs within the Cretaceous highlands. Large arroyos dissecting these highlands and the basin fill can convey substantial quantities of runoff during episodic wet years and act as pathways for focused recharge. Cross-formational flow from the underlying bedrock into the alluvial fill can occur locally through fractures and faults. Major springs issuing from Upper Cretaceous rocks in the Peyotes area provide substantial input to the Allende-Piedras Negras Valley aquifer between Zaragoza and Alamos. The return flow from irrigation and seepage from unlined canals can account for most of the aquifer recharge in areas where these operations exist. The Rio Grande floodplain in the Quemado valley receives an average 6.2 hm<sup>3</sup> of recharge every year, of which some 72 percent or 4.5 hm<sup>3</sup> is from canal seepage and from irrigation return flow.
- Groundwater is lost from the Allende-Piedras Negras Valley aquifer by irrigation pumping; by subsurface seepage to the Rio Grande, Río Escondido, and other gaining reaches in the region; by leakage to drains; and possibly by cross-formational flow into the underlying strata. Phreatophytes account for some evapotranspirative

discharge along the Rio Grande channel, creeks, and canal laterals. Water is artificially discharged from the aquifer by numerous wells used for domestic, sock, irrigation, and public water supply. Most of the active wells are located in Coahuila between the Rio Grande floodplain and El Amole creek. The greatest concentration of wells on the Texas side is in the Quemado valley of northwestern Maverick County. From 1980 through 1997, an average of 1.5 hm<sup>3</sup> of groundwater was pumped annually from the Allende-Piedras Negras Valley aquifer in Texas. Over 90 percent of this groundwater was used to meet needs within Maverick County. Irrigation use in this county accounts for the 46 percent of the annual average groundwater pumpage, whereas municipal and livestock uses have claimed 0.39 hm<sup>3</sup> (26 percent) and 0.31 hm<sup>3</sup> (20 percent) respectively of the annual groundwater production on the Texas side of the aquifer.

- Groundwater quality is predominantly fresh to slightly saline with TDS concentrations between 1,000 mg/l and 3,000 mg/l. Seven wells located on the edges of the basin south of Guerrero and one north of Eagle Pass have shown TDS concentrations of ranging from 3,100 mg/l to 30,500 mg/l. Salinities generally increase downgradient as groundwater dissolves aquifer minerals along its flowpath towards the Rio Grande and areas of groundwater pumpage. Increasing salinities in groundwater in the river valley downstream generally reflect the tendency for salts to be recycled in irrigation water, to return to the Rio Grande, and then to be reapplied to crops downstream as irrigation water. Samples from 186 wells within the study area had available analyses of major and minor ions. Of these, 72 samples exceeded the Environmental Protection Agency (EPA) secondary standards for sulfate. Thirty-five

samples surpassed the secondary standards for chloride, while six samples had nitrate (as  $\text{NO}_3^-$ ) concentrations above the maximum contaminant level.

- Carbonate dissolution/precipitation and gypsum dissolution are the main chemical processes impacting the groundwater chemistry of Allende-Piedras Negras Valley aquifer.

### **Carrizo-Wilcox Aquifer**

- The Carrizo-Wilcox aquifer is contained within the terrigenous clastic deposits of the Wilcox Group and the overlying Carrizo Formation of the Claiborne Group. The aquifer extends from northeastern Mexico into Texas, Arkansas, and Louisiana. In the study area the Carrizo-Wilcox aquifer underlies approximately 17,500  $\text{km}^2$  of which 14,200  $\text{km}^2$  are on the Texas side and 3,300- $\text{km}^2$  are on the Mexican side.
- In the Carrizo – Wilcox aquifer, hydraulic conductivity is lithofacies-dependent. Fine-grained sediments deposited in lacustrine, floodplain, or abandoned-channel-fill environments have the lowest hydraulic conductivity. The medium- to coarse-grained alluvial system sand bodies have the highest permeability and serve as pathways for the flow of groundwater in the aquifer. Estimates of aquifer transmissivity range from 12 to 808  $\text{m}^2/\text{day}$  with a mean of 447  $\text{m}^2/\text{day}$ ; hydraulic conductivity values range from 0.4 to 16.3  $\text{m}/\text{day}$ , with a mean of 7.5  $\text{m}/\text{day}$ ; and aquifer storativity range from 0.0001 to 0.00019.
- On the Texas side, the Carrizo-Wilcox potentiometric surface slopes to the east and southeast with steep hydraulic gradients in the aquifer outcrop and flatter gradients downdip. Heavy aquifer pumpage resulted in cones of depression along the Nueces

River from Crystal City to north of Asherton, and between Big Wells and Cotulla.

On the Mexican side, the potentiometric surface slopes to the east and northeast with gradients of up to 0.006 in the formation outcrop northeast of La Jarita. The gradient flattens ( $\sim 0.001$ ) towards the east. The highest hydraulic heads are found in the Carrizo outcrop areas south of San Ignacio (242 m) and in western Dimmit and Zavala counties (219 m). The lowest heads ( $\sim 70$  m) are downdip in the large cone of depression extending from Crystal City to the south, to Big Wells, and east to Cotulla.

- The Carrizo-Wilcox aquifer is recharged primarily by direct infiltration of precipitation in its outcrop area sands. Estimates of annual recharge to the aquifer on the Texas side averages about  $30.8 \text{ hm}^3$ . Additional recharge to the Carrizo-Wilcox aquifer occurs by cross-formational flow from the overlying Bigford Formation. Groundwater pumping on the Texas side has lowered the hydraulic heads in the Carrizo-Wilcox to levels below those encountered in the overlying strata. Mineralized groundwater from the Bigford percolates downward through aquitards and well bores and recharges the underlying Carrizo-Wilcox aquifer. Approximately  $7.6 \text{ hm}^3$  of groundwater leak into the Carrizo-Wilcox aquifer every year in the study area. Some recharge may take place by way of losing surface streams crossing the outcrop area.
- Groundwater leaves the Carrizo-Wilcox aquifer mainly by means of irrigation pumping. Subsurface seepage to the Leona River and other gaining reaches in the region and cross-formational flow into the overlying strata are two other discharge mechanisms. The amount of groundwater pumped from the Carrizo Sand rose steadily since the late 1930s or early 1940s, mainly to satisfy irrigation needs.

Widespread drought conditions during the 1950s, population increase, and industrial expansion in the area are other reasons for the regional increase in groundwater use during that time. In 1969, groundwater pumpage from the Carrizo Sand amounted to 314.5 hm<sup>3</sup>, which represented 97 percent of the entire irrigation pumpage in the Winter Garden area. From 1980 through 1997, an average of 111.6 hm<sup>3</sup> of groundwater was pumped annually from the Carrizo-Wilcox aquifer on the Texas side of the study area. On average, irrigation accounted for 100.1 hm<sup>3</sup> or 90 percent of the total amount of water used, while municipal pumping accounted for 7.9 hm<sup>3</sup> or seven percent of the average water use. Smaller amounts of groundwater were used for manufacturing, power generation, mining, and livestock.

- Groundwater on the Texas side is predominantly fresh to slightly saline, with TDS concentrations between 1,000 mg/l and 3,000 mg/l. The salinity in the Carrizo-Wilcox aquifer increases downgradient as meteoric, fresh recharge dissolves minerals along its flowpath and mixes with deep, high-TDS connate water expelled along fault zones. In contrast with the Texas side, the groundwater in Mexico is predominantly saline. Owing to the increase in clay content within the Carrizo and the Indio formations of Mexico, TDS concentrations in groundwater range from 482 mg/l to 9,334 mg/l. Of the 120 samples analyzed, 53 exceeded the U.S. Environmental Protection Agency secondary standards for sulfate. Fifty-six samples surpassed the secondary standards for chloride, while one sample had nitrate (as NO<sub>3</sub><sup>-</sup>) concentrations above the maximum contaminant level. Carrizo-Wilcox aquifer groundwaters evolve along flowpaths from a calcium, sodium, bicarbonate, and chloride-dominated composition encountered in shallow wells to a sodium-

bicarbonate facies encountered at depth. The main chemical processes impacting the groundwater chemical composition are carbonate dissolution and ion exchange reactions.

### **Susceptibility to non-point source contamination**

- The U.S. Environmental Protection Agency DRASTIC method was employed to assess the vulnerability to pollution of aquifers shared between Texas and Mexico between Del Rio/Ciudad Acuña and Laredo/Nuevo Laredo. The results indicate that approximately two-thirds of the study area has low vulnerability to groundwater pollution from non-point sources. There are many method-related assumptions and limitations that need to be understood before attempting make planning decisions based on DRASTIC outputs. The single-parameter sensitivity analysis revealed that the weights for each input parameter can vary widely from place to place and did not follow the method-prescribed weights. The analysis can thus be useful for model fine-tuning and targeting of areas within the model domain that need more detailed information and accuracy.



## TABLE OF CONTENTS

EXECUTIVE SUMMARY .....	1
Edwards-Trinity Aquifer System.....	2
Allende-Piedras Negras Valley Aquifer .....	5
Carrizo-Wilcox Aquifer.....	9
Susceptibility to non-point source contamination.....	12
CHAPTER 1: INTRODUCTION.....	19
Preface.....	19
Purpose.....	19
Participating agencies .....	20
Acknowledgments and disclaimer .....	20
Regional geographic setting.....	21
Location .....	21
Topography and drainage .....	25
Climate.....	26
Population and economy.....	27
History of groundwater development .....	32
Regional geologic setting.....	34
Geologic characteristics .....	34
Depositional history .....	34
References.....	38
CHAPTER 2: EDWARDS-TRINITY AQUIFER SYSTEM.....	41
Location and extent.....	41
Stratigraphy and structure.....	43
Water-bearing characteristics.....	52
Trinity Group .....	52
Fredericksburg and Lower Washita groups .....	54
Aquifer properties .....	55
Areal distribution of transmissivity and well yields .....	59
Potentiometric surface and water levels .....	61
Recoverable groundwater resources .....	70
Recharge areas .....	71
Discharge areas .....	78
Water quality.....	83
General hydrochemistry.....	83
Chemical Processes.....	91
References.....	95
CHAPTER 3: THE ALLENDE-PIEDRAS NEGRAS VALLEY AQUIFER.....	100
Location and extent.....	100
Stratigraphy and structure.....	100
Buda Formation .....	101
Eagle Ford Formation .....	101

Austin Chalk .....	102
Upson Clay.....	102
San Miguel Formation .....	103
Olmos Formation .....	103
Escondido Formation.....	103
Uvalde Gravel (Sabinas Conglomerate) .....	104
Quaternary Alluvium .....	105
Aquifer properties .....	107
Potentiometric surface and water levels .....	108
Recoverable groundwater resources .....	113
Recharge areas .....	113
Discharge areas .....	114
Groundwater quality .....	117
General hydrochemistry.....	117
Chemical processes.....	127
References.....	133
CHAPTER 4: CARRIZO – WILCOX AQUIFER .....	135
Location and extent.....	135
Stratigraphy and structure.....	136
Midway Group.....	141
Indio Formation or Wilcox Group .....	141
Carrizo Formation.....	142
Bigford Formation .....	143
El Pico Clay .....	143
Laredo Formation.....	143
Yegua Formation .....	144
Aquifer properties .....	144
Potentiometric surface and water levels .....	150
Recoverable groundwater resources .....	154
Recharge areas .....	155
Discharge areas .....	160
Groundwater quality .....	162
General hydrochemistry.....	162
Chemical processes.....	172
References.....	177
CHAPTER 5: AQUIFER VULNERABILITY TO CONTAMINATION .....	181
Introduction.....	181
Vulnerability assessment of the transboundary aquifers .....	181
Computing the DRASTIC Index .....	194
Model limitations .....	198
Single-parameter sensitivity analysis.....	199
Results and discussion .....	201
Conclusions.....	211
References.....	212

RECOMMENDATIONS .....	213
APPENDIX A .....	217
List of water-related agencies and institutions.....	217
APPENDIX B .....	221
Groundwater data sets and GIS coverages.....	221

## LIST OF FIGURES

Figure 1.1 Location of study area .....	22
Figure 1.2 Transboundary aquifers in the study area.....	23
Figure 1.3 Surface topography and drainage features in the study area .....	24
Figure 1.4 Geologic map of the study area .....	35
Figure 2.1 Edwards-Trinity aquifer location map.....	42
Figure 2.2 Geologic province areas within the Fredericksburg and Washita groups in Texas and northern Coahuila, Mexico. ....	47
Figure 2.3 East-west stratigraphic section of the Fredericksburg and Washita Groups in northern Coahuila, Mexico.....	48
Figure 2.4 Principal structural features of northern Coahuila, Mexico. ....	50
Figure 2.5 Histograms of transmissivity for the Edwards-Trinity aquifer in Texas.....	57
Figure 2.6 Histograms of hydraulic conductivity for the Edwards-Trinity aquifer in Texas. ....	58
Figure 2.7 Areal distribution of transmissivity and well yields in the Edwards-Trinity aquifer.....	60
Figure 2.8 Potentiometric surface map for the Edwards-Trinity aquifer.....	62
Figure 2.9 Potentiometric surface map for the Edwards-Trinity aquifer in Texas .....	64
Figure 2.10 Depth to water in Edwards-Trinity aquifer wells.....	65
Figure 2.11 Depth to water in Edwards-Trinity aquifer wells.....	67
Figure 2.12 Well hydrographs for the Edwards-Trinity aquifer.....	68
Figure 2.13 Plot of $\delta^2\text{H}$ versus $\delta^{18}\text{O}$ values for Edwards-Trinity aquifer.....	73
Figure 2.14 Areal distribution of $\delta^2\text{H}$ , $\delta^{18}\text{O}$ , $^{14}\text{C}$ , $\delta^{13}\text{C}$ , and $^3\text{H}$ . ....	75
Figure 2.15 Physiographic features of northern Coahuila, Mexico. ....	77
Figure 2.16 Groundwater pumpage from the Edwards-Trinity aquifer, 1980-1997.....	82
Figure 2.17 Hydrochemical Stiff map of the Edwards-Trinity aquifer. ....	85
Figure 2.18 Sulfate ion distribution in the Edwards-Trinity aquifer. ....	87
Figure 2.19 Nitrate ion distribution in the Edwards-Trinity aquifer.....	88
Figure 2.20 Areal distribution of hydrochemical facies in the Edwards-Trinity aquifer..	89
Figure 2.21 Major ion compositions for Edwards-Trinity aquifer groundwaters.....	90
Figure 2.22 Plot of Ca+Mg versus $\text{HCO}_3$ .....	92
Figure 2.23 Plot of Ca+Mg- $\text{SO}_4$ versus $\text{HCO}_3$ .....	92
Figure 2.24 Plot of Na-Cl versus Ca+Mg- $\text{SO}_4$ -0.5 $\text{HCO}_3$ .....	93
Figure 2.25 Calcite saturation indices for Edwards-Trinity.....	94

Figure 3.1 Well yields in the Allende-Piedras Negras Valley aquifer.....	106
Figure 3.2 Potentiometric surface map for the Allende-Piedras Negras Valley aquifer. ....	109
Figure 3.3 Well hydrographs for the Allende-Piedras Negras Valley aquifer .....	111
Figure 3.4 Relationship between land surface elevations and water levels in the Allende- Piedras Negras Valley aquifer.....	112
Figure 3.5 Hydrochemical Stiff map for the Allende-Piedras Negras Valley aquifer....	118
Figure 3.6 Chloride ion distribution in in the Allende-Piedras Negras Valley aquifer. .	119
Figure 3.7 Sulfate ion distribution in the Allende-Piedras Negras Valley aquifer. ....	120
Figure 3.8 Nitrate ion distribution in the Allende-Piedras Negras Valley aquifer .....	121
Figure 3.9 Mechanisms of groundwater salinization.....	123
Figure 3.10 Areal distribution of hydrochemical facies in the Allende-Piedras Negras Valley aquifer. ....	124
Figure 3.11 Major ion compositions in the Allende-Piedras Negras Valley aquifer.....	125
Figure 3.12 Plot of $\text{Na}^+$ versus $\text{Cl}^-$ .....	128
Figure 3.13 Plot of $\text{Ca}+\text{Mg}$ versus $\text{HCO}_3^-$ .....	130
Figure 3.14 Plot of $\text{Ca}+\text{Mg}$ versus $\text{SO}_4+\text{HCO}_3^-$ .....	131
Figure 3.15 Plot of $\text{Na}-\text{Cl}$ versus $\text{Ca}+\text{Mg}-\text{SO}_4-0.5 \text{HCO}_3^-$ .....	132
Figure 4.1 Structural elements of the Texas Coastal Plain. ....	137
Figure 4.2 High-sandstone trends, fluvial axes, and sediment input directions in the Winter Garden area of Texas. ....	138
Figure 4.3 Spatial distribution of transmissivity in the Carrizo Formation .....	148
Figure 4.4 Spatial distribution of transmissivity in the Wilcox Group.....	149
Figure 4.5 Potentiometric surface map for the Carrizo-Wilcox aquifer. ....	151
Figure 4.7 Distribution of $\delta^2\text{H}$ , $\delta^{18}\text{O}$ , $^{14}\text{C}$ , $\delta^{13}\text{C}$ , and $^3\text{H}$ in Carrizo-Wilcox aquifer ....	157
Figure 4.8 Plot of $\delta^2\text{H}$ versus $\delta^{18}\text{O}$ values for Carrizo-Wilcox aquifer.....	158
Figure 4.9 Estimated pumpage from the Carrizo Sand 1930-1969. ....	160
Figure 4.10 Estimated pumpage from the Carrizo-Wilcox aquifer 1980-1997.....	161
Figure 4.11 Hydrochemical Stiff map for Carrizo-Wilcox aquifer. ....	164
Figure 4.12 Sulfate ion distribution in Carrizo-Wilcox aquifer.....	166
Figure 4.13 Chloride ion distribution in Carrizo-Wilcox aquifer. ....	167
Figure 4.14 Major ion compositions for groundwater in Carrizo-Wilcox aquifer. ....	169
Figure 4.15 Hydrochemical groundwater facies in the Carrizo-Wilcox aquifer. ....	170
Figure 4.16 Plot of $\text{Na}^+$ versus $\text{Cl}^-$ .....	173
Figure 4.17 Plot of $\text{Ca}+\text{Mg}$ versus $\text{HCO}_3^-$ .....	173
Figure 4.18 Plot of $\text{Ca}+\text{Mg}$ versus $\text{SO}_4+1/2 \text{HCO}_3^-$ .....	175
Figure 4.19 Plot of $\text{Na}-\text{Cl}$ versus $\text{Ca}+\text{Mg}-\text{SO}_4-1/2 \text{HCO}_3^-$ .....	176
Figure 5.1. Ratings and depth intervals for the depth to groundwater layer.....	185
Figure 5.3 Ratings and rock types for the aquifer media layer.....	189
Figure 5.4 Ratings and soil types for the soil media layer.....	190
Figure 5.5 Ratings and percent slope ranges for the topography layer.....	192
Figure 5.6 Ratings and rock types for the impact of vadose zone layer .....	193
Figure 5.7 Ratings and value ranges for the hydraulic conductivity layer .....	195
Figure 5.8 DRASTIC Index distribution illustrating aquifer vulnerability to pollution..	197
Figure 5.9 Effective weight distribution for the impact of the vadose zone layer.....	203

Figure 5.10 Effective weight distribution for the depth to water layer.....	204
Figure 5.11 Effective weight distribution for the soil media layer .....	206
Figure 5.12 Effective weight distribution for the hydraulic conductivity layer .....	207
Figure 5.13 Effective weight distribution for the aquifer media layer .....	208
Figure 5.14 Effective weight distribution for the net recharge layer.....	209
Figure 5.15 Effective weight distribution for the topography layer .....	210

## LIST OF TABLES

Table 2.1 Correlation diagram for the Edwards-Trinity aquifer system.....	44
Table 2.2 Isotope composition in Edwards-Trinity groundwater samples .....	73
Table 2.3 Flow from selected springs in Coahuila .....	79
Table 2.4 Groundwater use in Val Verde, Edwards, Kinney, and Uvalde counties.....	81
Table 3.1 Historical groundwater use, Kinney and Maverick counties.....	119
Table 4.1 Stratigraphic relationships in south Texas.....	143
Table 4.2 Hydraulic conductivity and transmissivity, Carrizo-Wilcox aquifer.....	146
Table 4.3 Projections of groundwater availability from the Carrizo-Wilcox aquifer.....	154
Table 4.4 Isotope composition in Carrizo-Wilcox groundwater samples.....	156
Table 5.1. Comparison between assigned and effective parameter weights.....	200



## **CHAPTER 1: INTRODUCTION**

### **Preface**

#### **Purpose**

At the request of the U.S. Environmental Protection Agency (USEPA), the Texas Water Development Board (TWDB) undertook this study to characterize binational aquifers in parts of southern Texas, United States of America and northeastern Coahuila, Nuevo Leon, and Tamaulipas, Mexico. The study area lies along a corridor connecting the Del Rio/Ciudad Acuña and Laredo/Nuevo Laredo sister city pairs and extends 50 - 100 km on either side of the international border. The study uses well-established hydrogeological, hydrochemical, and isotopic techniques to trace groundwater flowpaths, to assess regional water quality, and to define aquifer recharge and discharge areas and areas susceptible to contamination.

Many of the surface and groundwater resources along the transboundary corridor are shared between the two nations, yet no binational study of these resources has been undertaken. Solutions to water-related problems can be derived only when a better understanding of transboundary water resources is attained. This study is an important step toward attaining a better understanding of these binational resources.

To complete this study, information from several sources had to be combined into one database. Geographic Information Systems (GIS) coverages of groundwater, surface water, and land use attributes were developed from the new database. This report provides the results of the study. Appendix B provides the documentation of GIS coverage

## **Participating agencies**

This report was prepared by the author under the general direction of William F. Mullican III, Deputy Executive Administrator for the Office of Planning, Gary L. Powell, Director -Hydrological and Environmental Monitoring Division, and Janie E. Hopkins, Chief – Groundwater Monitoring Section. TWDB team-members included Radu Boghici, project manager and principal investigator; Wan-Joo Choi, Mark Hayes, Christy-Ann Archuleta, and Erika Boghici, GIS analysts; Barry Hibbs, geohydrologist; and Steve Moore, Doug Coker, and John Derton, assistant hydrologists. Michael P. Vaughan and Ken Williams served as Project Officers for the U.S. EPA Region 6.

The Comisión Nacional del Agua (CNA), Mexico, provided hydrologic data and technical assistance. The Environmental Laboratory at the Lower Colorado River Authority in Austin performed the water-quality analyses on all the groundwater samples. The Coastal Science Laboratory in Austin, Texas, performed the stable isotope analyses, while the radiogenic isotope analyses were done by Beta Analytic, Inc., and the Tritium Laboratory, both located in Miami, Florida. The U.S. and Mexican sections of the International Boundary and Water Commission (respectively, IBWC and Comisión Internacional de Limites y Aguas, [CILA]) facilitated logistics of international data transfers.

## **Acknowledgments and disclaimer**

Research was supported by the U.S. Environmental Protection Agency under U.S. EPA contract number X-996343-01-0. The views and conclusions in this report are those of the TWDB and should not be interpreted as necessarily representing the official opinions of the USEPA, IBWC, CILA, or CNA. Adjunct research institutions and public agencies are credited



for providing technical and administrative assistance for this study. These include the Bureau of Economic Geology (BEG); the IBWC and CILA; the Texas Natural Resources Conservation Commission (TNRCC); and the Texas Natural Resources Information System (TNRIS). Several individuals are acknowledged for providing technical and administrative assistance and data. They include Dr. Robert Mace and Miguel Pavon of TWDB; Edward Collins of BEG; Debra Little, Jim Robinson, and Rong Kuo, of IBWC; and Antonio Rascon of CILA. Roberto Anaya, Ali Chowdhury, Janie Hopkins, Sanjeev Kalaswad, Robert Mace, Bill Mullican, Gary Powell, Richard Preston and Cindy Ridgeway, all of TWDB, reviewed this report. Their time and suggestions are much appreciated.

## **Regional geographic setting**

### **Location**

The area encompassed by this study lies between north latitudes 29° 59' 12" and 27° 15' 31" and west longitudes 98° 57' 26" and 101° 40' 51". The study area includes all or parts of Val Verde, Edwards, Real, Kinney, Uvalde, Maverick, Zavala, Frio, Dimmit, La Salle, and Webb counties, Texas. Part of northeastern Coahuila, Nuevo Leon, and Tamaulipas, Mexico, are included in the study area (figure 1.1). Total land surface area encompassed by the study is about 52,000 km<sup>2</sup>, of which nearly 22,100 km<sup>2</sup> is in Mexico. Principal transboundary aquifers in the region are the Edwards-Trinity aquifer, the Allende-Piedras Negras Valley aquifer, and the Carrizo-Wilcox aquifer (figure 1.2). Other water-bearing strata in the study area are the Bigford and Laredo formations (see the geologic map, figure 1.4). At the time this report was being written there was not enough geological and hydrological information to designate these units as binational aquifers.

# LOCATION OF STUDY AREA

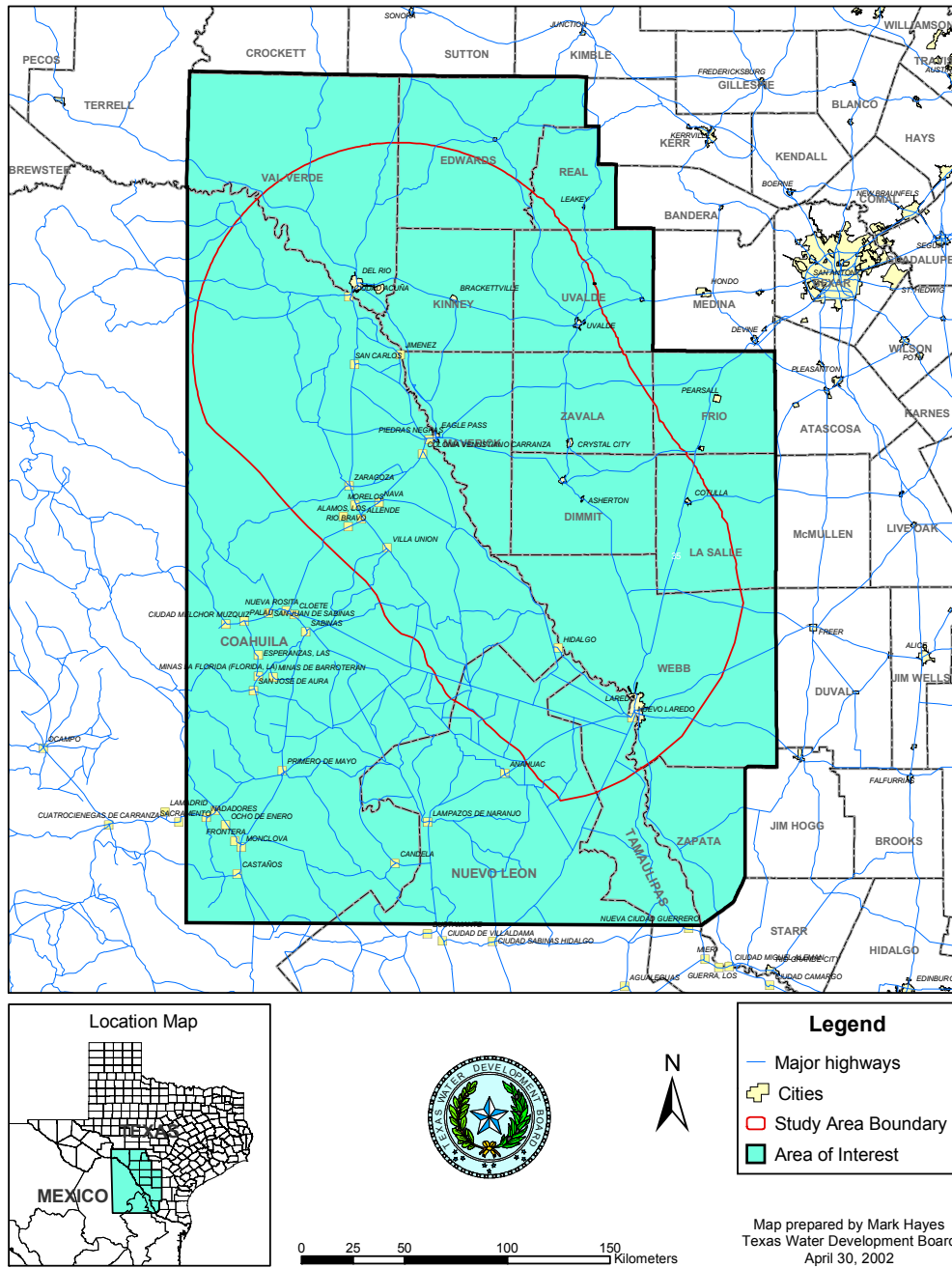


Figure 1.1 Location of study area.

# AQUIFERS WITHIN STUDY AREA

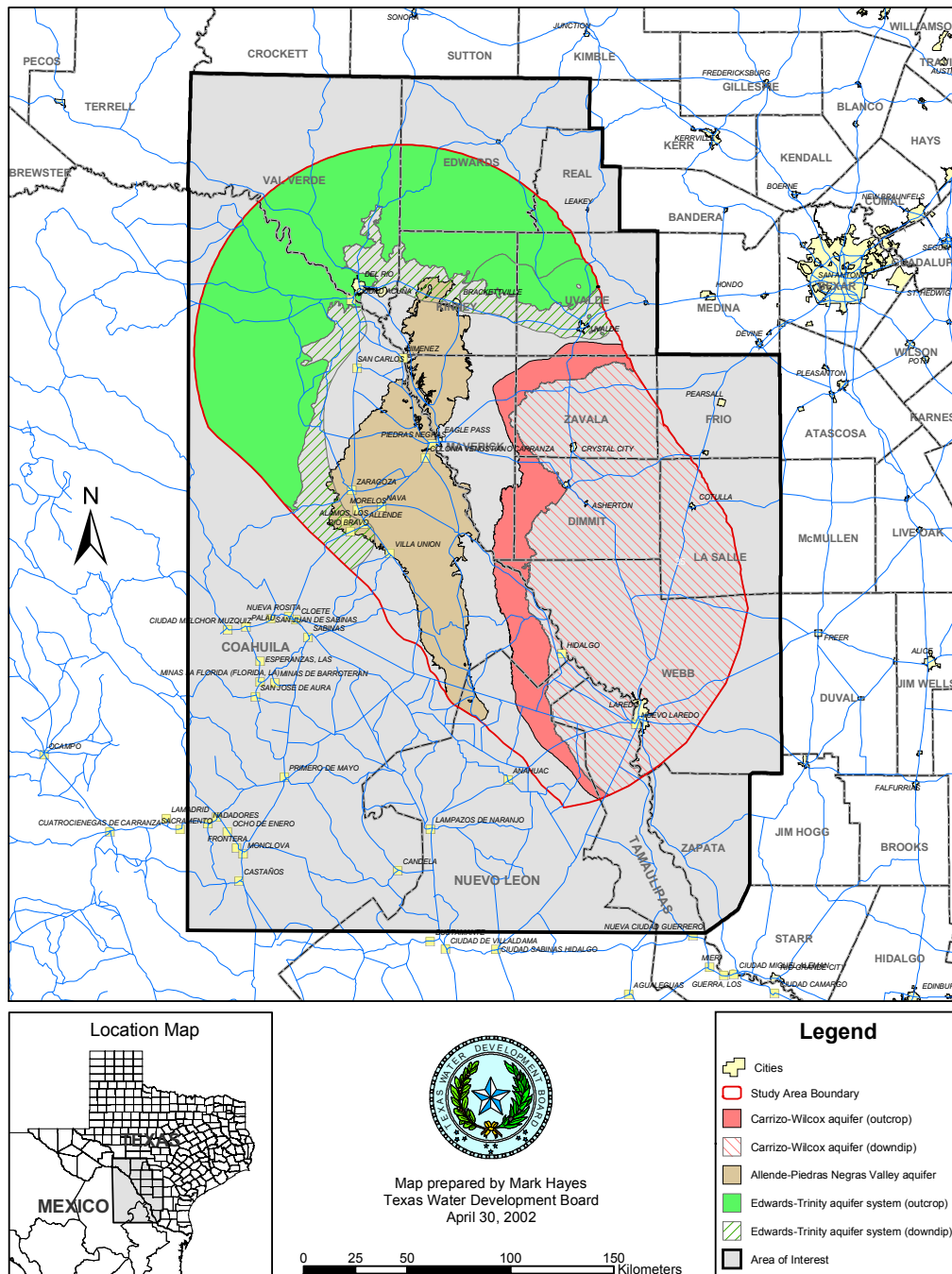
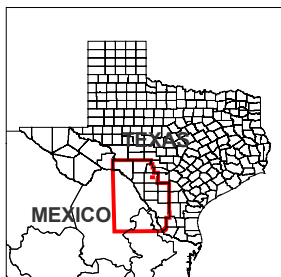
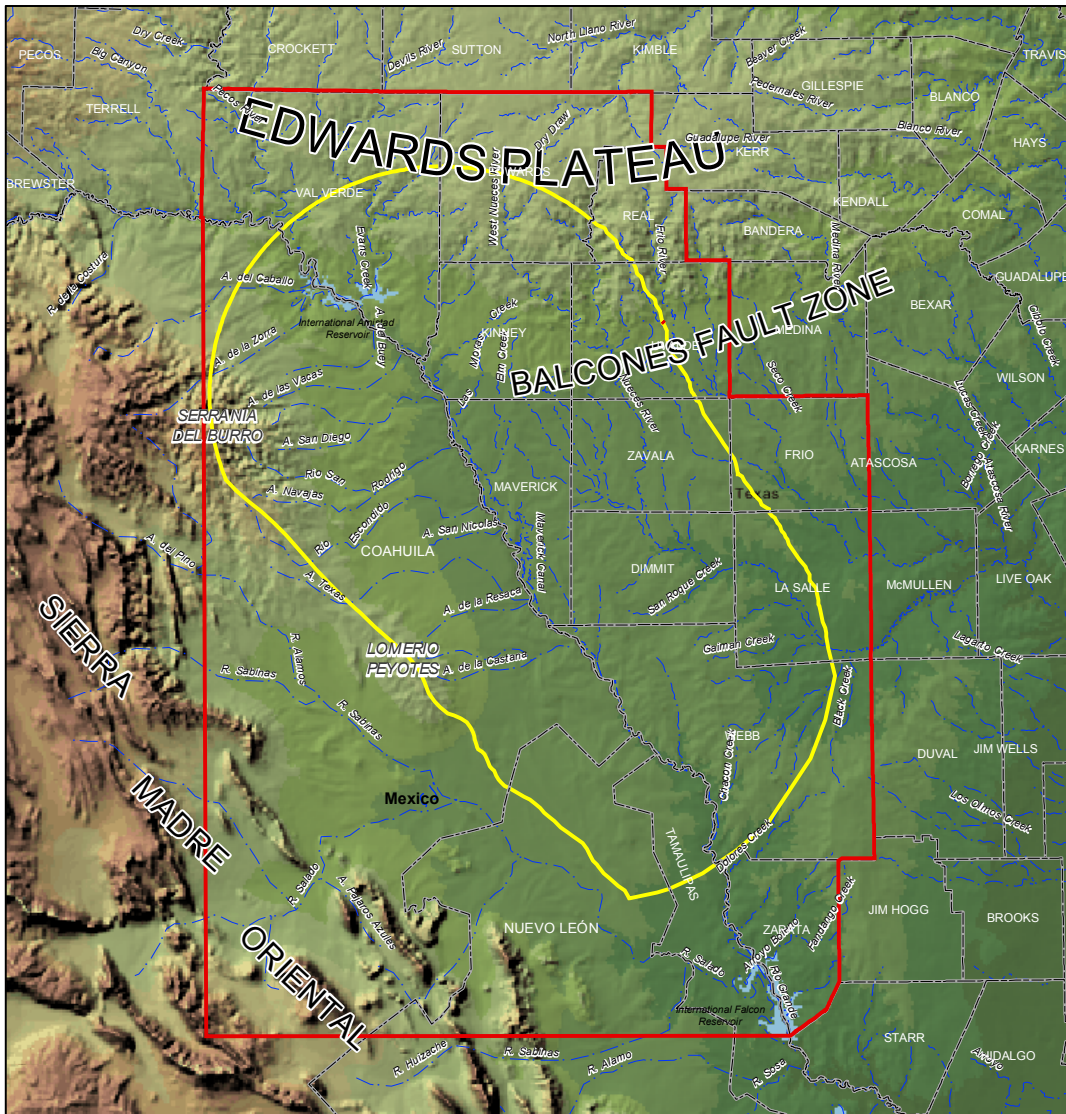
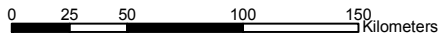


Figure 1.2 Transboundary aquifers in the study area.



**Legend**

-  Drainage
-  State and County boundaries
-  Study Area Boundary
-  Area of interest



Map prepared by Mark Hayes  
Texas Water Development Board  
May 24, 2002

Figure 1.3 Surface topography and drainage features in the study area

## **Topography and drainage**

The surface topography and the principal drainage are depicted in figure 1.3. Rough and rolling rocky plains that are sometimes dissected by deep, steep-walled canyons characterize the topography in the northwestern part of the area (Val Verde, Edwards, Real, and Kinney counties, Texas). The plains are bounded to the west and south by northwest-trending mountain ranges and alluvium-filled valleys.

The southeastern part of the study area has relatively low relief and slopes gently towards the Gulf of Mexico. The most prominent topographic feature in the study area is the Serranía del Burro mountain range in northeastern Coahuila, where elevations over 1,500 m are attained in the Oso Blanco area. The Peyotes Range, up to 700 m high, are a continuation of the Burro mountains to the southeast. Nuevo Laredo, Tamaulipas, has the lowest elevation in the study area (105 m).

Three major rivers, the Rio Grande, Nueces, and Frio dissect the study area and, together with their tributaries, drain the region. The Rio Grande flows southeastward and then east before emptying into the Gulf of Mexico. The Nueces and Frio Rivers drain the northeastern part of the region before merging with the Atascosa River and eventually flowing into the Gulf of Mexico. Other surface-water courses in the study area are: the Pecos River, Devils River, Las Moras Creek, Leona River on the Texas side and Arroyo Las Vacas, Río San Diego, Río San Rodrigo, and Río Escondido on the Mexican side (figure 1.3). In 1963, in accordance with the provisions of the 1944 Water Treaty, the United States and Mexico began construction on the Amistad Reservoir. The dam was completed during late 1969, and in September 1974 the reservoir was filled to near capacity with 19.67 km<sup>3</sup> of water (IBWC, 1987). The emplacement of the Amistad

Reservoir had a significant impact on the groundwater conditions in the area (Reeves and Small, 1973).

## **Climate**

The climate in the study area is subtropical and semiarid characterized by mild winters and hot summers. Average annual precipitation varies from as little as 300 mm/yr in northwestern Val Verde County to as much as 660 mm/yr in southern Webb County (NCDC, 1961-1990).

Climatological data have been collected for decades at and near the major metropolitan areas. The climate in Laredo and Nuevo Laredo is semiarid. Average annual precipitation in Laredo is 565.1 mm of which nearly one-half of precipitation is from thunderstorms that occur from June through September (Texas Almanac, 2000-2001). Mean annual temperature is 22.6°C in the Laredo/Nuevo Laredo area, with an average maximum temperature of 29.1°C and a minimum average temperature of 16.2°C.

The climate is arid to semiarid in the Eagle Pass/Piedras Negras area. Precipitation is mostly from thunderstorms that occur sporadically during the summer months. Precipitation records at several meteorological stations indicate that average annual rainfall along the Eagle Pass/Piedras Negras corridor is about 554 mm (most of it falling from April through September) and the temperature averages 21.2°C. The average minimum temperature at Eagle Pass is 14.5°C, while the average maximum temperature is 28°C.

The climate is arid to semiarid in the Del Rio/Ciudad Acuña area. The average annual precipitation at Del Rio is 481.3 mm. Most of the rainfall occurs from April through October mainly as showers or heavy downpours during thunderstorms. The average annual temperature in the Del Rio/Ciudad Acuña is 20.7°C. The average temperature ranges from 14.4°C (minimum) to 27.1°C (maximum). Based on climatic records from 1871 to 1975, Elizondo (1977, p. 13) indicates that precipitation on the Mexican side range from 525 mm in the Amistad Reservoir-Piedras Negras Basin (surface area 4,209 km<sup>2</sup>) to 517 mm in the Piedras Negras – Laredo Basin (surface area 9,829 km<sup>2</sup>)

### **Population and economy**

The statistics in this section have been compiled from the U.S. Census Bureau's 2000 Census datasets (USCB, 2000) and the 2000-2001 Texas Almanac for the Texas side and from El Instituto Nacional de Estadística, Geografía e Informática 2000 Census datasets (INEGI, 2000) for the Mexican side.

The year 2000 population of Dimmit County, Texas, was estimated to be 10,875, an increase of 4.4 percent from the 1990 census (pop.10,419). The 2000 census indicates that there were 3,308 households in Dimmit County with an average of 3.06 persons per household. In addition to the population estimates for Carrizo Springs (5,842), Asherton (1,658), Big Wells (829), and Catarina (45), the unincorporated areas had a total of 2,534 residents. The economy of Dimmit County is largely dependent upon private services which provided 2,064 jobs during 2000. Local and state employers provided 1,204 jobs, federal work provided 155 jobs, and 193 people were self-employed. Dimmit County is

an important producer of agricultural goods such as cattle, poultry, vegetables hay, and pecans amounting to \$19.9 million earned countywide during year 2000.

In 2000, the population of Edwards County numbered 2,162 people, an increase of 4.8 percent from the 2,063 inhabitants counted in the 1990 census. The 2000 census indicates that there were 801 households in Edwards County with an average of 2.66 persons per household. Larger towns in the county included Rocksprings (pop. 1,552), Barksdale (1,081), and Carta Valley (12), while the unincorporated areas were inhabited by 736 people. The economy of Edwards County is largely dependent upon private services and farming. In 2000, private services employed 487 people, local and state agencies employed 176, federal agencies employed 32, and 175 people were self-employed. Edwards County is a producer of agricultural goods such as cattle, goats and sheep. In 2000, \$9 million was earned in Edwards County through its ranches and farms. Edwards County is also known as a center of mohair-wool production, one of the largest segments of income countywide.

The year 2000 population of Kinney County was 3,379, or an increase of 9.1 percent from the 1990 census of 3,098. Between 1980 and 1990 population grew 26.5 percent. The 2000 census indicates that there were 1,314 households in Kinney County with an average of 2.55 persons per household. A total of 1,858 people resided in Bracketville, while Fort Clark Springs, Spofford, and the unincorporated areas had populations of 1,070; 66; and 1,042, respectively. The economy of Kinney County is largely dependent on agriculture, forestry, and fisheries. In 2000, these private services provided 637 jobs compared to local and state employers (209 jobs), federal agencies (62



jobs), and 113 self-employed. Kinney County has traditionally been an important producer of cattle, meat goats, angora goats, hay, wheat, cotton, and pecans.

A total of 47,297 people inhabited Maverick County in 2000, which was a 30 percent increase from the 1990 census. There were 13,089 households (an average of 3.60 persons per household) in Maverick County in 2000, with Eagle Pass (pop. 26,767), El Indio (148), and Quemado (426) being the largest towns. The unincorporated areas had a total of 7,036 inhabitants. The economy of Maverick County is largely dependent upon agriculture and manufacturing. In 2000, these private services provided 6,909 jobs compared to local and state agencies, which provided 2,162 jobs. Federal work provided 422 jobs, and the self-employed numbered 738. Maverick County has been an important producer of agricultural goods, such as cattle, pecans, vegetables, sorghum, wheat, goats and sheep. Countywide agricultural activities (sheep, goats cattle, and minor irrigation) provided a net cash return of \$2,498,000 in year 2000.

The population of Val Verde County was estimated to be 44,856 in 2000, or an increase of 16 percent from the 1990 census of 38,721. In 2000 there were 14,151 households in Val Verde County, averaging 3.11 persons per household. Del Rio (34,167), Comstock (375), and Langtry (145) were the largest towns, while the unincorporated areas had a total of 10,944 inhabitants. The economy of Val Verde County is dependent upon private services, retail trade, and farming. In 2000, these private services provided 7,338 jobs, while local and state employment provided 2,092 jobs. Val Verde County has traditionally been an important farming and ranching center. Val Verde County is ranked number one in the state of Texas in sheep sales (\$2,200,000

during year 2000). Overall, however, in year 2000 agriculture in Val Verde County (angora goats, cattle, meat goats, and minor irrigation) lost \$293,000.

The year 2000 population of Webb County of 193,117, was an increase of 45 percent from the 1990 census of 133,239. The increase between 1980 and 1990 was 34 percent. The 2000 census indicates that there were 50,740 households in Webb County with an average of 3.75 persons per household. With a population of 175,400, Laredo is the largest city in Webb County. Other towns include Río Bravo (4,131), El Cenizo (1,775), Mirando City (707), Oilton (585), and Bruni (581), and 2,299 inhabitants lived in unincorporated areas. The economy of Webb County is largely dependent on international trade, retail, tourism, manufacturing, meatpacking, and agriculture. In 1990, private services provided 32,651 jobs compared to local and state entities that provided 7,751 jobs. Federal work provided 1,656 jobs, and 3,504 were self-employed.

According to the 2000 census, Zavala County had a population of 11,600, down 4.6 percent from 1990 when it numbered 12,162 people. The largest cities in Zavala County were Crystal City (pop. 8,088), Batesville (1,275), and La Pryor (1,230). There were 3,248 households in Zavala County in 2000 with an average of 3.28 persons per household. The economy of Zavala County is largely dependent on agriculture, oil and gas, government, and services. In 1990, these private services provided 2,384 jobs whereas local and state agencies provided 856 jobs. Federal work provided 71 jobs, and 301 people were self-employed. Zavala County has traditionally been an important producer of agricultural goods, such as spinach, pecans, vegetables, sorghum, cotton, hay, cattle, goats, and sheep.

Coahuila de Zaragoza, third largest Mexican state after Chihuahua and Sonora, occupies the U.S.-Mexico border across from West Texas in the middle portion of the Rio Grande River. The capital city of Coahuila is Saltillo (2000 population 578,046). The largest border cities in northeastern Coahuila are Ciudad Acuña and Piedras Negras.

In 2000, the population of the Ciudad Acuña municipality was 110,487, up 7 percent from the 1990 census results. There were 25,643 households in Ciudad Acuña in 2000, with an average of 4.3 residents per household. Ciudad Acuña is an active economic center, predominantly of banking and manufacturing, but it also serves as an agricultural, cattle and trade transfer center for north and southbound trade traffic. In 2000, of the 44,838 people active economically, 60.4 percent were employed in commerce, transportation, government, and services while 35.8 percent were working in mining, oil and gas extraction, manufacturing, construction, and utilities (INEGI, 2000).

In the year 2000, 128,130 persons resided in the Piedras Negras municipality, a 2.7 percent increase from the 1990 census results. The 31,303 households in Piedras Negras averaged 4.1 people per household. In 2000, Of the active population (45,778) 48.4 percent were employed in commerce, transportation, government, and services, while 46.7 percent were working in mining, oil and gas extraction, manufacturing, construction, and utilities.

Other Coahuila municipalities included in the study area are Nava (pop. 23,019), Allende (20,943), Zaragoza (12,664), Jiménez (9,724), Morelos (7,263), and Villa Unión (6,159).

The Mexican state of Tamaulipas shares borders with Texas to the north, Nuevo Leon to the west, San Luis Potosi and Veracruz to the south, and the Gulf of Mexico to

the east. Its most populated municipality is Reynosa with 420,463 residents. The most important municipality along the border area with the U.S. is Nuevo Laredo, which in 2000 was inhabited by 310,915 people, a 3.6 percent increase from 1990. There were 73,676 households in Nuevo Laredo, and, on average, 4.2 people lived in each household. In 2000, 32.9 percent of the active population (115,976) were employed in commerce, transportation, government, and services, while 61.0 percent were working in mining, oil and gas extraction, manufacturing, construction, and utilities. Across the border from Laredo, TX, Nuevo Laredo is the principal inland port of entry to Mexico. According to port officials, 80 percent of Mexico's imports and exports are shipped across the Laredo/Nuevo Laredo border. The Nuevo Laredo-Laredo international bridge is the busiest commercial crossing point between the two countries. In 1999, thirty-eight percent of the total U.S./Mexico ground-based trade passed through Laredo, and \$30 billion in U.S. exports to Mexico crossed through Laredo (USDC, 2002). Nuevo Laredo's economy, traditionally based on banking and freight forwarding, has started to attract in-bond assembly plants (“maquilas”), which in 1999 employed about 20,000 people.

### **History of groundwater development**

Development of the Carrizo-Wilcox aquifer in south Texas prior to 1900 was chiefly for domestic, livestock, and public-supply uses. Roesler (1890) mentioned the completion of one of the early irrigation wells at Carrizo Springs, Dimmit County, in 1884. Many of the early wells in the Winter Garden area were flowing when first drilled. Large-scale aquifer pumping commenced in the early 1900s following the introduction of the deep-well turbine pumps (Klemm, 1976). Groundwater-level declines of up to 80 m

have taken place in Dimmit, Zavala, and eastern Maverick counties of Texas between 1929 and 1970 (Klemm et al., 1976). Groundwater withdrawals from the Carrizo-Wilcox aquifer peaked in the mid-1980s and have been on a declining trend ever since.

Presently, groundwater pumping for agriculture accounts for 90 percent of the volume of groundwater extracted from the Carrizo-Wilcox aquifer in the study area. Public water-supply uses claim seven percent of the groundwater withdrawn from the Carrizo-Wilcox aquifer.

Development of groundwater on the Texas side of the Edwards-Trinity aquifer began during the middle 1800s for the purpose of supplying U.S. Army Forts and stagecoach stops where springs and surface streams were not available (Walker, 1979). Early Edwards-Trinity water-supply wells were developed during the middle to late 1800s along the Butterfield Stage route in the northern part of the Edwards Plateau. The introduction of the windmill around 1880 signaled the beginning of the development of groundwater resources for livestock and rural domestic use. During 1920-30 groundwater pumped from industrial wells was used to supply oil and gas exploration uses, ice making, refineries, industrial complexes, and gasoline plants. The first irrigation well was drilled in Uvalde County in 1908, but groundwater was not used for irrigation in large quantities until 1925 (Welder and Reeves, 1962). Irrigation pumpage in Uvalde County increased gradually until 1947 and developed more rapidly afterwards. Smaller quantities of groundwater have been pumped for irrigation in Val Verde and Kinney counties.

## **Regional geologic setting**

### **Geologic characteristics**

Geologic units in the study area range from Cretaceous to recent (figure 1.4). The ages of strata in outcrop are primarily Cretaceous in the mountainous areas and plateaus, Paleocene and Eocene in the flatlands, and Pliocene – Holocene sediments can be found as valley fills. Consolidated rock types are important to the makeup of the hydrostratigraphy of the study area. They include Mesozoic (Cretaceous) carbonate rocks that are fractured and occasionally karstified; Cenozoic (Paleocene and Eocene) sandstone and siltstone; and some late Cretaceous-early Tertiary igneous rocks that are usually fractured and jointed.

Semi-consolidated to unconsolidated sediments include Pliocene and Quaternary alluvial deposits consisting largely of sand and gravel lenses interstratified with silt and clay. Lenses and beds are highly irregular in extent and thickness, and correlations across short distances are difficult or impossible to make with available data. Recent alluvial deposits not formed by the Rio Grande are associated with arroyos that drain the mountains. Typically these deposits are poorly sorted sands, silts, and gravels.

### **Depositional history**

The depositional hiatus between the Cretaceous strata that comprise the Edwards-Trinity aquifer and the underlying Paleozoic rocks marked a major change in the geologic history of the study area (Barker and Ardis, 1992). The study area was subaerially exposed for a period of approximately 60 million years, from the retreat of the Permian sea to the deposition of shallow-marine carbonates during early Cretaceous (Barker et al., 1994).

# GEOLOGY

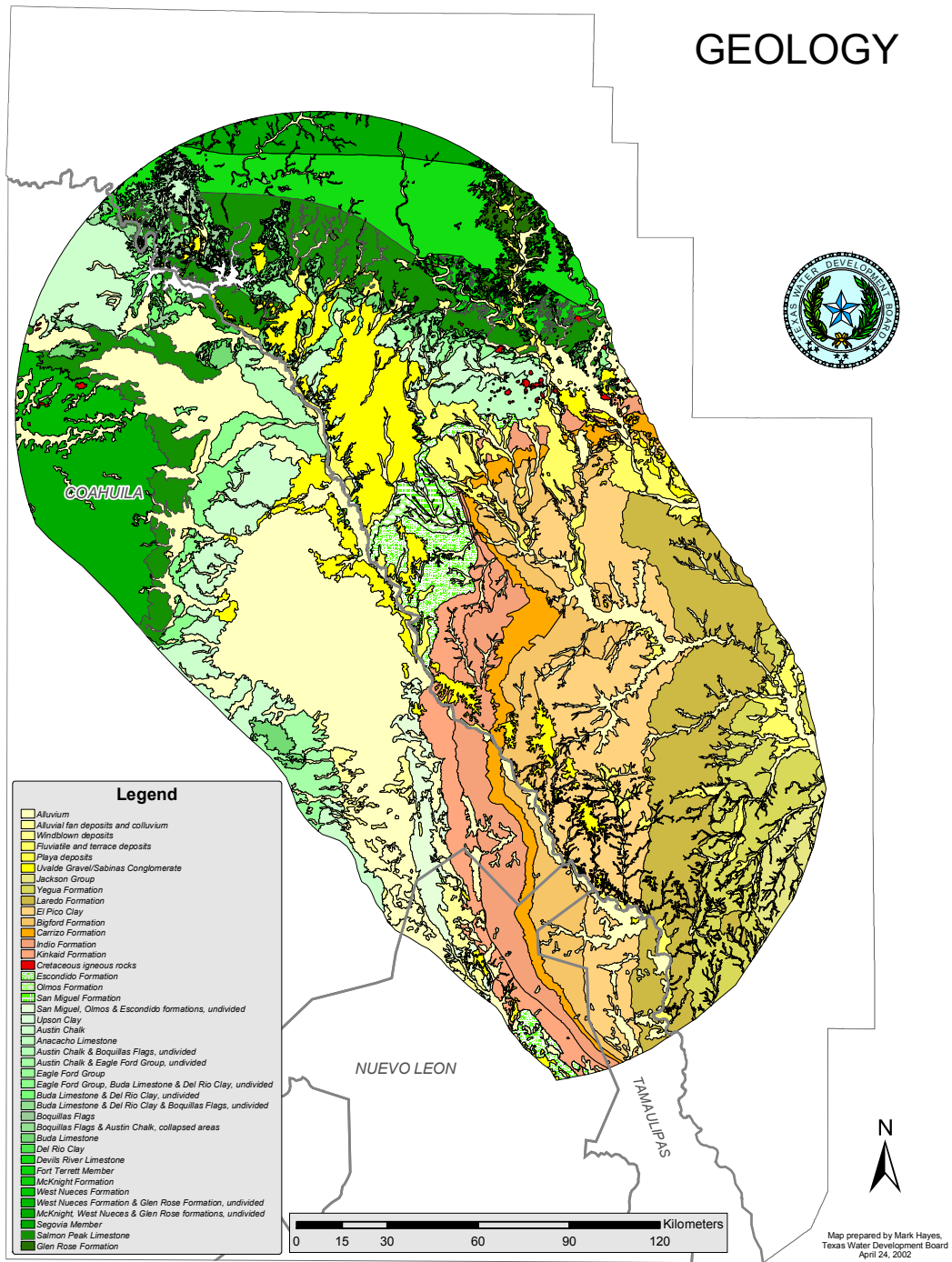


**Figure 1.4 Geologic map of the study area. Sources: Texas Bureau of Economic Geology geologic atlas sheets; El Instituto Nacional de Estadística, Geografía e Informática geologic sheets.**

From Permian through the end of Jurassic, the area also experienced crustal warping, erosion, and reversals of surface drainage patterns before being covered by the early Cretaceous sea (Sellards, 1933).

The early Cretaceous Trinity carbonates were deposited by a westward-advancing sea on the eroded surface of folded and faulted pre-Cretaceous rocks (Hill, 1901). The transgression of the sea was cyclic but persistent, with short-lived sea-level regressions that were controlled by variable rates of regional subsidence (Barker et al., 1994). During the late Trinity, the sea withdrew to the southeast (Lozo and Smith, 1964), and a fluvial-deltaic regime became dominant over parts of the study area.

A rapid sea-level rise during the early Fredericksburg favored the development of the Stuart City trend, a reef that extended from northern Coahuila into Texas (Winter, 1962). This reef controlled the regional Fredericksburg deposition: deep (> 300 m) marine conditions prevailed in the sea to the east of the reef, while shallow (~30 m), carbonate platform sediments were deposited landward. The Devils River trend, a narrow, carbonate reef developed around the northern and western rim of the Maverick basin, controlled the sedimentation in that basin through early Washitan time (Barker et al., 1994). During early to middle Washitan time the Stuart City reef began to disintegrate, and the connection between the two sedimentation centers improved (Smith, 1989 as cited in Barker et al., 1994). Following regional uplift during late Washitan time, the open-marine terrigenous Del Rio Clay blanketed the study area, but deep-sea conditions returned at the end of the Washitan time, as illustrated by the widespread deposition of Buda Limestone.



Thick, fine-grained, highly cemented, and virtually impermeable carbonates formed during Gulfian time when shallow marine, open shelf conditions prevailed (Barker et al., 1994). The Laramide orogeny of northern Mexico and southwestern U.S. uplifted the study area (Ewing, 1991) at the end of the Cretaceous. Extensive erosion of Gulfian rocks occurred prior to the deposition of Cenozoic strata over the Cretaceous beds.

The retreat of the Cretaceous sea was followed by deposition of thick, off-lapping Cenozoic deltaic sequences in the Rio Grande Embayment, which was a large bay peripheral to the ancestral Gulf of Mexico. Prior to Eocene deposition, the middle Wilcox mud-rich deltas prograded across the Midway Group shelf deposits (McCoy, 1991). Rivers then converged on the embayment carrying debris eroded from the inland mountains to the west. These sediments (Carrizo Formation) were deposited in sand-rich belts, aprons, or sheets coinciding with the fluvial axes (Galloway, 1981). Sea-level regression combined with subsidence and stacking of delta sequences, slowed the progradation of the Carrizo Formation. The end of the Carrizo Formation deposition was initiated by a marine transgression that inundated parts of the sandy coastal plain (Hamlin, 1988). Mixed alluvial sequences consisting of meandering river channels typify the end of the Carrizo Formation depositional episode, before the massive Bigford-Reklaw transgression inundated most of the Rio Grande Embayment (Hamlin, 1988).

Tertiary and Quaternary faulting, erosion, post-depositional solution and cementation, and structural collapse have affected the transmissive properties of the Cretaceous and Eocene water-bearing formations. Erosion of Mesozoic and Tertiary

strata produced large accumulations of permeable alluvium and terrace deposits, some of which make good aquifers today.

## References

- Barker, R. A. and Ardis, A. F., 1992, Configuration of the base of the Edwards-Trinity aquifer system and hydrogeology of the underlying pre-Cretaceous rocks, west-central Texas: U.S. Geologic Survey Water-Resources Investigations Report 91-4071, 25 p.
- Barker, R. A., Bush, P. W., and Baker, E. T., Jr., 1994, Geologic history and hydrogeologic setting of the Edwards-Trinity aquifer system, west-central Texas: U. S. Geological Survey Water-Resources Investigation Report 94-4039, 51 p.
- El Instituto Nacional de Estadística, Geografía e Informática, 2000: XII Censo General de Población y Vivienda,  
<http://www.inegi.gob.mx/difusion/espanol/poblacion/index.html>.
- Elizondo, J. R., 1977, Geología básica regional en la sub-cuenca hidrológica Acuña-Laredo: Comisión Federal de Electricidad, Series técnicas de CFE, 69 p.
- Ewing, T. E., 1991, The tectonic framework of Texas, with accompanying tectonic map of Texas: The University of Texas at Austin, Bureau of Economic Geology, 36 p.
- Galloway, W. E., 1981, Depositional architecture of Cenozoic Gulf Coastal Plain fluvial systems: Society of Economic Paleontologists and Mineralogists Special Publication No. 31, p. 127-155.
- Hamlin, H. S., 1988, Depositional and ground-water flow systems of the Carrizo-Upper Wilcox, south Texas: The University of Texas at Austin, Bureau of Economic Geology Report of Investigations No. 175, 61 p.
- Hill, R. T., 1901, Geography and geology of the Black and Grand Prairies, Texas, with detailed descriptions of the Cretaceous formations and special reference to artesian water: U.S. Geological Survey, 21<sup>st</sup> Annual Report, pt. 7, 666 p.
- IBWC, 1987, Amistad Reservoir area, report on hydrogeologic studies, Summary of report on effects of Amistad Reservoir on hydrologic regimen in the area, International Boundary and Water Commission, 99 p.
- Klemt, W. B., Duffin, G. L., and Elder, G. R., 1976, Groundwater resources of the Carrizo aquifer in the Winter Garden area of Texas: Texas Water Development Board Report 210, v. 1, 30 p.

- Lozo, F. E., Jr. and Smith, C. I., 1964, Revision of Comanche Cretaceous stratigraphic nomenclature, southern Edwards Plateau, southwest Texas: Transactions of Gulf Coast Association of Geological Societies, v. 14, p. 285-307.
- McCoy, T. W., 1991, Evaluation of ground-water resources of the western portion of the Winter Garden area, Texas: Texas Water Development Board Report 334, 64 p.
- NCDC, 1961-1990, National Climatic Data Center  
<ftp://www.ncdc.noaa.gov/pub/data/normal>
- Reeves, R. D., and Small, T. A., 1973, Ground-water resources of Val Verde County, Texas: Texas Water Development Board Report 172, 145 p.
- Roesler, F. E., 1890, Report (on the underground water supply in Texas): U.S. 51<sup>st</sup> Cong., 1<sup>st</sup> Sess., Ex. Doc222, v. 12 (U.S. Serial no. 2689), p. 243-319.
- Sellards, E. H., 1933, The pre-Paleozoic and Paleozoic Systems in Texas, *in* The geology of Texas, v. I, stratigraphy: The University of Texas at Austin, Bureau of Economic Geology Bulletin 3232, p. 15-238.
- Texas Almanac, 2000-2001, Millenium Edition: The Dallas Morning News, L.P., 672 p.
- U.S. Census Bureau, 2000, State and county QuickFacts:  
[http://quickfacts.census.gov/cgi-bin/state\\_QuickLinks?48000](http://quickfacts.census.gov/cgi-bin/state_QuickLinks?48000)
- U.S. Department of Commerce, 2002:  
<http://www.usatrade.gov/website/ccg.nsf/CCGurl/CCG-MEXICO2002-CH-2:-0047622B>
- Walker, L. E., 1979, Occurrence, availability, and chemical quality of ground water in the Edwards Plateau region of Texas: Texas Water Development Board Report 235, 336 p.
- Winter, J. A., 1962, Fredericksburg and Washita strata (subsurface Lower Cretaceous), southwest Texas, in Contributions to the geology of south Texas: San Antonio, Texas, South Texas Geological Society, p. 81-115.
- Welder, F. A. and Reeves, R. D., 1962, Geology and ground-water resources of Uvalde County, Texas: Texas Water Commission Bulletin 6212, 252 p.



## **CHAPTER 2: EDWARDS-TRINITY AQUIFER SYSTEM**

This section will describe the groundwater aquifers within the Edwards-Trinity aquifer system in the study area. The system (figure 1.2, p. 24) consists of two hydraulically interconnected aquifers, namely the Edwards-Trinity aquifer and the Edwards aquifer. The discussion that follows includes general information on aquifer location and extent, geology and water-bearing characteristics, aquifer properties, piezometry, hydrochemistry, and contamination potential.

### **Location and extent**

The segment of the Edwards-Trinity aquifer system discussed in this report underlies an area of 31,050 km<sup>2</sup>, of which 16,000 km<sup>2</sup> are located in Mexico. The limits of the study region at the northeast, northwest, and southwest are also the aquifer system limits (figure 2.1). The eastern boundary of the system in the study region is a hydrogeologic one: the "bad-water line", or the 1,000 mg/l line of total dissolved solids (TDS) concentration (Maclay et al., 1980). The "bad water line" has been traced south into Mexico and bounds the aquifer system to the east of Serranía del Burro and Peyotes anticline in Mexico (Lesser and Lesser, 1988).

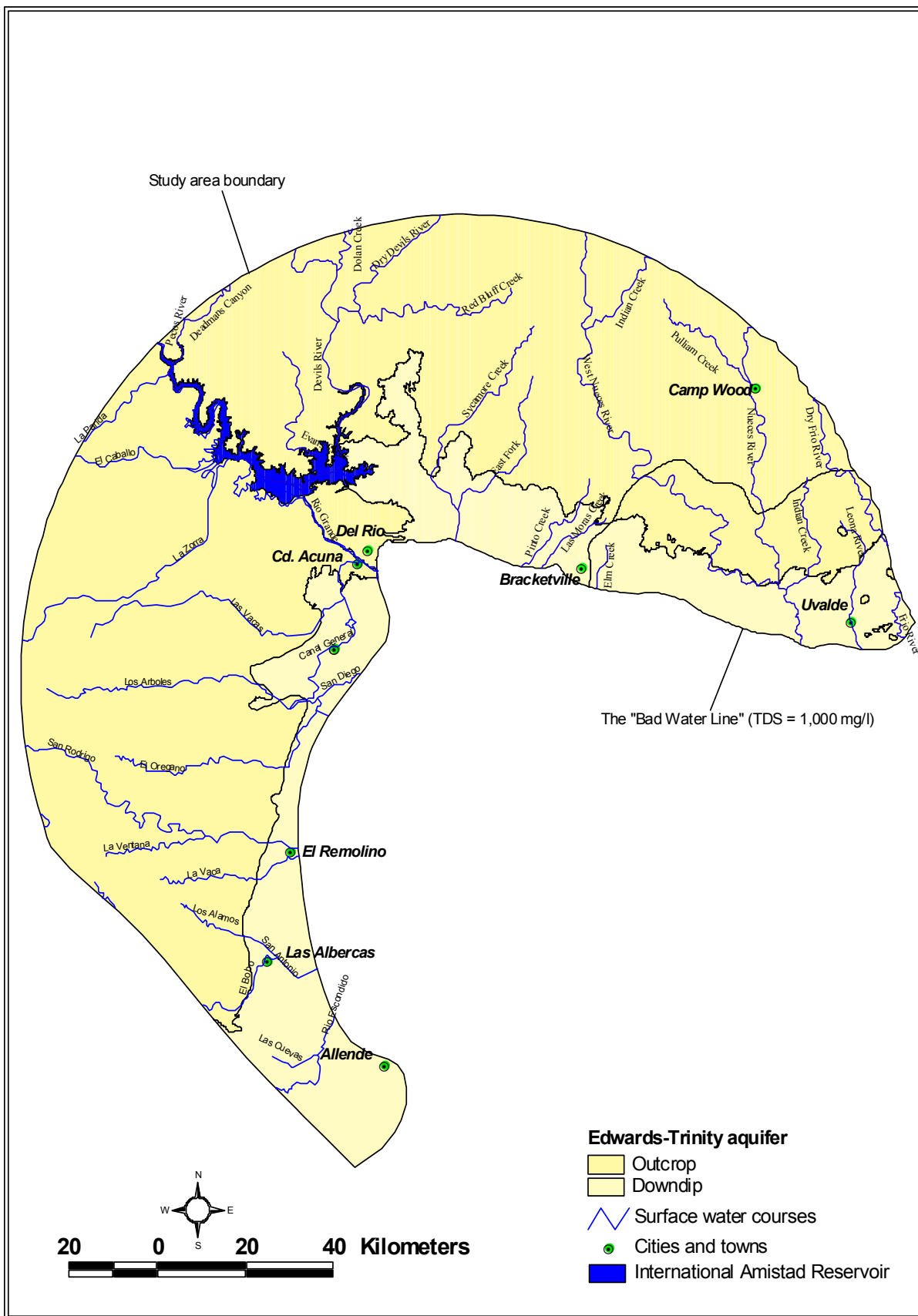


Figure 2.1 Location of the Edwards-Trinity aquifer

## Stratigraphy and structure

The lithostratigraphic and regional hydrogeologic units in the study area are summarized in table 2.1. The Edwards-Trinity aquifer system is hosted by lower Cretaceous rocks (Trinity, Fredericksburg, and lower Washita groups) which cover comparatively impermeable and structurally complex pre-Cretaceous rocks. They are overlain by the semi-permeable upper Cretaceous rocks (upper Washita through Navarro groups), which are locally regarded as confining units (Barker et al., 1994).

In northern Coahuila, Mexico, the Cretaceous System is divided into three series. From oldest to youngest these are the Coahuilan, Comanchean, and Gulfian (Smith, 1970), with the Gulfian referred to as the upper Cretaceous, and the Coahuilan and Comanchean together as the lower Cretaceous. In southwestern Texas the Cretaceous System includes the Comanchean and Gulfian Series. Some Coahuilan-equivalent strata are recognized by Loucks (1977) and included in the lower Comanchean.

The Comanchean in Texas begins with rocks of the Trinity Group, sediments that were deposited by a transgressive Early Cretaceous sea that advanced westward over an eroded, uneven surface of pre-Cretaceous rocks. Stratigraphically, the Trinity Group includes the Hosston, Sligo, and Pearsall formations; the Glen Rose Limestone; and the Maxon Sand.

The terrigenous Hosston Formation, consisting of siliciclastic siltstone and sandstone, is up to 270 m thick (Imlay, 1945, table 2). The overlying carbonate-rich Sligo Formation is composed of intertidal limestone and dolostone and evaporites (Bebout et al., 1981). Imlay (1945) estimates the Sligo Formation is at most 70 m thick.

ERATHEM	SYSTEM	SERIES	GROUP	UNITED STATES		MEXICO	
				DEVILS RIVER TREND	MAVERICK BASIN		
CENOZOIC	Quaternary			Alluvium			
	Tertiary			Uvalde Gravel	Sabinas Conglomerate		
MESOZOIC	CRETACEOUS	GULFIAN		Anacacho Limestone	Taylor & Navarro Groups		
				Austin Group			
				Eagle Ford Group			
				Buda Limestone			
				Del Rio Clay			
		COMANCHEAN	Washita Group	Devils River Formation	Salmon Peak Formation		
			Fredericksburg Group		McKnight Formation		
					West Nueces Formation		
		Trinity Group	Devils River Formation	Maxon Sand	Glen Rose Limestone		
				Basal Cretaceous Sand	Pearsall Fm.	La Pena Formation	
		Sligo Fm.		Cupido Formation			
		Hosston Formation					
PALEOZOIC	PERMIAN			Undivided			
	Cambrian through Pennsylvanian			Rocks of Ouachita Structural Belt			

EXPLANATION

- Allende - Piedras Negras Valley aquifer
- Cretaceous rocks not part of Edwards-Trinity aquifer system because they are discontinuous, unsaturated, or have low permeability
- Edwards-Trinity aquifer system

Modified from Barker et al., 1994, table 1

**Table 2.1 Correlation diagram showing geologic and hydrogeologic units in the Edwards-Trinity aquifer system, Texas and Coahuila**



The Pearsall Formation has been defined to include strata above the Sligo Formation and below the Glen Rose Limestone (Imlay, 1945, p. 1441). Barker and Ardis (1996) recognize three Pearsall members in the Balcones fault zone area, corresponding to the counties of Kinney and Uvalde in our study region. The Pearsall members are:

- (1) The Hammett Shale, composed of burrowed clay, silt, lime mud, and silt-sized dolomite (Amsbury, 1974);
- (2) The Cow Creek Limestone, represented by fine- to coarse-grained calcarenite, silty, cherty calcarenite, and beach deposits; and
- (3) The Hensel Sand, which comprises a mixture of limey sand, shale, chert and dolomite pebbles that typically form a basal conglomerate (Inden, 1974).

Under the Edwards Plateau, the Pearsall is not differentiated into members. According to Barker et al. (1994) the Pearsall Formation can be up to 130 m thick in the study area.

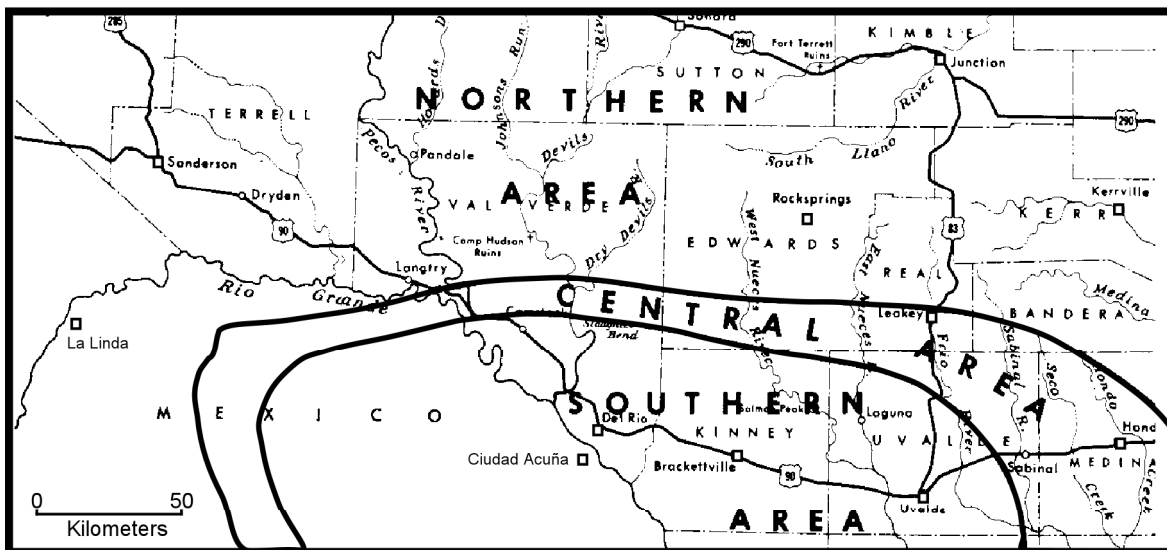
The Glen Rose Limestone is a fossiliferous, sandy limestone and dolostone, alternating with calcareous marl, shale, and clay, with laterally continuous beds of gypsum and anhydrite. Its thickness under the study area can reach 460 m (Welder and Reeves, 1962, table 1). In western Val Verde County, the Glen Rose Limestone is overlain by the Maxon Sand, which is a medium-to-coarse sandstone, alternating with conglomerate, limestone, and mudstone (Butterworth, 1970, p. 4).

In northern Coahuila the Cretaceous begins with the Coahuilan Series, where Smith (1970) mapped two formations: La Mula and Cupido. The La Mula lithology is predominantly a red-weathering, silty shale interbedded with fossiliferous lime mudstone. In the study area wells have intercepted about 75 m of La Mula material, which can get as thick as 760 m south of the study area (Smith, 1970, p. 17). At the top of La Mula rests

the transgressive Cupido Formation. Consisting of marine limestone and shale, the Cupido is 160-275 m thick (Smith, 1970, p. 18). According to Loucks (1977), the Cupido Formation is equivalent to the Hosston and Sligo formations described in Texas.

The Trinity Group in the subsurface of northern Coahuila, Mexico, is comprised of La Pena Formation and the overlying Glen Rose Formation. The La Pena beds are equivalent to the Pearsall Formation in Texas and are widely distributed over northern Mexico where they have been traced as a lithologically and faunally persistent unit (Smith, 1970). The La Pena Formation consists of about 60 m of black shale and gray lime mudstone with abundant Aptian ammonite and pelecypod fauna, all deposited in a marine environment. The Glen Rose Formation in northern Coahuila has been identified both in subsurface and in outcrop. The typical Glen Rose Formation as exposed in Serranía del Burro, is similar to the Glen Rose Formation of Texas, some of the same horizons being recognized in both areas. Smith (1970) mapped 490 m of Glen Rose strata exposed in a section at Sierra El Cedral, whereas 510 m of the same beds are overlying Fredericksburg marls at Cerro El Palomo.

The Fredericksburg and Washita Groups are genetically related rock formations that unconformably rest atop the Trinity. Lozo and Smith (1964, p. 291) divided the area occupied by the Fredericksburg and Lower Washita Groups into three geologically distinct regions: northern, central, and southern (figure 2.2). The lateral and vertical distributions of these rocks are summarized in figure 2.3.

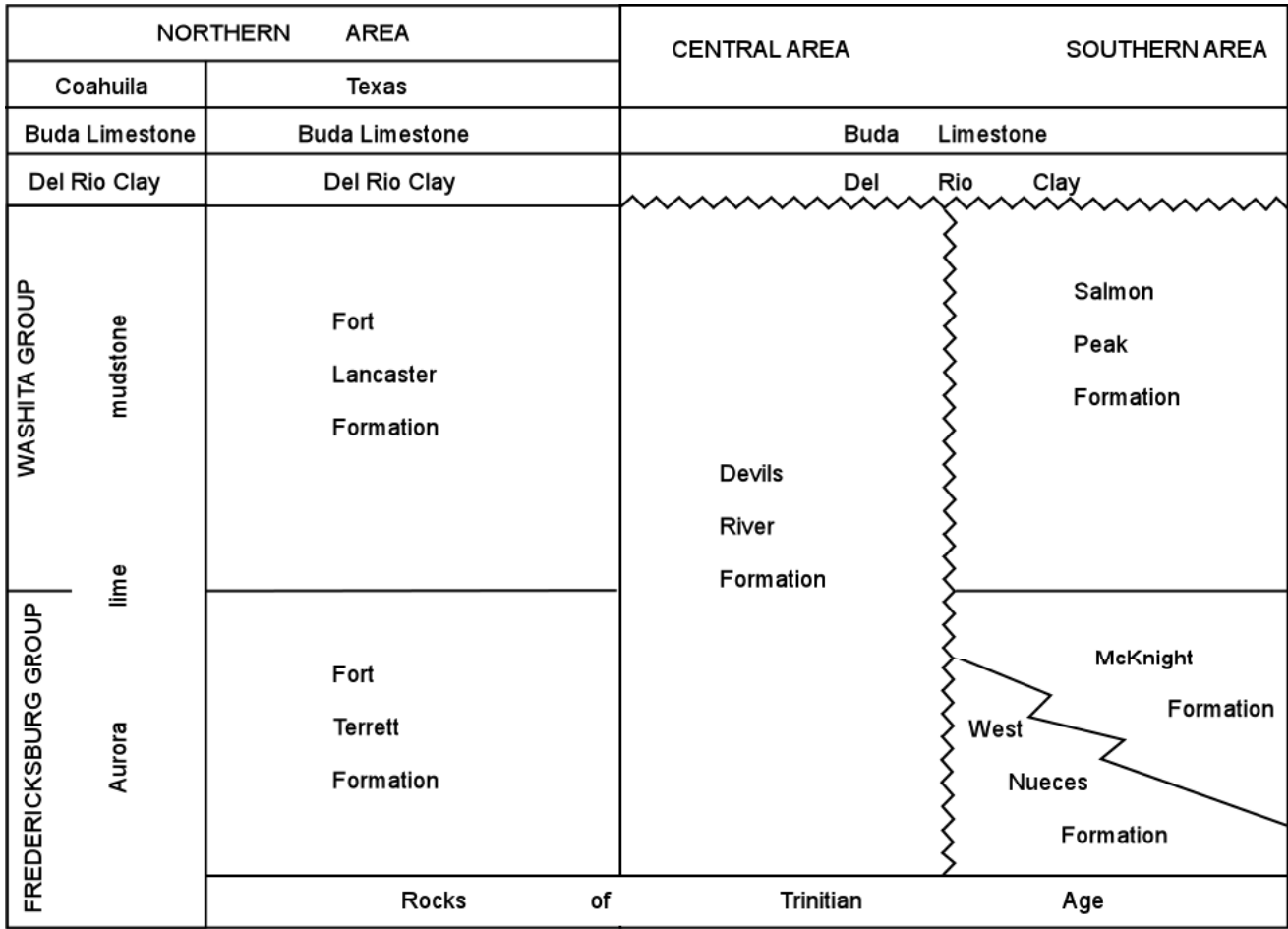


Map modified from Lozo and Smith (1964) and Smith (1970)

**Figure 2.2 Distribution of geologic province areas within the Fredericksburg and Washita groups in Texas and northern Coahuila, Mexico.**

The Upper Washita, represented by the Del Rio and Buda beds, overlies all three regions. In the northern region the Fredericksburg and Lower Washita Groups consist of rocks of the Fort Terrett and Fort Lancaster Formations. The Fort Terrett Formation is at most 100 m thick (Rose, 1972) and is made of limestone with dolomitic and gypsiferous intercalations. The Fort Lancaster Formation is a thick-bedded, rudist-bearing limestone, with a maximum thickness of 120 m (Barker et al., 1994, p. 26).

In the central region the Fort Terrett and Fort Lancaster formations can no longer be distinguished, and they grade into a narrow, oval carbonate bank that is known as the Devils River trend (figure 2.2). The Devils River trend is stratigraphically represented by the Devils River Formation, a 210-m-thick pack of dolostone, fossiliferous limestone, and reef debris (Lozo and Smith, 1964, p. 290-296).



Modified from Smith (1970), figure 15.

**Figure 2.3 East-west stratigraphic section of the Fredericksburg and Washita Groups in northern Coahuila, Mexico.**

The boundary between the central and southern regions coincides with the abrupt facies change from the massive Devils River limestone to rocks of the Maverick Basin (Winter, 1961). The Devils River trend wraps around the Maverick Basin at the west and northwest, and the Stuart City reef bounds the basin to the south. The Fredericksburg and Lower Washita units of the Maverick Basin (Lozo and Smith, 1964) are the West Nueces, McKnight, and Salmon Peak Formations. The West Nueces Formation can reach 80 m in thickness (Miller, 1984, p. 9) and consists of nodular, fossiliferous limestone closely resembling the basal transgressive Fort Terrett and Devils River Formations (Smith,

1979, p. 15). The McKnight Formation incorporates about 90 m of thin-bedded carbonate mudstone, petroliferous shale, and evaporitic deposits (Maclay and Small, 1983, p. 132). The 160 m-thick Salmon Peak Formation (Humphreys, 1984) concludes the Lower Washita succession with a dense, thick-bedded, deep-water mudstone that grades upward into a cross-bedded, fossiliferous grainstone (Smith, 1979, p. 16).

The terrigenous Del Rio Clay blanketed the Salmon Peak, Devils River, and Fort Lancaster Formations in the study area following late Washitan regional uplift. The unit is about 50 m thick near the city of Del Rio, Texas, and thins radially away from Del Rio. The Del Rio Clay consists of interbedded calcareous and siliceous flagstones and marly limestone (Adkins, 1933, p. 388-396). The Buda Limestone is about 30 m-thick in the study region, covers the Del Rio Clay, and is made of micritic limestone with marly interbeds (Rose, 1972).

The Upper Washita strata are overlain in parts of Kinney and Uvalde counties by rocks of the Eagle Ford, Austin, Taylor, and Navarro groups belonging to Gulfian Series. The Eagle Ford – Navarro sequence consists mainly of interbedded shale, siltstone, limestone, chalk, and marl (Bureau of Economic Geology, 1983) and serves locally as the confining unit for the westernmost segment of the Edwards aquifer in the Balcones Fault Zone. The Gulfian rocks are mostly absent in the rest of the area underlain by the Edwards-Trinity aquifer system. However Gulfian rocks with little known hydrologic significance separate the Washita from the overlying Tertiary deposits to the southeast.

The main structural feature in Northern Coahuila was produced during the Laramide Orogeny (late Cretaceous-middle Tertiary time) and consists of an elongated anticline running northwest to southeast, topographically expressed as the mountains of

Serranía del Burro and Lomerio de Peyotes (figures 2.4 and 1.1). This upwarp is folded into several smaller synclines and anticlines with axes paralleling the main structure, namely the Agua Verde Anticline, the Zavala Syncline, the Treviño – Chupadero Anticline, and the Eagle Pass Syncline (figure 2.4). Normal faults trending northwest to southeast and believed to have developed after the folding episodes, are also common in northern Serranía el Burro (Smith, 1970).

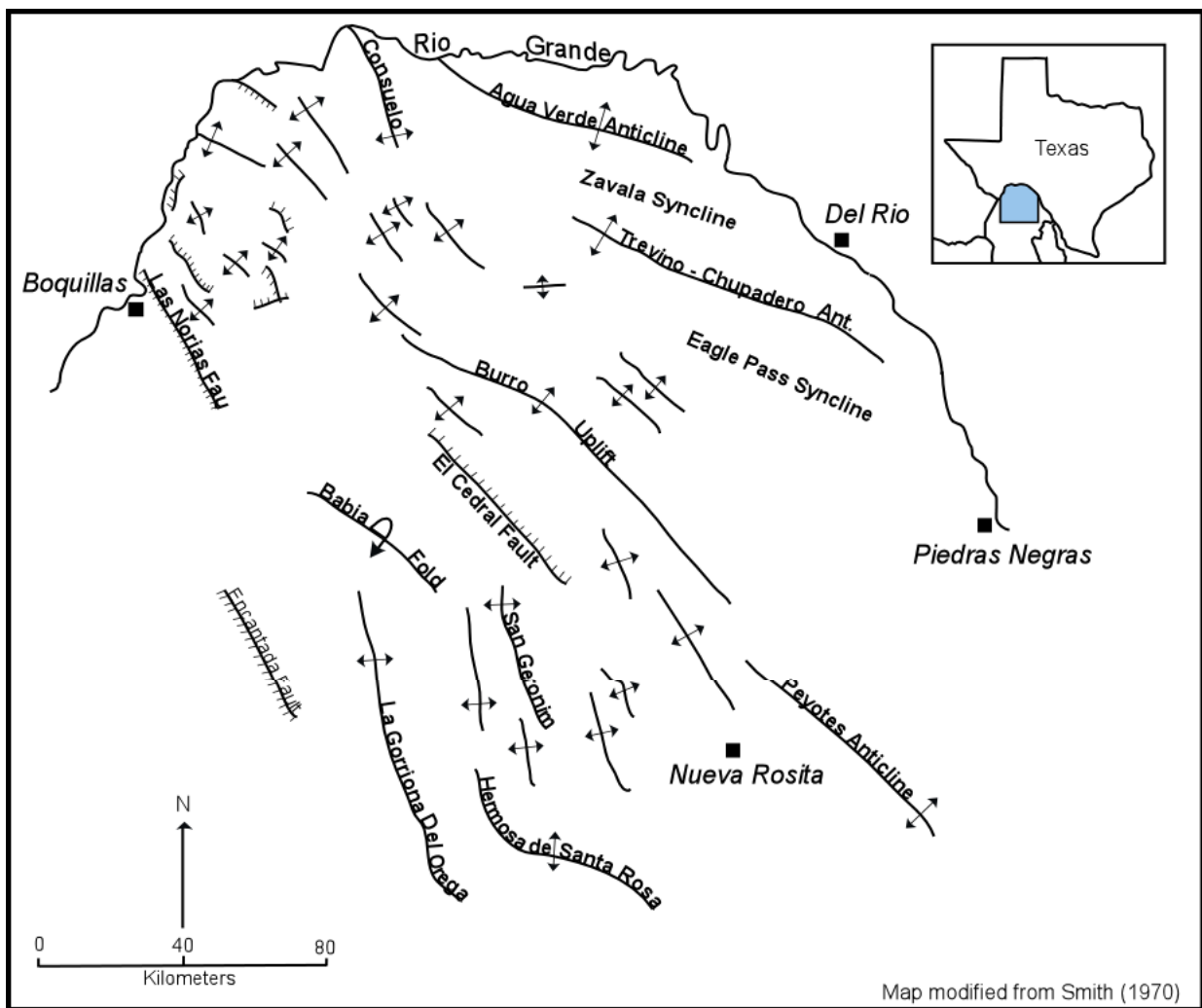


Figure 2.4 Principal structural features of northern Coahuila, Mexico.

Barker and Ardis (1992) have addressed the relationship between the regional structure and the Paleozoic topography and their impact upon the thickness of the Cretaceous strata. According to them, the Paleozoic depositional surface “was considerably flatter than the present-day base” which now shows the combined effects of subsidence, uplift, folding, faulting, and structural collapse caused by mineral dissolution. The configuration of the Edwards-Trinity aquifer bedding is, for the most part, the result of the Cretaceous overburden adjusting to the topography of its Paleozoic base (Barker and Ardis, 1991). The elevation of the Edwards-Trinity aquifer base in the study area ranges from over 1,500 m below sea level in southern Medina County to over 400 m above sea level in northern Val Verde County (Barker, 1996). No pre-Cretaceous structural information was available for the Mexican side of the study area at the time this report was being written. Under Val Verde County the aquifer base is sloping towards the south-southwest at an average rate of 10 m/km, but displays a steeper section (up to 12 m/km) in the northwestern part of the county. Under Edwards and Real counties the Paleozoic base is flatter (8 m/km) and trends toward the south, where it becomes much steeper under southern Uvalde County (61 m/km). This considerable plunge of the base coincides geographically with the western end of the Balcones Fault Zone and was caused by subsidence towards the ancestral Gulf of Mexico and by fault displacements atop the Ouachita structural belt (Flawn et al., 1961).

## **Water-bearing characteristics**

Rocks of the Trinity, Fredericksburg, and Washita groups host the Edwards – Trinity aquifer system, which, in the study area, is composed of two aquifers and the associated confining units. The aquifers are named the Edwards in the Balcones fault zone and the Edwards – Trinity (Plateau) in the Edwards Plateau. The Edwards – Trinity (Plateau) aquifer rocks outcrop over most of the study area, which also includes the western section of the Edwards aquifer in Kinney and Uvalde counties. Due to their hydraulic interconnectedness (Barker et al., 1994, p. 39), these individual aquifers will be discussed together and referred to as the Edwards – Trinity aquifer throughout this report.

The Edwards –Trinity aquifer is predominantly made of limestone and dolomite in its upper part and sand in its lower part. The aquifer includes all the Trinity and Fredericksburg strata, plus all the Washita rocks below the Del Rio Clay or Buda Limestone (where the Del Rio is missing) or land surface.

### **Trinity Group**

The lowermost Edwards-Trinity geohydrologic units belong to the Trinity Group. Throughout the Devils River trend and Maverick Basin, the Trinity Group begins with the Hosston and Sligo Formations, overlain by the Pearsall Formation, Glen Rose Limestone, and the Maxon Sand. To the north and northwest of Del Rio and outside the Maverick Basin, the Sligo and Glen Rose pinch out and the entire Trinity Group is referred to as the Basal Cretaceous Sands (Reeves and Small, 1973). Few water wells are deep enough to penetrate Trinity rocks in the study area, therefore the transmissive properties of these strata remain largely unknown.



In Val Verde County, the Hosston and Sligo formations are thin and contain small quantities of saline water whereas the Glen Rose Limestone yields very small to moderate amounts of brackish water (Reeves and Small, 1973). The Hosston and Sligo formations under Kinney County are not tapped by water wells: “They [Hosston and Sligo formations] probably contain water, but the quality is unknown” (Bennett and Sayre (1962). In Kinney County, neither the Pearsall formation nor the Glen Rose, are known to yield water to wells (TWDB groundwater database, 2001). Bennett and Sayre (1962) estimated that the Glen Rose Limestone might contain small amounts of moderately to highly saline (TDS > 3,000 mg/l) water. In Edwards County, the Basal Cretaceous Sands are water bearing and yield brackish groundwater (TDS > 1,000 mg/l) to four wells. The Hosston and Sligo formations in Uvalde County were encountered in several deep wells. The TWDB groundwater database lists only one Uvalde County well producing 1,000 mg/l TDS groundwater from the Hosston formation. The Upper Member of the Glen Rose limestone is generally interpreted to be a confining unit (Clark and Small, 1997). Several Uvalde County wells screened in the Glen Rose evaporitic sections are known to yield saline (TDS > 1,000 mg/l) groundwater to wells.

The La Mula and Cupido formations are the Mexican equivalents for the Hosston and Sligo of Texas. Leal (1992) classifies the La Mula – Cupido as an aquifer although its importance seems to be restricted to the area south of Serranía del Burro. Leal (1992) indicates that the La Mula – Cupido aquifer may be in hydraulic communication with the hydrostratigraphic units above due to profound fractures and faults (Leal, 1992, p. 20). Separated from the La Mula – Cupido aquifer by the La Peña aquitard, and overlain by the Telephone Canyon formation lies the Glen Rose aquifer. Glen Rose wells drilled in

the Burro and Peyotes anticlines encountered fresh (TDS < 1,000 mg/l) groundwater. Five regionally important springs (Zaragoza, Morelos, Nava, Allende, and Villa Union) located outside the Glen Rose subcrop area are interpreted as manifestations of Glen Rose aquifer discharge (Leal, 1992).

### **Fredericksburg and Lower Washita groups**

The Fredericksburg and lower Washita rocks are the primary water-producing strata in the study area. They consist of rocks of the Devils River Formation and of rocks of the Maverick basin (the Salmon Peak and McKnight formations).

The Devils River Formation is “one of the most porous and permeable” formations in the study area and displays extensive karst development (Clark and Small, 1997, p. 4). The Devils River is a prolific fresh water aquifer in central Val Verde and parts of Kinney and Uvalde counties.

Rocks of the Maverick Basin (the Salmon Peak and McKnight formations) underlie most of Kinney, southern Val Verde, and southeast Uvalde counties. The upper Salmon Peak Formation is permeable and porous and yields fresh to saline groundwater to wells. The lower Salmon Peak formation has low permeability and porosity, but can produce groundwater from fractured intervals (Barker et al., 1994). Both units can develop minor karst. The McKnight Formation generally displays low permeability and porosity and is classified as a confining unit in the study area (Clark and Small, 1997). Brecciated sections in the lower McKnight Formation are the result of gypsum, anhydrite, and halite dissolution and subsequent collapse. Such intervals can produce moderate amounts of groundwater rich in sulfate and chloride. The West Nueces Formation yields

groundwater to wells primarily from its “moderately permeable” upper part, whereas the lower members are “almost impermeable” (Barker et al., 1994) and do not transmit groundwater. In Northern Coahuila, the West Nueces, McKnight, and Salmon Peak formations crop out extensively throughout the Serranía del Burro where they are the main water-bearing units. Batzner (1976) investigated the chemical character of shallow groundwater and springs in the Peyotes area (figure 1.1), and concluded that the Fredericksburg strata in the El Burro area and Lomerio Peyotes are hydraulically connected.

Outside the Maverick Basin and to the north of the Devils River trend lie the Fort Terrett (of the Fredericksburg Group) and Fort Lancaster formations, the latter comprising the lower Washita Group. The Fort Lancaster Formation thickens southward from the Edwards Plateau, and can become water-saturated in north-central Val Verde County. Fort Terrett’s “burrowed zone” and the brecciated “Kirschberg evaporite zone” are highly permeable and the most important water-bearing units in the Edwards Plateau (Barker et al., 1994).

### **Aquifer properties**

Few aquifer test data are available for the Texas side of the study area, while no such information could be located for Mexico. However, specific capacity data for 119 wells mostly in Uvalde and Val Verde counties were available in the TWDB groundwater database. They were compiled and aquifer transmissivity estimates were computed using an automated algorithm developed by Mace (2001). In the absence of aquifer test data,

well yields were used as proxy for transmissivity and hydraulic conductivity on the Mexican side of the study area.

The specific capacity of a well is the ratio of the pumping rate to the total drawdown and is often used as an indicator of well productivity. Mace (2001) related transmissivity values to specific capacity data by using the analytical solution to the nonequilibrium equation (Theis, 1963) in an iterative fashion. An important assumption Mace has made is that the well loss is zero. The well loss is that part of the observed drawdown in a well resulting from the turbulent flow of water in the immediate vicinity of the well through the well screens in the casing. In reality, well losses are always involved in the measured specific capacity, which means that the transmissivities so calculated are underestimated (Domenico and Schwartz, 1990, p. 169).

Histograms show transmissivity ( $T$ , figure 2.5) and hydraulic conductivity ( $K$ , figure 2.6) for two subareas: the Edwards Plateau and the Balcones Fault Zone. The Edwards Plateau subarea encompasses parts of Val Verde, Edwards, Kinney and Uvalde counties commonly associated with the Edwards-Trinity (Plateau) aquifer. The Balcones Fault Zone includes portions of Kinney and Uvalde counties east of the Brackettville groundwater divide. Transmissivity and hydraulic conductivity each span several orders of magnitude, which is typical for carbonate rocks in karstic terranes.

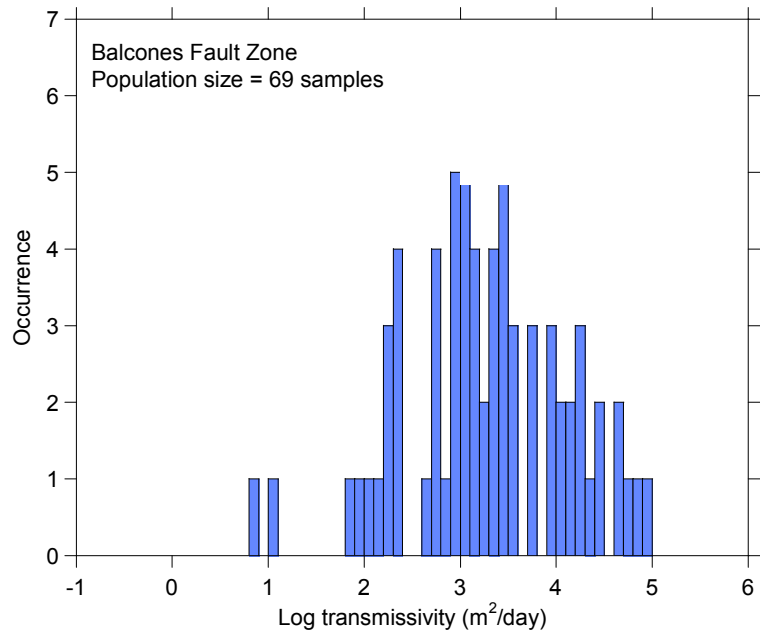
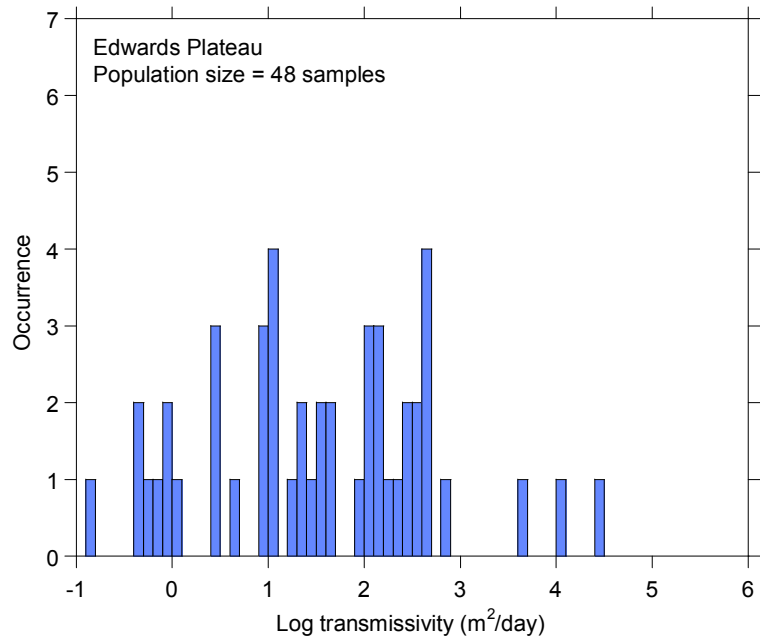


**Figure 2.5 Histograms of transmissivity for the Edwards-Trinity aquifer in Texas (data from Texas Water Development Board's groundwater database).**

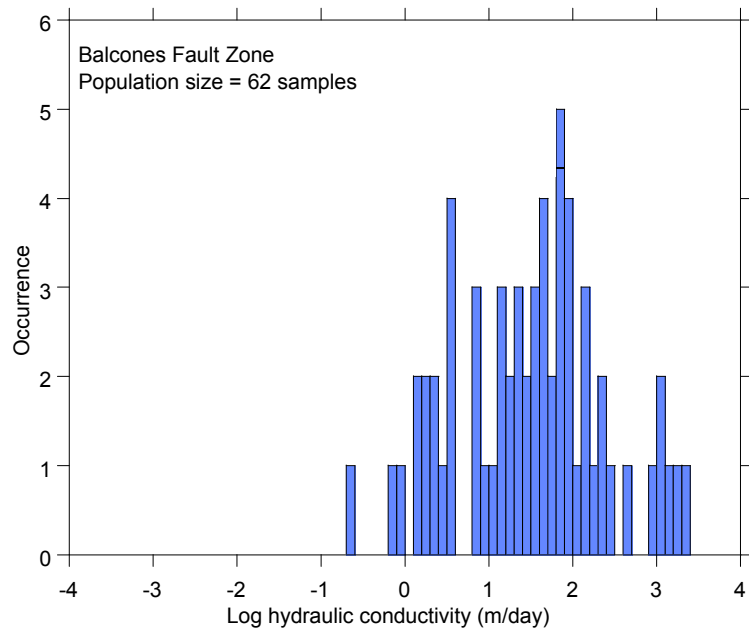
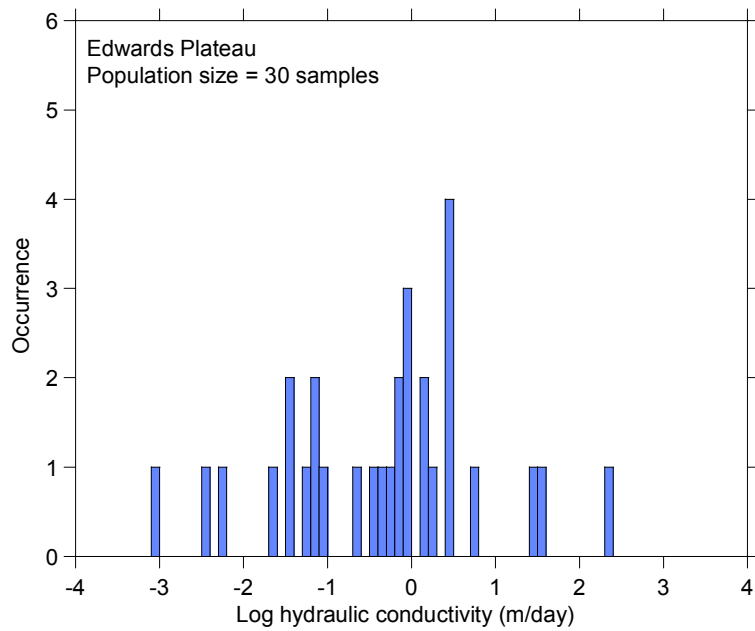


**Figure 2.6 Histograms of hydraulic conductivity for the Edwards-Trinity aquifer in Texas (data from Texas Water Development Board's groundwater database).**

In the Edwards Plateau transmissivity ranges from 0.15 to 25,100 m<sup>2</sup>/day, and hydraulic conductivity ranges from 0.0009 to 221 m/day, with median values of 38 m<sup>2</sup>/day and 0.7 m/day, respectively. The distributions of these parameters are uneven and suggest heterogeneity induced by multiple sample populations. Parameter distribution may illustrate distinct but overlapping populations controlled by both matrix and fracture permeability, but could also be due to insufficient number of samples.

In the Balcones Fault Zone transmissivity ranges from 7 to 97,300 m<sup>2</sup>/day, and hydraulic conductivity ranges from 0.2 to 2,400 m/day, with median values of 1,935 m<sup>2</sup>/day and 36 m/day, respectively. Parameter distributions (see figures 2.5 and 2.6) are closer to lognormal. The more even histogram grouping could be indicative of a single predominant control over aquifer permeability structure, possibly the effect of fractures.

### **Areal distribution of transmissivity and well yields**

The areal distribution of transmissivity on the Texas side and the available well yields on the Mexican side are shown on figure 2.7. Most of the wells in the study area have transmissivities of up to 20,000 m<sup>2</sup>/day. Transmissivity values of up to 90,000 m<sup>2</sup>/day were calculated in parts of Uvalde County. These values are in agreement with the transmissivity estimates used by Kuniansky and Holligan (1994, p. 27) in their numerical groundwater flow model for the Edwards-Trinity aquifer system.

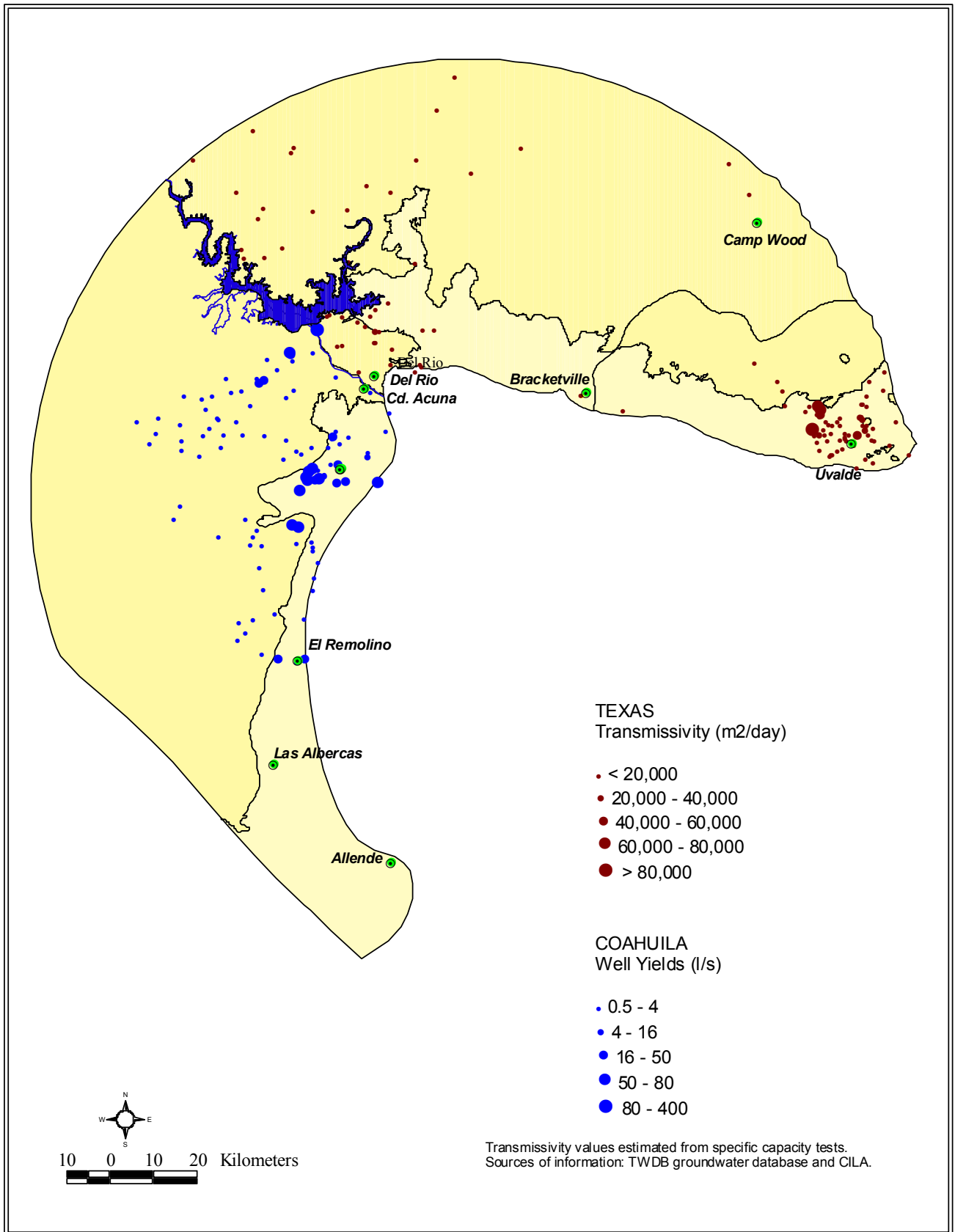


**Figure 2.7 Map showing areal distribution of transmissivity and well yields in the Edwards-Trinity aquifer.**



In Val Verde, Edwards, and northern Kinney counties Kuniatsky and Holligan (1994) estimated transmissivities ranging from 465 to 10,000 m<sup>2</sup>/day in the Edwards Plateau and from 9,300 to 45,000 m<sup>2</sup>/day around Del Rio and in east of the Bracketville divide. The same authors estimated transmissivities ranging from 46,500 m<sup>2</sup>/day to 460,000 m<sup>2</sup>/day in southeast Uvalde County.

Well yields in the Coahuila part of the Edwards-Trinity aquifer vary greatly. Most of the area wells with available yield data produce water from the Cretaceous bedrock. Well yields of 0.5 to 16 l/s are reported in the Serranía del Burro and on mountain flanks where the aquifer is predominantly unconfined (INEGI, 1979). Well yields increase in the confined area of the aquifer where 20 to 400 l/s are reported south of Ciudad Acuña and near Amistad Reservoir (INEGI, 1979).

### **Potentiometric surface and water levels**

Water-level data from 136 wells in Texas and Coahuila were collected between January 1980 and December 1981. Figure 2.8 shows the potentiometric surface of the Edwards-Trinity aquifer built using those data.

The 1980-81 potentiometric surface slopes towards the Rio Grande with hydraulic gradients of 0.016 in the uplands of Serranía del Burro and 0.006 along the Edwards Plateau escarpment between Red Bluff and Sycamore Creeks. The hydraulic gradient is very flat (~0.0001) immediately south of Amistad Reservoir and in Val Verde County west of Devils River and becomes steeper (0.003) in the Del Rio – Ciudad Acuña area. Hydraulic heads in excess of 715 m in the Burro area and 540 m in the Edwards Plateau, define areas of groundwater recharge.

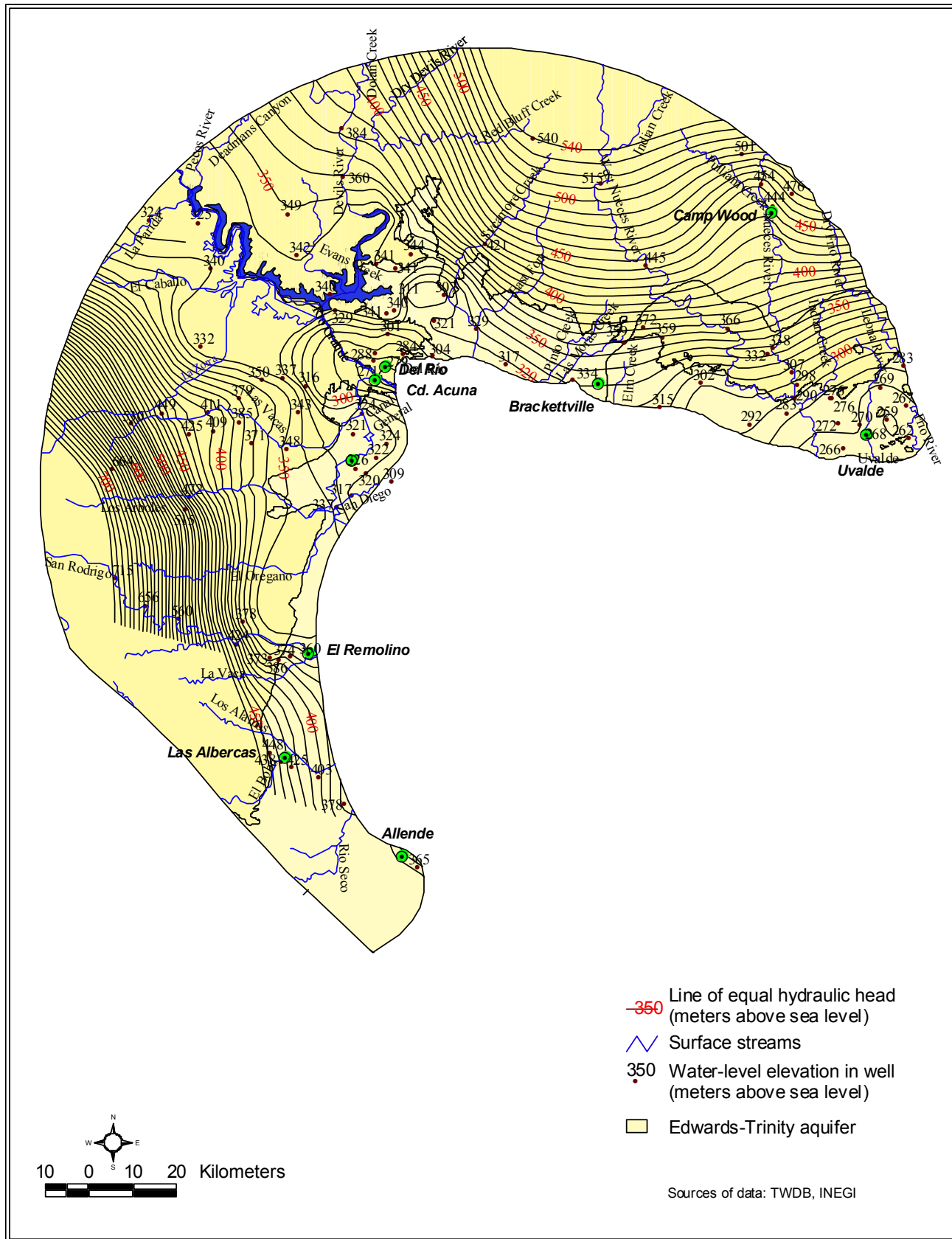


Figure 2.8 Potentiometric surface map for the Edwards-Trinity aquifer (data for 1980-1981).

The flat hydraulic gradient near Amistad Reservoir and northeast of Uvalde suggests that the aquifer there is very transmissive and large amounts of groundwater may flow through it. Groundwater moves generally from the highlands in Coahuila and Texas towards Amistad Reservoir or Rio Grande where hydraulic heads range from 270 m to 340 m above sea level. Surface drainage variations, as well as groundwater pumping, can modify the regional potentiometric pattern. Gaining stream conditions in rivers such as Devils, Sycamore, and Nueces in Texas, and Arroyo Las Vacas, Río San Diego, Río San Rodrigo, and Río Escondido in Coahuila cause the contour lines in figure 2.8 to flex upstream along the river channel. A mild pumping cone of depression has reversed the hydraulic gradient northeast of Uvalde.

In the absence of recent water-level measurements in Coahuila, water-level data collected by TWDB from December 1999 through March 2000 from 37 wells were used to generate an updated potentiometric map for the Texas side of the study area only (figure 2.9). A comparison between the 2000 and the 1981 map shows only minor changes in the potentiometric surface configuration. Groundwater in the aquifer moves toward the Rio Grande and Amistad Reservoir and displays slight perturbations along rivers reaches and near pumpage centers. Devils, Nueces, and West Nueces rivers are being fed by Edwards-Trinity groundwater, and a very mild cone of depression is still noticeable near Uvalde, Texas.

In 1980, the depth to groundwater in study area wells varied between 1.9 m and 112 m with an average of 25.8 m (figure 2.10). Depths to water of less than 15 m were measured in wells in the low-lying areas around Del Rio and Ciudad Acuña along river courses and creeks in the Lomerio Peyotes area and north and west of Uvalde.

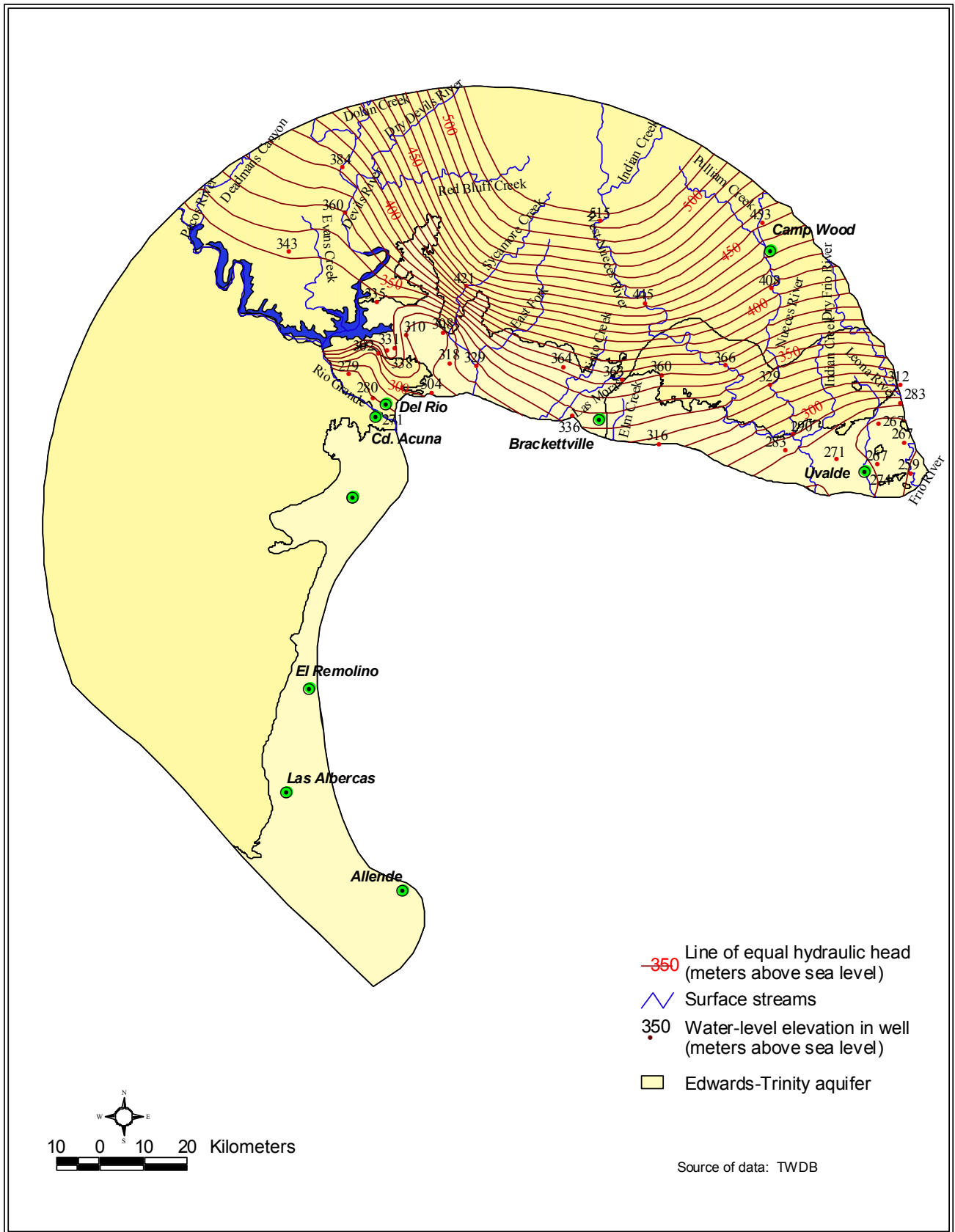


Figure 2.9 Potentiometric surface map for the Edwards-Trinity aquifer in Texas. Hydraulic head data gathered during 2000.

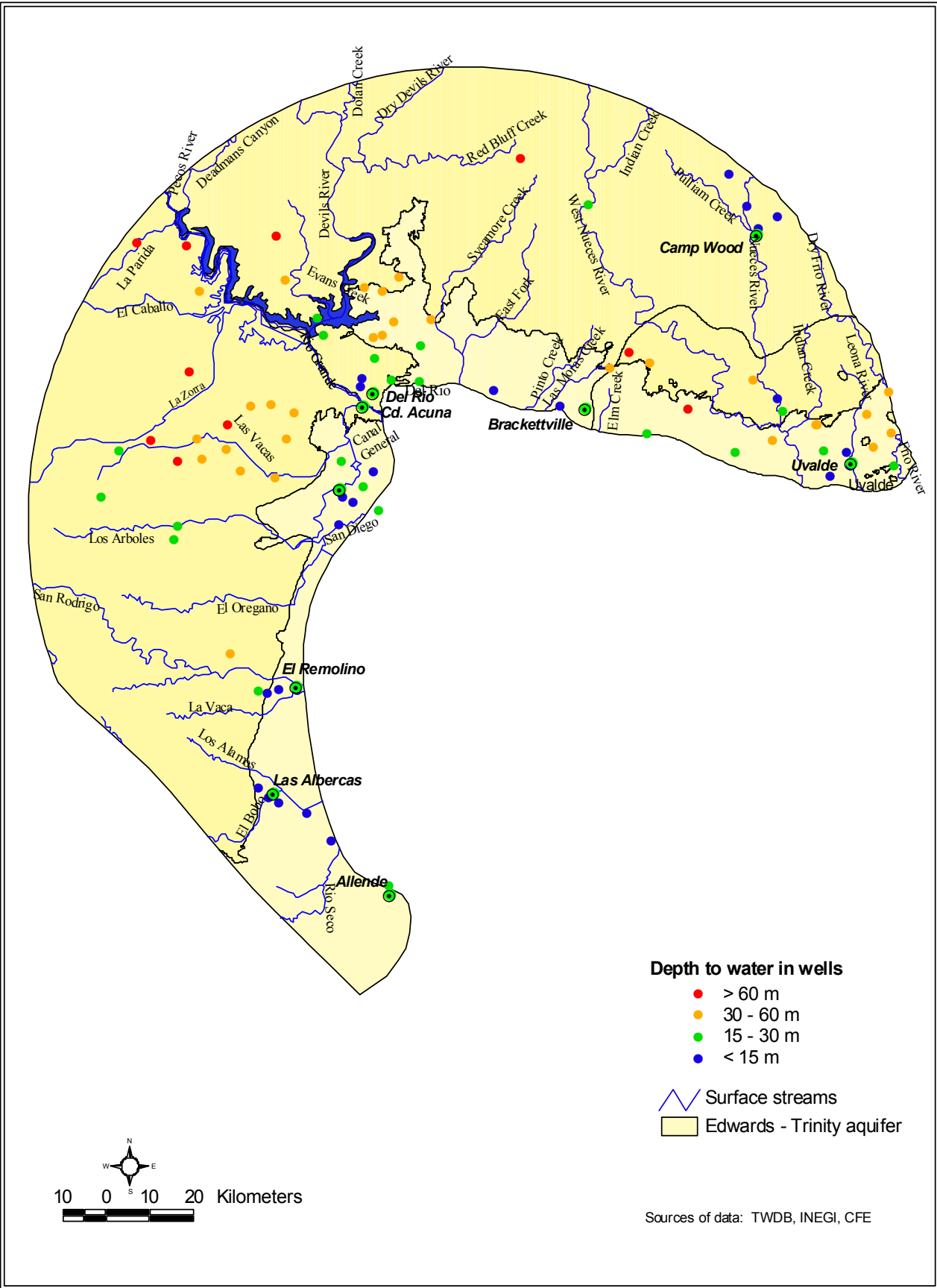


Figure 2.10 Depth to water in Edwards-Trinity aquifer wells, 1980-1981.

Deeper water levels of up to 112 m were generally encountered in the Edwards Plateau of Texas and Serranía del Burro in Coahuila. Because well depth and completion information are unavailable for Mexico, it can not be verified at this time whether the shallow water levels measured in Lomerio Peyotes are representative of Edwards-Trinity aquifer conditions or not. In this area where the aquifer is confined, the Fredericksburg strata being overlain by rocks of the Eagle Ford Group (Gulf Series), which is known to yield moderate quantities of water to wells in Kinney County, Texas. However, Batzner (1976) concluded, based on structural and geochemical evidence, that Edwards – Trinity groundwater from the Burro region moves through the subsurface towards Lomerio Peyotes where it upwells into the overlying strata.

A plot of depth to groundwater in these wells versus their corresponding land surface elevation (figure 2.11) shows two distinct trends. In some of the wells, the depth to groundwater increases abruptly with land surface elevation, a situation characteristic of confined aquifers. The second trend is illustrated by wells with depths to water that closely follow the local topography, a situation commonly associated with unconfined aquifer conditions.

Time series hydrographs of selected Texas wells (figure 2.12) illustrate long-term temporal water-level fluctuations and, generally, explain changes in the potentiometric surface map. Water-level fluctuations are caused by changes in aquifer storage, which is a function of recharge and discharge. If groundwater use exceeds recharge, then the excess demand would be satisfied at the expense of aquifer storage. This causes water levels to decline. Conversely, a reduction in groundwater use and/or an increase in

aquifer recharge would help replenish the storage and water levels would rise accordingly.

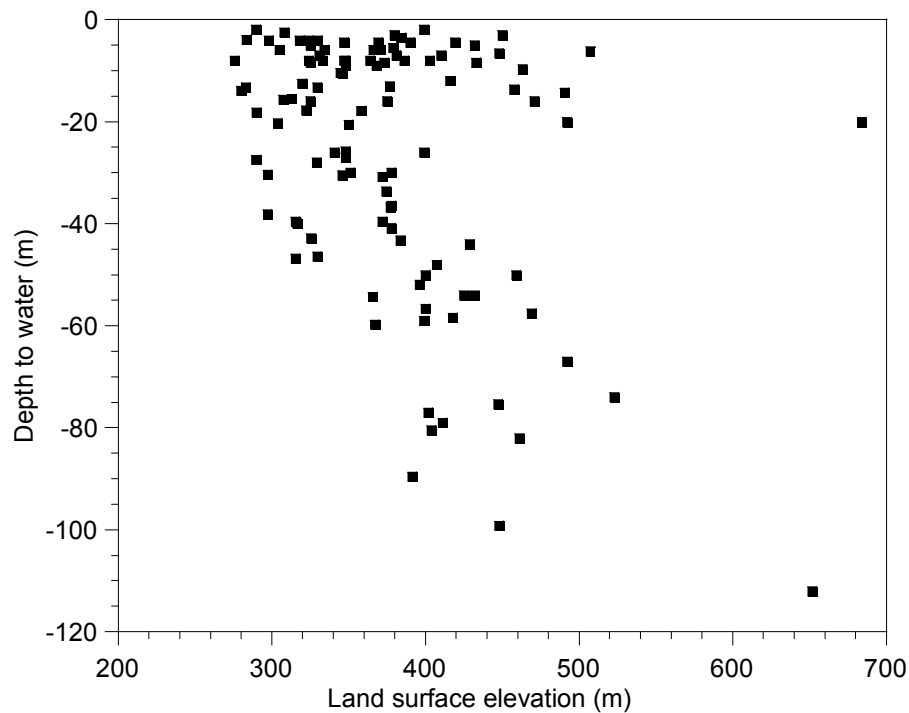


**Figure 2.11 Relationship between land surface elevations and water levels in the Edwards-Trinity aquifer (data from Texas Water Development Board and Instituto Nacional de Estadística, Geografía e Informática).**

Several wells located immediately adjacent to Amistad Reservoir exhibited pronounced increases in water levels soon after the lake was emplaced in 1968. Net water-level changes of up to 80 m have been measured in wells 70-25-603, 71-23-901, 71-32-401, and 71-40-201 in Val Verde County, Texas, and it took approximately seven years for the groundwater levels to stabilize (see figure 2.12). The effects of this enormous increase in aquifer storage extended some 15 km to the southeast (all the way to Del Rio) and as far 40 km north of the reservoir (Armstrong, 1995, p. 48).

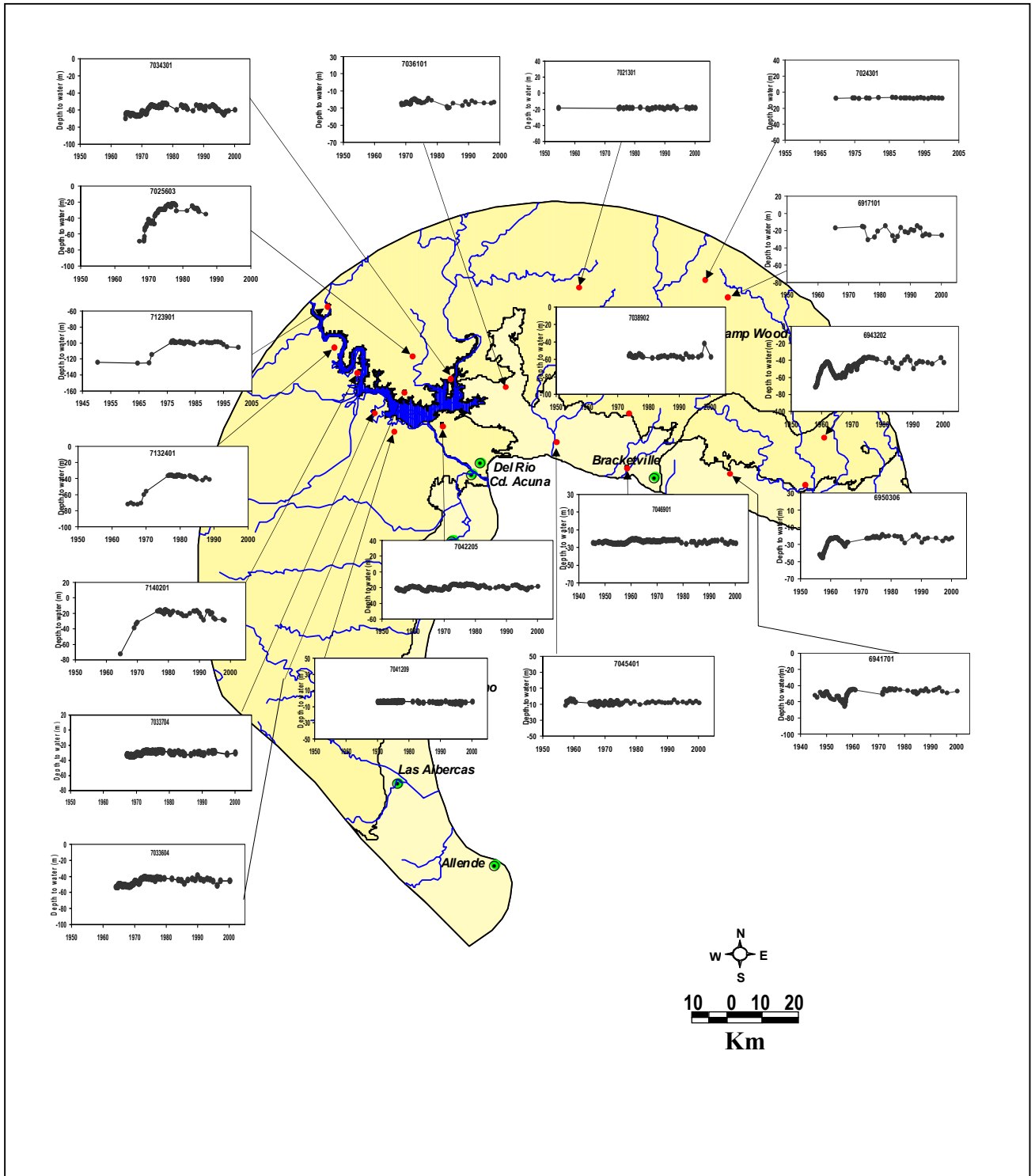


Figure 2.12 Well hydrographs for the Edwards-Trinity aquifer (data from Texas Water Development Board's groundwater database).



Since the completion of the reservoir, baseflow from streams and creeks in both Texas and Chihuahua have increased by more than 77 percent for treaty streams and 228 percent for non-treaty streams, and a large number of springs that formerly flowed into the reservoir area were inundated (IBWC, 1990).

Hydrographs for selected wells in the Edwards Plateau between Del Rio and Uvalde are characteristic of areas with little or no groundwater development, as denoted by rather stable water levels over time with only minor seasonal variations. Fluctuations in aquifer storage in this region are explained by the interplay of cyclical precipitation patterns and well withdrawals (Barker et al., 1994). In contrast, water levels in wells 69-41-701, 69-50-306, and 69-43-202, all in Uvalde County, have fluctuated as much as 40 m from the mid 1950s through the mid-1960s and 20 m since the mid-1980s while being on a slightly ascending trend (figure 2.12). The fluctuations were the combined effect of wide variations in aquifer recharge from rainfall and in water use patterns (see the hydrograph for the monitor well 69-41-701 in figure 2.12). Irrigation pumping in Uvalde County increased gradually from 1925 to 1947 and developed very rapidly afterwards. In 1956 about 100 wells pumped 70.28 hm<sup>3</sup> of Edwards groundwater to irrigate approximately 3,250 ha (Welder and Reeves, 1962). The downward trend in pre-1957 water levels was exacerbated by the widespread drought of the 1950s and by the concurrent excess demand for groundwater. The drought was broken in 1957 when record rainfall of 160 percent of normal for the area helped recharge the aquifer and diminish the stress on groundwater resources. Water levels rose rapidly, only to decline again in the early to mid-1960s in response to diminished rainfall and increasing groundwater use (52.89 hm<sup>3</sup> pumped county-wide in 1964). The wet 1970s brought

about a sustained water-level recovery, while the dry mid-1980s saw the aquifer storage being depleted to the 1970 level. The last decade has been, on average, normal with regard to precipitation in Uvalde County. This, and local efforts to conserve groundwater, have led to somewhat stable water levels in wells during the 1990s.

### **Recoverable groundwater resources**

Several studies have been conducted in Texas to estimate the amount of recoverable fresh (TDS < 1,000 mg/l) water in the Edwards – Trinity aquifer in the study area. Calculations require an estimate of the volume of water-saturated rock and an estimate of the storativity of the aquifer, which can vary from  $10^{-7}$  for confined aquifers to 0.4 for unconfined aquifers (Domenico and Schwartz, 1990). The storativity under unconfined conditions is also referred to as specific yield. Recoverable resources are computed by multiplying the storativity by the volume of fresh groundwater held in the aquifer.

The volumes of groundwater available in the year 2000 from the Edwards-Trinity aquifer for the Texas side of the study area were determined using ArcView<sup>®</sup> GIS map algebra techniques. First, the volume of the saturated portion of the aquifer (rock and water) was computed by multiplying the surface area of the study region by the saturated thickness of the aquifer. The saturated thickness was calculated by subtracting the elevation of the aquifer bottom (Barker and Ardis, 1992) from the water-level elevations in wells as measured during year 2000. To account for the less productive Trinity strata, a storativity of 0.015 and a 25 percent recoverable yield were applied to the total saturated volume to arrive at a total of 11,231 hm<sup>3</sup> estimated recoverable groundwater

reserves. Recoverable groundwater values are approximate due to uncertainty in estimates of aquifer saturated thickness and spatial variability of specific yield. Due to the paucity of geologic and aquifer properties data in Mexico, no attempt has been made to estimate recoverable groundwater resources within Coahuila.

### **Recharge areas**

Mechanisms of recharge to the Edwards-Trinity aquifer system in the Edwards Plateau are different from those active in the Balcones Fault Zone. In the Edwards Plateau, recharge is mostly by direct infiltration of precipitation and streamflow on the outcrops of Trinity, Fredericksburg and lower Washita strata. During rainfall events, the soil moisture is replenished first, and, after field capacity has been attained, the additional water percolates downward through solution openings, joints, and fractures in the underlying strata and to the water table. A small amount of recharge may occur along faults and fractures and by cross-formational flow through semi-confining beds.

Solution-widened fractures and sinkholes facilitate the recharge to the Edwards Plateau section of the aquifer in Texas. These solution features are particularly abundant on the steeper slopes and in the beds of streams on the southern edge of the Edwards Plateau, but tend to be less common elsewhere. The Edwards-Trinity aquifer in Val Verde, Edwards, and Kinney counties has a recharge area approximately 16,800 km<sup>2</sup> in size. It extends from Lozier Canyon in Terrell County north to Sheffield in Pecos County, east – northeast from Sheffield to Eldorado in Schleicher County, southeast from Eldorado to Bracketville in Kinney County, and west to Del Rio (Reeves and Small, 1973, p. 28).

In the Balcones Fault Zone, the aquifer is recharged by the perennial streams crossing highly permeable rocks of the Devils River Formation; by direct infiltration of precipitation on the aquifer outcrop; and by cross-formational flow from the adjacent Trinity aquifer (Barker et al., 1994).

Various researchers have estimated the amount of recharge to the Edwards-Trinity aquifer in the study area based on streamflow measurements and base-flow separation techniques, and expressed it as fraction of annual rainfall reaching the aquifer. The long-term recharge rates for Real, Kinney, and Edwards counties are 50.8 mm/year (Long, 1958, p. 21), 35.6 mm (Bennett and Sayre, 1962, p. 76), and 33.02 mm/year (Long, 1963, p. J24) respectively. Reeves and Small (1973) calculated the yearly recharge rate in Val Verde County to be approximately 38.1 mm. In the development of their groundwater flow model, Kuniansky and Holligan (1994, p. 29) estimated recharge rates for the year 1974 ranging from 6.32 mm in Val Verde and western Kinney and Edwards counties to over 100 mm in portions of Uvalde County.

During January 2002, the author collected six groundwater samples from wells and springs in Val Verde, Edwards, and Kinney counties and had them analyzed for stable and radiogenic isotopes. Deuterium ( $\delta^2\text{H}$ ) and Oxygen-18 ( $\delta^{18}\text{O}$ ) are stable isotopes used to investigate the provenance of groundwater, and tritium ( $^3\text{H}$ ) and Carbon-14 ( $^{14}\text{C}$ ) are radioisotopes used to determine the age of the water. The results are shown in table 2.2.

State Well Number	$\delta^2\text{H}$ (‰) SMOW	$\delta^{18}\text{O}$ (‰) SMOW	Apparent $^{14}\text{C}$ Age <sup>1</sup>	pmC <sup>2</sup>	$\delta^{13}\text{C}$ (‰)	Tritium (TU) <sup>3</sup>
50-44-801	-33.5	-5.1	2870±40	0.6990	-10.6	1.14
70-41-301	-33.5	-5.3	2400±40	0.7410	-11.8	1.85
71-15-401	-37.5	-5.95	8130±40	0.3630	-9.6	0.79
70-45-505	-32.5	-4.9	4030±40	0.6050	-10.3	2.01
55-63-702	-36.0	-5.3	5960±40	0.4760	-8.4	0.98
70-29-101	-33.5	-5.1	2650±50	0.7190	-11.1	2.64

<sup>1</sup>Reported as radiocarbon years before present ("present" = 1950 A.D.)

<sup>2</sup>Percent modern carbon; <sup>3</sup>Tritium Units

**Table 2.2 Isotope composition in Edwards-Trinity groundwater samples, Val Verde, Edwards, and Kinney counties**

A graph of  $\delta^2\text{H}$  and  $\delta^{18}\text{O}$  (figure 2.13) shows the samples plotting on or slightly below the Global Meteoric Water Line (GMWL) (Craig, 1961). The proximity of the data points to GMWL indicates that the groundwaters originated as precipitation and also that  $\delta^2\text{H}$  and  $\delta^{18}\text{O}$  values have not been altered significantly by water-rock interaction (Banner and Hanson, 1990).

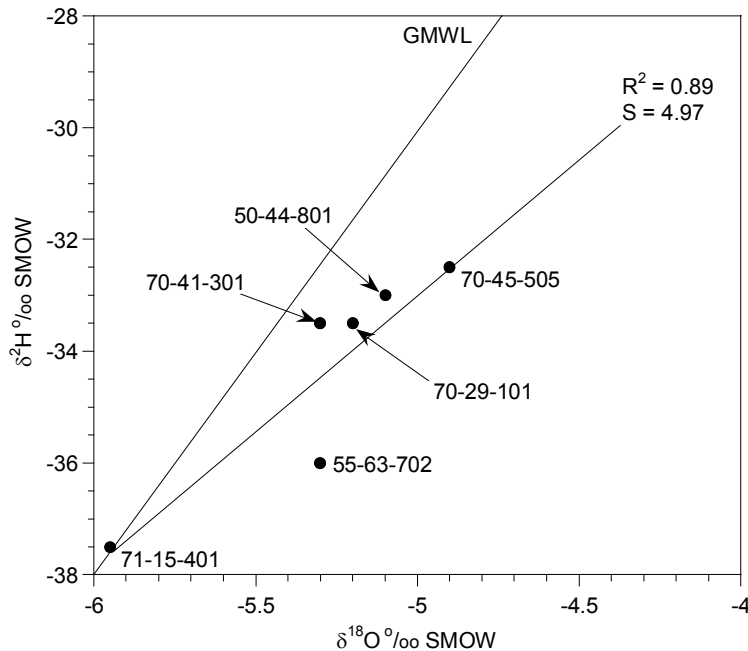


**Figure 2.13 Plot of  $\delta^2\text{H}$  versus  $\delta^{18}\text{O}$  values for Edwards-Trinity aquifer. Data plot along an evaporation line, indicating evaporative enrichment of water prior to recharge. Source of data: Texas Water Development Board's groundwater database.**

The data describe a trendline with a slope of almost 5, which is typical of evaporative isotope enrichment (Clark and Fritz, 1997, p. 86). This suggests that the Edwards-Trinity aquifer is dominated by recharge from summer rains - characterized by larger isotope fractionation effects-as opposed to winter rains which, in arid climates, tend to plot closer to the global line (Clark, 1987). Water can be lost by evaporation from surface waters during runoff prior to infiltration, during infiltration through the unsaturated zone, or from the water table-if it is shallow enough. The trendline slope being close to 5 suggests that the former may be the predominant evaporation mechanism (Clark and Fritz, 1997).

Tritium concentrations greater than 0.8 TU, coupled with radiocarbon activities ranging from 36 to 74 pmC, indicate that the samples represent a mixture between submodern (recharged prior to 1952) and recently recharged groundwaters. Tritium and radiocarbon in groundwater vary in a non-uniform fashion along flowpaths in the aquifer (figure 2.14). The existence of preferential flow conduits permitting fast, focused recharge to the water table with limited mixing taking place, could explain this behavior. Recharge to the Coahuila part of the Edwards-Trinity aquifer occurs both inside and outside the study area by infiltration of rainwater on the outcrops of Trinity, Fredericksburg, and lower Washita strata and by seepage along various streambeds. The recharge zone of the Trinity portion of the aquifer corresponds with the extensive Glen Rose outcrops throughout Serranía del Burro arroyos and canyons incised in the mountain.

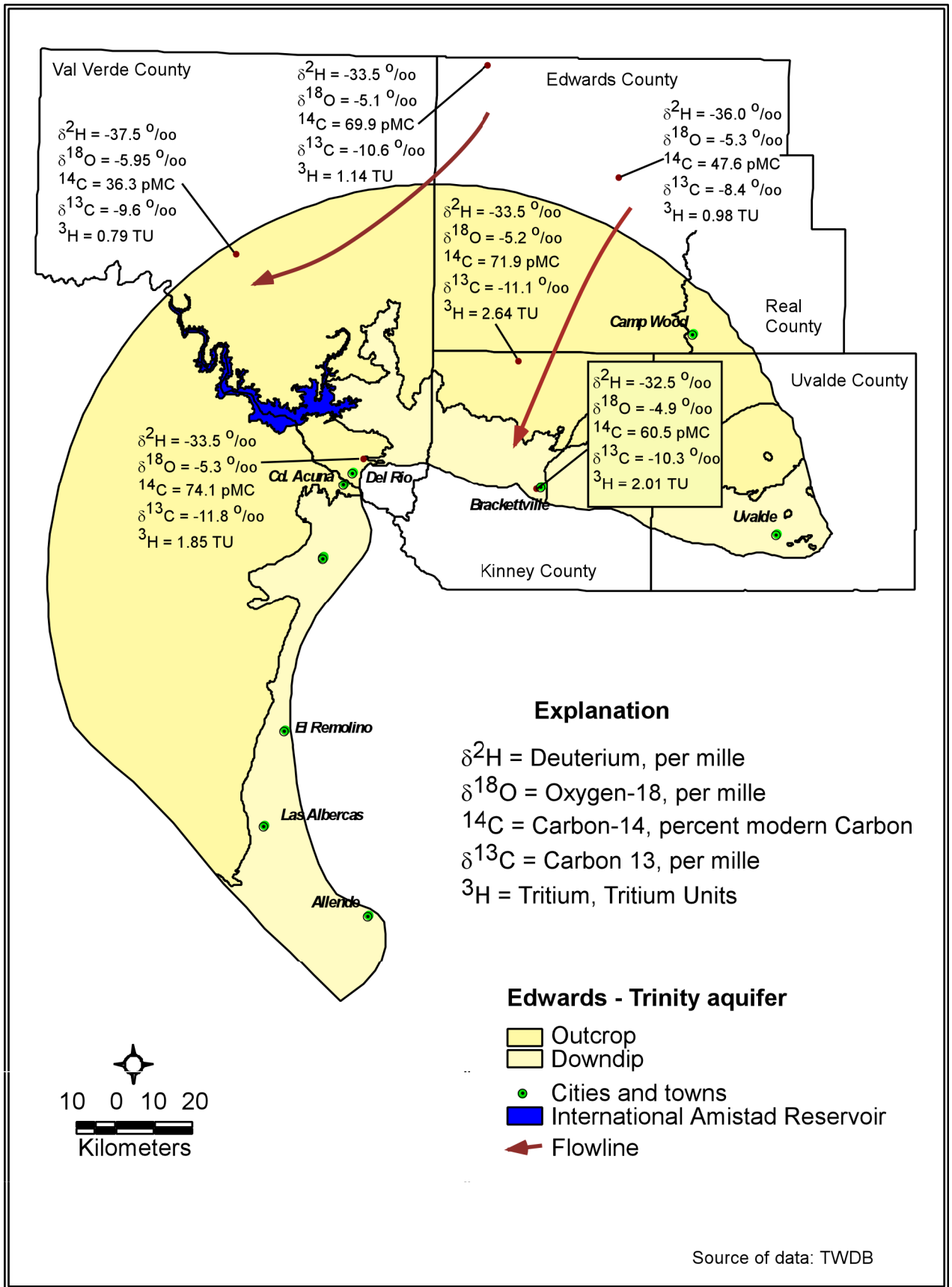
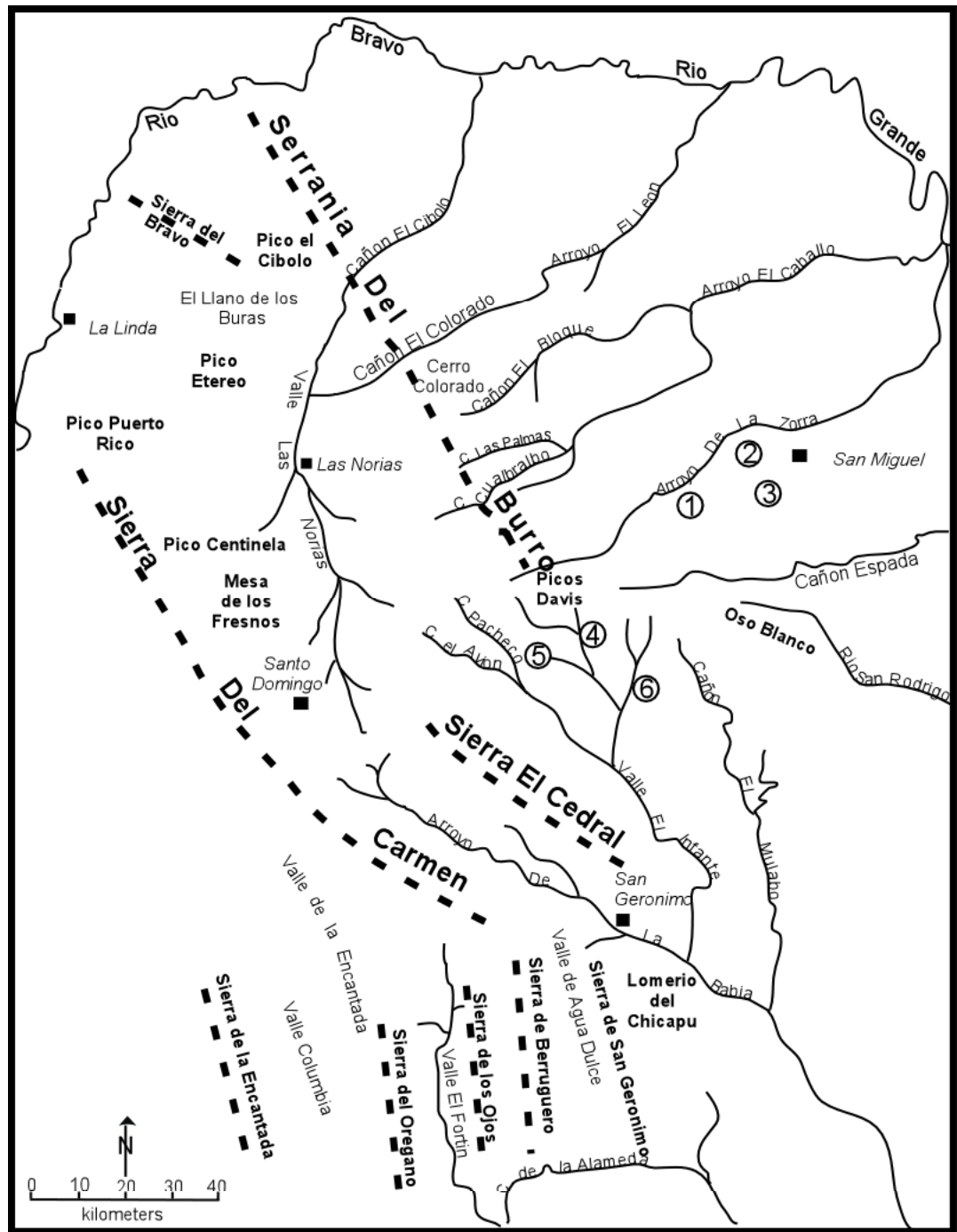


Figure 2.14 Areal distribution of  $\delta^2\text{H}$ ,  $\delta^{18}\text{O}$ ,  $^{14}\text{C}$ ,  $\delta^{13}\text{C}$ , and  $^3\text{H}$  in Edwards-Trinity aquifer groundwater.

The most important are Cañon de la Espada, Arroyo de la Zorra, Cerro el Palomo, Cerro el Centinela, Cañon San Rodrigo, Picacho San Agustin, and Oso Blanco (figure 2.15). Cañon de los Caballos, Valle del Huincar, Picos Davis, Cañon de Fortin, and the northeastern flank of Sierra El Cedral also receive recharge.

The units comprising the Fredericksburg and lower Washita groups in the Maverick Basin are recharged in the El Treinta, El Comandante, and El Tule ranches located on the southern flank of Serranía del Burro (Leal, 1992). Recharge to the Devils River Formation in Coahuila takes place along San Juan Valley to the west of Nueva Rosita, Coahuila (Leal, 1992).





**EXPLANATION**

- 1 - Cerro el Palomo
- 2 - Cerro el Centinela
- 3 - Picacho San Agustín
- 4 - Cañon de los Caballos
- 5 - Valle de Huincar
- 6 - Cañon del Fortín

Map modified from Smith (1970)

**Figure 2.15** Physiographic features of northern Coahuila, Mexico.

## Discharge areas

Groundwater discharges from the Edwards-Trinity aquifer as springs and seeps, as baseflow to gaining streams, and through well withdrawals. Locally, where the water table is shallow, some discharge may take place by evapotranspiration.

Most of the discharge from the Edwards-Trinity aquifer in the study area is by springflow. Among the largest springs on the Texas side are San Felipe, Goodenough, and Las Moras Springs. San Felipe Springs, the fourth largest in Texas (Brune, 1981), issues from ten orifices along San Felipe Creek northeast of Del Rio in Val Verde County. The City of Del Rio relies in part on the springs for their water supply. From 1961 through 1967, San Felipe Springs discharged an average of 2.26 m<sup>3</sup>/s (IBWC, 2001). The filling of Lake Amistad with water has resulted in increased springflows of 3.38 m<sup>3</sup>/s on average since 1968.

The Goodenough Springs, also called Hinojosa Springs, are now submerged by Amistad Reservoir. Before 1968, when they were inundated by the lake, they were the third largest group of springs in Texas, with an average flow of 3.9 m<sup>3</sup>/s (Brune, 1981). Now 46 m under the top of the lake, their flow is reduced due to the hydraulic pressure induced by the column of water above the springs' orifice. Underwater investigations by cave divers have revealed that the springs still discharge a significant amount of water (M. Gary, 1999, personal communication). Las Moras Springs rise on the grounds of Fort Clark in Bracketville, Texas, and, with an average flow of 0.622 m<sup>3</sup>/s, was the ninth-largest spring in the state (Brune, 1981). Until 1964, when they temporarily ceased flowing, Las Moras Springs had been the sole public water source for the City of

Bracketville, which has since switched to water wells. Presently, the springs are feeding a large pool used by a vacation resort.

In Coahuila there are no less than 13 major springs grouped in a relatively small area (700 km<sup>2</sup>) encompassing the cities of Zaragoza, Morelos, Nava, Allende, and Villa Union (figure 2.1). Most of the springs issue from Tertiary and Quaternary conglomerates and upper Cretaceous limestone at the northern edge of Peyotes anticline. Nevertheless, Elizondo, (1977) and Leal (1992) have determined that these springs are fed by Glen Rose Limestone and Salmon Peak Formation groundwaters recharged in the Serranía del Burro to the northwest, hence their inclusion in this discussion. Table 2.3 lists several springs and their flow as measured by S.A.R.H. technicians at various times from 1971 through 1976:

**Springflow (m<sup>3</sup>/s)**

<b>Spring Name</b>	<b>Sept. 1971</b>	<b>Apr. 1974</b>	<b>Oct. 1974</b>	<b>Jan. 1976</b>	<b>Feb. 1976</b>	<b>Apr. 1976</b>
Allende	1.386	1.200	1.205	1.499	1.542	1.462
Chamacueros	0.06	0.06				
Las Corrientes	1.566	1.566	0.846			
Villagigedo		0.2	0.093			
Guadalupe	0.15	0.15	0.211		0.407	0.433
La Zanja	1.696	1.775				1.698
Patinos	0.336	0.2				
Morelos		1.5		1.707	1.552	1.288
El Socavon	1.2	1.2	0.9			
El Remolino	0.52	0.83	0.583			
Nava		1.1	1.41			
Las Albercas		0.3				

**Table 2.3 Flow from selected springs in Coahuila. Source of data: Elizondo (1977)**

Smaller springs have been identified throughout Serranía del Burro on the several ranches outside the study area (Leal, 1992).

Pumping from the Edwards – Trinity aquifer in Texas is for municipal, industrial, irrigation, and livestock water-supply purposes. The Texas Water Development Board maintains a database showing groundwater use from 1980 through 1997. More recent information is currently being compiled. Groundwater use summaries for Val Verde, Edwards, Kinney, and Uvalde counties are shown in table 2.4.

**VAL VERDE COUNTY**

<b>Year</b>	<b>Municipal</b>	<b>Manufact.</b>	<b>Power</b>	<b>Mining</b>	<b>Irrigation</b>	<b>Livestock</b>	<b>Total use</b>
1980	0.912	-	-	-	0.111	1.041	2.064
1984	5.947	-	-	0.122	0.907	0.465	7.441
1985	2.197	-	-	0.122	0.756	0.488	3.563
1986	6.250	-	-	0.004	0.141	0.538	6.932
1987	5.578	-	-	0.107	-	0.588	6.274
1988	8.648	-	-	0.117	0.528	0.678	9.971
1989	5.999	-	-	0.117	0.476	0.670	7.261
1990	3.963	-	-	0.117	0.432	0.682	5.193
1991	7.910	-	-	0.121	0.445	0.739	9.214
1992	6.578	-	-	0.121	0.446	0.653	7.799
1993	8.812	-	-	0.121	0.371	0.667	9.971
1994	8.007	-	-	0.121	0.448	0.584	9.160
1995	6.631	-	-	0.121	0.379	0.557	7.688
1996	7.873	-	-	0.122	0.375	0.526	8.896
1997	7.825	-	-	0.122	0.375	0.459	8.780

**EDWARDS COUNTY**

<b>Year</b>	<b>Municipal</b>	<b>Manufact.</b>	<b>Power</b>	<b>Mining</b>	<b>Irrigation</b>	<b>Livestock</b>	<b>Total use</b>
1980	0.416	-	-	0.014	0.184	1.002	1.615
1984	0.477	0.002	-	0.014	-	0.504	0.997
1985	0.406	0.002	-	0.014	-	0.508	0.930
1986	0.377	0.002	-	0.006	-	0.439	0.825
1987	0.377	-	-	-	-	0.480	0.857
1988	0.399	-	-	-	-	0.546	0.946
1989	0.498	-	-	-	-	0.543	1.041
1990	0.506	-	-	-	-	0.546	1.052
1991	0.451	-	-	0.007	-	0.592	1.051
1992	0.469	-	-	0.007	-	0.607	1.083
1993	0.499	-	-	0.007	0.176	0.587	1.270
1994	0.534	-	-	0.007	0.164	0.594	1.300
1995	0.488	-	-	0.007	0.164	0.588	1.248
1996	0.568	-	-	0.007	0.176	0.420	1.173
1997	0.494	-	-	0.007	0.176	0.418	1.096

**KINNEY COUNTY**

<b>Year</b>	<b>Municipal</b>	<b>Manufact.</b>	<b>Power</b>	<b>Mining</b>	<b>Irrigation</b>	<b>Livestock</b>	<b>Total use</b>
1980	1.264	-	-	-	11.477	0.499	13.240
1984	1.317	-	-	-	11.249	0.390	12.955
1985	1.288	-	-	-	5.714	0.379	7.381
1986	1.327	-	-	-	6.165	0.459	7.950
1987	1.298	-	-	-	2.568	0.510	4.377
1988	1.475	-	-	-	3.335	0.549	5.359
1989	1.729	-	-	-	12.944	0.501	15.173
1990	1.446	-	-	-	8.248	0.504	10.198
1991	1.238	-	-	-	8.248	0.524	10.009
1992	1.176	-	-	-	6.643	0.545	8.365
1993	1.348	-	-	-	11.128	0.477	12.953
1994	1.343	-	-	-	9.222	0.448	11.012
1995	1.327	-	-	-	7.224	0.433	8.984
1996	1.396	-	-	-	9.947	0.375	11.717
1997	1.398	-	-	-	8.615	0.316	10.329

**UVALDE COUNTY**

<b>Year</b>	<b>Municipal</b>	<b>Manufact.</b>	<b>Power</b>	<b>Mining</b>	<b>Irrigation</b>	<b>Livestock</b>	<b>Total use</b>
1980	7.306	-	-	0.386	91.137	0.912	99.741
1984	7.769	0.377	-	0.026	184.268	0.862	193.302
1985	6.685	0.377	-	0.370	184.283	0.824	192.539
1986	6.197	0.404	-	0.412	147.748	0.578	155.340
1987	5.848	0.413	-	0.128	121.975	0.600	128.964
1988	7.169	0.413	-	0.471	162.221	0.577	170.851
1989	7.657	0.446	-	0.492	186.649	0.567	195.811
1990	6.377	0.687	-	0.492	169.976	0.576	178.108
1991	6.520	0.482	-	0.491	139.034	0.602	147.129
1992	5.706	0.575	-	0.562	50.684	0.867	58.394
1993	6.868	0.406	-	0.906	130.194	0.830	139.203
1994	6.403	0.456	-	0.906	112.960	0.788	121.513
1995	6.426	0.414	-	0.642	79.133	0.784	87.400
1996	7.346	0.391	-	0.642	103.254	1.081	112.715
1997	6.699	0.382	-	0.651	72.606	0.766	81.104

**Table 2.4 Groundwater use in Val Verde, Edwards, Kinney, and Uvalde counties, expressed as hm<sup>3</sup>.  
Source of data: Texas Water Development Board water use survey.**

From 1980 through 1997, an average of 155.92 hm<sup>3</sup> of Edwards–Trinity groundwater was used every year to meet the needs within Val Verde, Edwards, Kinney,

and Uvalde counties. More water was used for irrigation than for any other purpose in the study area. From 1980 to 1997, irrigation pumpage was on average 137.74 hm<sup>3</sup> or 88.3 percent of the total amount of Edwards–Trinity groundwater used every year. Irrigation pumping in Uvalde County has been on average 82 percent of the total groundwater extracted area-wide for all uses. Yearly municipal pumping accounted for 14.76 hm<sup>3</sup> or 9.5 percent of the groundwater use. Average annual livestock and industrial (manufacturing, power, and mining) uses were 2.39 hm<sup>3</sup> (1.5 percent) and 1.03 hm<sup>3</sup> (0.7 percent) respectively.

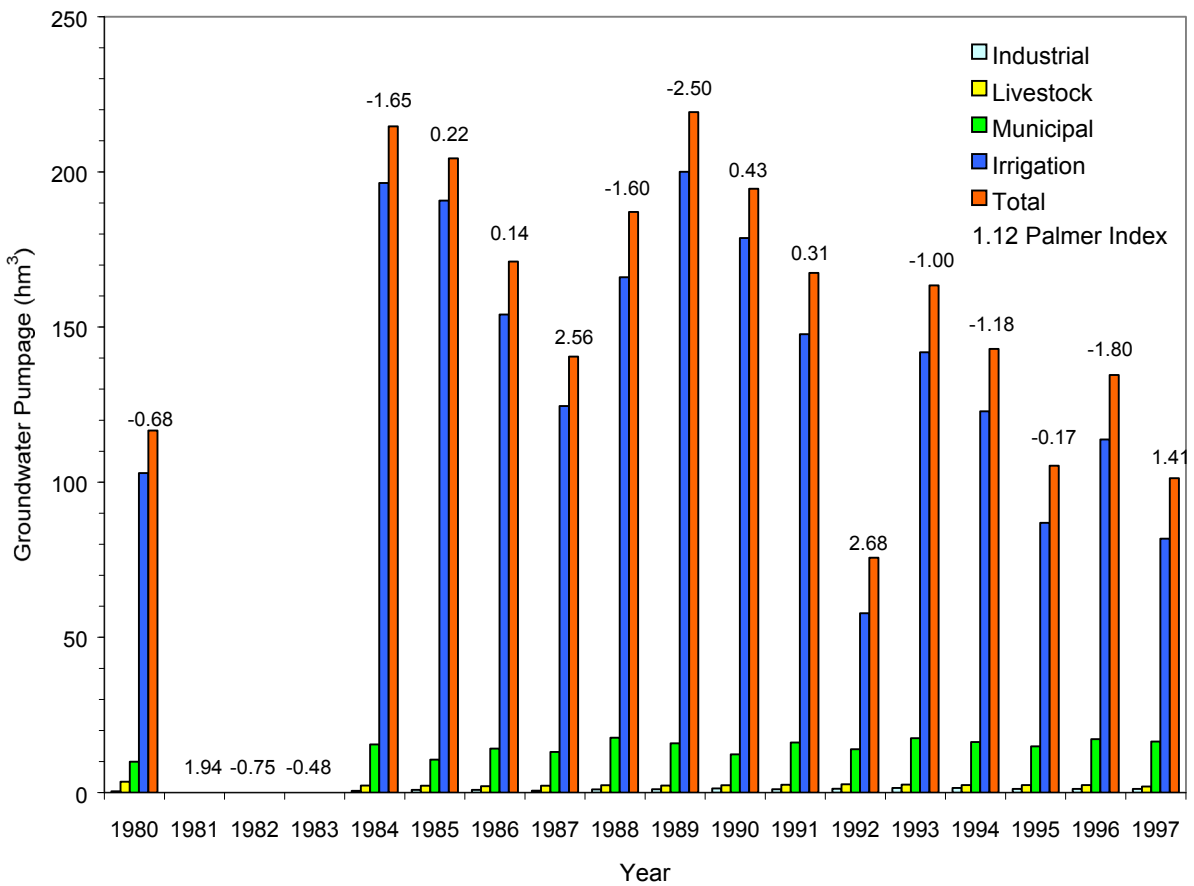


**Figure 2.16 Groundwater pumpage from the Edwards-Trinity aquifer, 1980-1997. Source of data: Texas Water Development Board.**

Figure 2.16 depicts trends in groundwater pumpage from the Edwards-Trinity aquifer on the Texas side of the study area. The yearly volumes of water extracted from the aquifer from 1980 through 1997 have been highly variable. Annual changes in groundwater use of 4 to 116 percent have been recorded. The main factor controlling the groundwater use has been the area-wide precipitation availability from year to year. The numbers shown above each column in figure 2.16 are the Drought Palmer Drought Severity Indices (PDSI) as calculated by the Texas Water Development Board for the Edwards Plateau area for the time interval 1980-1997. The PDSI (Palmer, 1965) uses temperature and rainfall information in a formula to determine dryness and is most effective in determining long term drought. A PDSI of zero signifies normal conditions, negative numbers indicate drought, and positive PDSI values suggest wetter than normal conditions. There is a good correlation between the groundwater withdrawal rates and PDSI for the period of record (figure 2.16). Drier than normal conditions during the early and late 1980s resulted in increased pumpage from the Edwards-Trinity aquifer. Groundwater use dropped in 1985 to 1987, 1990 to 1992, and 1997 when the area received above average precipitation.

## **Water quality**

### **General hydrochemistry**

General groundwater quality in the Edwards-Trinity aquifer is shown on the Stiff map (figure 2.17). The hydrochemical data displayed were collected in 1980-1981 in Coahuila and between 1981 and 2000 in Texas. Groundwater in both Coahuila and Texas was predominantly fresh (TDS < 1,000 mg/l). Several wells drilled near the

downdip limit of the aquifer (the “bad water zone”) in both Texas and Coahuila had higher TDS concentrations of up to 2,970 mg/l (well H-14-7-95 near San Carlos, Coahuila). Low-TDS groundwaters - indicated by the blue, narrow Stiff diagrams in figure 2.17 - are associated with active recharge areas in the Edwards Plateau and in Serranía del Burro and Lomerio Peyotes. TDS concentrations increase downgradient as groundwater dissolves aquifer minerals along its flowpath towards the downdip limit of the aquifer. A number of samples with TDS concentrations in the 1,000 to 3,000 mg/l range are located near Nava, Allende, Villa Union, and San Carlos, Coahuila, and north of Camp Wood, Texas. They have a distinct chemical character, reflecting different aquifer lithology and location within the flow system with respect to recharge and discharge.

The presence of the sulfate and chloride ions suggests that the dissolution of evaporite minerals may have contributed to these samples’ chemical composition. The likely sources for these minerals are the gypsum and halite sequences in the McKnight and Glen Rose formations. Samples from 212 wells within the study area were analyzed for major and minor ions. Of these, 16 samples showed sulfate concentrations of 300 mg/l or higher (figure 2.18) and five samples had nitrate (as  $\text{NO}_3^-$ ) concentrations greater than 44.3 mg/l (figure 2.19). In the United States, the maximum contaminant levels (MCLs) are set at 250 mg/l for sulfate (secondary standards) and 44.3 mg/l for nitrate.

Four general water types could be identified based on their hydrochemical signatures (see figure 2.20):



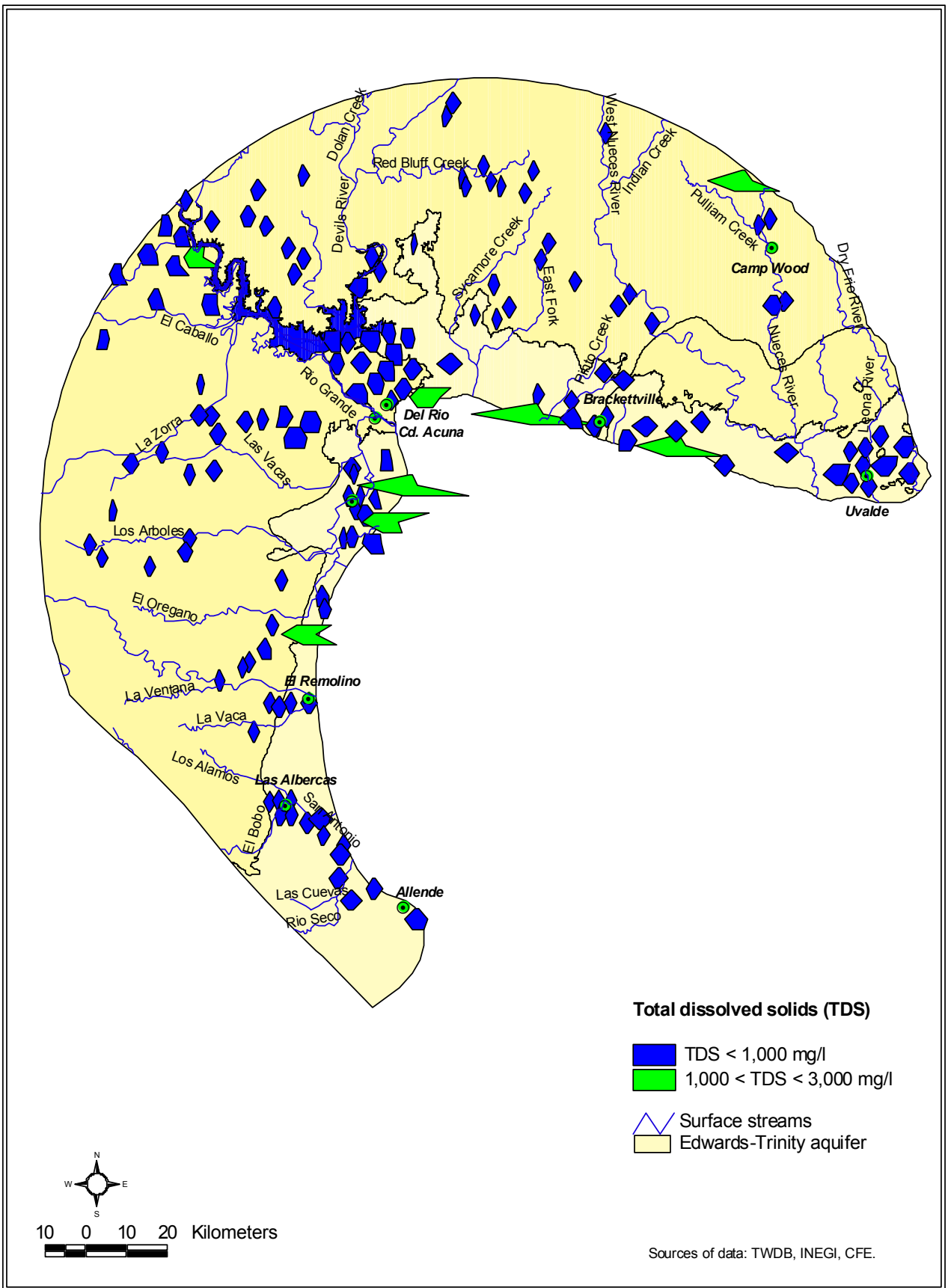


Figure 2.17 Stiff diagrams illustrating hydrochemical facies for the Edwards-Trinity aquifer.

- (1) A Ca-HCO<sub>3</sub> type which is predominant (76 percent of all samples) throughout the Edwards-Trinity aquifer in both Coahuila and Texas. Fresh (less than 1,000 mg/l TDS) Ca-HCO<sub>3</sub> groundwater occurs not only in the highlands of Serranía del Burro and Edwards Plateau, but also in wells along the mountain fronts.
- (2) A Ca-SO<sub>4</sub> type encountered primarily in fresh and slightly saline wells dotting the downdip limit of the aquifer in both Texas and Coahuila, and in few isolated wells around Brackettville and Camp Wood, Texas.
- (3) A Ca-Mixed Anion type where no single anion species exceeds 50 percent of the total anion equivalent weight, and calcium is the dominant cation. Within this water type, a Ca-HCO<sub>3</sub>-SO<sub>4</sub> sub-facies has been identified in wells west of San Carlos in Coahuila, and just north of Del Rio in Texas. Several samples near Uvalde, and one just east of Del Rio show a Ca-HCO<sub>3</sub>-Cl signature.
- (4) A Mixed Cation-Mixed Anion type where the ion with the greatest concentration is less than 50 percent of the total ionic equivalent weight.

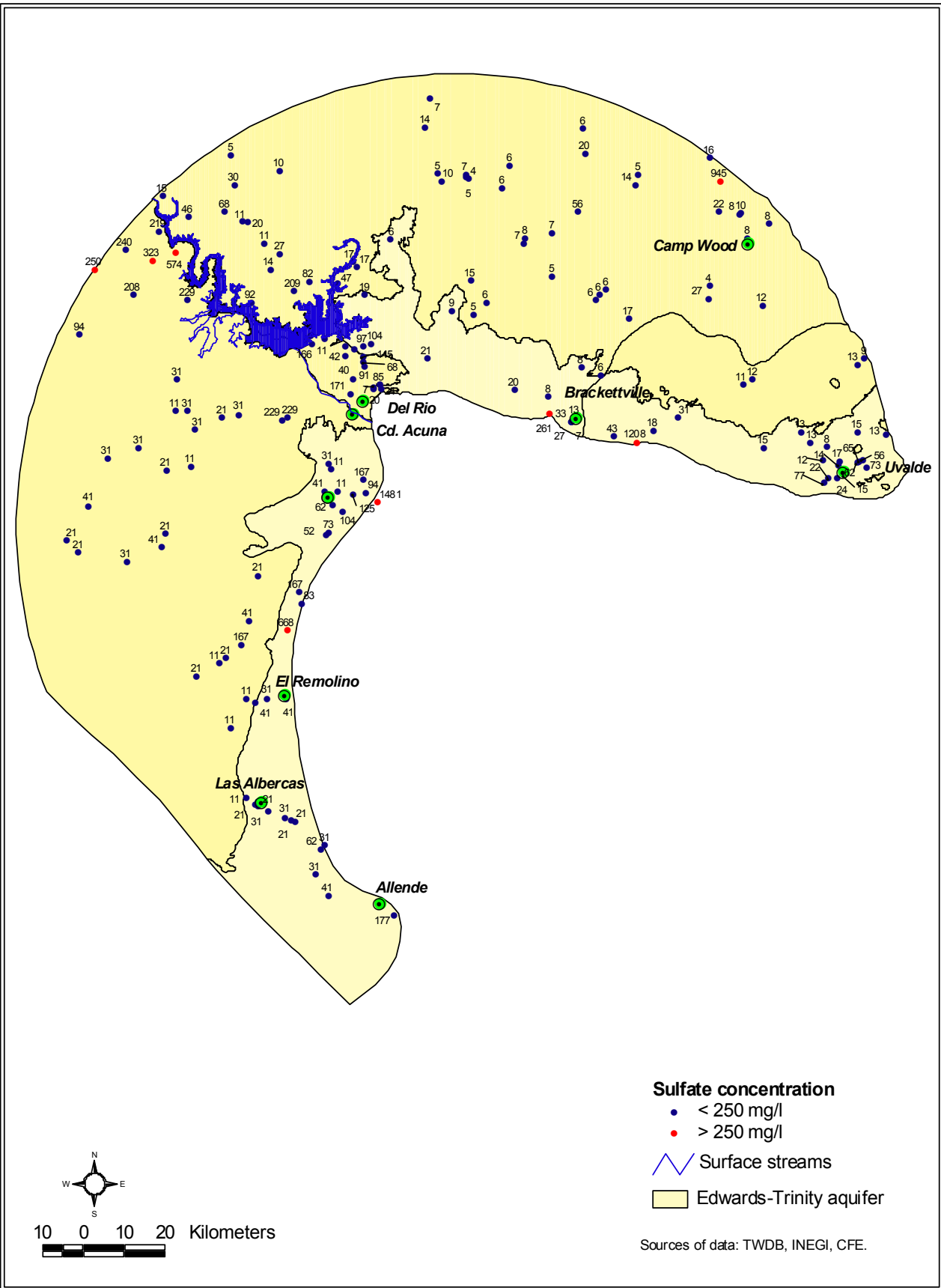


Figure 2.18 Map showing the distribution of sulfate in the Edwards-Trinity aquifer.

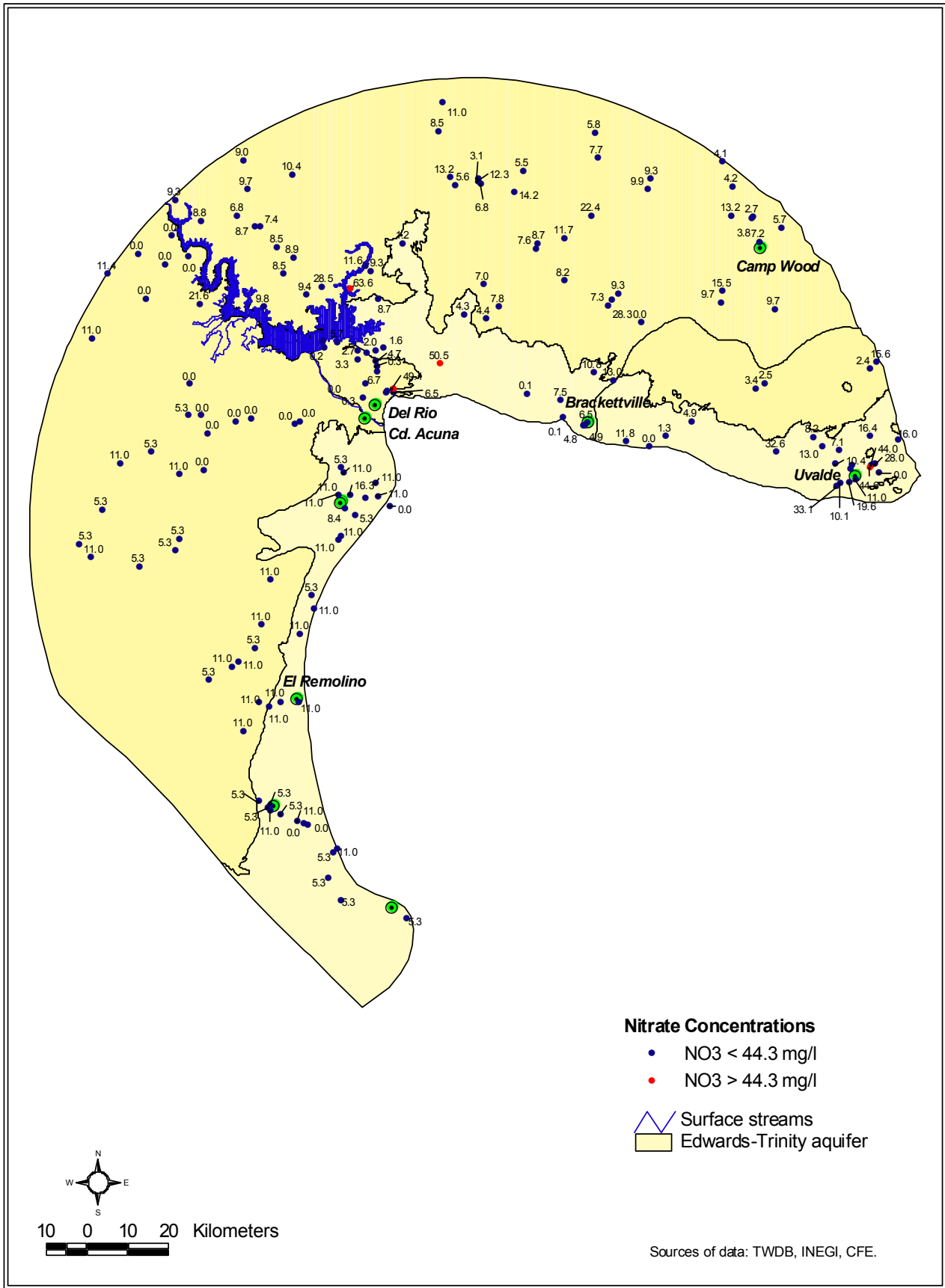


Figure 2.19 Map showing the distribution of nitrate in the Edwards-Trinity aquifer.

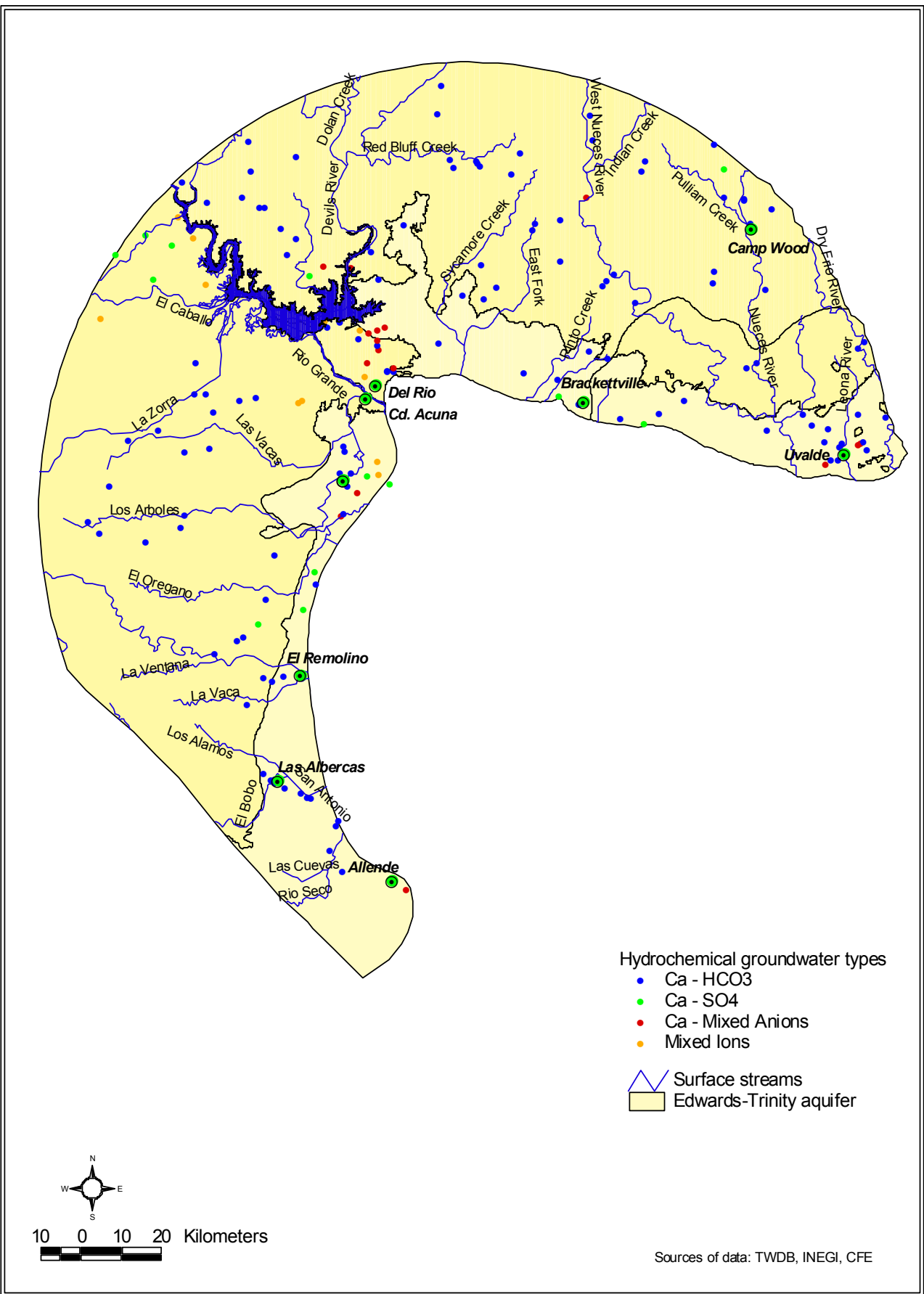
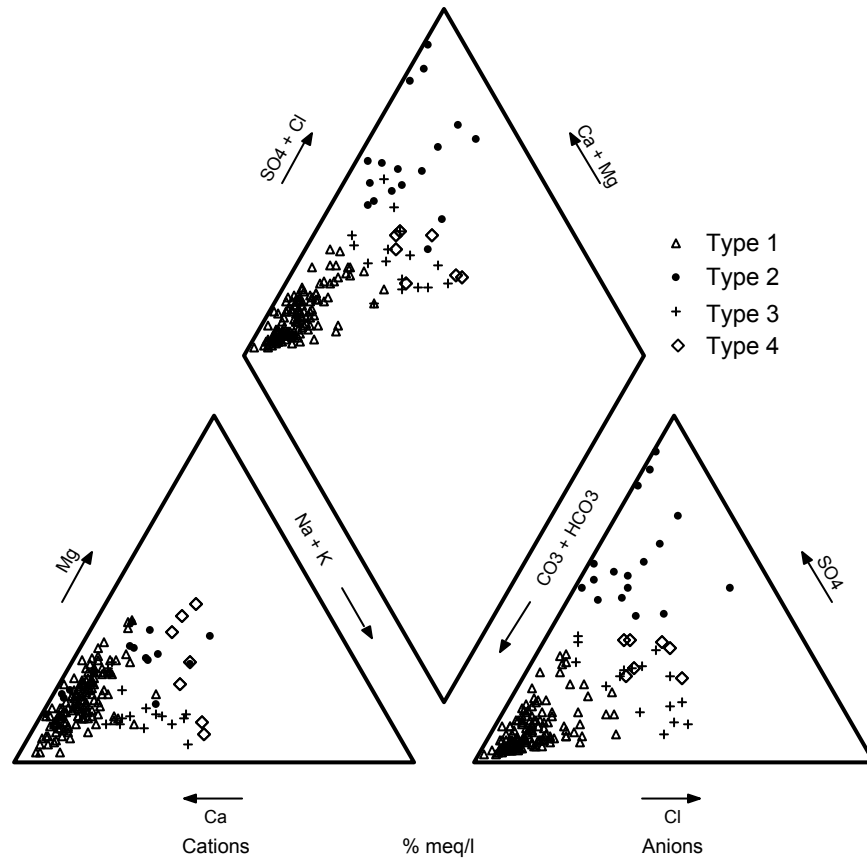


Figure 2.20 Areal distribution of hydrochemical facies in the Edwards-Trinity aquifer.

These fresh waters (less than 1,000 mg/l TDS) have been sampled in the Del Rio–Acuña area wells and at several locations along the Rio Grande upstream from Amistad reservoir.



**Figure 2.21 Piper diagrams showing major ion compositions for Edwards-Trinity aquifer. Sources of data: TWDB, INEGI, and CFE.**

Figure 2.21 illustrates potential evolutionary paths for Edwards-Trinity aquifer groundwaters. Fresh, type 1 waters gradually change their composition downgradient to the more saline types 3 and 4 through the addition of Cl and Na ions and the loss of Ca and HCO<sub>3</sub>. These changes in chemical composition suggest that halite dissolution, calcite precipitation, and possibly ion exchange reactions may take place. These reactions are discussed in more detail in the following section. Groundwater may evolve along a

flowpath from type 1 to type 2 through the addition of Ca, Mg, and SO<sub>4</sub>, and loss of HCO<sub>3</sub>, consistent with the dissolution of calcite, dolomite, and evaporite minerals.

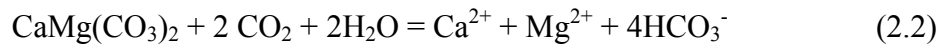
### Chemical Processes

Following are the governing equations for prominent mineral dissolution and precipitation reactions occurring in aqueous systems:

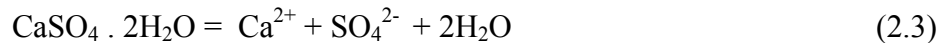
Calcite dissolution and precipitation:



Dolomite dissolution:



Gypsum dissolution:



Halite dissolution:



Ion exchange:

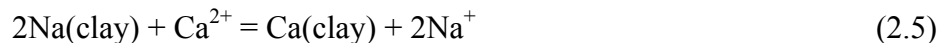


Figure 2.22 shows the relationship between the concentration of Ca<sup>2+</sup> + Mg<sup>2+</sup> versus HCO<sub>3</sub><sup>-</sup> concentration. If all Ca<sup>2+</sup> + Mg<sup>2+</sup> were derived from calcite and dolomite dissolution, then data would plot along a line with slope 1:2, as stated by equation 2.1. All points are above the 1:2 line, indicating an additional source of Ca<sup>2+</sup> and Mg<sup>2+</sup>.

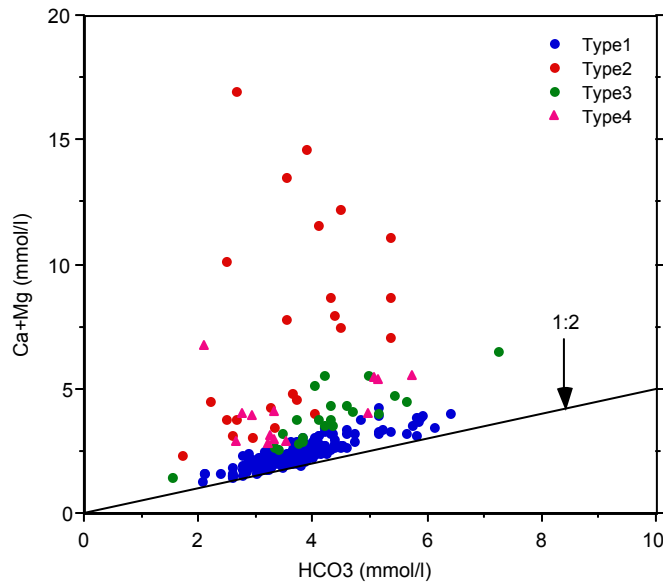


Figure 2.22 Plot of Ca+Mg versus HCO<sub>3</sub>

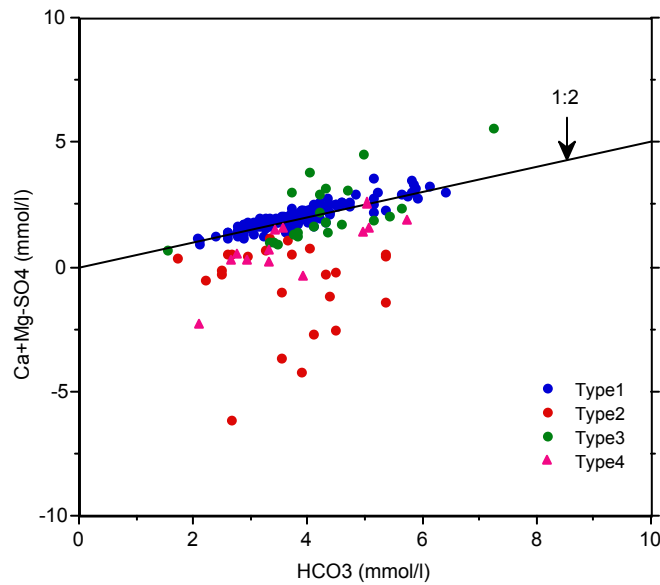
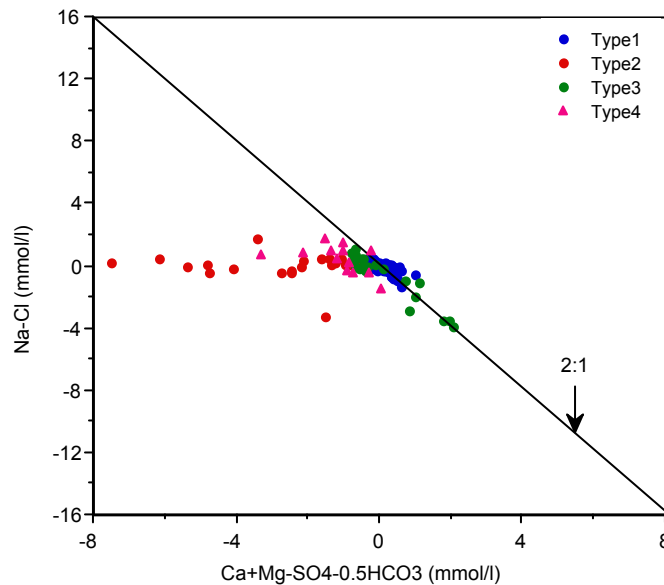


Figure 2.23 Plot of Ca+Mg-SO<sub>4</sub> versus HCO<sub>3</sub>

A potential source of additional Ca<sup>2+</sup> is the gypsum-bearing McKnight Formation of the Maverick Basin. To account for the Ca<sup>2+</sup> derived from gypsum dissolution, the SO<sub>4</sub><sup>2-</sup> concentration is subtracted from Ca<sup>2+</sup> + Mg<sup>2+</sup> and is then plotted as a function of HCO<sub>3</sub><sup>-</sup> (figure 2.23). Most of the samples group near the 1:2 line, indicating that carbonate and gypsum dissolution explains much of the variations in Ca<sup>2+</sup>, Mg<sup>2+</sup>, and HCO<sub>3</sub><sup>-</sup>



concentrations. Most of type 2 water samples, however, plot well below the 1:2 line. This indicates that other processes such as ion exchange between  $\text{Ca}^{2+}$  and/or  $\text{Mg}^{2+}$  and  $\text{Na}^+$  or calcite precipitation may be removing  $\text{Ca}^{2+}$  and/or  $\text{Mg}^{2+}$  from solution in type 2 samples.



**Figure 2.24** Plot of Na-Cl versus  $\text{Ca}+\text{Mg}-\text{SO}_4-0.5 \text{HCO}_3$

To test the ion exchange hypothesis, the concentration of  $(\text{Na}^+-\text{Cl}^-)$  is plotted against  $(\text{Ca}^{2+}+\text{Mg}^{2+}-\text{SO}_4^{2-}-0.5\text{HCO}_3^-)$ . The quantity  $(\text{Na}^+-\text{Cl}^-)$  represents "excess"  $\text{Na}^+$ , that is,  $\text{Na}^+$  coming from sources other than halite dissolution, assuming all  $\text{Cl}^-$  is derived from halite. The quantity  $(\text{Ca}^{2+}+\text{Mg}^{2+}-\text{SO}_4^{2-}-0.5\text{HCO}_3^-)$  represents the  $\text{Ca}^{2+}$  and/or  $\text{Mg}^{2+}$  coming from sources other than gypsum and carbonate dissolution. These two quantities represent the maximum amount of  $\text{Na}^+$  and  $\text{Ca}^{2+}+\text{Mg}^{2+}$  available for ion exchange processes. Some of the type 1, 3, 4, and 5 waters (figure 2.24) plot near a line with slope of 2:1 suggesting that limited cation exchange reactions may be taking place. However, this process cannot explain the calcium deficit in type 2 groundwaters, which are plotting well to the left of the base exchange line in figure 2.24.

To test the hypothesis that  $\text{Ca}^{2+}$  is being removed from solution by precipitation, saturation indices (SI) for calcite ( $\text{CaCO}_3$ ) were examined for each groundwater type. The saturation index is a function of the ionic activity of the ions in the water sample and the solubility product of a mineral phase of interest (in this case, calcite). If SI equals zero, then the water is at equilibrium with the mineral phase in question. If SI is positive, then the water is oversaturated with respect to the mineral phase in question and will tend to precipitate. If SI is negative, then the water is undersaturated with respect to the mineral phase in question, and will tend to dissolve more of the mineral if it is present.

Calcite equilibria for the Edwards-Trinity samples are plotted in figure 2.25. Waters range from undersaturated to oversaturated. Average saturation indices are highest for the type 2 groundwater samples (average SI = 0.49). The other waters are at equilibrium or slightly saturated with respect to calcite (SI = 0.09-0.22).

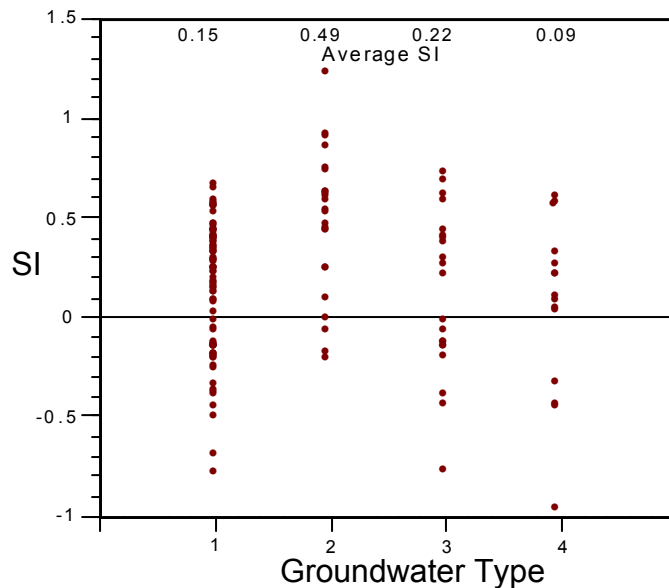


**Figure 2.25 Calcite saturation indices for Edwards-Trinity waters**

The higher saturation in type 2 samples is caused by the addition of calcium ions from the dissolution of gypsum (the common ion effect). This process increases the ionic

strength of the solution by reducing  $\text{Ca}^{2+}$  and  $\text{CO}_3^{2-}$  activity coefficients and elevating calcite solubility, thus resulting in calcite oversaturation.

In conclusion, carbonate dissolution/precipitation and gypsum dissolution are the main chemical processes responsible for the Edwards-Trinity groundwater chemistry. Dissolution of specific minerals is a function of their spatial variability at locations in the aquifer. Carbonate rocks are predominant, and they impart a calcium-bicarbonate character to groundwater in most of the study area. Locally, the gypsum present in the Fredericksburg strata of Maverick Basin is altering this signature. Other minerals such as halite appear to contribute little to the overall dissolved load of these groundwaters.

### References

- Adkins, W. S., 1933, The Mesozoic Systems in Texas, *in* The geology of Texas, Bureau of Economic Geology Bulletin 3232, p. 239-518.
- Amsbury, D. L., 1974, Stratigraphic petrology of Lower and Middle Trinity rocks on the San Marcos platform, south-central Texas, *in* Perkins, B. F., ed., Aspects of Trinity division geology-a symposium: Louisiana State University, Geoscience and man, v. 8, p. 1-35.
- Armstrong, A. W., 1995, The use of stable isotope ratios to investigate the relative importance of Amistad Reservoir to recharge of the McKnight and associated limestones, southwestern Val Verde County, Texas: Unpublished M.S. thesis, The University of Texas at San Antonio, 95 p.
- Banner, J. L. and Hanson, G. N., 1990, Calculation of simultaneous isotopic and trace element variations during water-rock interaction with applications to carbonate diagenesis: *Geochimica et Cosmochimica Acta*, v. 54, p. 3123-3137.
- Barker, R. A. and Ardis, A. F., 1992, Configuration of the base of the Edwards-Trinity aquifer system and hydrogeology of the underlying pre-Cretaceous rocks, west-central Texas: U.S. Geologic Survey Water-Resources Investigations Report 91-4071, 25 p.

- Barker, R. A. and Ardis, A. F., 1996, Hydrogeologic framework of the Edwards-Trinity aquifer system, west-central Texas: U. S. Geological Survey Professional Paper 1421-B, 61 p.
- Barker, R. A., Bush, P. W., and Baker, E. T., Jr., 1994, Geologic history and hydrogeologic setting of the Edwards-Trinity aquifer system, west-central Texas: U. S. Geological Survey Water-Resources Investigation Report 94-4039, 51 p.
- Barnes, V. E., 1977, Del Rio sheet: The University of Texas at Austin, Bureau of Economic Geology, Geologic Atlas of Texas, scale 1:250,000.
- Batzner, J. C., 1976, The hydrogeology of Lomerio de Peyotes, Coahuila, Mexico: Unpublished M.S. thesis, University of New Orleans, 64 p.
- Bebout, D. G., Budd, D. A., and Schatzinger R. A., 1981, Depositional and diagenetic history of the Sligo and Hosston formations (Lower Cretaceous) in south Texas: The University of Texas at Austin, Bureau of Economic Geology Report of Investigations 109, 70 p.
- Bennett, R. R. and Sayre, A. N., 1962, Geology and ground-water resources of Kinney County, Texas: Texas Water Development Board Bulletin 6216, 163 p.
- Brune, G., 1981, Springs of Texas, volume I: Branch-Smith, Inc., Fort Worth, Texas, 566 p.
- Butterworth, R. A., 1970, Sedimentology of the Maxon Formation (Cretaceous), west Texas: The University of Texas at Austin, Department of Geological Sciences unpublished M. A. thesis, 132 p.
- Clark, A. K. and Small, T. A., 1997, Geologic framework of the Edwards aquifer and upper confining unit, and hydrogeologic characteristics of the Edwards aquifer, south-central Uvalde County, Texas: U.S. Geologic Survey Water-Resources Investigations Report 97-4094, 11 p.
- Clark, I. D., 1987, Groundwater resources in the Sultanate of Oman: origin, circulation times, recharge processes and paleoclimatology. Isotopic and geochemical approaches: Université de Paris-Sud, Orsay, France, Unpublished doctoral thesis, 264 p.
- Clark, I. D. and Fritz, P., 1997, Environmental isotopes in hydrogeology: Lewis Publishers, 328 p.
- Domenico, P. A. and Schwartz, F. W., 1990, Physical and chemical hydrogeology: John Wiley & Sons, Inc., 824 p.

- Elizondo, J. R., 1977, Geologia basica regional en la sub-cuenca hidrologica Acuña-Laredo: Comisión Federal de Electricidad, Series tecnicas de CFE, 69 p.
- Flawn, P. T., Goldstein, A., Jr., King, P. B., and Weaver, C. E., 1961, The Ouachita system: The University of Texas at Austin, Bureau of Economic Geology Publication 6120, 401 p.
- Imlay, R. W., 1945, Subsurface Lower Cretaceous formations of south Texas: American Association of Petroleum Geologists Bulletin, v. 29, p. 1416-1469.
- Inden, R. F., 1974, Lithofacies and depositional model for a Trinity Cretaceous sequence, central Texas, *in* Perkins, B. F., ed., Aspects of Trinity division geology-a symposium: Louisiana State University, Geoscience and man, v. 8, p. 37-52.
- International Boundary and Water Commission (IBWC), 1990, Amistad Reservoir area, report on hydrogeologic studies, Summary of report on effects of Amistad Reservoir on hydrologic regime in the area, 99 p.
- International Boundary and Water Commission (IBWC), 2001, Flow of the Rio Grande and tributaries and related data: [http://www.ibwc.state.gov/wad/rio\\_grande.htm](http://www.ibwc.state.gov/wad/rio_grande.htm)
- Kuniansky, E. L. and Holligan, K. Q., 1994, Simulations of flow in the Edwards-Trinity aquifer system and contiguous hydraulically connected units, west-central Texas: U.S. Geological Survey Water-Resources Investigations Report 93-4039, 40 p.
- Leal, J. A. R., 1992, Estudio geohidrologico en la region carbonifera de Sabinas, Coahuila, Etapa de perfectabilidad: Comisión Federal de Electricidad, Superintendencia de Estudios Zona Norte, Area de Geohidrologia, Nueva Rosita, Coahuila, 25 p.
- Lesser, J. M. and Lesser, G., 1988, Region 9, Siera Madre Oriental, *in* Back, W., Rosenshein, J. S., and Seaber, P. R., ads., Hydrogeology: Boulder, Colorado, Geological Society of America, The Geology of North America, v. O-2.
- Long, A. T., 1958, Ground-water geology of Real County, Texas: Texas Board of Water Engineers Bulletin 5803, 46 p.
- Long, A. T., 1963, Ground-water geology of Edwards County, Texas: U. S. Geological Survey Water-Supply paper 1619-J, 29 p.
- Loucks, R. G., 1977, Porosity development and distribution in shoal-water carbonate complexes-subsurface Pearsall Formation (Lower Cretaceous) south Texas, *in* Bebout, D. G., and Loucks, R. G., eds., Cretaceous carbonates of Texas and Mexico, applications to subsurface exploration: The University of Texas at Austin, Bureau of Economic Geology Report of Investigations 89, p. 97-126.

- Lozo, F. E., Jr. and Smith, C. I., 1964, Revision of Comanche Cretaceous stratigraphic nomenclature, southern Edwards Plateau, southwest Texas: Transactions of Gulf Coast Association of Geological Societies, v. 14, p. 285-307.
- Mace, R. A., 2001, Estimating transmissivity using specific capacity data: The University of Texas at Austin, Bureau of Economic Geology Geological Circular 01-2, 44 p.
- Maclay, R. W. and Small, T. A., 1983, Hydrostratigraphic subdivisions and fault barriers of the Edwards aquifer, south-central Texas, U.S.A., *in* Back, W. and LaMoreaux, P. E., eds., V. T. Stringfield symposium, Processes in karst hydrology: Journal of Hydrology v. 61, p. 127-146.
- Maclay, R. W., Rettman, P. L., and Small, T. A., 1980, Hydrochemical data for the Edwards aquifer in the San Antonio area: Texas Department of Water Resources LP-131, 38 p.
- Miller, B. C., 1984, Physical stratigraphy and facies analysis, Lower Cretaceous, Maverick basin and Devils River trend, Uvalde and Real Counties, Texas, *in* Smith, C. I., ed., Stratigraphy and structure of the Maverick basin and the Devils River trend, Lower Cretaceous, southwest Texas-A field guide and related papers: South Texas Geological Society, p. 3-33.
- Palmer, W. C., 1965, Meteorological drought: U.S. Department of Commerce Weather Bureau, Washington, D.C., Research paper no. 45.
- Reeves, R. D., and Small, T. A., 1973, Ground-water resources of Val Verde County, Texas: Texas Water Development Board Report 172, 145 p.
- Rose, P. R., 1972, Edwards Group, surface and subsurface, central Texas: The University of Texas at Austin, Bureau of Economic Geology Report of Investigations 74, 198 p.
- Smith, C. I., 1970, Lower Cretaceous stratigraphy, northern Coahuila, Mexico: The University of Texas at Austin, Bureau of Economic Geology Report of Investigations 65, 101 p.
- Smith, C. I., 1979, The Devils River trend and Maverick basin sequence, *in* Rose, P. R., ed., Stratigraphy of the Edwards Group and equivalents, eastern Edwards Plateau, Texas-guidebook for Gulf Coast Association of Geological Societies field trip 1, October 9-10, 1979: South Texas geological Society, p. 14-18.
- Theis, C. V., 1963, Estimating the transmissivity of a water-table aquifer from the specific capacity of a well, *in* U. S. Geological Survey Water-Supply Paper 1536-I, p. 332-336.

Welder, F. A. and Reeves, R. D., 1962, Geology and ground-water resources of Uvalde County, Texas: Texas Water Commission Bulletin 6212, 252 p.

Winter, J.A., 1962, Fredericksburg and Washita strata (subsurface Lower Cretaceous), southwest Texas, in Contributions to the geology of south Texas: San Antonio, Texas, South Texas Geological Society, p. 81-115.

## **CHAPTER 3: THE ALLENDE-PIEDRAS NEGRAS VALLEY AQUIFER**

This section describes the Allende-Piedras Negras Valley aquifer in the study area (figure 1.3). The discussion includes general information on aquifer location and extent, geology and water-bearing characteristics, aquifer properties, potentiometric surface, and hydrochemistry.

### **Location and extent**

The Allende-Piedras Negras Valley aquifer underlies an area of 5,368 km<sup>2</sup> in the northeast part of the state of Coahuila and extends north into Texas where it covers 1,498 km<sup>2</sup> in Kinney and Maverick counties. The aquifer lies within the Río Bravo-Conchos hydrologic region of Coahuila (the Rio Grande basin in Texas) and comprises the sub-basins of the Río Escondido-Río San Antonio, and Castaños Arroyo. The principal cities in the aquifer region are Allende, Villa Union, Morelos, Zaragoza, Nava, Guerrero, with the Piedras Negras-Eagle Pass city pair standing out as the largest.

The aquifer limits follow the geologic contacts between the unconsolidated deposits of the Piedras Negras Valley and the surrounding Cretaceous and Eocene outcrops (see figure 1.4).

### **Stratigraphy and structure**

The Allende-Piedras Negras Valley aquifer is made of thin (up to 50 m thick) alluvial terraces, alluvial bolsons conglomerates, and floodplain deposits such as clays, silt, sands, and gravels. These unconsolidated sedimentary deposits are the result of



erosion and transport of limestones that constitute the higher topographic elevations. In large part, the geology of the area is represented by Upper Cretaceous marine carbonates overlain by Quaternary terrigenous sequences.

The following briefly describes the physical characteristics of the litho-stratigraphic units that are relevant to the aquifer, starting with the oldest and ending with the most recent [descriptions from Barnes, 1976, 1977; U.S.-Mexico Foundation for Science (FUMEC), 1999]:

### **Buda Formation**

The Buda Formation is a light-gray to pale-orange, fine-grained, bioclastic, and fossiliferous limestone about 30 m thick in Coahuila and 15 to 35 m thick in Texas. Several Buda Formation outcrops border the northern edge of the Allende-Piedras Negras Valley aquifer in Texas south of the Balcones fault zone. In Texas the Buda Formation yields very little water to stock wells in Val Verde and Uvalde counties and is considered to be relatively impermeable. In Coahuila the Buda Formation is intensively deformed and fractured and can be encountered to the southeast of the town of Allende (FUMEC, 1999).

### **Eagle Ford Formation**

The Eagle Ford Formation consists of 25 to 100 m of alternating thin layers of shale, siltstone, and flaggy limestone with laminar structure. In the study area, the Eagle Ford Formation crops out in a northwest-southeast-trending belt from eastern Val Verde County to lower West Nueces River in Kinney County. The formation is a source of

groundwater only in the outcrop areas and only where fractures are present (Bennett and Sayre, 1962).

### **Austin Chalk**

The Austin Chalk is represented by alternating thin limestone, chalk, and marl and is massive in outcrop. At several locations in Texas the Austin Chalk is very fossiliferous and contains beds composed primarily of shells (Bennett and Sayre, 1962). In Coahuila, the Austin Chalk crops out toward the western part of the towns of Zaragoza, Morelos, Allende, and Villa Union and is up to 300 m thick and faulted (FUMEC, 1999). The formation is water-bearing and can produce large yields from shallow wells near Uvalde, Texas.

### **Upson Clay**

In Texas the Upson Clay crops out in several spots along the eastern edge of the aquifer (in Mustang and Quemado Creeks and just east of Spofford), and consists of pro-deltaic and shelf calcareous gray clays with marine megafossils. In Coahuila the Upson Clay contains dark gray shales with some interbeds of silts; in the upper part, it contains sandstones deposited in a deltaic environment. The formation does not crop out in the area of the Allende – Piedras Negras Valley aquifer in Mexico. The thickness of the Upson Clay is probably in excess of 200 m in Coahuila and southern Texas but thins out rapidly to the north (Barnes, 1976). Because it is made principally of fine terrigenous material, the Upson Clay can be conceptualized as an aquitard.

### **San Miguel Formation**

The San Miguel Formation conformably overlies the Upson Clay and consists of delta-front gray and greenish hard calcareous sandstone and sandy limestone alternating with clay beds. The sandstone beds become more numerous and coarser upwards (Caffey, 1978). The 130 to 150 m thick formation is exposed just east of the Allende-Piedras Negras Valley aquifer limit in Texas where it dips gently to the southeast (Bennett and Sayre, 1962). In Texas, the San Miguel Formation yields small amounts of highly mineralized groundwater to stock wells.

### **Olmos Formation**

The Olmos Formation was deposited in a deltaic-front environment and consists of dark gray carbonaceous shales interrupted by sandstone layers. The 1 to 5 m thick sandstone beds are upward-fining and cannot be correlated over more than 1 to 2 km (Caffey, 1978, p. 26). Seams of coal and lignite up to two meters thick are common.

The Olmos Formation is not known to transmit water to wells in Texas. Several friable sandstone beds in the upper Olmos Formation have been mapped in Kinney County, but their limited continuity probably precludes the movement of groundwater.

### **Escondido Formation**

The Escondido Formation, the youngest Cretaceous formation in the area, is exposed in northeastern Maverick County and has a lithology characteristic of interdeltic and marine shelf environments. The 70-360 m thick Escondido Formation is made of alternating siltstone, sandstone, and mudstone beds that overlay the Olmos

Formation. In Coahuila the unit crops out amply in the southeast and eastern parts, bordering north to south the western part of the Rio Grande and continuing toward the west below the Sabinas Conglomerate (next section). The permeability of the Escondido unit is generally low, although several stock wells in Maverick County are known to pump from this unit.

### **Uvalde Gravel (Sabinas Conglomerate)**

Coarse Pliocene alluvial deposits blanket the Upper Cretaceous rocks in the study area and, together with the younger, Quaternary deposits, comprise the Allende-Piedras Negras Valley aquifer. In Texas, the Pliocene deposits are described as the Uvalde Gravel, while in Coahuila they are known as the Sabinas Conglomerate. The formation is composed mainly of well-cemented pebbles and cobbles of limestone, 1 to 5 cm in diameter, chert and fragments of igneous rocks, caliche, clay, and calcareous sandstone. The thickness of the gravel varies from zero to over 50 m. The formation is up to 25 m thick on the Texas side and thickens to an average of 40 m into Coahuila (FUMEC, 1999). The gravel is distributed extensively in the entire Piedras Negras Valley, where it is sometimes mixed with recent alluvium such as clays and sands.

Its fossil content suggests that the Uvalde Gravel resulted from the erosion of the Edwards Limestone (Holt, 1959), which was exposed during most of the Tertiary. During late Pliocene to early Pleistocene, the Edwards Plateau was uplifted along the Balcones Fault Zone, which resulted in steeper topographic gradients and stronger streams. The streams carried and spread the gravel well to the south of its source area. Based on the mineralogical composition of igneous rock pebbles found in the gravel,

Getzender (1930) suggested that some of the material might have been transported from as far as Trans-Pecos. Later erosion incised deep valleys into the ancient plain, leaving the gravel-capped highlands as remnants.

The permeability of these units is high, and many wells in Coahuila produce good quality groundwater for public supply, irrigation, and stock uses from the Sabinas Conglomerate and the associated alluvium. Few wells have been completed in the Uvalde Gravel on the Texas side of the aquifer.

### **Quaternary Alluvium**

Quaternary Alluvium is made of unconsolidated Pleistocene and Holocene (Recent) age deposits. Pleistocene sediments form fluvial terraces that are underlying the modern river floodplains and consist of gravel, sand, silt, and clay. When adjacent to Cretaceous limestone outcrops, these deposits are predominantly gravel, limestone, and chert are the product of the weathering and erosion of the highlands.

The Holocene Quaternary alluvium fills all the valley streams crossing the Allende-Piedras Negras Valley aquifer. The alluvium contains silt, sand, clay, and gravel resulted from the weathering of the adjacent formations. Most of the youthful streams draining the Edwards Plateau are blanketed by limestone cobbles and gravels in large quantities. The alluvium bordering the Rio Grande is generally finer grained and can contain igneous and sedimentary rocks transported from Trans-Pecos, Coahuila, and even New Mexico (Barnes, 1976). The Quaternary alluvium has high permeability and yields water to many wells in both Texas and Coahuila.

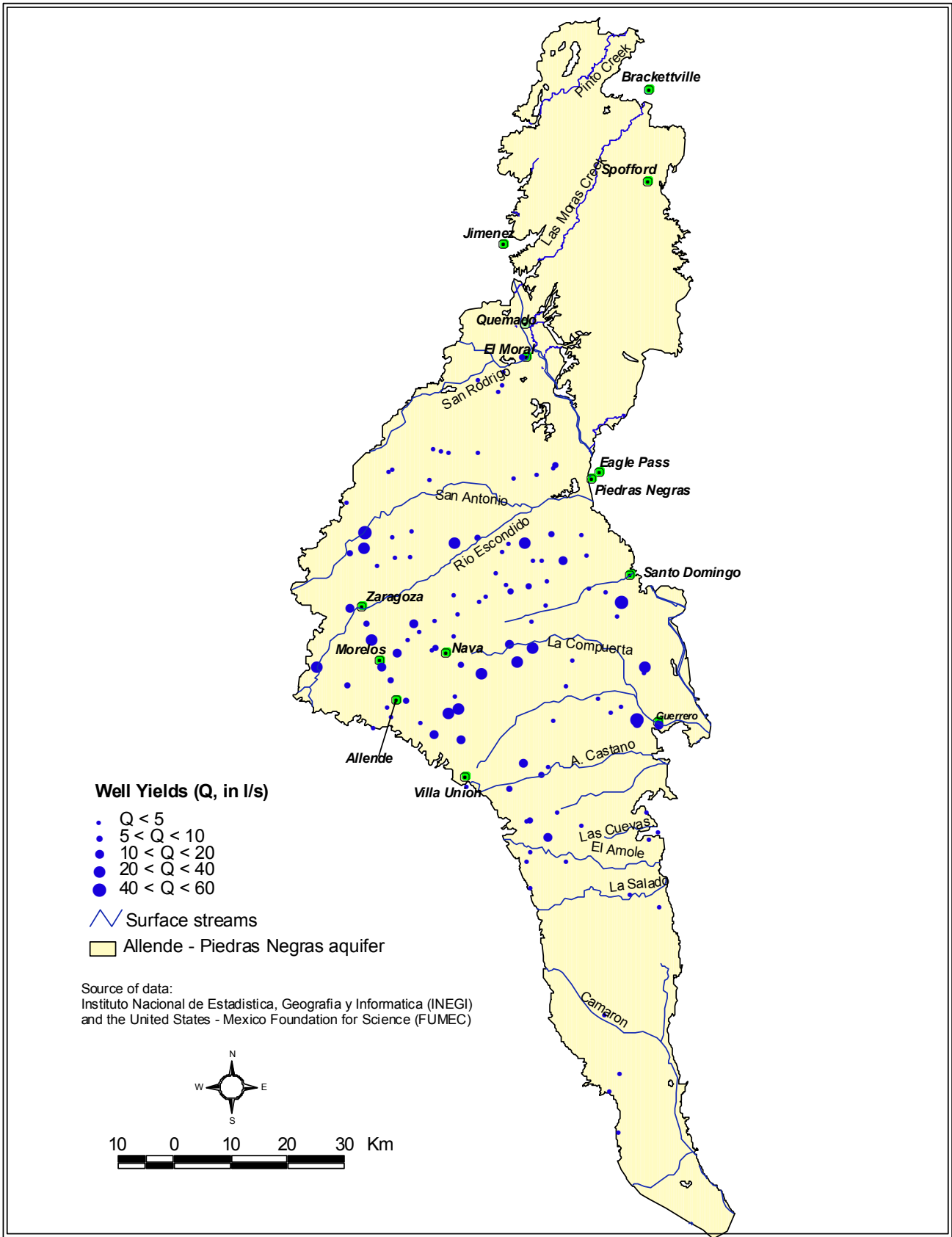


Figure 3.1 Well yields in the Allende-Piedras Negras Valley aquifer.

## **Aquifer properties**

On the Texas side, the majority of the Allende – Piedras Negras wells yield water from the alluvium in the Quemado Valley, a portion of the Rio Grande floodplain in northwestern Maverick County, Texas. Aquifer tests indicate that the alluvial aquifer in the Quemado Valley has the capability of transmitting moderate to large quantities of groundwater to wells (Bluntzer, 1992).

Estimates of aquifer transmissivity range from 1,800 to 3,000 m<sup>2</sup>/day in the Holocene alluvium adjacent to the Rio Grande and are about 1,200 m<sup>2</sup>/day in the less permeable Pleistocene terrace deposits away from the river. Corresponding hydraulic conductivity values for the aquifer in the Quemado Valley vary from 160 to 430 m/day.

Little is known about the transmissive properties of the Uvalde Gravel. There are very few wells completed in this formation on the Texas side, and no well yields are reported. Given its composition and structure, the Uvalde Gravel is likely to have high hydraulic conductivity. However, because of its limited thickness, the transmissivity of the Uvalde Gravel is probably low.

Well yields in the Coahuila part of the Allende-Piedras Negras Valley aquifer vary between 0.5 l/s and 80 l/s with a median yield of 2 l/s (figure 3.1). In 1999, the majority of the wells in the area pumped 5 l/s or less. As expected, most of the low yields are associated with windmills and hand-operated pumps, whereas the higher yields come from irrigation and public water-supply wells.

## Potentiometric surface and water levels

The Allende-Piedras Negras Valley aquifer potentiometric surface map was created using water-level information from 86 wells in Coahuila (figure 3.2). Comisión Nacional del Agua (CNA) personnel measured these wells in September 1999. No water-level information of this vintage exists for the Texas side.

The 1999 potentiometric surface slopes west to east towards the Rio Grande with hydraulic gradients as steep as 0.015 across Peyotes hill just west of Allende. The gradient flattens to 0.003 between Morelos and Nava and becomes very flat ( $\sim 0.0001$ ) between Nava and the Rio Grande near Santo Domingo. Hydraulic heads in excess of 400 m in the Peyotes area define areas of groundwater recharge. The flat hydraulic gradient in the Rio Grande floodplain between Santo Domingo and Guerrero suggests that the aquifer there is very transmissive and that large amounts of groundwater may flow through it and discharge into the Rio Grande.

On the Texas side, the water-level information for the Allende – Piedras Negras Valley aquifer is sparse and dated. Water levels measured in 1938 in alluvial wells north of the Spofford parallel indicate that regional flow was from the highlands west of Brackettville towards the Rio Grande. Hydraulic gradients were 0.005 along Pinto Creek west of Brackettville and 0.004 along Las Moras Creek from Spofford on to the south. Water-level measurements in the Quemado Valley indicate gentle hydraulic gradients (0.0009 to 0.0018) sloping towards the Rio Grande (Bluntzer, 1992).



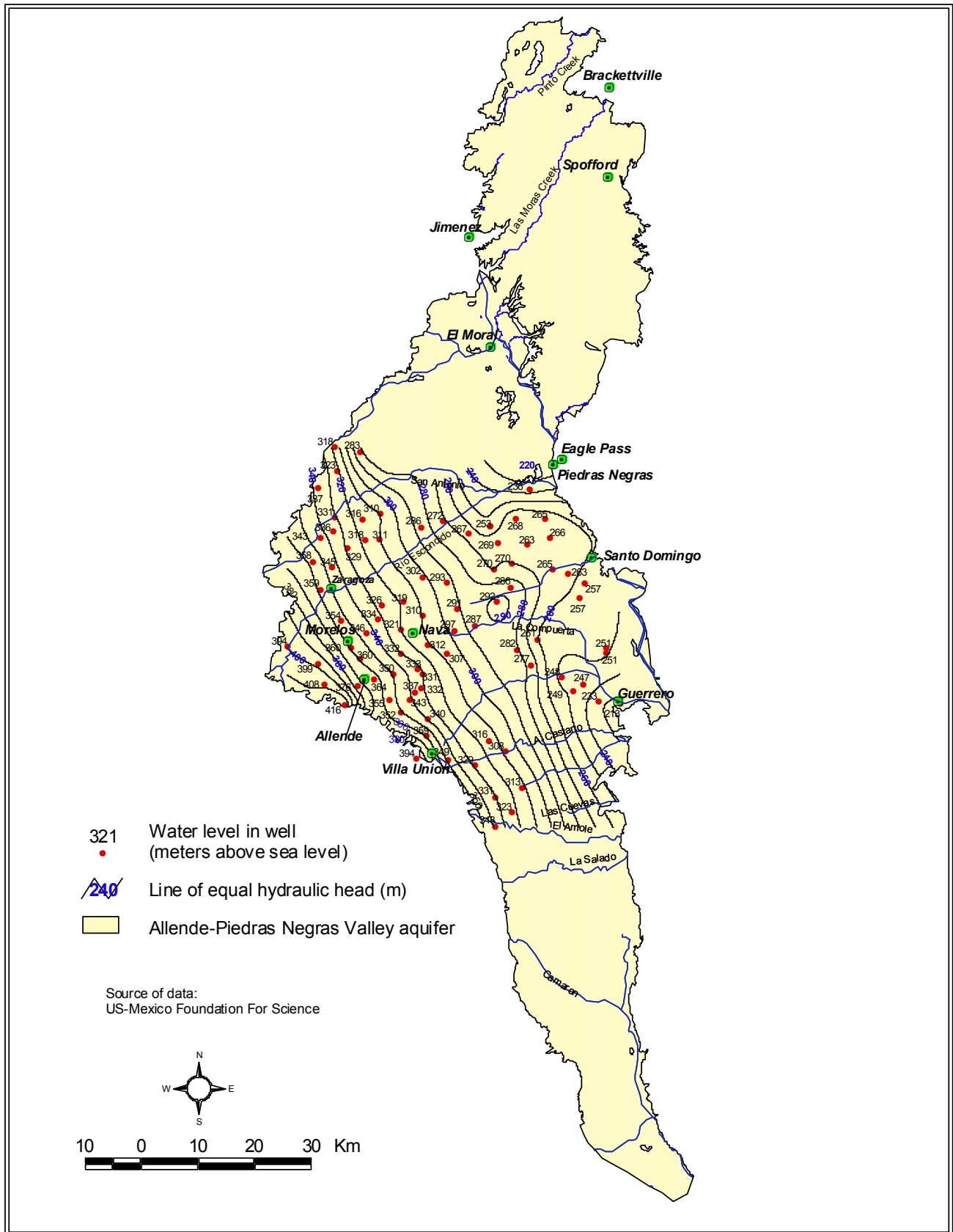


Figure 3.2 Potentiometric surface map for the Allende-Piedras Negras Valley aquifer. Water-level data collected in 1999.

In 1938, hydraulic heads on the Texas side were as high as 344 m in well 70-45-102 (located 9 km northwest of Brackettville and along Pinto Creek) to 297 m in well 70-52-601 (located 9 km west of Spofford and along Las Moras Creek). Hydraulic heads along the Rio Grande floodplain aquifer ranged from 237.8 m in well 76-03-302 downstream from Jimenez to 211.7 m in well 76-12-902 located 5 km upstream from Eagle Pass (Bluntzer, 1992).

Surface drainage and groundwater pumping can impact the regional potentiometric pattern. The configuration of the potentiometric surface suggests that gaining stream and underflow conditions prevail along the Rio Grande and Río Escondido. Las Moras Creek captures the flow from the Las Moras Springs below Brackettville. The other creeks in the study area are ephemeral, losing streams. Groundwater pumping for irrigation and mining may explain the contour line flexures mapped near Allende and southwest of Piedras Negras (FUMEC, 1999).

Well hydrographs prepared with data collected from 1991 to 1999 illustrate annual changes in water levels (figure 3.3). Water-level fluctuations mirror changes in aquifer storage. The addition of water to storage results in a water-level rise, while a decline in water level would indicate storage depletion. The paucity of time-series water-level measurements is evident, and the conclusions that can be drawn from them are limited. Most of the hydrographs suggest that between 1991 and 1999 the Allende – Piedras Negras Valley aquifer storage has been declining slightly, as shown by the downward trend in hydrographs. The areas of the aquifer north of Zaragoza and between Nava and Villa Union (wells CNA 429, 270, and 322) have sustained groundwater withdrawals in amounts less than the effective recharge, which

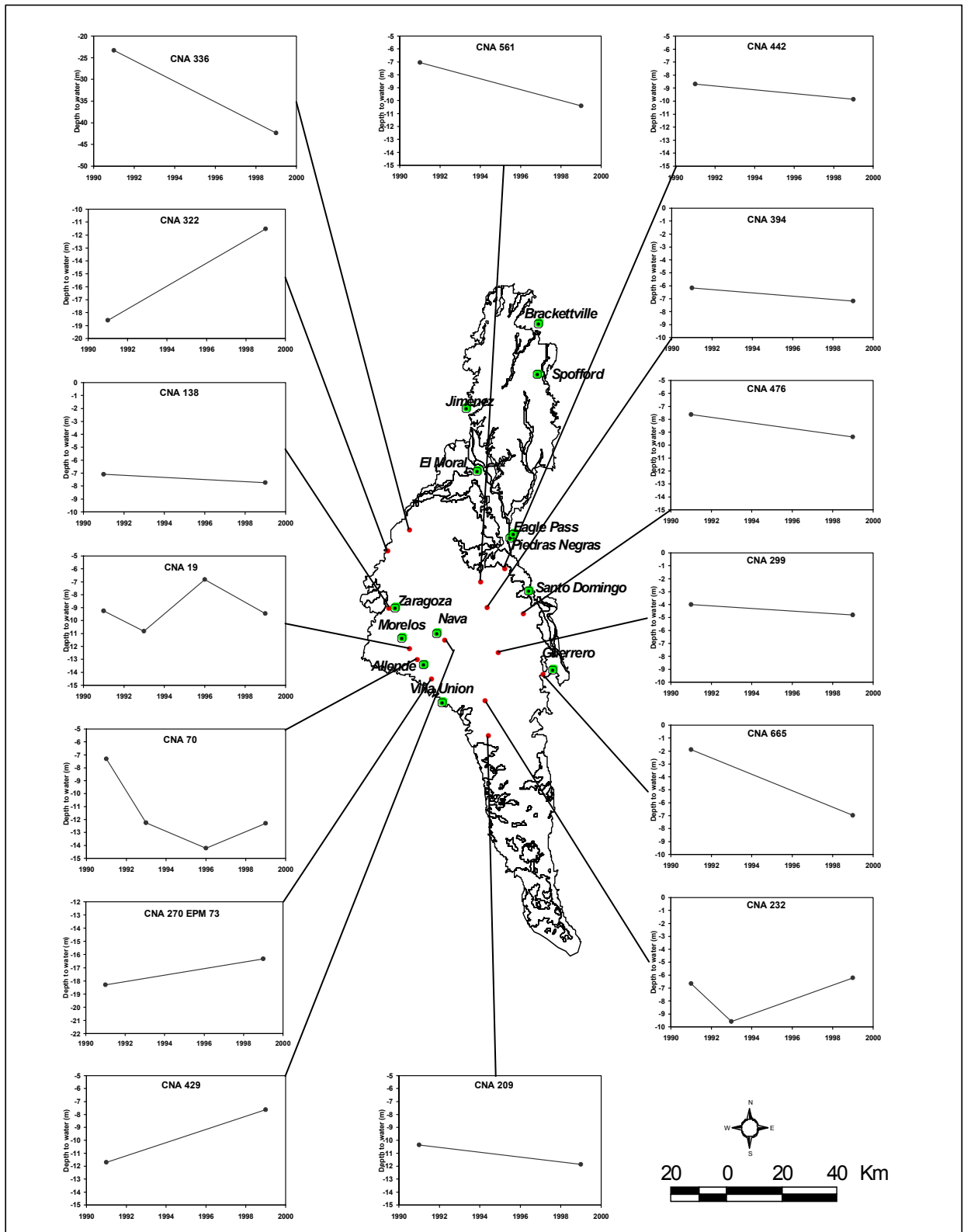
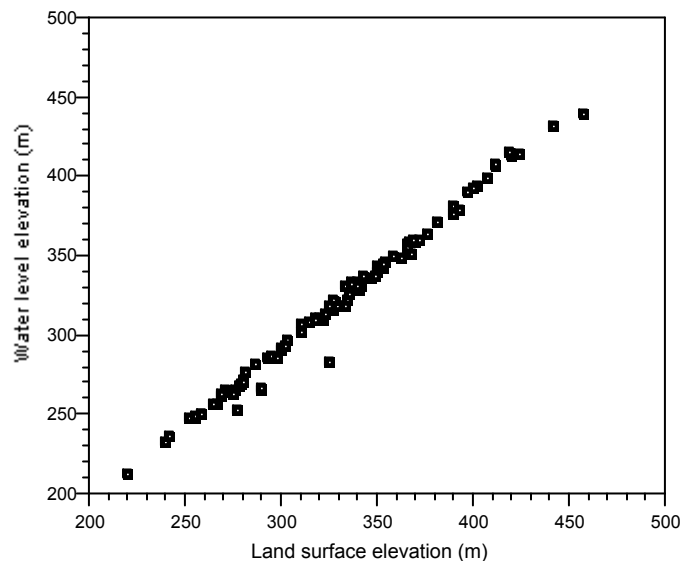


Figure 3.3 Time series well hydrographs for the Allende-Piedras Negras Valley aquifer (source of data, U.S.-Mexico Foundation for Science – FUMEC)

resulted in stationary or rising water levels. Well hydrographs for CNA 70 and 232 give a more detailed account of the changes in aquifer storage through time. They show storage depletion from 1991 to 1996 followed by a rebound from 1996 to 1999. According to FUMEC (1999), some of the irrigation wells active during 1996 have been later abandoned because of poor construction or simply because it had become uneconomical for the small irrigators to continue pumping them.

In 1999, depths to groundwater in the Allende-Piedras Negras Valley aquifer ranged from 2.2 m to 42.3 m below land surface. Shallow water levels (less than 10 m below land surface) were encountered in most of the wells regardless of location. The good correlation between the topography and water levels in wells confirms that the aquifer is unconfined (figure 3.4). The water table deepens to approximately 25 m south of the Río San Antonio and Río Escondido confluence. This is the area affected by the dewatering operations at the Micare coal mine.



**Figure 3.4 Graph showing a linear relationship between land surface elevations and water levels in the Allende-Piedras Negras Valley aquifer. Sources of data: U.S. Mexico Foundation for Science – FUMEC and Instituto Nacional de Estadística, Geografía e Informática – INEGI).**

### **Recoverable groundwater resources**

Estimates of the quantity of water for the Allende-Piedras Negras Valley aquifer cannot be accurately derived because lithologic and geophysical records are not sufficient to permit analysis. Total quantity of water is estimated by calculating the volume of saturated fill between the water table and bedrock surface and by multiplying this volume by 0.22, an average specific yield deemed typical for this kind of aquifer material. Saturated aquifer thicknesses of zero to 10 m on the Texas side (Bluntzer, 1992) and 10 to 60 m on the Coahuila side (FUMEC, 1999) were used in these computations. It is estimated that the total amount of water stored in the Allende-Piedras Negras Valley aquifer is about 24,500 hm<sup>3</sup>. Of this amount, 900 hm<sup>3</sup> are stored in the Texas part of the aquifer and 23,600 hm<sup>3</sup> are stored in the Mexican part of the aquifer. This figure does not include water stored in the Cretaceous bedrock. The distribution of saturated thickness and well yields suggest that the best potential for groundwater development is in Coahuila, particularly between Rio Grande and the Villa Union parallel. Bluntzer (1992) estimates that, during wet years, the aquifer in the Quemado Valley would have about 100 hm<sup>3</sup> of groundwater in storage that is available for development, of which 75 hm<sup>3</sup> are physically recoverable by wells. During drought, approximately 75 hm<sup>3</sup> of water would be in total storage with 56 hm<sup>3</sup> available for extraction by wells.

### **Recharge areas**

The Allende-Piedras Negras Valley aquifer is recharged in part by direct infiltration of precipitation on the valley floor. The annual potential evapotranspiration in

Piedras Negras Valley is four to six times greater than the yearly precipitation rate (CFE, 1979) suggesting that direct percolation of rainwater through the basin floor may take place only following sustained rains. Additional precipitation recharge to the basin occurs within the Cretaceous highlands (the Edwards Plateau and the Peyotes anticline near Allende, Morelos, and Zaragoza bordering the alluvial basin). Large arroyos dissecting these highlands and the basin fill can convey substantial quantities of runoff during episodic wet years and act as pathways for focused recharge. Cross-formational flow from the underlying bedrock into the alluvial fill can occur locally through fractures and faults. Major springs issuing from Upper Cretaceous rocks in the Peyotes area (see previous chapter for description) provide substantial input to the Allende-Piedras Negras Valley aquifer between Zaragoza and Alamos. The return flow from irrigation and seepage from unlined canals can account for most of the aquifer recharge in areas where these operations exist. Prominent examples of man-made diversions are the Maverick County canal and the canal network between Villa Union and Zaragoza.

According to Bluntzer (1992), the Rio Grande floodplain in the Quemado Valley receives an average  $6.2 \text{ hm}^3$  of recharge every year, of which some 72 percent or  $4.5 \text{ hm}^3$  is from canal seepage and from irrigation return flow. Further quantification of the amounts and spatial variability of recharge to the alluvial aquifer is not feasible with the available information.

### **Discharge areas**

Groundwater is lost from the Allende-Piedras Negras Valley aquifer by irrigation pumping; by subsurface seepage to the Rio Grande, Río Escondido, and other gaining

reaches in the region; by leakage to drains; and, possibly, by cross-formational flow into the underlying Cretaceous bedrock. Phreatophytes account for some evapotranspirative discharge along the Rio Grande channel, Las Moras Creek, and canal laterals.

Water is artificially discharged from the aquifer by numerous wells used for domestic, stock, irrigation, and public water supply. Most of the active wells are located in Coahuila between the Rio Grande floodplain and El Amole creek. The greatest concentration of wells on the Texas side is in the Quemado Valley of northwestern Maverick County.

#### KINNEY COUNTY

<b>Year</b>	<b>Municipal</b>	<b>Manufact.</b>	<b>Power</b>	<b>Mining</b>	<b>Irrigation</b>	<b>Livestock</b>	<b>Total use</b>
1980	0.01	-	-	-	-	0.11	0.12
1984	0.01	-	-	-	-	0.09	0.09
1985	0.01	-	-	-	-	0.08	0.09
1986	0.01	-	-	-	-	0.10	0.11
1987	-	-	-	-	-	0.11	0.12
1988	-	-	-	-	-	0.12	0.12
1989	0.01	-	-	-	-	0.11	0.12
1990	0.04	-	-	-	-	0.11	0.15
1991	0.04	-	-	-	-	0.12	0.16
1992	0.04	-	-	-	-	0.12	0.16
1993	0.04	-	-	-	-	0.11	0.15
1994	0.04	-	-	-	-	0.10	0.14
1995	0.05	-	-	-	-	0.10	0.14
1996	0.05	-	-	-	-	0.08	0.13
1997	0.05	-	-	-	-	0.07	0.12

**MAVERICK COUNTY**

<b>Year</b>	<b>Municipal</b>	<b>Manufact.</b>	<b>Power</b>	<b>Mining</b>	<b>Irrigation</b>	<b>Livestock</b>	<b>Total use</b>
1980	1.21	0.01	-	0.00	0.00	1.26	2.47
1984	0.31	0.01	-	0.24	0.50	0.21	1.26
1985	0.40	0.01	-	0.28	0.74	0.20	1.63
1986	0.19	0.01	-	0.00	0.00	0.20	0.40
1987	0.26	-	-	0.26	0.00	0.15	0.68
1988	0.03	-	-	0.26	1.86	0.10	2.25
1989	0.29	-	-	0.24	0.21	0.10	0.85
1990	0.40	-	-	0.24	1.86	0.11	2.62
1991	0.46	-	-	0.15	1.92	0.11	2.64
1992	0.30	-	-	0.15	1.98	0.11	2.54
1993	0.28	-	-	0.15	0.00	0.12	0.55
1994	0.43	-	-	0.15	0.06	0.14	0.79
1995	0.42	-	-	0.15	0.23	0.09	0.89
1996	0.29	-	-	0.15	0.25	0.06	0.74
1997	0.27	-	-	0.15	0.00	0.06	0.48

**Table 3.1 Historical groundwater use, Kinney and Maverick counties, Texas, 1980 to 1997.**  
**Water quantity in hm<sup>3</sup>. Source of data: TWDB water use survey.**

Historical groundwater use data, including pumpage from the Cretaceous bedrock, are available for the Texas side of the aquifer (table 3.1). From 1980 through 1997, an average of 1.5 hm<sup>3</sup> of groundwater was pumped annually from the Allende-Piedras Negras Valley aquifer in Texas. Over 90 percent of this groundwater was used to meet needs within Maverick County. Irrigation use in this county accounts for 46 percent of the annual average groundwater pumpage, whereas municipal and livestock uses have claimed 0.39 hm<sup>3</sup> (26 percent) and 0.31 hm<sup>3</sup> (20 percent) respectively of the annual groundwater production on the Texas side of the aquifer.



## Groundwater quality

### General hydrochemistry

General groundwater quality in the Allende-Piedras Negras Valley aquifer is shown in the regional Stiff map (figure 3.5) created with data of various vintages. In Coahuila most of the available data come from wells sampled in 1996. Several wells, located principally south of El Amole River have been sampled in 1980. On the Texas side, the most recent information available is from 1992 through 1997 and pertains to wells in the Rio Grande floodplain. With one exception, all water quality data for the wells north of the Spofford parallel are 1938 vintage.

Groundwater in both Coahuila and Texas is predominantly fresh to slightly saline with TDS concentrations between 1,000 mg/l and 3,000 mg/l. Seven wells located on the edges of the basin south of Guerrero and one north of Eagle Pass have TDS concentrations ranging from 3,100 mg/l to 30,500 mg/l. Low-TDS groundwaters are indicated by the blue, narrow diagrams in figure 3.5 and occur within the aquifer recharge areas (Edwards Plateau between Bracketville and Spofford, and along Lomerio Peyotes between Zaragoza and Villa Union). Salinities increase generally downgradient as groundwater dissolves aquifer minerals along its flowpath towards the Rio Grande and areas of groundwater pumpage. Several wells located in a north-south trending band between La Compuerta Creek and Nava and between the creeks of Las Cuevas and La Salada, Coahuila were pumping slightly saline groundwater (see figure 3.5). Their chemical composition is different from the other recharge area wells west of the Villa Union meridian. The predominance of sulfate and calcium ions in the slightly saline

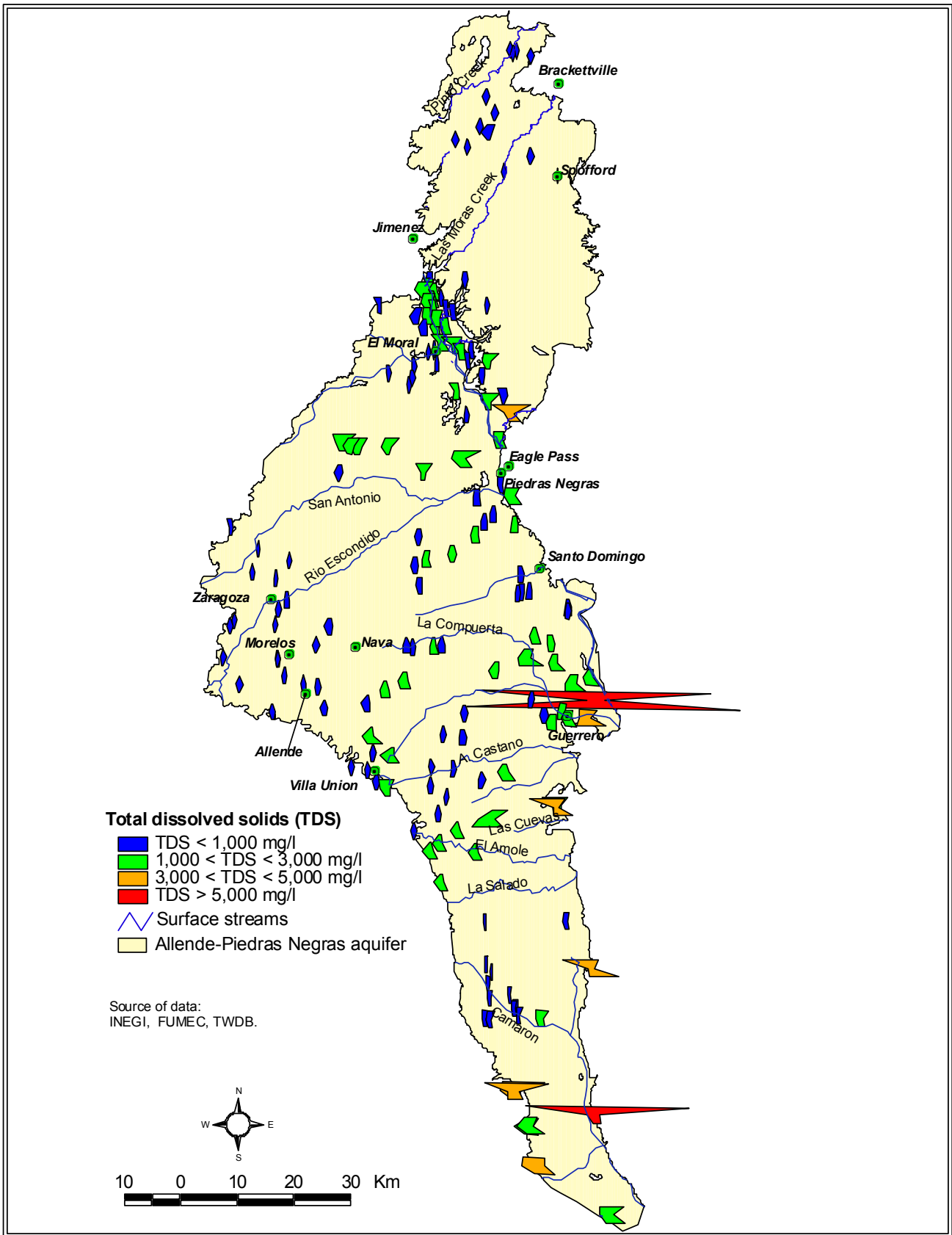


Figure 3.5 Stiff diagrams illustrating hydrochemical types for the Allende-Piedras Negras Valley aquifer.

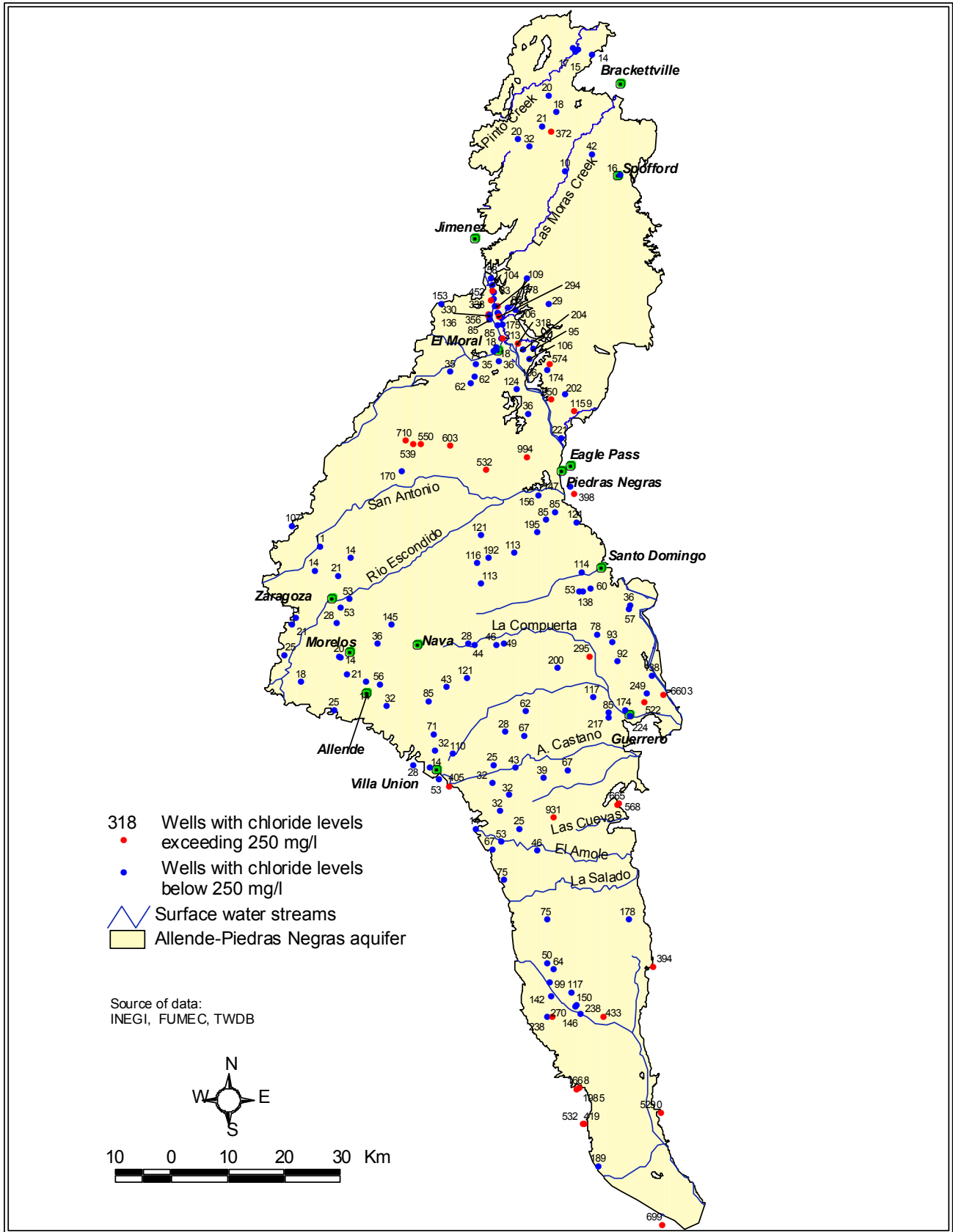


Figure 3.6 Map showing the distribution of chloride in the Allende-Piedras Negras Valley aquifer.

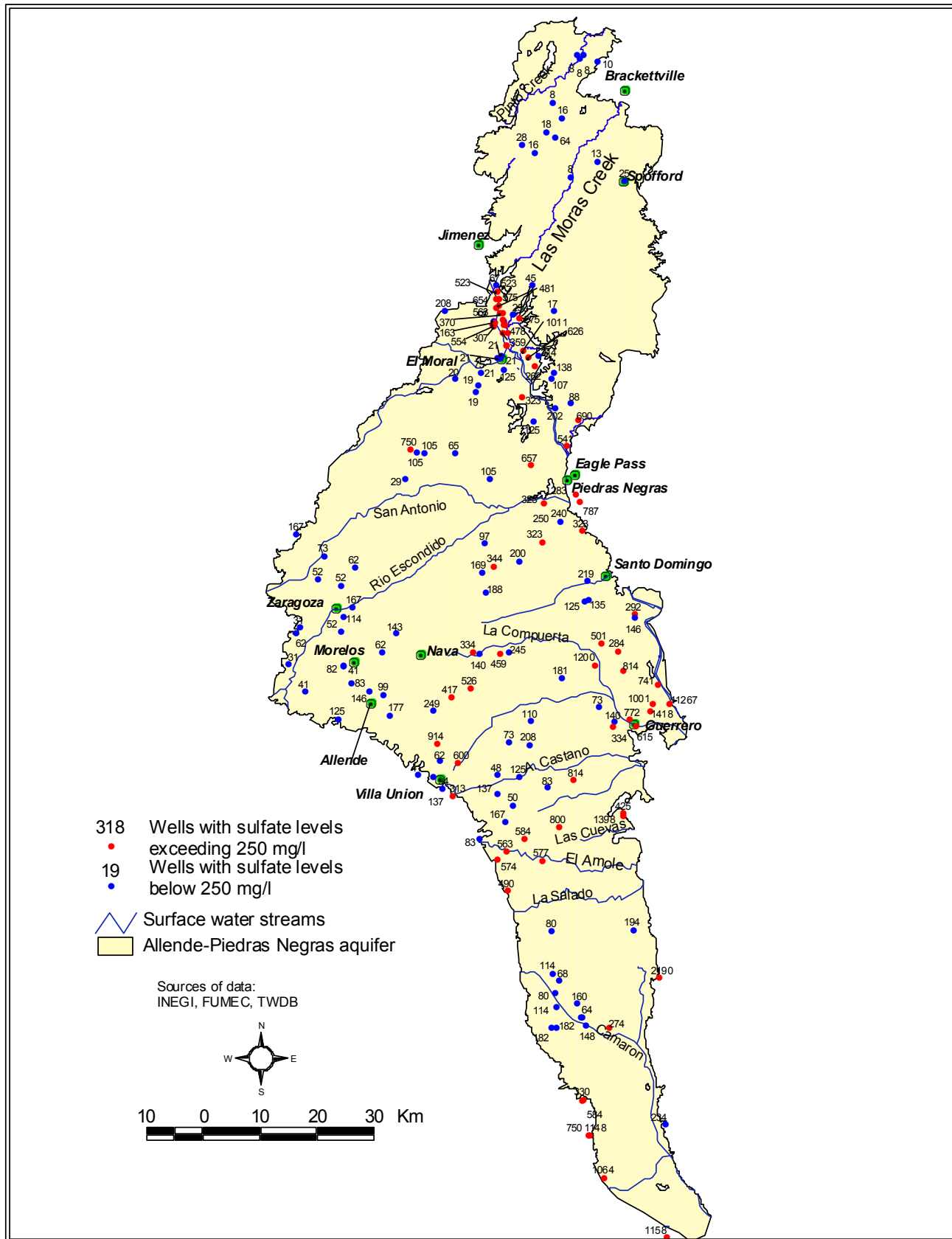


Figure 3.7 Map showing the distribution of sulfate in the Allende-Piedras Negras Valley aquifer.



waters suggests that the dissolution of evaporitic minerals such as gypsum may be one of the chemical processes impacting the groundwater quality. The likely source for gypsum are the Lower Cretaceous McKnight Formation of the Maverick Basin, part of the underlying Edwards-Trinity aquifer (see the previous section). Cross-formational flow from the Edwards-Trinity aquifer is the main recharge mechanism to the Allende-Piedras Negras Valley aquifer in the Peyotes area (Batzner, 1976). It is thus possible that slightly saline, sulfate-rich water from the McKnight Formation may be upwelling and mixing with the fresh Allende-Piedras Negras groundwater.

Samples from 186 wells within the study area had analyses of major and minor ions. Of these, 72 samples exceeded the U. S. Environmental Protection Agency secondary standards for sulfate (figure 3.7). Thirty-five samples surpassed the secondary standards for chloride (figure 3.6), and six samples had nitrate (as  $\text{NO}_3^-$ ) concentrations above the maximum contaminant level (figure 3.8). In the United States, maximum contaminant levels are set at 250 mg/l for sulfate and chloride (secondary standards) and 44.3 mg/l for nitrate as  $\text{NO}_3^-$ .

Many of the high sulfate and chloride concentrations and all the high-nitrate samples come from irrigation wells along the Rio Grande Valley between Eagle Pass and Jimenez. Salts in irrigation water become concentrated in soils due to low atmospheric moisture and high evaporation rates. These salts can be readily remobilized by leaching to the shallow aquifer table. Increasing salinities in groundwater in the river valley (figure 3.5) generally reflects the tendency for salts to be recycled in irrigation water, to return to the Rio Grande, and then to be reapplied to crops downstream (figure 3.9). This

process is a basic function of evaporation, consumptive use, and salt-enriched irrigation return flow (Hibbs and Boghici, 1999).

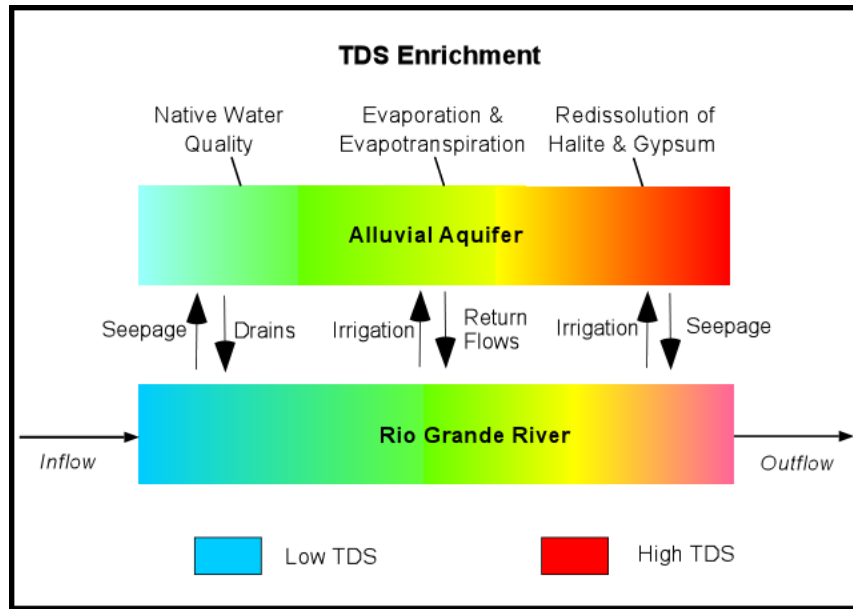


**Figure 3.9 Mechanisms of groundwater salinization through aquifer – river interactions. Modified from Hibbs and Boghici (1999).**

Four general water types could be identified based on their hydrochemical signatures (figure 3.10):

- (1) A Ca-Mg-HCO<sub>3</sub> facies encountered in fresh groundwaters from the El Moral and Zaragoza-Villa Union-Nava-Guerrero regions of Coahuila and from the Edwards Plateau uplands of Texas. Lenses of predominantly fresh Ca- HCO<sub>3</sub> facies groundwater have been mapped west-southwest of Guerrero along the Castanos Creek and just south of El Moral, Coahuila.

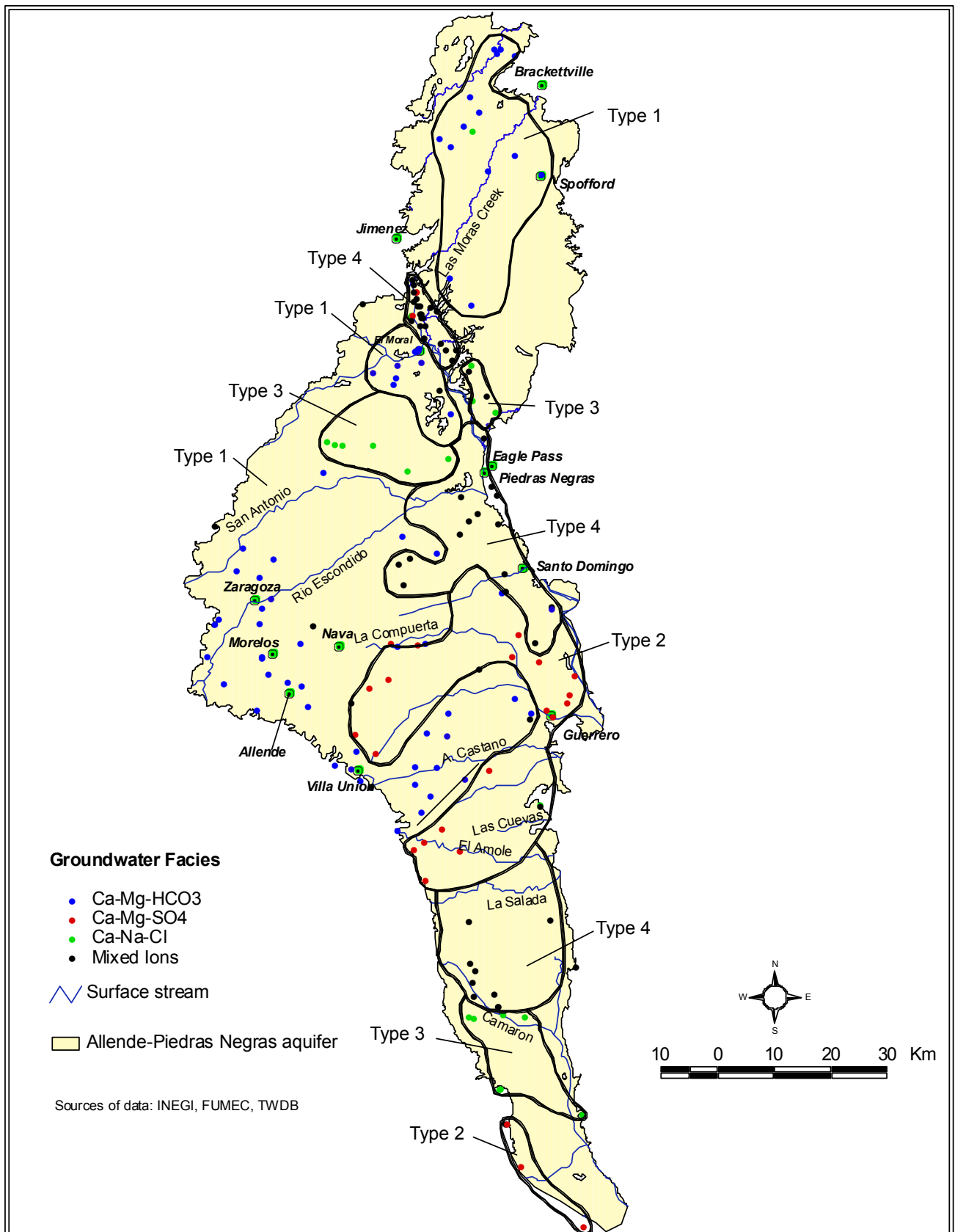
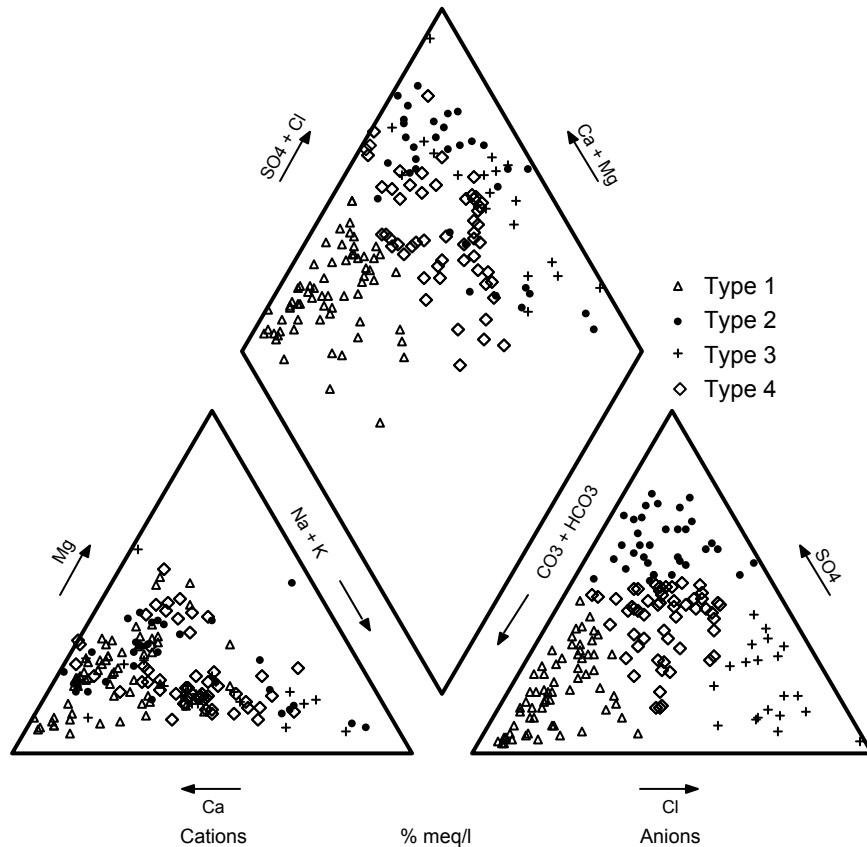


Figure 3.10 Areal distribution of hydrochemical facies in the Allende-Piedras Negras Valley aquifer.





**Figure 3.11 Piper diagram showing major ion compositions for groundwater in the Allende-Piedras Negras Valley aquifer. Source of data: Texas Water Development Board and Instituto Nacional de Estadística, Geografía y Informática.**

(2) A Ca-Mg-SO<sub>4</sub> facies characteristic of fresh and slightly saline groundwater in the Guerrero-Villa Union-Nava region. Groundwater samples representative of this facies are distributed in an arcuate belt stretching north from Villa Union to La Compuerta creek, turning east-southeast to Guerrero, and then southwest towards the El Amole-La Salada interfluvium.

(3) A Ca-Na-Cl facies recognized in slightly saline groundwater from wells west of Piedras Negras, Coahuila, along the Rio Grande Valley between Eagle Pass, Texas

and El Moral, Coahuila. This facies has also been identified in fresh to saline samples from wells south of Camaron Valley, Coahuila.

- (4) A Mixed Ion facies was mapped in Coahuila between the La Salada and Camaron valleys, the area delimited by La Compuerta to the south, Río Escondido to the north, and the Nava and Guerrero meridians to the west and east, respectively. Similar chemical characteristics were also identified in groundwater sampled along the Río Grande plain upstream from El Moral, Coahuila.

The Piper diagram suggests that water mixing processes, carbonate and evaporite dissolution, and ion exchange reactions may be controlling the groundwater chemical composition (figure 3.11).

Groundwaters of type 4 appear to be the result of mixing between endmember waters of types 1, 2, and 3. If two waters mix, the composition of the mixture will lie on a straight line joining the endmembers. The fresher type 4 waters plot along mixing lines between waters of types 1 and 2, and 1 and 3, respectively (figure 3.11). Similarly, mixing between 2 and 3 results in a slightly saline mixture of facies 4. However, the distribution of groundwater types (figure 3.10) and the groundwater flow directions towards the Río Grande (figure 3.2) only partially support this mixing theory.

Fresh Ca-Mg-HCO<sub>3</sub> waters of type 1 in the Zaragoza-Nava-Allende region flow downgradient towards the east where they mix with the type 2 sulfate-rich waters south of La Compuerta and with type 3 chloride-rich waters west of the Río San Antonio-Río Escondido confluence. Similarly, mixing between type 1 groundwater immediately adjacent to the Río Grande and type 2 groundwater just upstream from Eagle Pass may

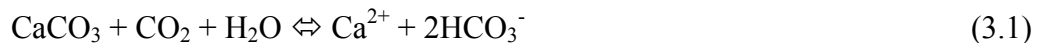
result in the type 4 water encountered in Quemado Valley. The absence of hydraulic head data for the segment of the aquifer south of El Amole Valley precludes the interpretation of groundwater facies distribution in that region.

### **Chemical processes**

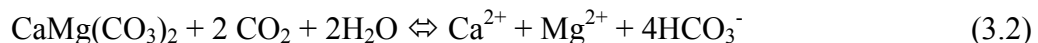
The variable hydrochemical signature in Allende-Piedras Negras Valley ground water (figures 3.5, 3.10, and 3.11) can be attributed to the varying solubilities of aquifer minerals, cation exchange, and mixing. Calcium and magnesium concentrations are controlled by the weathering of Ca- and Mg-bearing minerals, such as calcite and dolomite, and also by sulfate dissolution and by ion exchange processes.

Following are the governing equations for prominent mineral dissolution and precipitation reactions occurring in aqueous systems.

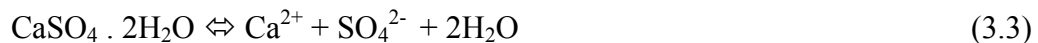
Calcite dissolution and precipitation:



Dolomite dissolution:



Gypsum dissolution:



Halite dissolution:



Ion exchange:



A plot of sodium against chloride (figure 3.12) indicates that some sodium and chloride may come from halite.

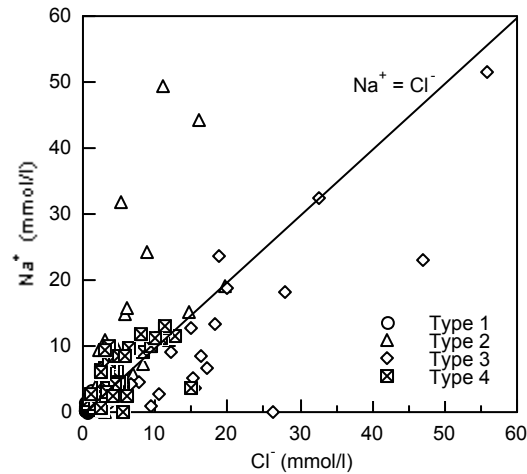


**Figure 3.12** Plot of  $\text{Na}^+$  versus  $\text{Cl}^-$

The predominance of sodium over chloride in some of the type 2 waters suggests a source of sodium beyond halite dissolution, possibly ion exchange between dissolved calcium or magnesium and adsorbed sodium. This hypothesis is discussed later in this section.

Many of the type 3 waters come from irrigation wells and show sodium to chloride ratios of less than unity. Mayer (1997) describes a similar situation in irrigation groundwater samples in the Dell City area of Texas and hypothesizes that reverse ion exchange, in which dissolved sodium is exchanged for adsorbed calcium, may take place. A succinct discussion of ion exchange equilibrium is offered below.

Equation 5 yields the following selectivity coefficient for calcium-sodium exchange (Drever, 1988, p. 92):

$$k = \frac{Na_2X[Ca^{2+}]}{CaX[Na^+]^2} \quad (3.6)$$

where  $X$  denotes mole fraction in the solid phase and the terms inside the brackets denote concentrations in groundwater. The selectivity coefficient is not constant, but changes as a function of the ratio of sodium to calcium on the solid. These changes in  $k$ , however, are much smaller than those caused by concentration changes in groundwater (Sayles and Mangelsdorf, 1979). The relationship between the concentrations of dissolved calcium and sodium are related to the adsorbed mole fraction as follows:

$$\frac{Na_2X}{CaX} = k \frac{[Na^+]^2}{[Ca^{2+}]} \quad (3.7)$$

Equation 3.7 shows that the ratio of adsorbed species is proportional to the relative concentrations of dissolved species. However, because of the squared term  $[Na^+]^2$  in equation 3.7, a uniform change in total concentration, such as by evaporation or dilution, will also change the ratio of adsorbed species. Bohn et al. (1985) termed this the “valence dilution effect”, whereby as water is being diluted, the exchange medium will selectively remove calcium from the groundwater. Conversely, sodium will be removed from solution by the exchange solid as the water is being concentrated by evaporation. It then follows that, in samples with sodium to chloride ratios of less than unity, evaporative concentration of irrigation water may favor the adsorption of sodium over calcium, and thus would lead to low sodium to chloride ratios such as those encountered in type 3 groundwaters.

Figure 3.13 shows the relationship between the concentration of calcium and magnesium versus bicarbonate. If calcium and magnesium originate entirely from

dissolution of carbonates, the molar ratio of Ca and Mg to  $\text{HCO}_3^-$  would be 0.5 (Sami, 1992). Ratios less than 0.5 may be attributed to the loss of Ca and Mg through cation exchange, whereas ratios greater than 0.5 may indicate additional sources of Ca and Mg, possibly associated with the dissolution of sulfate minerals. Some of the type 1 data points plot on the 1:2 line, although the rest of the samples are above the 1:2 line, indicating an additional source of calcium and magnesium.

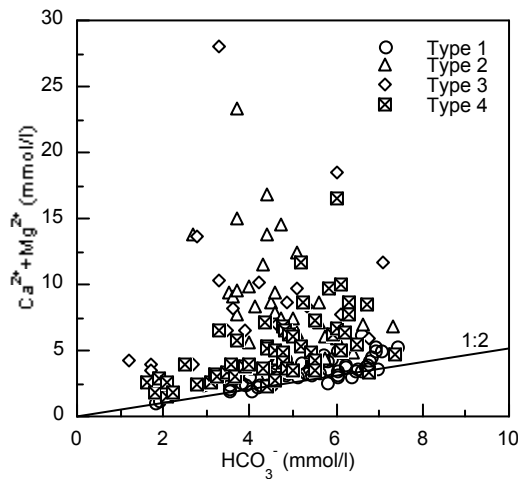


**Figure 3.13 Plot of Ca+Mg versus  $\text{HCO}_3^-$**

No specific mention exists in the geologic literature regarding the presence of evaporite deposits in the Allende-Piedras Negras Valley aquifer area. However, sulfate-rich groundwater from the underlying McKnight Formation (Lower Cretaceous) may be upwelling and mixing with the fresh Allende-Piedras Negras groundwater in the Guerrero-Villa Union-Nava region (Batzner, 1976).

To account for the calcium derived from gypsum dissolution, calcium and magnesium molar concentrations are summed up and plotted against the sum of sulfate and half of bicarbonate concentration (figure 3.14). The major ion water chemistry

suggests that the calcium, magnesium, sulfate, and bicarbonate present in the water are the result of a simple dissolution of the available dolomite or magnesium-calcite along with gypsum or anhydrite. In an ideal case, such dissolution reactions would result in these samples plotting on a straight line through the origin with a slope of one. In figure 3.14, type 1 and 4 waters plot along lines with slopes close to unity, have good coefficients of correlation ( $R^2 = 0.98$  and  $0.86$  respectively), and intercepts near zero.

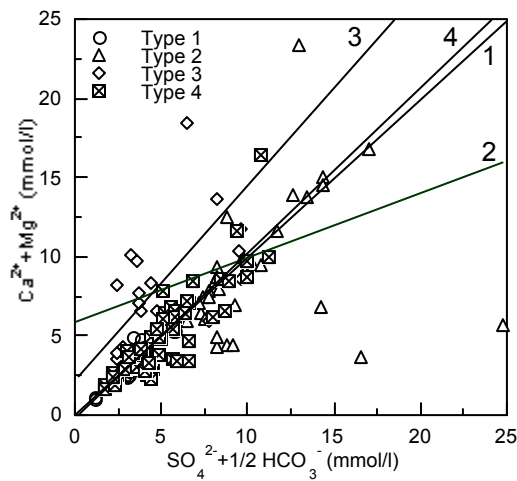


**Figure 3.14** Plot of  $\text{Ca}+\text{Mg}$  versus  $\text{SO}_4+\text{HCO}_3$

Samples of types 2 ( $R^2 = 0.29$ ) and 3 ( $R^2 = 0.62$ ) define trend lines with slopes of 0.3 and 1.3 respectively. The slope of the type 2 trend line suggests that there is a partial loss of calcium plus magnesium relative to the amount of bicarbonate and sulfate present. This is consistent with a partial cation exchange where some of the calcium plus magnesium is lost from the water and sodium is gained. This interpretation explains why most of these water samples have a higher ionic concentration of sodium than chloride (see figure 3.12), which indicates that there is a source of sodium beyond halite dissolution.

Figure 3.15, a plot of  $(\text{Na}^+ - \text{Cl}^-)$  against  $(\text{Ca}^{2+} + \text{Mg}^{2+} - \text{SO}_4^{2-} - 0.5\text{HCO}_3^-)$ , best illustrates the interrelationship between calcium, magnesium, and sodium, as it allows for direct evaluation of the significance of exchange and mineral weathering on concentrations of these cations (Sami, 1992). The quantity  $(\text{Na}^+ - \text{Cl}^-)$  represents "excess" sodium, that is, sodium coming from sources other than halite dissolution, assuming all chloride is derived from halite. The quantity  $(\text{Ca}^{2+} + \text{Mg}^{2+} - \text{SO}_4^{2-} - 0.5\text{HCO}_3^-)$  represents the calcium and/or magnesium coming from sources other than gypsum and carbonate dissolution. These two quantities represent the maximum amount of sodium and calcium plus magnesium available for ion exchange processes.

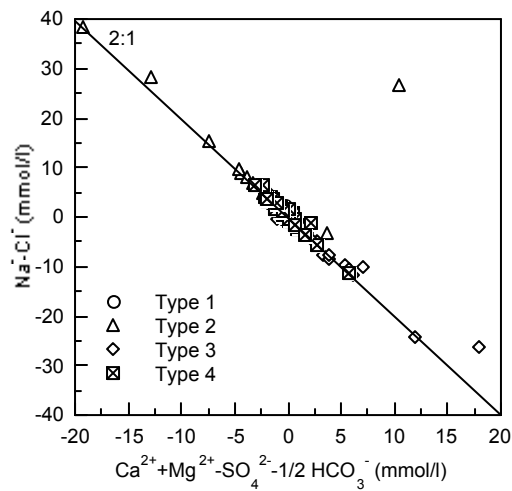


**Figure 3.15** Plot of  $\text{Na}-\text{Cl}$  versus  $\text{Ca}+\text{Mg}-\text{SO}_4-0.5 \text{HCO}_3$

The linearity indicates a highly correlated relationship between the increase of sodium and the loss of the divalent cations calcium and magnesium. Specifically, sodium increases at slightly more than twice the loss rate of calcium and magnesium, as would be expected from cation exchange. Waters undergoing exchange of calcium and magnesium



for bound sodium on clays will gradually become of sodium-sulfate type. The fact that calcium is still the dominant cation in most of these samples indicates that exchange reactions have not yet occurred extensively. However, a close examination of these data shows that the cation exchange is somewhat more involved than this. There is more magnesium in the water than can be accounted for by the dissolution of dolomite. It is believed that these data also represent a significant amount of ionic exchange where calcium is lost and magnesium is gained.

### References

- Barnes, V. E., 1976, Crystal City – Eagle Pass sheet: The University of Texas at Austin, Bureau of Economic Geology, Geologic Atlas of Texas, scale 1:250,000.
- Barnes, V. E., 1977, Del Rio sheet: The University of Texas at Austin, Bureau of Economic Geology, Geologic Atlas of Texas, scale 1:250,000.
- Batzner, J. C., 1976, The hydrogeology of Lomerio de Peyotes, Coahuila, Mexico: Unpublished M.S. thesis, University of New Orleans, 64 p.
- Bennett, R. R. and Sayre, A. N., 1962, Geology and ground-water resources of Kinney County, Texas: Texas Water Development Board Bulletin 6216, 163 p.
- Bluntzer, R. L., 1992, An overview report on the ground-water conditions in the Quemado Valley of northwestern Maverick County, Texas: Texas Water Development Board unpublished report, 8 p.
- Bohn, H. L., McNeal, B. L., and O'Connor, G. A., 1985, Soil Chemistry, 2<sup>nd</sup> edition: John Wiley & Sons, 341 p.
- Caffey, K. C., 1978, Depositional Environments of the Olmos, San Miguel, and Upson Formations (Upper Cretaceous), Rio Escondido Basin, Coahuila, Mexico: Unpublished M.A. Thesis, Department of Geological Sciences, The University of Texas at Austin, 86 p.

- Comisión Federal de Electricidad (CFE), 1979, Estudio Geohidrológico de Gran Visión en el Área Comprendida entre Nuevo Laredo y Lampazos Estados de Tamaulipas y Nuevo León: Informe No. 79023, 20 p.
- Drever, J. I., 1988, The geochemistry of natural waters: Englewood Cliffs, N.J.: Prentice-Hall, 437 p.
- Getzender, F. M., 1930, A geologic section of the Rio Grande embayment, Texas and implied history: American Association of Petroleum Geologists Bulletin, v. 14, p. 1425-37.
- Hibbs, B. J. and Boghici, R., 1999, On the Rio Grande aquifer: flow relationships, salinization, and environmental problems from El Paso to Fort Quitman, Texas: Environmental & Engineering Geoscience, vol. V, no. 1, Spring 1999, p. 51-59.
- Holt, C. L. R., Jr., 1956, Geology and ground-water resources of Medina County, Texas: Texas Board of Water Engineers Bulletin 5601, 277 p.
- Mayer, J. R., 1995, The role of fractures in regional groundwater flow – field evidence and model results from the basin-and-range of Texas and New Mexico: Unpublished Ph.D. dissertation, Department of Geological Sciences, The University of Texas at Austin, 221 p.
- Sami, K., 1992, Recharge mechanisms and geochemical processes in a semi-arid sedimentary basin, Eastern Cape, South Africa: Journal of Hydrology, v. 139, p. 27-48.

## **CHAPTER 4: CARRIZO – WILCOX AQUIFER**

This section describes the Carrizo-Wilcox aquifer in the study area (figure 1.2). The discussion includes general information on aquifer location and extent, geology and water-bearing characteristics, aquifer properties, potentiometric surface, and hydrochemistry.

### **Location and extent**

The Carrizo-Wilcox aquifer is contained in the terrigenous clastic deposits of the Wilcox Group and the overlying Carrizo Formation of the Claiborne Group. The aquifer extends from northeastern Mexico into Texas, Arkansas, and Louisiana.

In the study area the Carrizo-Wilcox aquifer underlies approximately 17,500 km<sup>2</sup> in both Mexico and the United States, of which 14,200 km<sup>2</sup> are in parts of Maverick, Dimmit, Uvalde, La Salle, Zavala, and Webb counties, Texas. South of the Rio Grande, the Carrizo-Wilcox aquifer extends under a 3,300-km<sup>2</sup> area spanning the Mexican States of Coahuila, Nuevo Leon, and Tamaulipas. The portion of Texas discussed in this section is part of the Winter Garden Area, which is defined as the region of Texas between the San Marcos and Rio Grande rivers where the Carrizo Formation contains fresh to slightly saline water (Klemt et al., 1976). Within the Winter Garden Area is the Winter Garden District, an agricultural region which relies on irrigation for late winter and early spring vegetable production in Dimmit, Zavala, and eastern Maverick counties (Klemt et al., 1976).

The Carrizo-Wilcox aquifer lies within the Río Bravo – Rio Grande hydrologic basin of Coahuila, Nuevo Leon, Tamaulipas, and Texas. Physiographically, the study

area belongs to the Burgos Basin province (Lalo, 1979) in Mexico and to the South Texas Coastal Plains physiographic province (McCoy, 1991) in the U. S.

According to the U.S. Department of Housing and Urban Development (1988), the largest cities in the region are Laredo (population 188,166) and Nuevo Laredo (estimated population 650,000). Other cities in the study area are La Pryor, Batesville, Crystal City, Carrizo Springs, Asherton, Cotulla, Encinal, and El Cenizo on the Texas side and Villa Hidalgo, Colombia, San Ignacio, and La Jarita on the Mexican side.

The Carrizo-Wilcox aquifer is bound to the west and north by the Midway Group-Wilcox Group geologic contact (figure 1.4). To the east, its downdip limit is the line of 3,000 mg/l total dissolved solids in groundwater. For the purpose of this study, the aquifer limits coincide with the study area boundary.

### **Stratigraphy and structure**

The Carrizo-Wilcox aquifer is contained mainly in Tertiary sand with gravel, silt, clay, and lignite intercalations deposited in a fluvial-deltaic environment. Following is a brief depositional history of the units comprising the Paleocene and lower Eocene strata in the study area.

The Rio Grande Embayment of south Texas (figure 4.1) has controlled the deposition of sediments in the southern Gulf Coast Basin beginning with the late Paleozoic (Flawn, 1961). Marine carbonates and clastics filled this depocenter until late Paleocene times, when the transgressive shoreline and coastal-plain Wilcox terrigenous clastics were deposited (Fisher and McGowen, 1967).

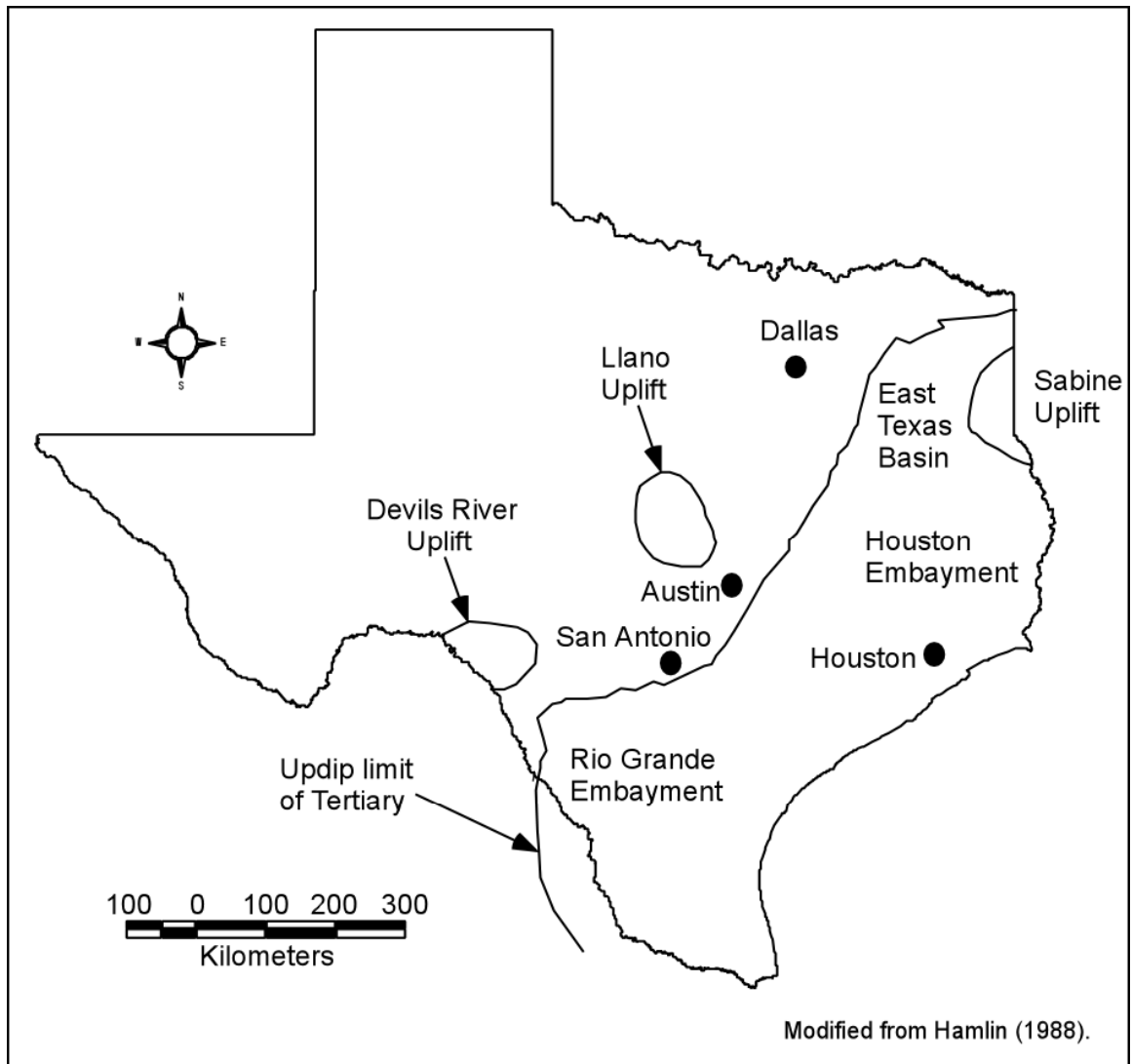


**Figure 4.1 Structural elements of the Texas Coastal Plain.**

They were followed by the deposition of the sandy, non-marine Carrizo Formation and its downdip equivalent, the upper Wilcox Group at the beginning of the Eocene, some 55 million years ago (Ma). At that time, several fluvial systems were flowing into the Rio Grande Embayment from the west, northwest, and north (figure 4.2), transporting terrigenous material eroded from elevated areas to the west and northwest of the depocenter (Belcher, 1975).

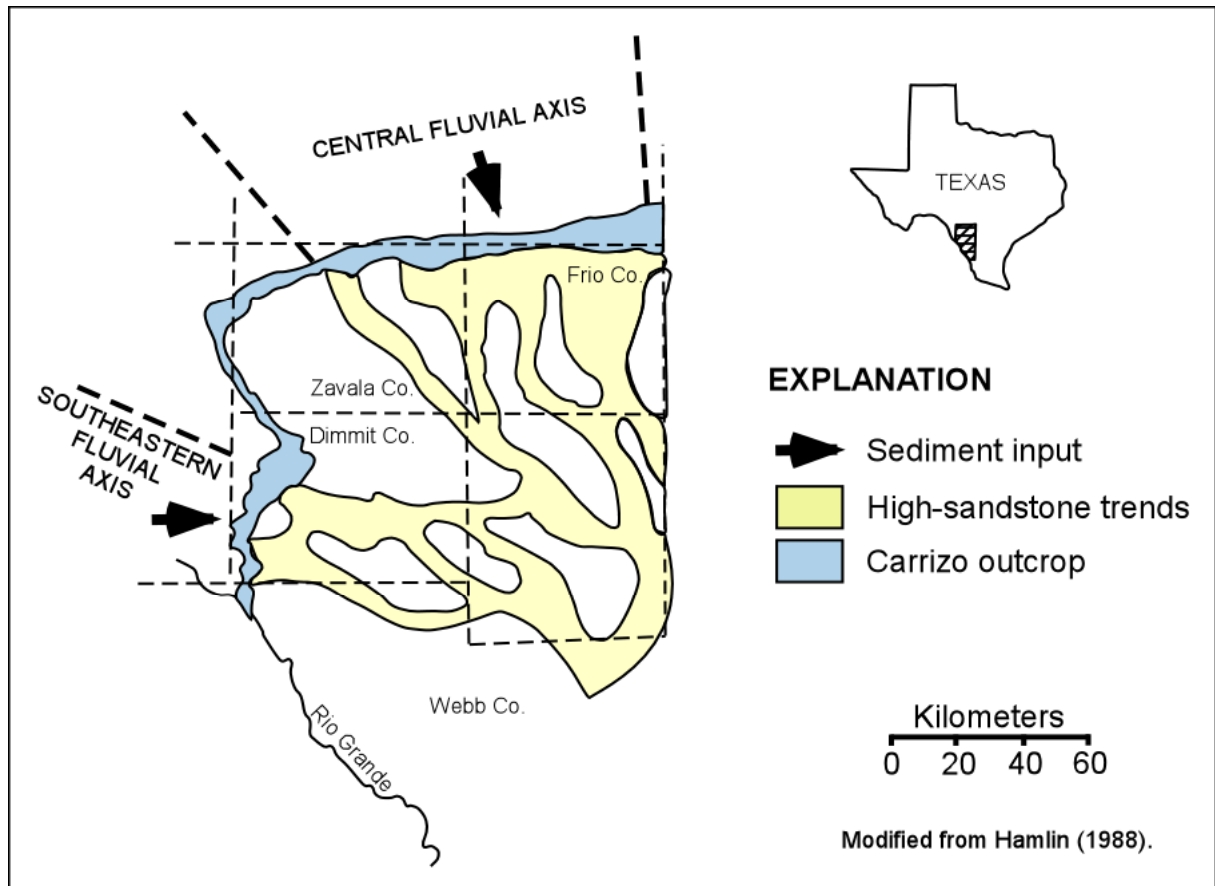


**Figure 4.2 Map of Carrizo Formation high-sandstone trends, fluvial axes, and sediment input directions in the Winter Garden area of Texas.**

Sedimentation in the Carrizo Formation was initiated by shoreline regression followed by the progradation of upper Wilcox mudstone deltas over the shelf edge. Rapid subsidence resulted in overlapping delta facies and in a slower seaward advance of Carrizo Formation - upper Wilcox Group (Hamlin, 1988). Concurrently, bed-load fluvial systems migrated coastward depositing the massive, permeable sand beds that make the Carrizo Formation such a prolific aquifer. The end of the Carrizo deposition was initiated by a marine transgression that inundated parts of the sandy coastal plain (Hamlin, 1988). Mixed alluvial sequences consisting of meandering river channels typify

the end of the Carrizo depositional episode, before the massive Bigford-Reklaw transgression inundated most of the Rio Grande Embayment (Hamlin, 1988).


The Bigford Formation, El Pico Clay, and Laredo Formation and their marine counterparts (the Reklaw, Queen City, Weches, Sparta, and Cook Mountain formations) blanketed the Carrizo during middle Eocene time. With the exception of the Sparta sands, which were deposited during a regressive episode, all other sequences enumerated above are transgressive (McCoy, 1991). Towards the end of the Eocene or approximately 37 Ma, the sea retreated, and the subaerial deposition of the Yegua Formation commenced. The humid tropical climate that characterized the early Eocene favored the growth of abundant vegetation in the study area (Habicht, 1979). Fossilized remnants such as petrified wood fragments and root structures are commonly found in the sands of the Carrizo Formation (Hamlin, 1988).

All the geologic units discussed in this section crop out in north-south striking bands on the Texas side of the study area and in a northwest-southwest direction in Mexico (figure 1.4) where they dip to the southeast. Table 4.1 shows the stratigraphic relationships between these units in the study area.

CHRONOSTRATIGRAPHY		LITHOSTRATIGRAPHY			
Series	Stage	Outcrop/shallow subsurface		Deeper subsurface (>1300 m)	
		Southwest	Northeast		
Eocene	Lutetian	El Pico Clay	Weches Fm.	Queen City Fm.	Mount Selman Formation, lower Claiborne Group
		Bigford Fm.	Queen City Fm.		
	Ypresian		Carrizo Formation	Reklaw Fm.	
		upper Wilcox		Wilcox Group	
Paleocene	Thanetian	Indio Formation	Wilcox Group		middle Wilcox
		Danian	Midway Group		lower Wilcox

Modified from Hamlin (1988)

Explanation

 Carrizo - Wilcox aquifer

**Table 4.1 Paleocene to lower Eocene stratigraphic relationships in south Texas.**

The position of the Carrizo Formation in the Eocene succession has long been the subject of debates. While early outcrop mapping by Plummer (1932) suggested that the Carrizo strata belong in the Claiborne Group, more recent subsurface studies indicated they might in fact be part of the underlying Wilcox Group (Hargis, 1962 and 1985; Eargle, 1968; Fisher, 1969; Bebout et al., 1982). For the purpose of this study, the stratigraphic relationships established by Hamlin (1988) are followed (table 4.1).

The following briefly describes the lithological and water-bearing properties of the Eocene stratigraphic units, starting with the oldest to the most recent. Descriptions are from Barnes (1976), Klemm et al. (1976), Kaiser et al. (1980), Hamlin (1988), and McCoy (1991).



## **Midway Group**

The Late Paleocene Midway Group can be up to 500 m thick (Upitis, 1998) and consists of dark gray, fossiliferous shale alternating with some sandstone and limestone intervals. The Midway Group is a confining unit and constitutes the base of the Carrizo-Wilcox aquifer described in this section.

## **Indio Formation or Wilcox Group**

The Indio Formation (known as the Wilcox Group in the subsurface) consists of alternating layers of fine-grained, thin-bedded sandstone, sandy, carbonaceous shale, and lignite. The thickness of the Indio Formation ranges from 122 to 427 m and increases southward. This formation yields fresh to brackish water to wells in Medina County, which is outside the study area boundary. In the study area very few wells are completed in the Indio Formation. They have small yields (1l/s or less) and produce brackish to saline groundwater.

At depth, the Indio-equivalent Wilcox Group consists of interbedded sand, clay, and silt, with discontinuous beds of lignite, and rare occurrences of gypsum. Wilcox sediments have a mean sand content of approximately 55 percent (Mace et al., 2000). The Wilcox yields small to moderate quantities (1 to 20 l/s) of fresh to brackish water to wells in Maverick, Zavala, and Dimmit counties on the Texas side. On the Mexican side, wells with yields under 1 l/s pump fresh to saline groundwater. The quality of water in the Wilcox group deteriorates with depth. The Wilcox Group and the overlying Carrizo Formation are commonly thought to be hydraulically connected. Klemm et al. (1976)

indicate that “the waters probably commingle to some degree, although most of the sand beds in the Wilcox Group are less permeable and most contain poorer water quality than the Carrizo Sand”.

### **Carrizo Formation**

The Carrizo Formation was named for the town of Carrizo Springs in Dimmit County, Texas (Owen, 1889). The Carrizo Formation is composed of massive, cross-bedded, medium-grained sands that range in thickness from 50 to 400 m. The formation has a mean sand content of 85 percent (Mace et al., 2000). While the overall sand content in the Carrizo Formation decreases downdip, the individual sand bodies are larger downdip (Hamlin, 1988, p.8-9). Several fine-textured marine flooding sequences occur within both the underlying Wilcox Group and the Carrizo Formation and form semi-permeable hydrologic barriers. The high permeability of these laterally connected sand bodies and the large amounts of groundwater contained in them make the Carrizo-Wilcox aquifer one of the most productive aquifers in Texas, with most of the aquifer discharge occurring during irrigation pumpage. Wells completed in the Carrizo sands on the Texas side usually have large yields (30 l/s or more) and produce fresh to brackish groundwater. On the Mexican side, the Carrizo Formation gradually thins to the southeast and displays a “major increase in clay content” (Elizondo, 1977). The few Carrizo wells recorded on the Mexican side have low yields (~0.25 l/s) and produce water of poor quality (figure 4.12).

### **Bigford Formation**

The Bigford Formation is made of calcareous, gypsiferous clays alternating with coarse, crossbedded sandstone, shale, and frequent plant remains, with the shale making up 25 percent of the formation outcrop (Eargle, 1968). The Bigford Formation thickens southwards, with thickness ranging from 60 m in Zavala County, Texas, to 240 m in Frio County, Texas. Water wells on the Texas side are reported to yield 0.2 to 6 l/s of fresh to saline water, although dual-completion wells (Bigford Formation and Carrizo Formation) can produce of up to 92 l/s. The few Bigford wells recorded on the Mexican side have low yields (0.25 l/s) and produce water of poor quality.

### **El Pico Clay**

The El Pico Clay is a confining unit comprised mostly of partly gypsiferous clays, alternating with finely grained sandstone and coal lenses. The 210 to 275 m thick formation yields small amounts of highly mineralized groundwater to stock wells.

### **Laredo Formation**

The Laredo Formation is a marine unit composed of fine-grained sandstone layers at the base grading into sandy clay and clay at the top and reaches a thickness of 180 to 210 m. In Texas, wells completed in the Laredo Formation yield up to 3 l/s to stock, household, and industrial wells.

## **Yegua Formation**

The Yegua Formation has a thickness ranging from 210 to over 300 m and is made of lignitic, sandy, laminated clay and fine-grained, massive, quartzitic sandstone. The Yegua Formation yields small amounts of brackish water to wells in its outcrop, but it can be a prolific aquifer to the northeast of the study area.

### **Aquifer properties**

Aquifer test data for the Carrizo–Wilcox aquifer are abundant in the Winter Garden district on the Texas side, and are absent on the Mexican side of the study region. Klemt et al. (1976), Hamlin (1988), Thorkildsen et al. (1989), Prudic (1991), and Mace et al. (2000) are a few of the researchers who investigated the hydraulic properties of this aquifer.

Estimates of aquifer transmissivity range from 12 to 808 m<sup>2</sup>/day with a mean of 447 m<sup>2</sup>/day; hydraulic conductivity values range from 0.4 to 16.3 m/day, with a mean of 7.5 m/day; and aquifer storativity ranges from 0.0001 to 0.00019 (Hamlin, 1988, p. 22). Klemt et al. (1976) provided hydraulic conductivity values from aquifer tests ranging from 0.4 to 15 m/day and storage coefficients of 0.25 in the outcrop area (unconfined conditions) and 0.0005 downdip (confined conditions). Klemt et al. (1976) also determined hydraulic conductivity from hydraulic tests on core samples from Carrizo wells in the Winter Garden area and from granulometric analysis of drill cuttings. The values obtained (1.6 to 38 m/day for cores and 22 to 28 m/day for drill cuttings) were greater than the estimates derived from pumping tests. Thorkildsen et al. (1989) estimated hydraulic conductivities in the Carrizo–Wilcox aquifer by using well

geophysical logs to map shale, channel, and interchannel deposits, and by assigning predetermined hydraulic conductivity values to the mapped deposits. Their assigned hydraulic conductivity values were 0.04 m/day for shales, 1 to 2 m/day for interchannel deposits, and 6 to 20 m/day for channel deposits.

Aquifer-wide transmissivity determined by Mace et al. (2000) range from 0.1 to 929 m<sup>2</sup>/day and has a geometric mean of 27.9 m<sup>2</sup>/day. Hydraulic conductivity ranges from 0.003 to 1,219 m/day and has a geometric mean of about 1.8 m/day (Mace et al., 2000, p. 32).

Hamlin (1988) noted that in the Carrizo–Wilcox aquifer, hydraulic conductivity is lithofacies-dependent. Fine-grained sediments deposited in lacustrine, floodplain, or abandoned-channel-fill environments have the lowest hydraulic conductivity. The medium- to coarse-grained alluvial system sand bodies (see figure 4.2) have the highest permeability and serve as conduits for the flow of groundwater in the aquifer (Hamlin, 1988). Various researchers have reported vertical and lateral variations in permeability within the Carrizo–Wilcox aquifer. Due to its larger sand content, the Carrizo portion of the aquifer has transmissivity and hydraulic conductivity that are higher (two and a half to eleven times higher for transmissivity and two to six times higher for hydraulic conductivity) than those of the Wilcox Group as a whole (Mace et al., 2000, p. 43). Areally, the aquifer transmissivity decreases from the east to the west, a trend that can be correlated with a westward reduction in sand content and a northeast to southwest thinning of Carrizo strata (Hamlin, 1988). On an aquifer-wide scale, hydraulic conductivity in the Carrizo–Wilcox aquifer increases from an average of 4.3 m/day in the northeast to an average of 6.7 m/day in the southwest (Prudic, 1991). His conclusion is

supported by the findings of Mace et al. (2000, p.53), who report mean hydraulic conductivity values of 2 m/day in the northeast and 8.8 m/day in the southeast. Estimates of Carrizo–Wilcox hydraulic conductivity for the Winter Garden area by Prudic (1991) range from 0.1 to 67 m/day with an average of 52 m/day and a median of 28 m/day. Using aquifer test and specific capacity data from TWDB groundwater database, Mace et al. (2000) reported the following hydraulic conductivity and transmissivity values for the Carrizo–Wilcox for the different counties in the area pertaining to this study (table 4.2):

County	Hydraulic Conductivity (m/day)						
	n	25 <sup>th</sup>	50 <sup>th</sup>	75 <sup>th</sup>	90 <sup>th</sup>	x <sup>a</sup>	s <sup>b</sup>
Dimmit	12	1.1	1.2	3.7	20.0	1.9	0.35
La Salle	5	1.9	2.0	3.0	3.4	2.3	0.14
Maverick	1	-	-	-	-	0.2	-
Webb	3	0.0	0.5	0.5	0.5	0.1	0.4
Zavala	8	6.7	14.6	27.1	45.7	12.8	0.56

County	Transmissivity (m <sup>2</sup> /day)						
	n	25 <sup>th</sup>	50 <sup>th</sup>	75 <sup>th</sup>	90 <sup>th</sup>	x <sup>a</sup>	s <sup>b</sup>
Dimmit	24	87.4	112.4	232.6	334.6	131.2	0.34
La Salle	7	148.7	223.0	288.1	390.3	223.0	0.23
Maverick	2	-	-	-	-	11.1	-
Webb	4	1.8	3.1	11.2	85.5	6.4	1.20
Zavala	15	418.2	697.0	864.3	1115.2	557.6	0.31

<sup>a</sup> Based on log transformation of original data

<sup>b</sup> Log-transformed standard deviation

**n** number of values

**25<sup>th</sup>** 25<sup>th</sup> percentile

**50<sup>th</sup>** 50<sup>th</sup> percentile (median)

**75<sup>th</sup>** 75<sup>th</sup> percentile

**90<sup>th</sup>** 90<sup>th</sup> percentile

**x** mean

**s** standard deviation

**Table 4.2 Hydraulic conductivity (m/day) and transmissivity (m<sup>2</sup>/day) for different counties in the study area. Table from Mace et al. (2000).**

Using statistical techniques, Mace et al. (2000) showed that transmissivity and hydraulic conductivity values in the Carrizo Sand and Wilcox Group are spatially correlated over about 10 and 15.5 km, respectively. However, their data distribution also suggests a large amount of randomness due to local-scale heterogeneity and measurement errors, particularly for the Wilcox Group tests. Kriged maps of transmissivity for the Carrizo Formation and Wilcox Group in southern Texas are shown in figures 4.3 and 4.4.

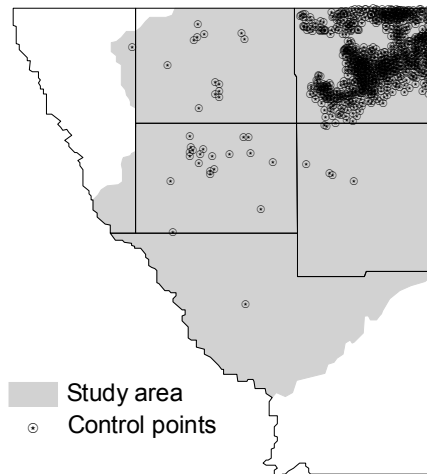
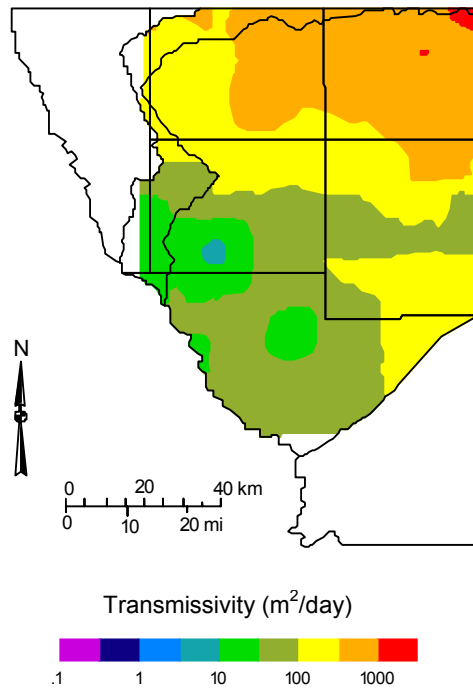


**Figure 4.3 Spatial distribution of transmissivity in the Carrizo Formation using kriging values from the TWDB database (upper map). Location of control points shown on lower map. Modified from Mace et al. (2000).**



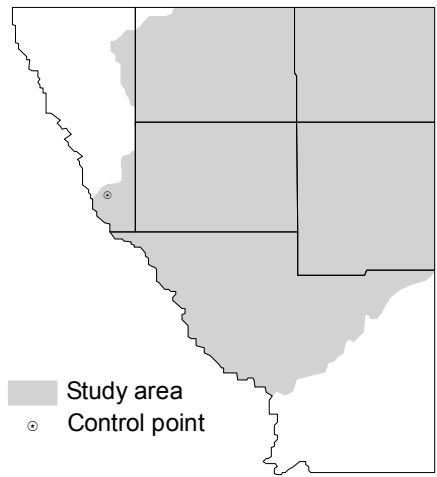
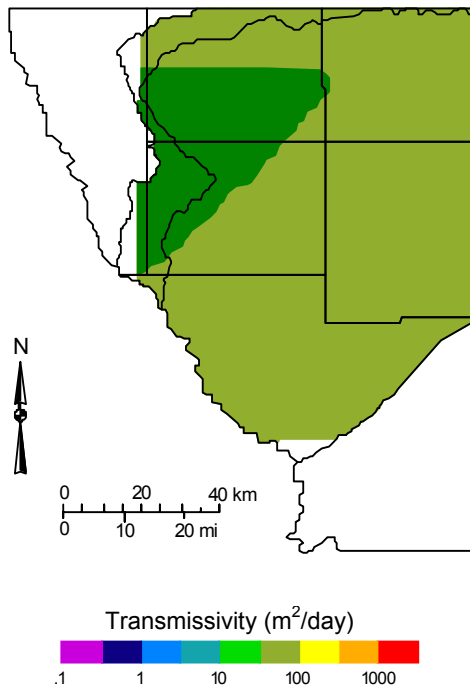


**Figure 4.4 Spatial distribution of transmissivity in the Wilcox Group using kriging values from the TWDB database (upper map). Location of control points shown on lower map. Modified from Mace et al. (2000).**

### **Potentiometric surface and water levels**

Figure 4.5 shows the Carrizo-Wilcox aquifer potentiometric surface map built using 1981-vintage water-level data from 113 wells in Texas, Coahuila, and Nuevo Leon. More recent water-level readings on the Mexican side were not available at the time this report was being written.

On the Texas side, the potentiometric surface slopes to the east and southeast with steep hydraulic gradients (0.01 along Nueces River west of La Pryor and 0.014 just west of Carrizo Springs) in the formation outcrop. Where valley streams cross the formation outcrop the isolines flex upwards (along Nueces River) or downwards (along Leona River and Rio Grande), indicating aquifer-stream interactions may take place (losing stream and gaining stream conditions, respectively). The gradient flattens to 0.001 between Batesville and Big Wells and becomes very flat (~0.0007) east of Cotulla. Heavy aquifer pumpage resulted in cones of depression along the Nueces River from Crystal City to north of Asherton and between Big Wells and Cotulla (see figure 4.5).

On the Mexican side, the potentiometric surface slopes to the east and northeast with gradients of up to 0.006 in the formation outcrop northeast of La Jarita. The gradient flattens (0.001) towards the east along a flowline between Villa Hidalgo to Cotulla.

The highest hydraulic heads are found in the outcrop areas south of San Ignacio (242 m) and in western Dimmit and Zavala counties (219 m). The lowest heads are downdip in the large cone of depression extending from Crystal City to the south, to Big Wells, and east to Cotulla. Groundwater flows downgradient from areas of high hydraulic head to areas of lower hydraulic head.

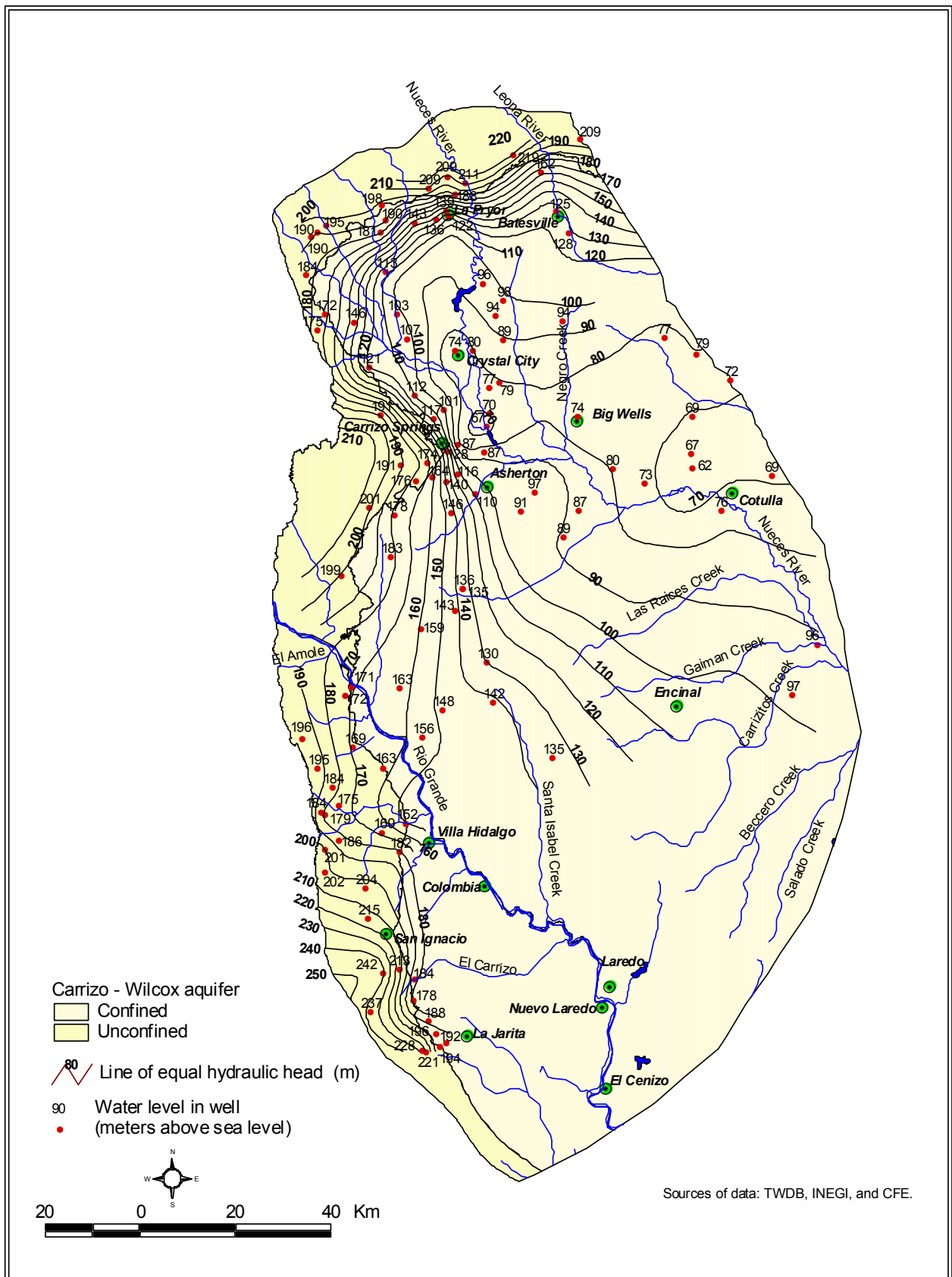


Figure 4.5 Potentiometric surface for the Carrizo-Wilcox aquifer. Map made using data gathered in 1981.

Where the Carrizo-Wilcox heads have not been lowered by pumpage, they exceed the hydraulic heads in the overlying water-bearing units (McCoy, 1991). This indicates a potential for cross-formational flow of groundwater from the Carrizo-Wilcox aquifer up into the Bigford Formation. Based on evidence of decreasing aquifer transmissivity downdip, Hamlin (1988) suggests that cross-formational flow into the overlying units occurs in the deeper parts of the Carrizo-Wilcox aquifer. Downwards leakage of groundwater from the superjacent Bigford Formation has been documented in areas of intensive pumpage in Dimmit and Zavala counties on the Texas side (Mason, 1960). Numerical groundwater flow models by Klemm et al. (1977) estimated the amount of leakage from the Bigford into the Carrizo to be almost 12.3 million m<sup>3</sup>.

Well hydrographs prepared with data collected from wells on the Texas side (figure 4.6) illustrate long-term hydraulic head fluctuations and explain changes in the potentiometric surface map.

Lowering of hydraulic heads is apparent in the confined portion of the aquifer under Dimmit, Zavala, and La Salle counties where intensive groundwater production for agriculture has taken place. From the 1960s to 2002, as much as 40 m of net decline has occurred in wells in this area. Large fluctuations in hydraulic head over short periods of time accompany their long-term declining trend and reflect seasonal variations in pumpage (McCoy, 1991).

Head data from the unconfined area of the aquifer show a stationary trend and little short-term variation (figure 4.6). The high transmissivity of the Carrizo Sand and the location of these wells in the recharge area could dampen the effects of groundwater extraction on the potentiometric surface.

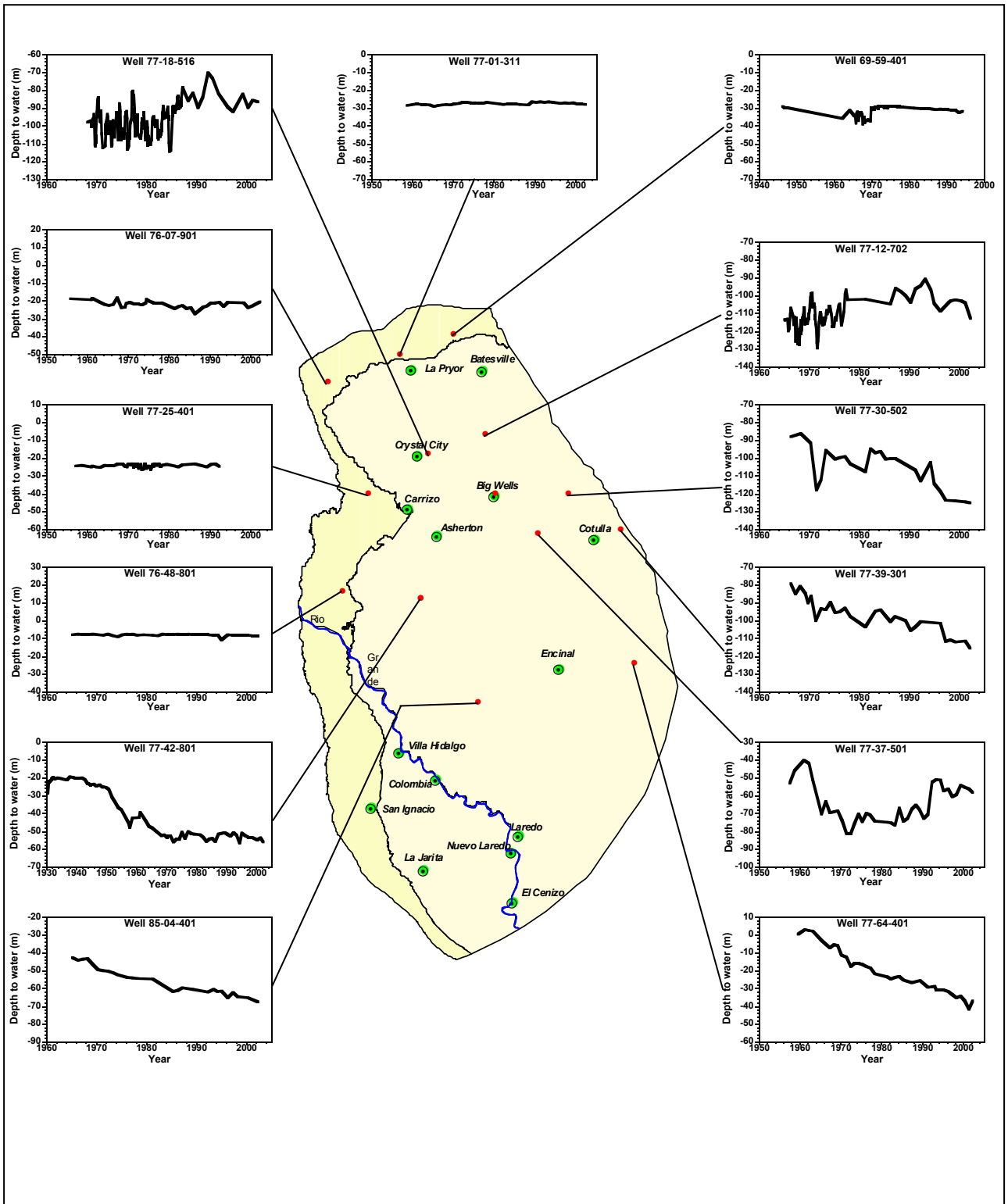


Figure 4.6 Time series well hydrographs for Carrizo-Wilcox aquifer. Source of data: Texas Water Development Board's groundwater database.

In 1981, depths to groundwater in the Carrizo-Wilcox aquifer ranged from 1.5 m to 111.9 m below land surface. Shallow water levels of up to 20 m below the land surface were encountered in most of the wells in the outcrop area. Water levels were deeper (over 100 m below land surface) in the confined part of the aquifer, particularly in areas in Texas affected by groundwater pumpage. Hamlin (1988, p. 24) noted a good correlation between water levels and topography in the unconfined area. The correlation was poor in the confined part of the aquifer Hamlin (1988, p. 24).

### **Recoverable groundwater resources**

Several groundwater availability studies have been conducted in Texas to estimate the amount of recoverable water in the Carrizo-Wilcox aquifer in the study area. McCoy (1991) estimated that 145.6 hm<sup>3</sup> of groundwater would be available for development on an annual basis from the Carrizo-Wilcox aquifer in the Winter Garden area.

The 2001 Texas State water plan (Rio Grande and South-Central Regions) projects quantities of groundwater available between the years 2000 and 2050 as follows:

County Name	Available Water (hm <sup>3</sup> )					
	2000	2010	2020	2030	2040	2050
Dimmit	37.3	37.3	37.3	15.0	15.0	15.0
La Salle	42.9	42.9	42.9	15.6	15.6	15.6
Maverick	5.1	5.1	5.1	3.3	3.3	3.3
Uvalde	5.5	5.5	5.5	2.0	2.0	2.0
Webb	36.7	36.7	36.7	20.9	20.9	20.9
Zavala	37.6	37.6	37.6	13.6	13.6	13.6
<b>TOTAL</b>	<b>165.1</b>	<b>165.1</b>	<b>165.1</b>	<b>70.4</b>	<b>70.4</b>	<b>70.4</b>

**Table 4.3 Projections of groundwater availability from the Carrizo-Wilcox aquifer in the study area from 2000 to 2050. Source of data: 2001 Texas State Water Plan.**

Due to the paucity of geologic and aquifer properties data, no attempt has been made to estimate recoverable groundwater resources on the Mexican side.

### **Recharge areas**

The Carrizo-Wilcox aquifer is recharged primarily by direct infiltration of precipitation in its outcrop area sands. Annual recharge to the aquifer in the Texas counties of Dimmit, Maverick, and Zavala averages about 30.8 hm<sup>3</sup> (Turner et al., 1948). Klemt et al. (1972) indicated that the average annual rate of aquifer recharge in the Winter Garden Area is about 123.3 hm<sup>3</sup>. Hamlin (1988, p. 22) estimated that recharge by outcrop infiltration in parts of Webb, Dimmit, Maverick, and Zavala counties amounts to 19.7 hm<sup>3</sup> per year. Additional recharge to the Carrizo-Wilcox aquifer occurs by cross-formational flow from the overlying Bigford Formation. Groundwater pumping in Dimmit, Zavala, and Frio counties lowered the hydraulic heads in the Carrizo-Wilcox aquifer to levels below those encountered in the overlying strata. Mineralized groundwater from the Bigford percolates downward through aquitards and well bores to recharge the underlying Carrizo-Wilcox aquifer. Approximately 7.6 hm<sup>3</sup> of groundwater leak into the Carrizo-Wilcox aquifer every year in the study area (Hamlin, 1988). The configuration of the Carrizo-Wilcox potentiometric surface map (figure 4.6) suggests some recharge may also take place by way of losing surface streams crossing the outcrop area (e.g., Nueces River).

During January 2002, six Carrizo-Wilcox wells in Zavala, Dimmitt, and Webb counties were sampled by the author for stable and radiogenic isotopes. Deuterium ( $\delta^2\text{H}$ )

and oxygen-18 ( $\delta^{18}\text{O}$ ) are stable isotopes used to investigate the provenance of groundwater. Tritium ( $^3\text{H}$ ) and Carbon-14 ( $^{14}\text{C}$ ) are radioisotopes used to determine the age of the water. The results and the locations of the wells are shown in table 4.4 and figure 4.7 respectively.

State Well Number	$\delta^2\text{H}$ (‰) SMOW	$\delta^{18}\text{O}$ (‰) SMOW	Apparent $^{14}\text{C}$ Age <sup>1</sup>	pmC <sup>2</sup>	$\delta^{13}\text{C}$ (‰)	Tritium (TU) <sup>3</sup>
77-18-407	-28.5	-4.2	10460±80	0.2720	-9.9	0.00
69-57-904	-31.0	-4.6	32680±1200	0.0100	-11.8	-0.06
85-21-501	-30.5	-4.5	35490±1500	0.0120	-10.7	-0.02
77-39-407	-30.5	-4.6	28950±200	0.0270	-9.6	-0.02
77-35-802	-30.5	-4.4	27600±200	0.0320	-12.1	-0.01
76-48-803	-33.5	-5.1	13650±80	0.1830	-18.1	-0.14

<sup>1</sup>)Reported as radiocarbon years before present (“present” = 1950 A.D.)

<sup>2</sup>) Percent modern carbon; <sup>3</sup>)Tritium Units

**Table 4.4 Isotope composition in Carrizo-Wilcox groundwater samples, Zavala, Dimmit, and Webb counties**

The samples are virtually devoid of tritium and exhibit low radiocarbon activities, which is typical for older waters in slow moving flow systems with very limited active recharge. The very low  $^{14}\text{C}$  values are indicative of groundwater that was recharged several thousands of years ago. Highly accurate age estimates based exclusively on carbon isotopes, however, are difficult to derive because of the complex nature of carbon chemistry in groundwater systems. Geochemical processes such as dilution and isotope exchange can strongly alter the initial  $^{14}\text{C}$  activity in groundwater, resulting in an artificial aging of groundwaters. The apparent ages listed in table 4.4 have not been corrected for radiocarbon dilution and are assumed to represent maximum limits. Previous work by Pearson and White (1967) showed that the age of Carrizo waters in Atascosa and neighboring counties ranged from zero at the outcrop to 27,000 years downdip and that groundwater velocities ranged from 1.6 m/year to 2.4 m/year.



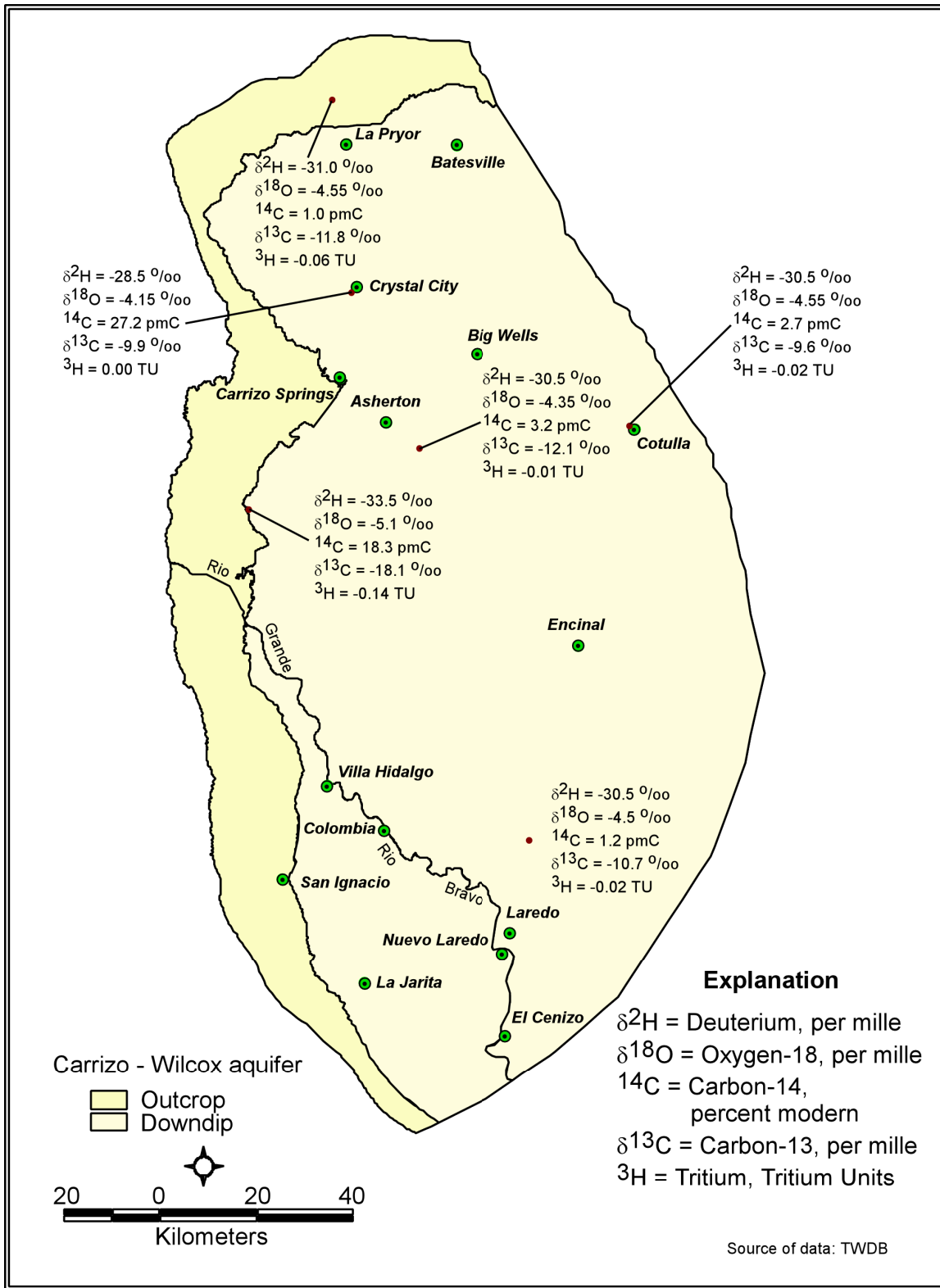
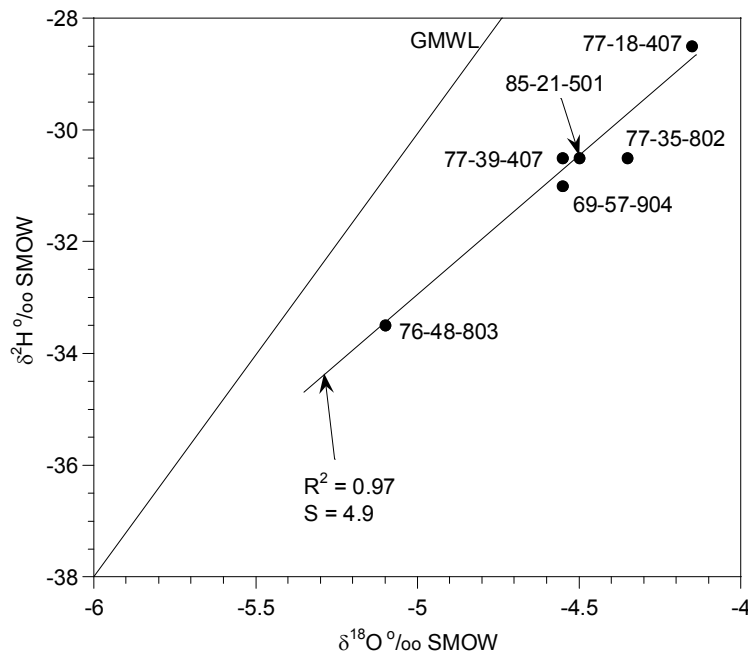


Figure 4.7 Areal distribution of  $\delta^2\text{H}$ ,  $\delta^{18}\text{O}$ ,  $^{14}\text{C}$ ,  $\delta^{13}\text{C}$ , and  $^3\text{H}$  in Carrizo-Wilcox aquifer groundwater.

The results of the TWDB sampling generally agree with the findings of Pearson and White (1967). Radiocarbon activities decrease along flowpaths from 27 pmC in shallower wells to 1 pmC in deep, downdip samples (see figure 4.8). However, a shallow, high-TDS water sample from Zavala County yielded very low  $^{14}\text{C}$  values and no measurable tritium despite its provenance from the aquifer recharge area. Bicarbonate concentrations ranging from 615 mg/l to 732 mg/l have been measured in groundwater from this well (69-57-904). Such values are typical of deeper parts of the flow system where mixing between meteoric water and formation water takes place (Hamlin, 1988, p. 37).



**Figure 4.8 Plot of  $\delta^2\text{H}$  versus  $\delta^{18}\text{O}$  values for Carrizo-Wilcox aquifer. The  $\delta^{18}\text{O}$  shift from GMWL is probably caused by water-rock interaction. Source of data: Texas Water Development Board's groundwater database.**

As shown in figure 4.8, the  $\delta^2\text{H}$  and  $\delta^{18}\text{O}$  data plot below the Global Meteoric Water Line (GMWL) (Craig, 1961), where they form a rather well-defined linear trend with a very good coefficient of determination ( $R^2$ ). The slope of the line of best fit ( $S = 4.9$ ) could indicate that evaporative isotope enrichment processes occurred prior to recharge (Clark and Fritz, 1997, p. 86). Given the old ages of these groundwaters, however, it is possible that water-rock interactions have modified their original meteoric signature. The groundwater temperatures at these locations range from 27°C to 43°C, not hot enough to explain the positive  $^{18}\text{O}$  shift from the global line as high-temperature exchange between the fluids and the rocks.

However, cases of  $^{18}\text{O}$  enrichment accompanied by minor  $^2\text{H}$  enrichment at low temperatures have been documented in formation waters in the Gulf Coast and other sedimentary basins around the world (Clayton et al., 1966; Fleischer et al., 1977). The deviation from GMWL for these waters has been attributed to  $^{18}\text{O}$  exchange with carbonate minerals at elevated temperatures (Clayton et al., 1966),  $^2\text{H}$  exchange with hydrocarbon, hydrogen sulfide, and hydrated minerals, and mixing with meteoric waters (Longstaffe, 1983; Bein and Dutton, 1993; Musgrove and Banner, 1993). Of these processes, the mixing of deep-basin formation waters and fresh recharge is known to occur in the Carrizo Formation (Kreitler, 1979).

The flow regime prevalent in the deeper Carrizo Formation is characterized by upward gradients and results in the outward expulsion of formation waters (Galloway, 1984). Deep faults provide the conduits for their flow updip where they mix with descending, younger meteoric recharge.

## Discharge areas

Groundwater leaves the Carrizo-Wilcox aquifer mainly by means of irrigation pumping. Subsurface seepage to the Leona River and other gaining reaches in the region and cross-formational flow into the overlying strata are two other discharge mechanisms.

Pumping of the aquifer began in 1884 when S.D. Frazier completed the first flowing well at Carrizo Springs in Dimmit County, Texas (Roesler, 1890). Many of the early wells in the Winter Garden Area were flowing when first drilled. From 1900 to 1930, irrigation pumpage using turbines became predominant, first in Dimmit and Zavala counties, and later in the rest of the Winter Garden area.

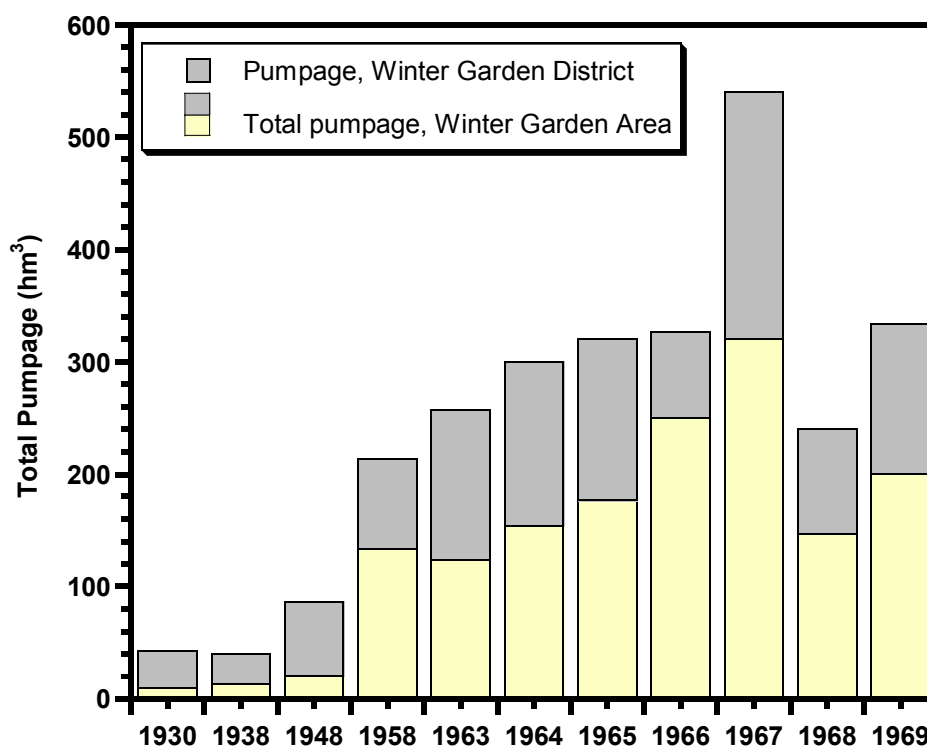


Figure 4.9 Estimated pumpage from the Carrizo Sand for irrigation, public supply, and industrial use, 1930-1969. Modified from Klemt et al. (1976).

Figure 4.9 shows the estimated quantities of water pumped from the Carrizo Formation in the study area from 1930 to 1969. The amount of groundwater pumped from the Carrizo Formation rose steadily since the late 1930s or early 1940s, mainly to satisfy irrigation needs. Widespread drought conditions during the 1950s, population increase, and industrial expansion in the area are other reasons for the regional increase in groundwater use during that time (Klemt et al., 1976). In 1969, groundwater pumpage from the Carrizo Sand amounted to 314.5 hm<sup>3</sup>, which represented 97 percent of the entire irrigation pumpage in the Winter Garden Area (Klemt et al., 1976).

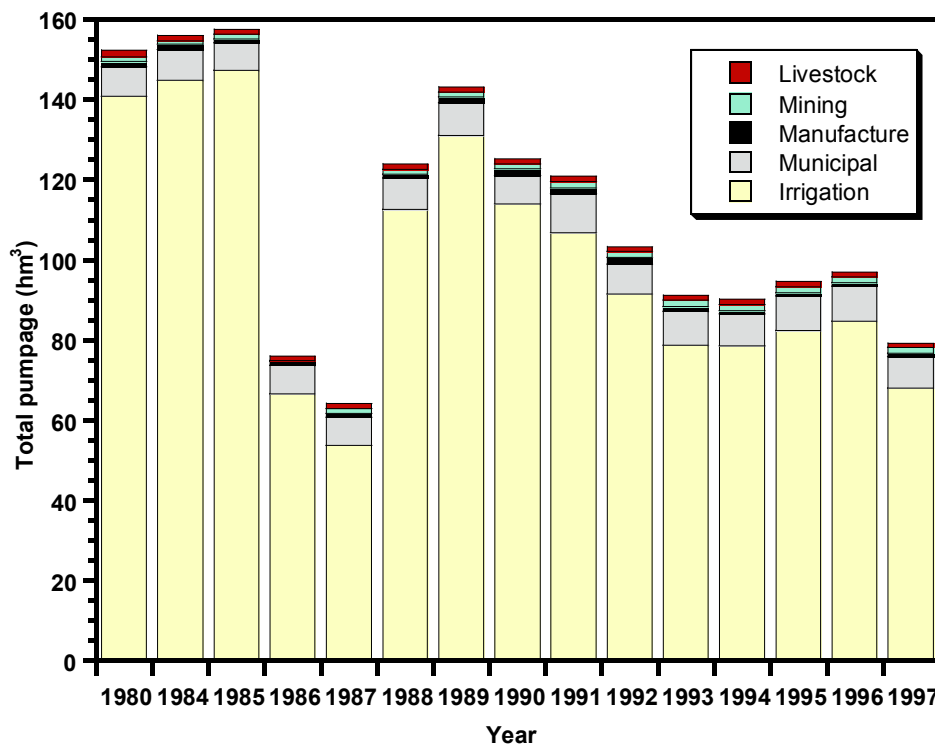


Figure 4.10 Estimated pumpage from the Carrizo-Wilcox aquifer in Dimmit, Maverick, La Salle, Uvalde, Webb, and Zavala counties, 1980-1997. Source of data: TWDB's water use survey.

Historical groundwater use for the Texas side of the study area is shown in figure 4.10. From 1980 through 1997, an average of 111.6 hm<sup>3</sup> of groundwater was pumped annually from the Carrizo-Wilcox aquifer in Dimmit, Maverick, La Salle, Uvalde, Webb, and Zavala counties. Users in Zavala County have been extracting an average of 85.1 hm<sup>3</sup> of groundwater every year, which represents 76 percent of the overall area-wide use. More water was used for irrigation than for any other purpose in the study area. On average, irrigation accounted for 100.1 hm<sup>3</sup> or 90 percent of the total amount of water used. Area-wide municipal pumping accounted for 7.9 hm<sup>3</sup> or seven percent of the average water use. Smaller amounts of groundwater were used for manufacturing, power generation, mining, and livestock.

Groundwater pumping on the Texas side has been on a declining trend since the middle 1980s owing to reduced irrigation demands (see figure 4.10). A drastic reduction in irrigation pumpage took place during 1986 and 1987, two of the wettest years on record for Zavala and Dimmit counties.

## **Groundwater quality**

### **General hydrochemistry**

The general groundwater quality in the Carrizo-Wilcox aquifer is shown in the regional Stiff map (figure 4.11), which was created with data of various vintages from 120 wells. On the Mexican side, the only data available were collected during 1980 and 1981, a time when very little water quality sampling took place in the Carrizo-Wilcox of Texas. On the Texas side, water-quality data from 1997 and 1998 were used.

Groundwater on the Texas side was predominantly fresh to slightly saline with TDS concentrations between 1,000 mg/l and 3,000 mg/l. Salinities in water samples from outcrop wells ranged from 270 mg/l to 1,200 mg/l owing to lithologic heterogeneities in aquifer material and, possibly, reduced recharge rates (Hamlin, 1988). Groundwater samples from three outcrop wells (76-08-503, 76-24-903, and 76-40-401) had dissolved solids content ranging from 4,000 to 6,500 mg/l (see figure 4.11). This may be due to contamination from improperly cased wells or cross-formational flow from more saline aquifers (Hamlin, 1988). The salinity in the Carrizo-Wilcox aquifer increases downgradient as meteoric, fresh recharge dissolves minerals along its flowpath and mixes with deep, high-TDS connate water expelled along fault zones (Kreitler, 1979).

On the Mexican side, the majority of the samples came from outcrop wells. In contrast with the Texas side, the groundwater in Mexico was predominantly saline. Owing to the increase in clay content within the Carrizo and the Indio formations of Mexico, TDS concentrations in groundwater there ranged from 482 mg/l to 9,334 mg/l (see figure 4.11).

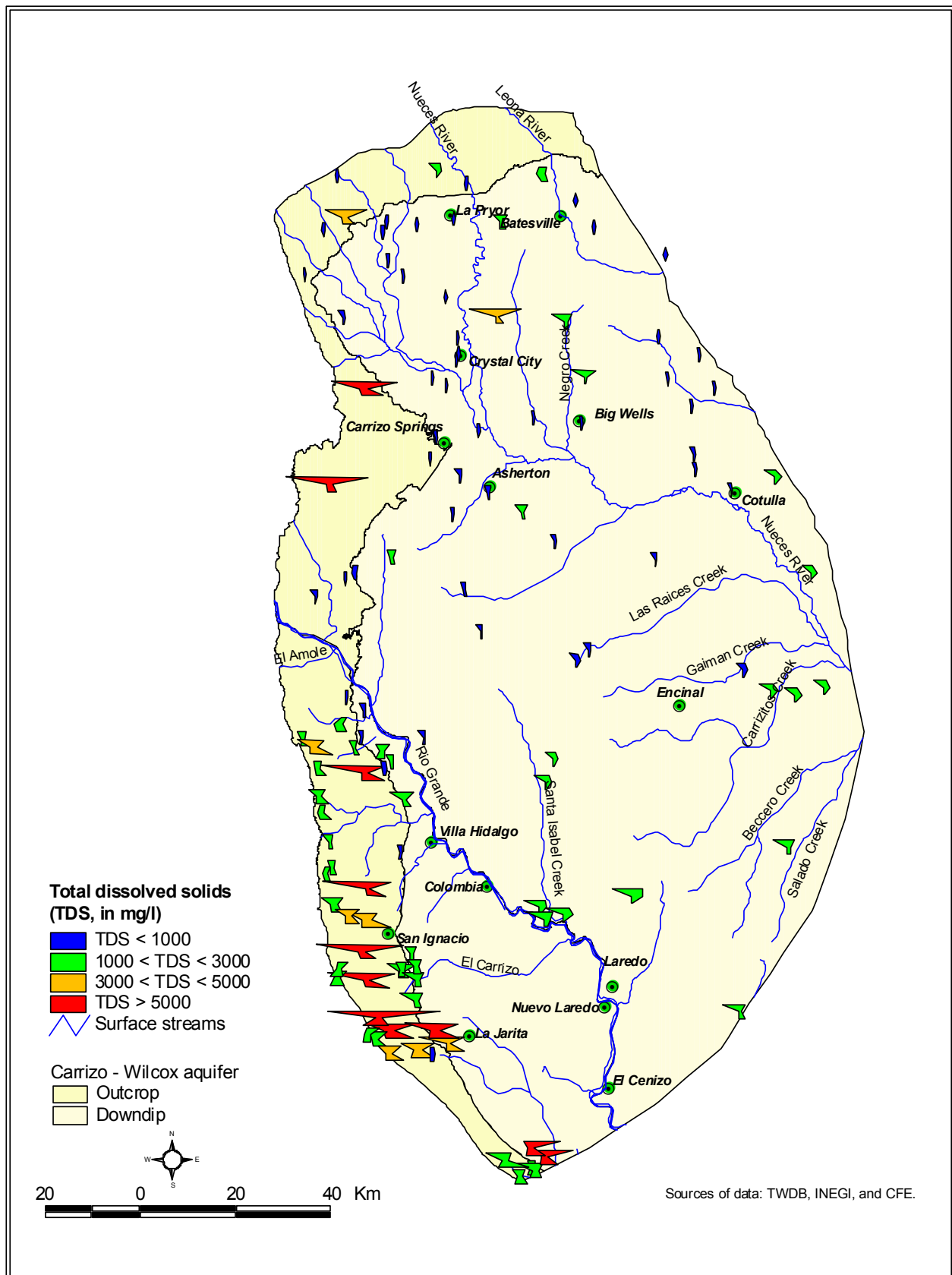


Figure 4.11 Stiff diagrams illustrating hydrochemical facies for the Carrizo-Wilcox aquifer.



Of the 120 samples analyzed, 53 exceeded the U.S. Environmental Protection Agency secondary standards for sulfate (figure 4.12). Fifty-six samples surpassed the secondary standards for chloride (figure 4.13), while one sample had nitrate (as  $\text{NO}_3^-$ ) concentrations above the maximum contaminant level. In the U. S., maximum contaminant levels are set at 250 mg/l for sulfate and chloride (secondary standards) and 44.3 mg/l for nitrate.

The Piper diagram in figure 4.14 shows the relative proportion of ionic species in the Carrizo-Wilcox aquifer groundwaters. Figure 4.15 depicts a map view of the groundwater types and their areal distribution in the aquifer. The composition of groundwater in the Carrizo-Wilcox aquifer is highly variable in the outcrop and shallow confined areas but tends to become more uniform with depth. Where the aquifer is shallow, calcium, bicarbonate and chloride-dominated facies prevail. Downdip, through enrichment in sodium and loss of calcium, the water shifts to a sodium-bicarbonate composition. The chemical variability is greatest on the Mexican side. The presence of heterogeneous mud-rich overbank sediments interspersed with cleaner sand intervals in the Carrizo-Wilcox aquifer of Mexico could explain the abrupt facies changes over short distances, as well as the abundance of chloride and sulfate ions in those samples.

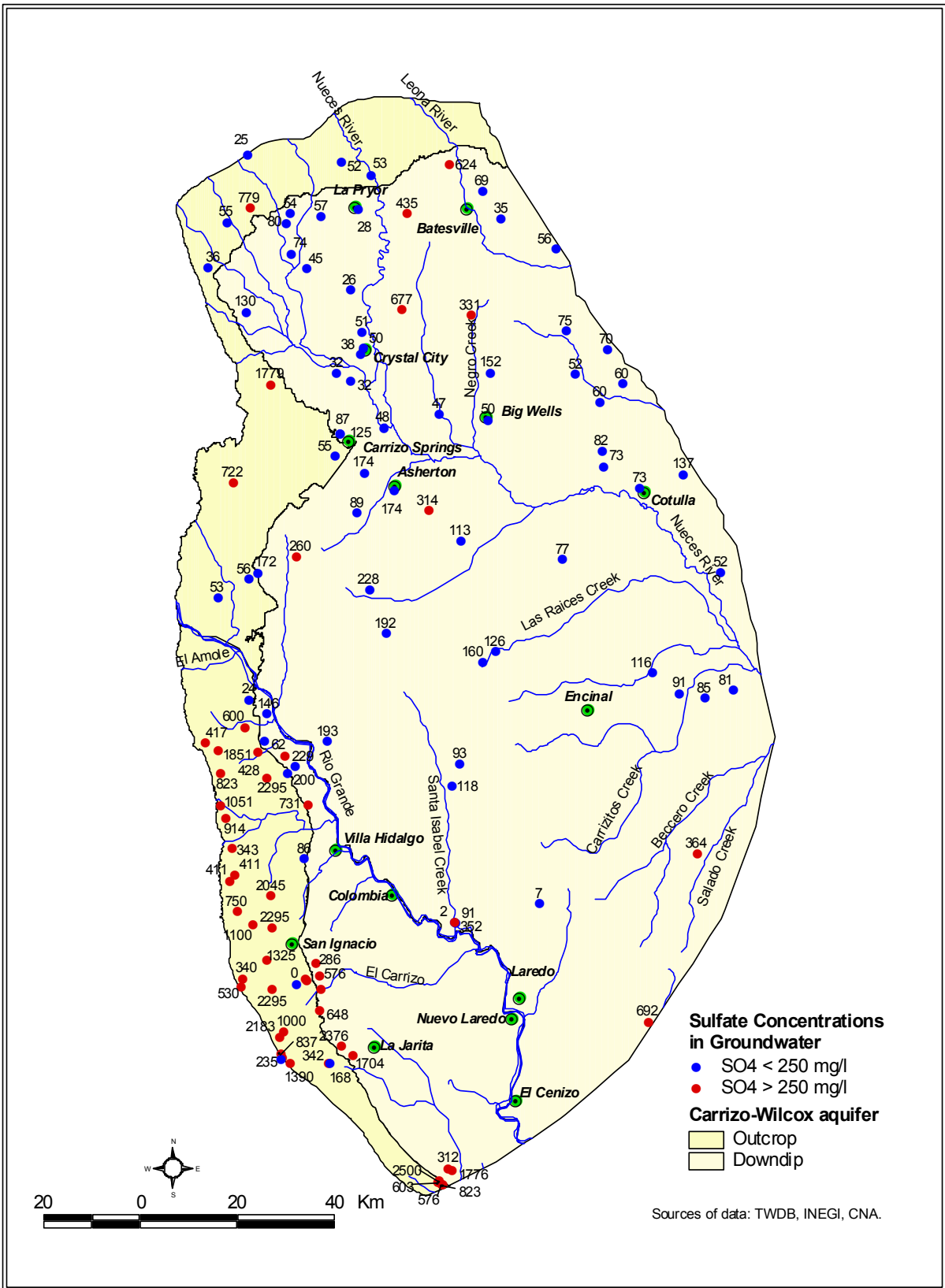


Figure 4.12 Map showing the distribution of sulfate in the Carrizo-Wilcox aquifer.

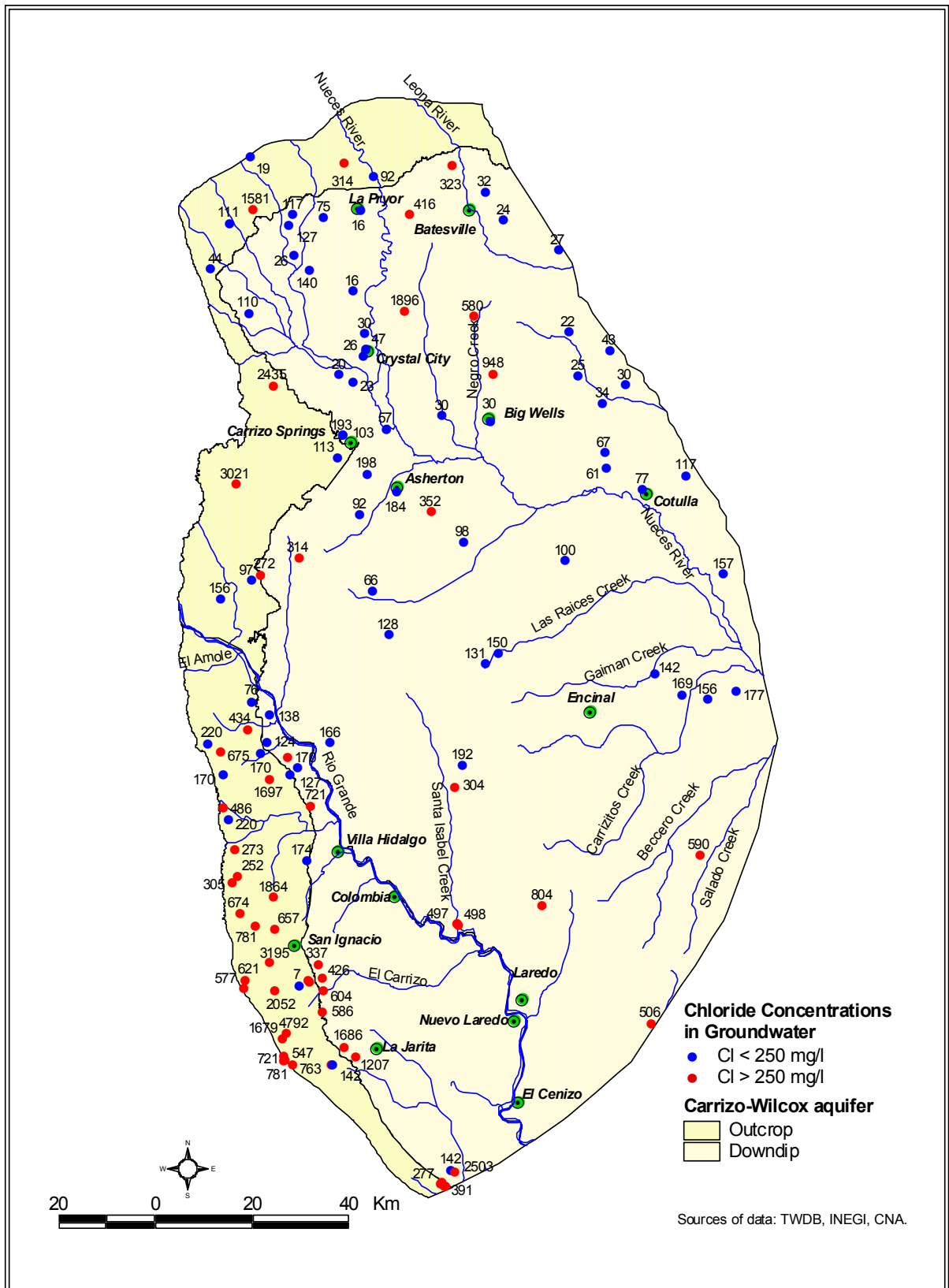
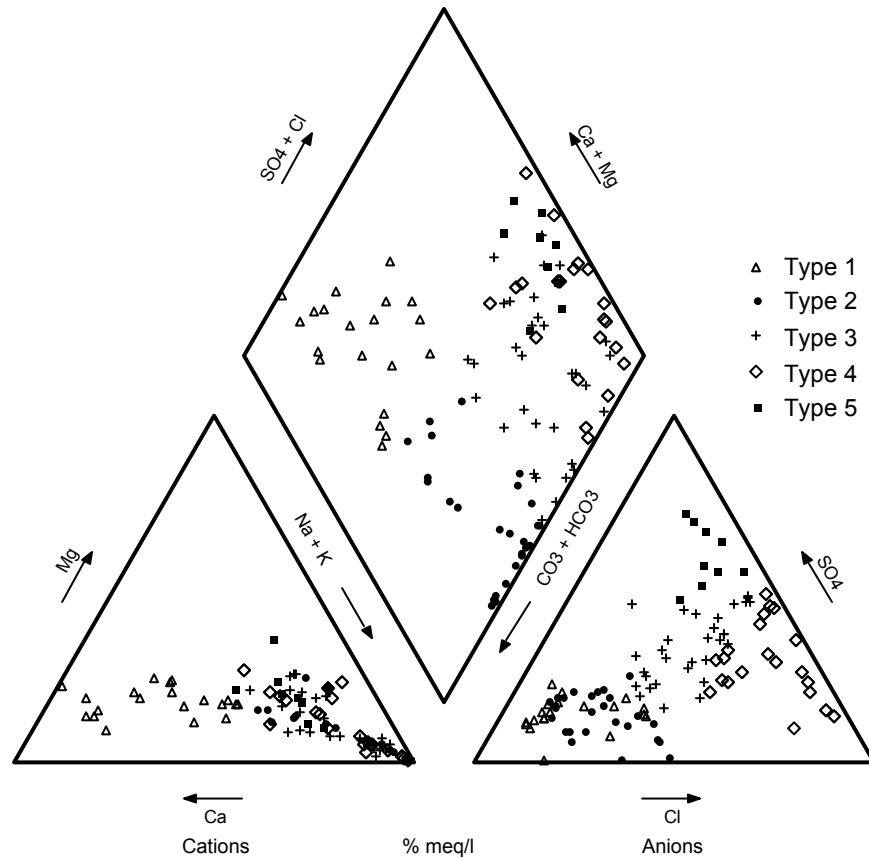


Figure 4.13 Map showing the distribution of chloride in the Carrizo-Wilcox aquifer.

Five general water types could be identified based on their hydrochemical signatures (see figures 4.14 and 4.15):

- (1) A Ca-Na-HCO<sub>3</sub> facies encountered in fresh and slightly saline groundwaters in the recharge area of Zavala County, extending south and southeast towards Crystal City, La Pryor, and Batesville;
- (2) A Na-HCO<sub>3</sub> facies characteristic of fresh and slightly saline groundwaters sampled in the eastern half of the aquifer on the Texas side. Groundwater samples representative of this facies are distributed south and east of a line running from Big Wells to Carrizo Springs, turning east-southeast to Asherton, southwest along Las Raices Creek, and south and southeast along Santa Isabel Creek and towards Laredo;
- (3) A Na-Mixed Anion facies recognized in fresh and slightly saline groundwaters wells to the west of (2). Most of the samples on the Mexican side were representative of this facies;
- (4) A Na-Cl facies encountered in saline water samples between Crystal City and Negro Creek, west and south of Carrizo Springs, and west and southwest of San Ignacio. Isolated Na-Cl type samples have been identified within all other groundwater types listed above;
- (5) A Na-SO<sub>4</sub> facies found in several slightly saline groundwater samples between Villa Hidalgo and El Amole Creek on the Mexican side.

Calcium-bicarbonate groundwaters occur in an east-west-trending belt across the outcrop area in Zavala County on the Texas side. The dissolution of caliche (calcite concretions present in the shallow subsurface) by meteoric recharge water could explain the predominance of calcium ions in this facies (Hamlin, 1988).



**Figure 4.14 Piper diagram showing major ion compositions for groundwater in the Carrizo-Wilcox aquifer. Source of data: Texas Water Development Board and Instituto Nacional de Estadística, Geografía y Informática.**

As groundwater moves downdip, it changes to a sodium-dominated chemical composition, owing in part to ion exchange reactions; calcium ions dissolved in groundwater are exchanged for sodium ions bound on clay particles in the aquifer material.

In the western and central parts of the aquifer, the groundwater composition evolves along flowpaths from a sodium-mixed type to a sodium-bicarbonate facies by addition of bicarbonate at depth.

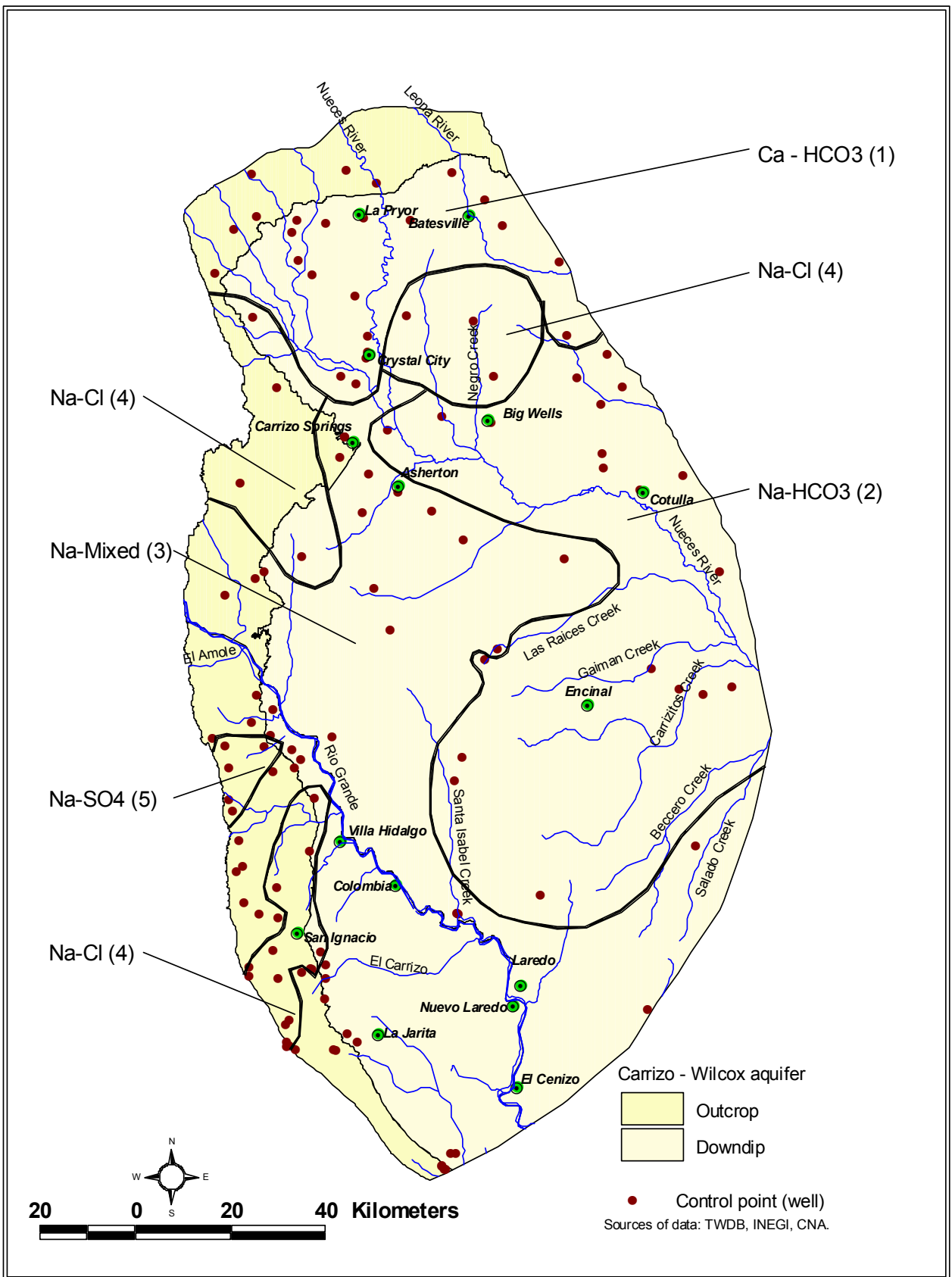
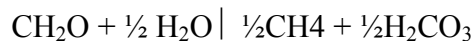


Figure 4.15 Map showing the areal distribution of hydrochemical groundwater facies in the Carrizo-Wilcox aquifer.

Bicarbonate concentration is closely dependent of the pH and the degree of openness of the carbonate system with respect to carbonic acid (Freeze and Cherry, 1979). Hamlin (1988, p. 37) has examined the changes in bicarbonate concentrations and pH along groundwater flowpaths in the Carrizo aquifer of Texas. He noted that pH increases downgradient while the supply of carbonic acid in water is being exhausted (closed system). The pH finally stabilizes at around values of 8.0 to 8.6, while the bicarbonate continues to increase. This indicates that an additional source is supplying carbonic acid to the solution, thus opening the carbonate system. Hamlin (1988) indicates that, for this portion of the aquifer, methane fermentation can supply the additional carbonic acid following the reaction below:



Hydrocarbons and carbonic acid accompany the deep connate waters expelled upward along downdip growth faults. These solutions mix with Carrizo-Wilcox groundwater and re-open the carbonate system by adding carbonic acid into solution (Hamlin, 1988).

Sodium-chloride facies are predominant in areas of Texas that have experienced significant lowering of Carrizo-Wilcox hydraulic heads due to groundwater pumping. This has facilitated the cross-formational flow of saline groundwater into the aquifer in the Crystal City – Carrizo Springs area. Groundwater use patterns on the Mexican side were unknown at the time this report was being written. It is therefore impossible to say if the saline samples from wells around San Ignacio are the result of irrigation return

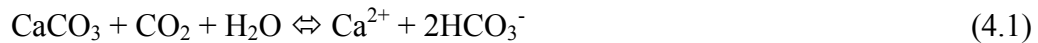
flow, leakage from underlying water-bearing strata, or are related to local lithologic variations.

### Chemical processes

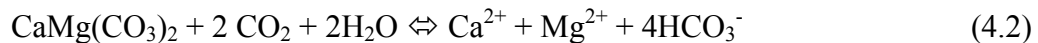
The aquifer mineralogy, mineral equilibria, and chemical composition suggest that carbonate and ion exchange may be the main chemical processes affecting the groundwater in the Carrizo-Wilcox aquifer.

Following are the governing equations for prominent mineral dissolution and precipitation reactions occurring in aqueous systems.

Calcite dissolution and precipitation:



Dolomite dissolution:



Gypsum dissolution:



Halite dissolution:



Ion exchange:



A graph of chloride against sodium (figure 4.16) shows the data points plotting mostly below the halite dissolution line. At lower salinities (less than 5 mmol/l Na and Cl), some of the sodium and chloride may come from halite, as indicated by the points plotting on the 1:1 line.



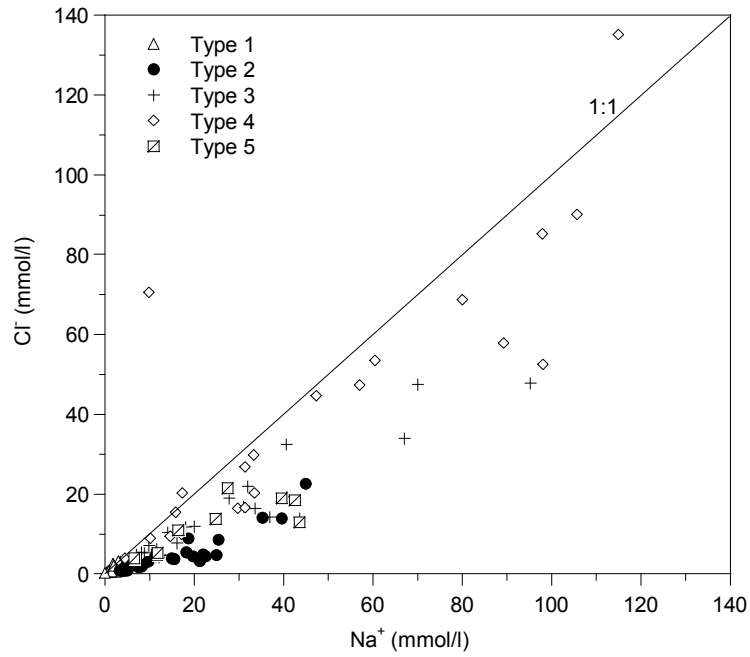


Figure 4.16 Plot of  $\text{Na}^+$  versus  $\text{Cl}^-$

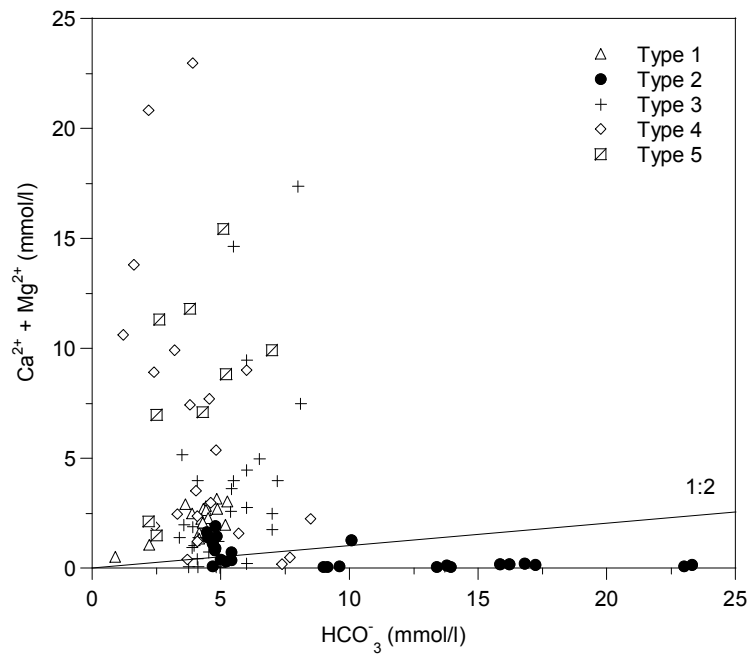


Figure 4.17 Plot of  $\text{Ca} + \text{Mg}$  versus  $\text{HCO}_3^-$

However, the predominance of sodium over chloride in most of the samples indicates a source of sodium beyond halite dissolution, possibly ion exchange between dissolved calcium or magnesium and adsorbed sodium. This hypothesis is discussed later in this section. Figure 4.17 shows the relationship between the concentration of calcium and magnesium versus bicarbonate. If all calcium and magnesium were derived from calcite and dolomite dissolution, then data would plot along a line with slope 1:2, as stated by equation (4.1). Some of the type 1 data points plot on the 1:2 line, but the rest of the samples are above the line, indicating an additional source of calcium and magnesium.

Calcium concentrations above those resulted from calcite dissolution are usually attributed to gypsum or anhydrite dissolution. Lithological descriptions mention the presence of gypsum layers and sulfur fragments in Carrizo and Wilcox strata on the Mexican side (INEGI, 1982).

To account for the calcium derived from gypsum dissolution, calcium and magnesium molar concentrations are summed up and plotted against the sum of sulfate and half of bicarbonate concentration (figure 4.18). The major ion water chemistry suggests that the calcium, magnesium, sulfate, and bicarbonate present in the water are the result of a simple dissolution of the available dolomite or magnesium-calcite along with gypsum or anhydrite. In an ideal case, such dissolution reactions would result in these samples plotting on a straight line through the origin with a slope of one. In figure 4.18, all but four samples plot below the 1:1 line, indicating that there is a partial loss of calcium plus magnesium relative to the amount of bicarbonate and sulfate present. This is consistent with a partial cation exchange where some of the calcium plus magnesium is

lost from the water and sodium is gained. This interpretation explains why most of these water samples have a higher ionic concentration of sodium than chloride (see figure 4.16).

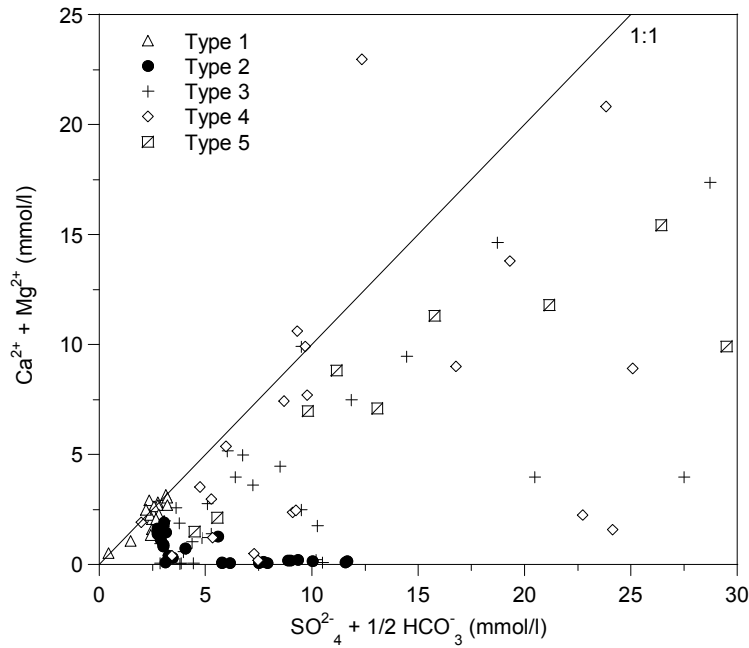


**Figure 4.18** Plot of Ca+Mg versus  $\text{SO}_4 + 1/2 \text{HCO}_3$

The oxidation of iron sulfides in shallow groundwaters releases sulfate into the solution (Hamlin, 1988), therefore accentuating the calcium and magnesium deficit.

To test the ion exchange hypothesis, the concentration of  $(\text{Na}^+ - \text{Cl}^-)$  is plotted against  $(\text{Ca}^{2+} + \text{Mg}^{2+} - \text{SO}_4^{2-} - 0.5\text{HCO}_3^-)$ . The quantity  $(\text{Na}^+ - \text{Cl}^-)$  represents "excess" sodium, that is, sodium coming from sources other than halite dissolution, assuming all chloride is derived from halite. The quantity  $(\text{Ca}^{2+} + \text{Mg}^{2+} - \text{SO}_4^{2-} - 0.5\text{HCO}_3^-)$  represents the calcium and/or magnesium coming from sources other than gypsum and carbonate dissolution.

These two quantities represent the maximum amount of sodium and calcium plus magnesium available for ion exchange processes.

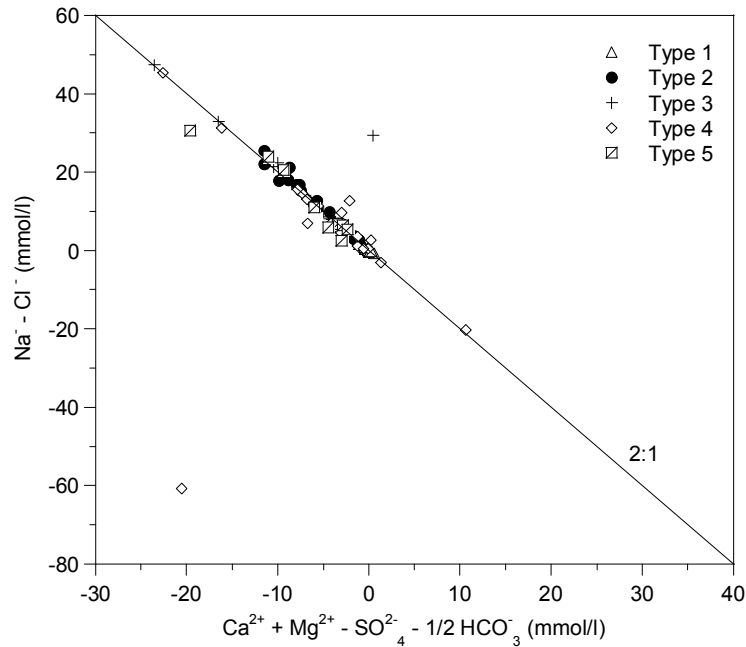


**Figure 4.19 Plot of Na-Cl versus Ca+Mg-SO<sub>4</sub>-1/2 HCO<sub>3</sub>**

The samples (figure 4.19) plot tightly on a line with slope of 2:1 indicating that ion exchange reactions are occurring. Waters undergoing exchange of calcium and magnesium for bound sodium on clays will gradually become of sodium-sulfate type. Only a handful of samples, categorized as type 5 groundwaters (see figures 4.14 and 4.15) on the Mexican side have reached this stage.

Carrizo-Wilcox groundwaters evolve along flowpaths from a calcium, sodium, bicarbonate, and chloride-dominated composition encountered in shallow wells to a sodium-bicarbonate facies encountered at depth. The main chemical processes impacting

the groundwater chemical composition are carbonate dissolution and ion exchange reactions.

### References

- Barnes, V. E., 1976, Crystal City-Eagle Pass sheet: The University of Texas at Austin, Bureau of Economic Geology Geologic Atlas of Texas, scale 1:250,000.
- Barnes, V. E., 1976, Laredo sheet: The University of Texas at Austin, Bureau of Economic Geology Geologic Atlas of Texas, scale 1:250,000.
- Bebout, D. G., Weise, B. R., Gregory, A. R., and Edwards, M. B., 1982, Wilcox sandstone reservoirs in the deep subsurface along the Texas Gulf Coast, their potential for production of geopressured geothermal energy: The University of Texas at Austin, Bureau of Economic Geology Report of Investigations No. 117, 125 p.
- Bein, A. and Dutton, A. R., 1993, Origin, distribution, and movement of brine in the Permian Basin (U.S.A.): A model for displacement of connate brine: Geological Society of America Bulletin, 105, p. 695-707.
- Belcher, R. C., 1975, The geomorphic evolution of the Rio Grande: Waco, Texas, Baylor University, Baylor Geological Studies Bulletin 29, 64 p.
- Clark, I. D. and Fritz, P., 1997, Environmental isotopes in hydrogeology: Lewis Publishers, 328 p.
- Clayton, R. N., Friedman, I., Graff, D. L., Mayeda, T. K., Meents, W. F. and Shimp, N. F., 1966, The origin of saline formation waters. 1. Isotopic composition: Journal of Geophysical Research, 71, p. 3869-3882.
- Craig, H., 1961, Isotopic variations in meteoric waters: Science, 133, p. 1702-1703.
- Elizondo, J. R., 1977, Geologia basica regional en la sub-cuenca hidrologica Acuña-Laredo: Comisión Federal de Electricidad, Series tecnicas de CFE, 69 p.
- Eargle, D. H., 1968, Nomenclature of formations of the Claiborne Group, Middle Eocene, Coastal Plain of Texas: U.S. Geological Survey Bulletin 1251-D, 25 p.
- Fisher, W. L., 1969, Facies characterization of Gulf Coast Basin delta systems, with some Holocene analogues: Gulf Coast Association of Geological Societies Transactions, v. 19, p. 239-261.

- Fisher, W. L., and McGowen, J. H., 1967, Depositional systems in the Wilcox Group of Texas and their relationship to occurrence of oil and gas: Gulf Coast Association of Geological Societies Transactions, v. 17, p. 105-125.
- Flawn, P. T., 1961, Appendix: part 1. summary reports on wells penetrating rocks of the Ouachita belt and immediately adjacent foreland in Texas, *in* Flawn, P. T., and others, The Ouachita System: The University of Texas at Austin, Bureau of Economic Geology Publication No. 6120, p. 211-338.
- Fleischer, E., Goldberg, M., Gat, J. R. and Magaritz, M., 1977, Isotopic composition of formation waters from deep drillings in southern Israel: *Geochimica et Cosmochimica Acta*, 41, p. 511-525.
- Freeze, R. A., and Cherry, J. A., 1979, Groundwater: Englewood Cliffs, New Jersey, Prentice-Hall, 604 p.
- Galloway, W. E., 1984, Hydrogeologic regimes of sandstone diagenesis, *in* McDonald, D. A., and Surdam, R. C., eds., Clastic diagenesis: American Association of Petroleum Geologists Memoir No. 37, p. 3-13.
- Habicht, J. K. A., 1979, Paleoclimate, paleomagnetism, and continental drift: American Association of Petroleum Geologists Studies in Geology No. 9, 31 p.
- Hamlin, H. S., 1988, Depositional and ground-water flow systems of the Carrizo-Upper Wilcox, south Texas: The University of Texas at Austin, Bureau of Economic Geology Report of Investigations No. 175, 61 p.
- Hargis, R. N., 1962, Stratigraphy of the Carrizo-Wilcox of a portion of South Texas and its relationship to production: Gulf Coast Association of Geological Societies Transactions, v. 12, p. 9-25.
- Hargis, R. N., 1985, Proposed lithostratigraphic classification of the Wilcox Group of South Texas: Gulf Coast Association of Geological Societies Transactions, v. 35, p. 107-116.
- INEGI, 1982, Carta Geologica Piedras Negras, escala 1:250 000.
- Kaiser, W. R., Ayers, W. B., Jr., and LaBrie, L. W., 1980, Lignite resources in Texas: The University of Texas at Austin, Bureau of Economic Geology Report of Investigations No. 104, 52 p.
- Klemt, W. B., Duffin, G. L., and Elder, G. R., 1976, Groundwater resources of the Carrizo aquifer in the Winter Garden area of Texas: Texas Water Development Board Report 210, v. 1, 30 p.

- Kreitler, C. W., 1979, Ground-water hydrology of depositional systems, in Galloway, W. E., and others, Depositional and ground-water flow systems in the exploration for uranium, a research colloquium: The University of Texas at Austin, Bureau of Economic Geology, p. 118-176.
- Lalo, R. C., 1979, Estudio geohidrologico de gran vision en el area comprendida entre Nuevo Laredo y Lampazos Estados de Tamaulipas y Nuevo Leon: Comisión Federal de Electricidad, Informe No. 79023, 20 p.
- Longstaffe, F. J. 1983. Diagenesis 4: Stable isotope studies of diagenesis in clastic rocks. *Geoscience Canada*, v. 10, p. 43-58.
- Lonsdale, J. T., and Day, J. R., 1937, Geology and groundwater resources of Webb County, Texas: U.S. Geological Survey Water-Supply Paper 778, 104 p.
- Mace, R. E., Smyth, R. C., Xu, L., and Liang, J., 2000, Transmissivity, hydraulic conductivity, and storativity of the Carrizo-Wilcox aquifer in Texas: Data and analysis: The University of Texas at Austin, Bureau of Economic Geology, Technical report prepared for Texas Water Development Board under TWDB Contract No. 99-483-279, Part 1, 76 p.
- Mason, C. C., 1960, Geology and groundwater resources, Dimmit County, Texas: Texas Board of Water Engineers Bulletin 6003, 234 p.
- McCoy, T. W., 1991, Evaluation of ground-water resources of the western portion of the Winter Garden area, Texas: Texas Water Development Board Report 334, 64 p.
- Musgrove, M. and Banner, J. L., 1993, Regional ground-water mixing and the origin of saline fluids: Midcontinent, United States: *Science*, 259 p. 1877-1882.
- Owen, J., 1889, Report of geologists for southern Texas, in Dumble, E. T., ed., First report of progress, 1888: Texas Geological Survey, p. 69-74.
- Pearson, F. J., Jr., and White, D. E., 1967, Carbon-14 ages and flow rates of water in Carrizo Sand, Atascosa County, Texas: *Water Resources Research*, v. 3, no. 1, p. 251-261.
- Prudic, D. E., 1991, Estimates of hydraulic conductivity from aquifer-test analyses and specific-capacity data, Gulf Coast regional aquifer systems, south-central United States: U. S. Geological Survey, Water-Resources Investigations, WRI 90-4121, 38 p.
- Roesler, F. E., 1890, Report (on the underground water supply in Texas): U.S. 51<sup>st</sup> Cong., 1<sup>st</sup> Sess., Ex. Doc222, v. 12 (U.S. Serial no. 2689), p. 243-319.

- Turner, S. F., Robinson, T. W., White, W. N., Outlaw, D. E., George, W. O., 1960, Geology and groundwater resources of the Winter Garden district, Texas, 1948: U.S. Geological Survey Water-Supply Paper 1481, 247 p.
- Upitis, G. W., 1998, Paleocene-Early Middle Eocene lithostratigraphy and sequence stratigraphy in the Rio Grande River Valley, Texas: The University of Texas at Austin, Unpublished M.A. thesis, 156 p.



## **CHAPTER 5: AQUIFER VULNERABILITY TO CONTAMINATION**

### **Introduction**

Large parts of the study area rely on groundwater as a drinking water source or for irrigation, manufacturing, and domestic use. Preserving the quality of the area's groundwater resources stresses the need for a proactive approach to guard these resources against contamination.

Different landuse activities have different impacts on the groundwater resources, and aquifers have varying susceptibilities to contamination. Effective groundwater protection involves conducting both pollution risk evaluations and aquifer vulnerability assessments. Pollution risk evaluations take in consideration pollutants' source and characteristics, and aquifer vulnerability assessments examine the intrinsic characteristics of an aquifer and its response to an imposed contaminant load.

The purpose of this section is to present results of an aquifer vulnerability assessment conducted for the area along the Rio Grande between Del Rio/Ciudad Acuña and Laredo/Nuevo Laredo.

### **Vulnerability assessment of the transboundary aquifers**

The examination of groundwater pollution potential between Del Rio/Ciudad Acuña and Laredo/Nuevo Laredo is an example of transboundary research products that result from integrating U.S. and Mexican data. This assessment employs the U.S. Environmental Protection Agency's DRASTIC method (Aller et al., 1987) within a Geographic Information System (GIS) to map the relative sensitivity of aquifers to

contamination. This method is well suited to gridded sets of factors affecting aquifer vulnerability. ArcInfo GIS (ESRI, 1990) was chosen for manipulation and displaying aquifer vulnerability factors because of its analytical capabilities as a grid-based cell modeling environment.

In the DRASTIC method, the vulnerability assessment consists of rating seven hydrogeological parameters throughout the study area and combining them into a numerical value (the “DRASTIC index”) indicative of the aquifers’ susceptibility to pollution. The seven parameters were **D**epth to water, **R**echarge, **A**quifer media, **S**oils, **T**opography, **I**mpact of vadose zone, and hydraulic **C**onductivity. Each parameter is classified into ranges (for continuous variables) or significant media types (for thematic data) that have impacts on vulnerability to pollution. Weight multipliers are then used for each parameter to fine-tune their importance. The DRASTIC index ( $D_I$ ) is calculated using the expression:

$$D_I = D_r D_w + R_r R_w + A_r A_w + S_r S_w + T_r T_w + I_r I_w + C_r C_w \quad (5.1)$$

where  $D$ ,  $R$ ,  $A$ ,  $S$ ,  $T$ ,  $I$ , and  $C$  are the seven parameters described above,  $w$  is the weight associated with each parameter, and  $r$  is the rating assigned to each parameter.

The weights associated with each parameter are as follows (Aller et al., 1987):

Depth to groundwater	$D_w = 5$
Recharge	$R_w = 4$
Aquifer media	$A_w = 3$
Soils	$S_w = 2$
Topography (% slope)	$T_w = 1$
Impact of vadose zone	$I_w = 5$
Conductivity (hydraulic)	$C_w = 3$

The DRASTIC method can employ a second set of weights to be used where aquifers are susceptible to contamination by pesticides (Aller et al., 1987). For this study only the regular, non-pesticide weights were used.

Data incorporated in the model include topography, geology, hydrology, soils information, water levels in wells, aquifer tests results, and well logs. The data were extracted from digital files and paper records provided by participating U.S. and Mexican state and federal agencies. Following are brief descriptions of the data sources and technical procedures employed to build the DRASTIC input files and coverages.

#### 1. Depth to groundwater

Depth to groundwater is significant because it is indicative of the distance and time necessary for the contaminant to reach the aquifer. A water well database containing latitude and longitude locations and depth to water data was produced for both

Texas and Mexico sides. The sources of the information were the Texas Water Development Board's groundwater database for the Texas side and the 1:250,000 scale Carta Hidrologica de Aguas Subterranas (groundwater hydrologic maps) published in 1981 by Instituto Nacional de Estadística, Geografía e Informática (INEGI) for the Mexican side. The downdip portions of the transboundary aquifers are under confined conditions and, therefore, are less vulnerable to land surface pollution. To keep the focus on the shallow parts of the aquifers, only information from wells 100 m deep or shallower was used. The data were gridded and contoured using a kriging interpolation method, and a map was created based on the DRASTIC rating scheme (figure 5.1).

## 2. Recharge

Net aquifer recharge is, arguably, the most difficult groundwater parameter to estimate. The recharge layer was created by combining digital annual precipitation contour maps of Texas and Mexico, assuming that part of precipitation recharges the aquifers. For the Texas part, an Arc/Info annual precipitation polygon coverage was downloaded from the U.S. Natural Resources Conservation Service (NRCS) file transfer protocol (ftp) site which contains coverages of average monthly and annual precipitation for the period 1961-90. For the Mexico side, annual precipitation contour lines were digitized from INEGI's 1:250,000 scale Carta Hidrologica de Aguas Superficiales (surface water hydrologic map) sheets which display average precipitation data collected over the 1950-1975 period.

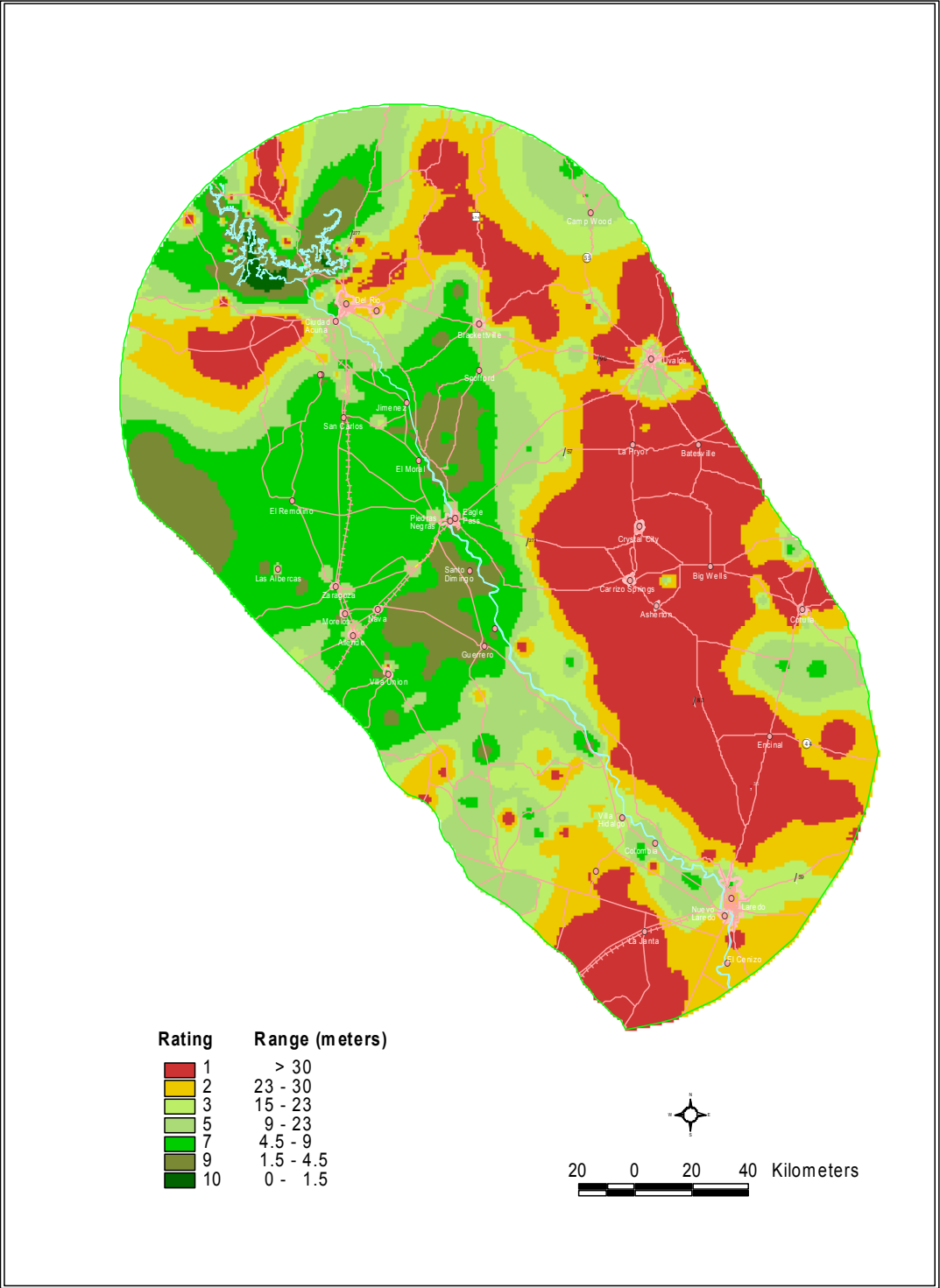


Figure 5.1. Ratings and depth intervals for the depth to groundwater DRASTIC layer

Annual recharge was assumed to be two percent of annual precipitation, a value commonly employed in numerical groundwater flow models in arid regions (Orr and Risser, 1992). Similar recharge rates of (12 to 50 mm per year) have been used by Kuniatsky and Holligan (1993) in their Edwards-Trinity aquifer groundwater flow simulations. Recharge values were then classified based on the DRASTIC classification scheme. Both Texas and Mexico sides of the study area were within the recharge range of 0 - 25 mm per year and a DRASTIC rating of 1 was assigned to the entire study area except over the open bodies of water (Lake Amistad and Lake Casa Blanca), which were assigned a rating of 9 (figure 5.2).

### 3. Aquifer Media

Aquifer media is defined by Aller et al. (1987) as the consolidated and unconsolidated rocks that constitute the water-bearing units. For this study it was assumed that the aquifer media would have characteristics similar to those of the overlying geology, which may not always be true. The digital geology database was created by combining the 1:250,000 digital Geologic Atlas of Texas sheets, Laredo (1976), digitized by the Texas Bureau of Economic Geology; Crystal City-Eagle Pass (1976) digitized by Blackland Research Center; Del Rio (1977), San Antonio (1982) sheets both digitized by TWDB, and joining INEGI's 1:250,000 Carta Geologica sheets (Ciudad Acuña, Piedras Negras, Nueva Rosita, and Nuevo Laredo, digitized by TWDB). The digitized information was converted to a GIS polygon coverage.

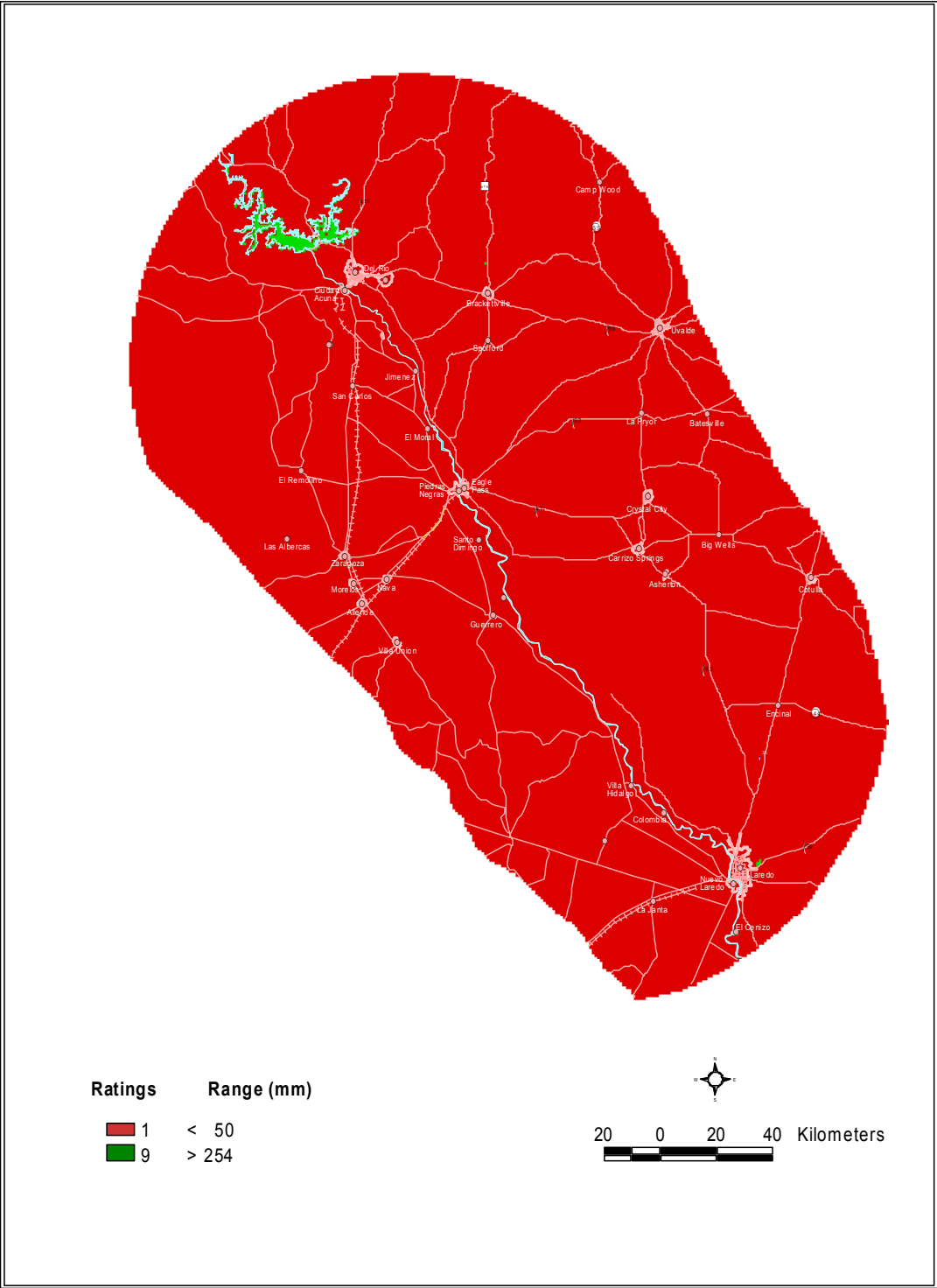


Figure 5.2. Ratings and rates of aquifer recharge for the net recharge layer

Each polygon was coded according to the legend on the paper maps and rated based on the DRASTIC scheme (figure 5.3).

#### 4. Soil Media

The term soil media refers to the uppermost portion of the vadose zone (Aller et al., 1987). Soil cover characteristics influence the downward movement of contaminants therefore greatly impacting aquifer vulnerability. The digital soil database was created by combining the 1:250,000 Texas STATSGO soil layer (1995) and Mexican 1:1,000,000 Carta Edafologica, Monterrey sheet (1987) digitized by TWDB. The resulting polygon coverage received DRASTIC ratings based on the Mexican soil map. The ratings for the Texas side were assigned according to the surface texture parameter in the STATSGO database. Both soil coverages were reprojected to UTM-14, joined together into a polygon coverage, and then converted to ArcInfo GRID model (figure 5.4).

#### 5. Topography

Topography indicates whether or not a pollutant would run off or pond on the land surface and percolate through the vadose zone to the water table. Digital Elevation Model (DEM) files (1994) were downloaded from the U.S. Geological Survey website for Texas side and from TWDB Borderlands Information Center (BIC) website for the



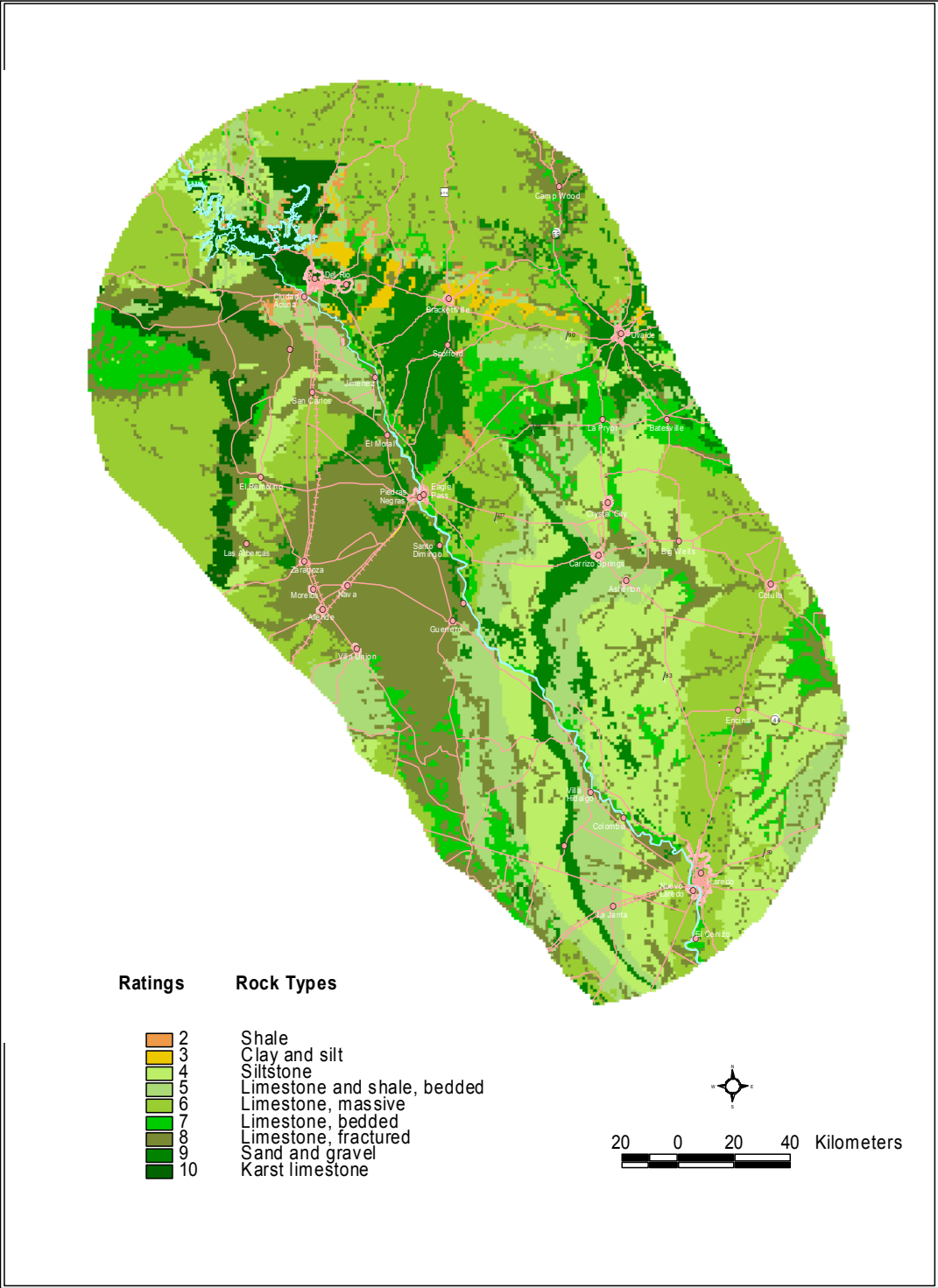


Figure 5.3 Ratings and rock types for the aquifer media DRASTIC layer

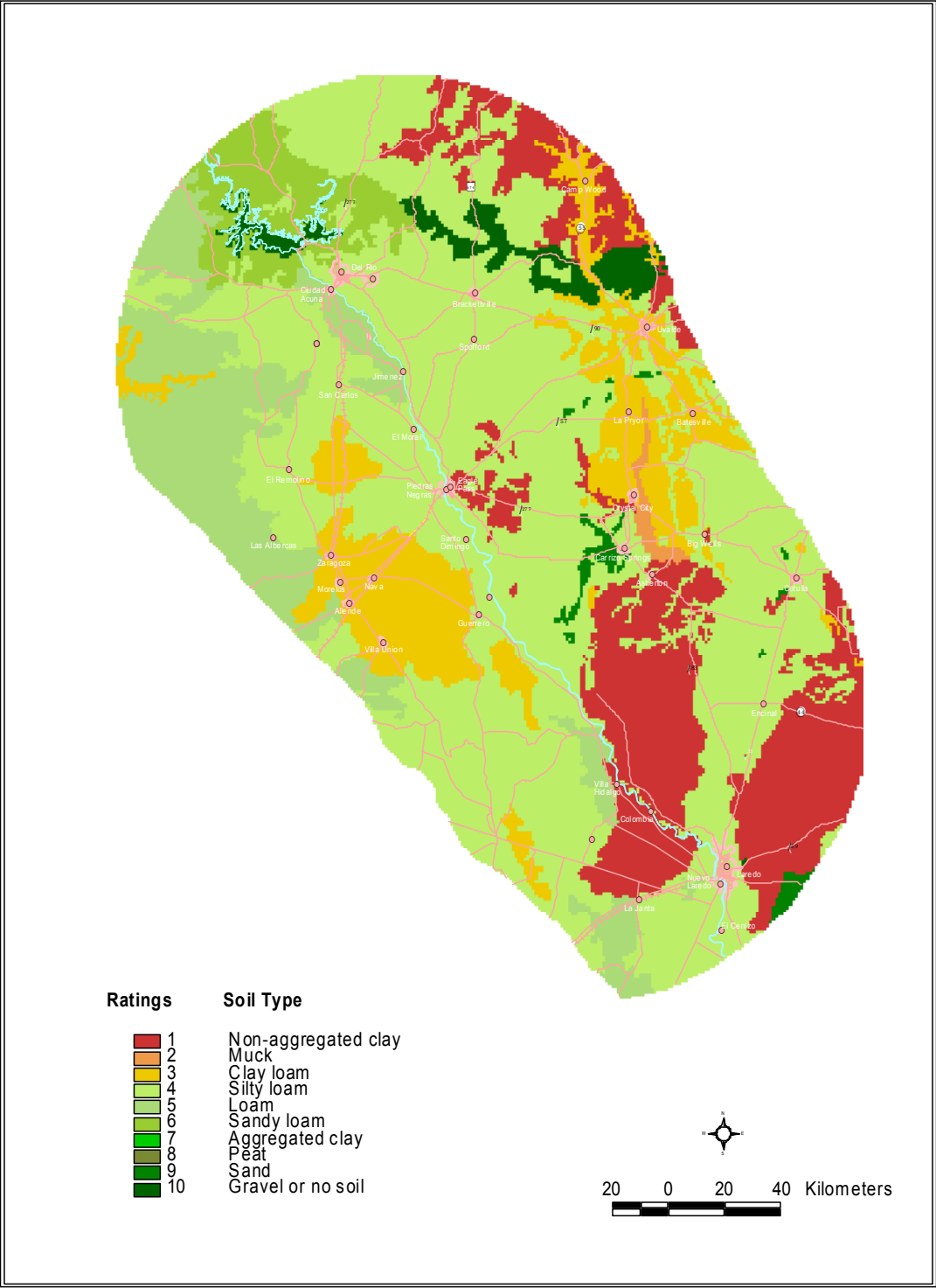


Figure 5.4 Ratings and soil types for the soil media DRASTIC layer

Mexican side. The DEM files were converted to ArcInfo GRID model and joined together. The GRID file was then resampled to 1000-meter cells to meet the DRASTIC cell size requirements. Surface slopes (percent rise) were calculated within ArcInfo GRID and DRASTIC ratings were assigned based on the slope values (see figure 5.5).

## 6. Impact of the Vadose Zone

The vadose (unsaturated) zone is the ground section found above the water table and the saturated portion of the capillary fringe where the pores are generally filled with both liquid water and air (Domenico and Schwartz, 1990). The vadose zone can affect the aquifer vulnerability to contamination in essentially the same way as the soil cover. The properties of geologic formations below the soil cover also need consideration for areas with deeper water tables. For areas where the water table is shallow (less than 10 m) it was assumed that the soil cover properties had a greater influence on aquifer vulnerability than the underlying geology. In such cases (the Plio-Pleistocene Uvalde and Sabinas gravels and conglomerates and the Rio Grande Quaternary alluvium) the soils have been used as a proxy for the vadose zone properties. For the rest of the study area the DRASTIC rating followed the regional geologic descriptions (figure 5.6).

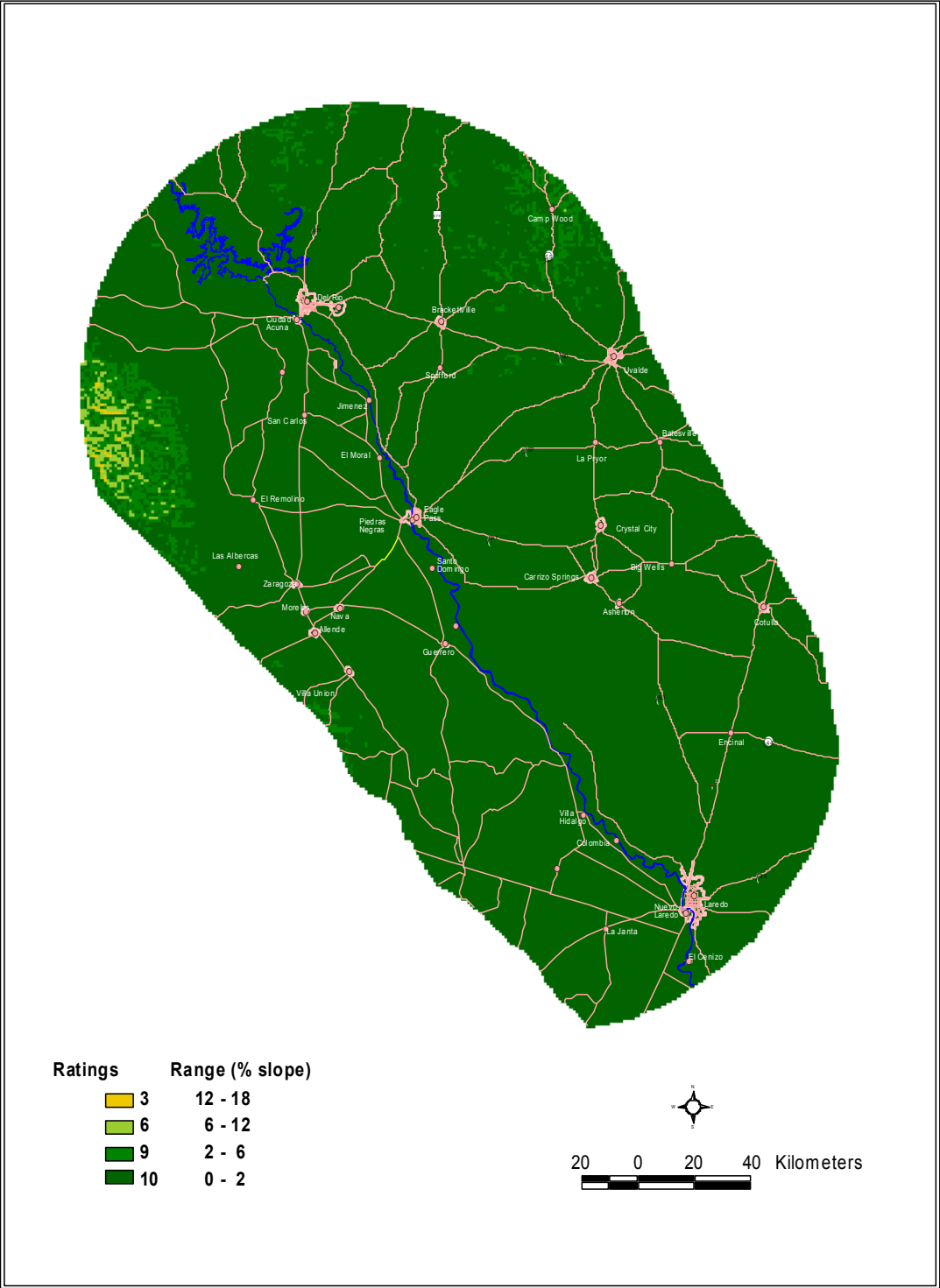


Figure 5.5 Ratings and percent slope ranges for the topography DRASTIC layer

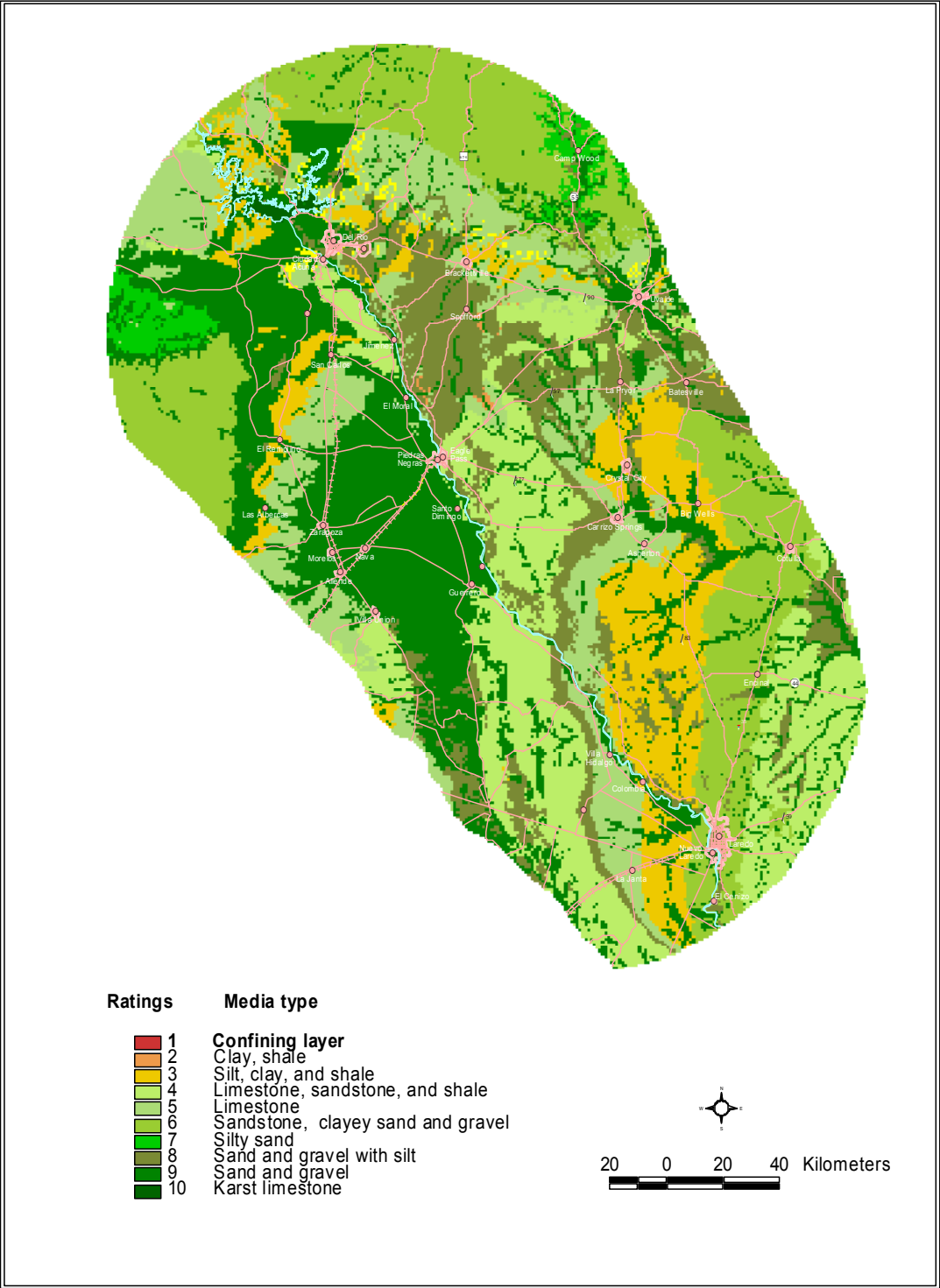


Figure 5.6 Ratings and rock types for the impact of vadose zone DRASTIC layer

## 7. Hydraulic Conductivity

Hydraulic conductivity characterizes the ability of the aquifer to transmit water and depends on a variety of physical factors including porosity, particle size and distribution, shape of particles, arrangement of particles, presence and distribution of fractures and faults, among other factors. Hydraulic conductivity, representative of the properties of both the aquifer and the fluid, is a critical factor controlling the migration of the pollutant from the source point within the saturated zone. The hydraulic conductivity coverage (see figure 5.7) was calculated from published pumping test data for Texas (Myers, 1969, Klemm et al., 1970, Kuniandy et al., 1991), estimated from specific-capacity tests using the methodology developed by Mace and others (1998), and from various unpublished reports. No aquifer-test data were available for the Mexican side of the study area. The hydraulic conductivity ratings for Mexico were geology-based and obtained by extrapolating the corresponding Texas ratings south of Rio Grande, based on the Mexican 1:250,000 scale Carta Hidrologica de Aguas Subterraneas (1981).

### **Computing the DRASTIC Index**

GRID models were developed for each of the DRASTIC parameters, and a natural sensitivity map for the entire study area was generated from the GRID map calculation (figure 5.8). The DRASTIC index values are a measure of the aquifers' natural vulnerability ranging from a minimum value of 26 to a maximum of 228.

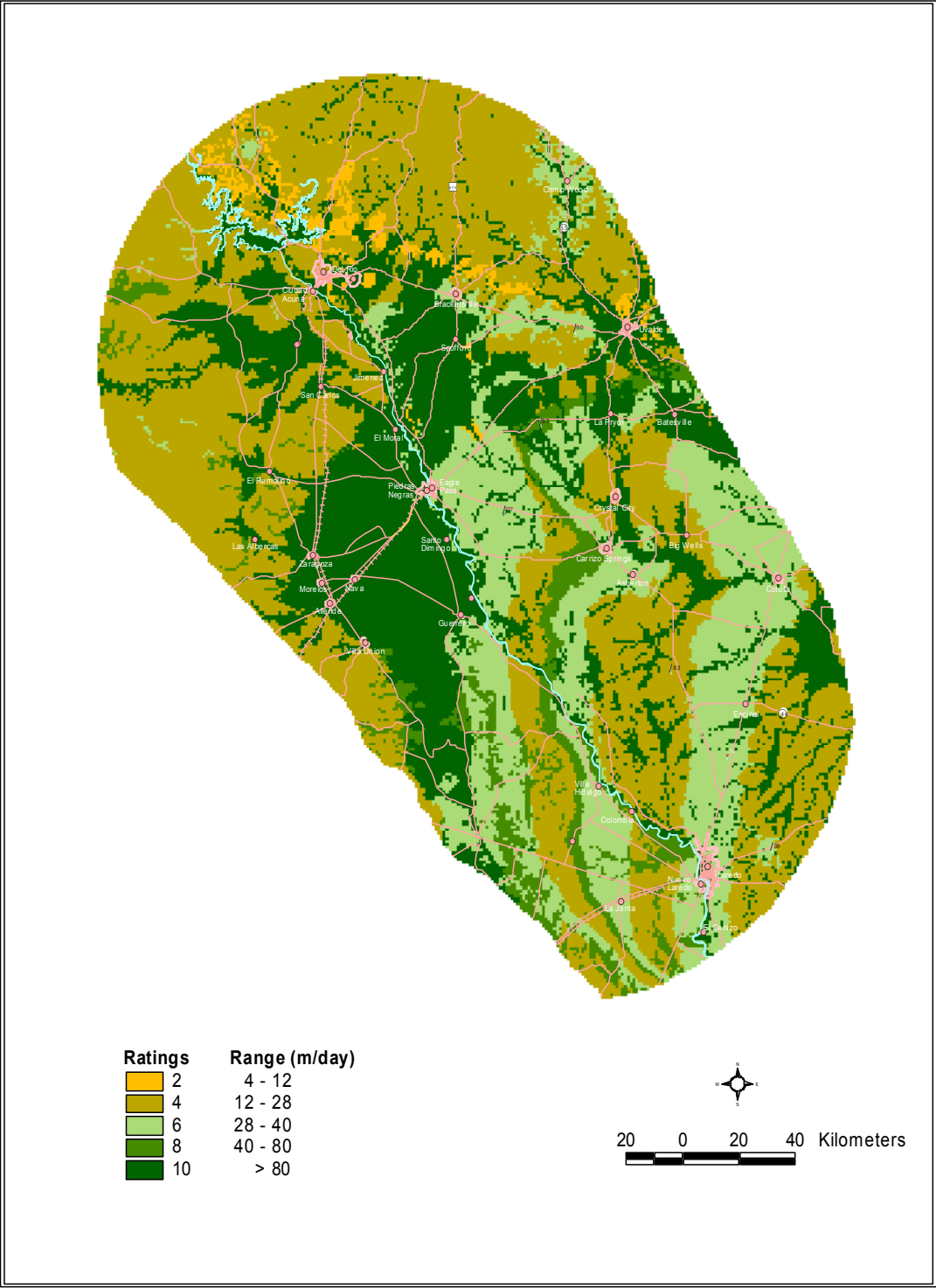


Figure 5.7 Ratings and hydraulic conductivity ranges for the hydraulic conductivity DRASTIC layer

The aquifers' vulnerability to contamination by infiltrating pollutants is directly proportional to the computed DRASTIC index ( $D_I$ ) and was classified as follows:

Very slight	$D_I < 79$ ;
Slight	$80 \leq D_I \leq 99$ ;
Low	$100 \leq D_I \leq 119$ ;
Moderate	$120 \leq D_I \leq 139$ ;
High	$140 \leq D_I \leq 159$ ;
Very high	$160 \leq D_I \leq 179$ ;
Severe	$180 \leq D_I \leq 199$ ;
Extreme	$D_I \geq 200$

The map indicates that approximately two-thirds of the study area has low vulnerability to groundwater pollution illustrated by a DRASTIC index of less than 120. These areas correspond mainly to less permeable Paleocene and Eocene mudstones and sandstones outcropping from El Indio, Texas to El Cenizo, Mexico. Index values of 140-179 (high to very high vulnerability) are associated with the shallow Uvalde and Sabinas formations—a 25-mile wide band of Plio-Pleistocene gravels and conglomerates exposed from Bracketville, Texas in the north through El Moral and Piedras Negras, Mexico to the south.



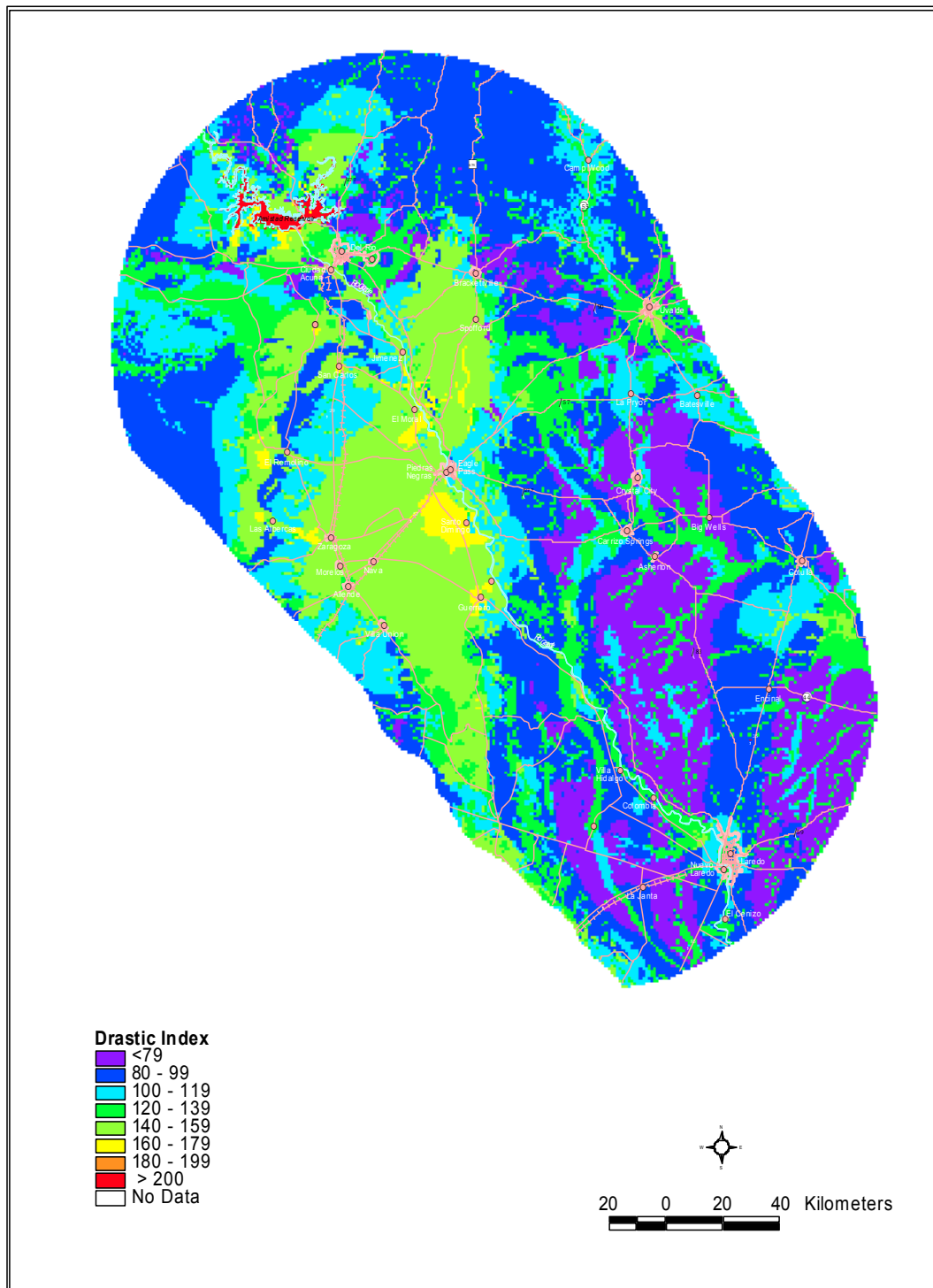


**Figure 5.8 DRASTIC Index distribution illustrating aquifer vulnerability to pollution. The aquifer vulnerability to contamination increases with the DRASTIC Index.**

The Quaternary alluvium deposited along the Rio Grande/Río Bravo and other alluvial valleys displays an index of 120 to 160 indicative of moderate to high susceptibility to contamination. The intensely karstified Salmon Peak limestone of Cretaceous age extending from central Val Verde County, Texas, through El Remolino and Las Albercas, Mexico, is another high-risk area. DRASTIC index values of 200 and greater have been calculated around Amistad Reservoir where the shallow water levels and the magnitude of the karst phenomena make this area extremely susceptible to contamination.

### **Model limitations**

According to its authors, “the DRASTIC index provides only a relative evaluation tool and is not designed to provide absolute answers” (Aller et al., 1987). The model discussed in this chapter has a coarse spatial resolution with a cell size of 1 km by 1 km. This restricts its use to relative evaluations on a regional basis and does not allow site-specific investigations.

The DRASTIC method does not consider the human impact on groundwater quality, nor does it allow distinguishing between man-induced versus naturally occurring water quality problems. Some important factors that can significantly impact the vulnerability evaluation but are not considered by the method include aquifer and vadose zone anisotropy and heterogeneity; precipitation duration and intensity; and natural soil attenuation capabilities. In addition, DRASTIC assumes the contaminant is introduced at the ground surface, is flushed into the aquifer by precipitation, and has the mobility of water. Although these assumptions have led to criticism, the strength of DRASTIC lies

in the fact that it considers most of the major factors controlling groundwater susceptibility to pollution, unlike any other tool of this kind. Care must be exercised when interpreting DRASTIC vulnerability maps not to read into them more than what the method is designed to produce.

### **Single-parameter sensitivity analysis**

The DRASTIC method involves the selection, rating, and weighing of seven physical parameters deemed to be critical for the aquifer vulnerability analysis. The inherent subjectivity associated with these procedures can significantly affect the model results. One way to evaluate the contribution of the input parameters on the model output is by performing a sensitivity analysis. Sensitivity analysis could reveal the effective or real weight each DRASTIC parameter gets in the context of the values of the other parameter in a given area.

The analysis performed here is based on the use of unique condition subareas within the model domain as implemented by Napolitano and Fabbri, (1996). In brief, the seven parameter rating maps are combined to extract all the possible combinations of cells' ratings throughout the study area, new effective weights for each layer are computed, and the rating maps are then reclassified to show the effective weight for each parameter in each subarea.

A unique condition subarea is defined as “one or more polygons consisting of pixels [cells] with a unique combination of  $D_i$ ,  $R_i$ ,  $A_i$ ,  $S_i$ ,  $T_i$ ,  $I_i$ , and  $C_i$ , where  $D_i$ ,  $R_i$ ,  $A_i$ ,  $S_i$ ,  $T_i$ ,  $I_i$ , and  $C_i$  are the rating values of the seven layers used to compute the vulnerability index, and  $1 \leq i \leq 10$ ” (Napolitano and Fabbri, 1996). All possible ratings combinations

(51,838 in all) of the seven layers were computed and pixels (cells) with identical ratings combinations were grouped together in 1,169 unique condition subareas. An analysis was then made to compare the effective weight for each parameter in each subarea with the theoretical weight assigned by the DRASTIC method. The effective weight,  $W_{pi}$ , depends on both the DRASTIC-assigned weight and on the value of each single parameter in the context of the values of the other parameters. The effective weight in each unique condition subarea was computed using the equation (Napolitano and Fabbri, 1996):

$$W_{pi} = \frac{P_{Ri} \cdot P_{Wi}}{D_i} \cdot 100 \quad (2)$$

where  $P_{Ri}$  and  $P_{Wi}$  are the ratings and the weights respectively of parameter  $P$  assigned to subarea  $i$  and  $D_i$  is the DRASTIC index as calculated by equation (1). The effective weights for each parameter, together with the method-assigned weights, and several statistical measures are shown in table 5.1.

Parameter	Theoretical Weight	Theoretical Weight (%)	Effective Weight (%)	Standard Deviation (%)	Median (%)	Minimum Value (%)	Maximum Value (%)
<i>D</i>	5	21.74	14.76	9.61	17.70	3.55	51.14
<i>R</i>	4	17.39	4.05	2.13	3.64	2.12	26.49
<i>A</i>	3	13.04	17.91	3.51	17.14	5.94	26.32
<i>S</i>	2	8.70	7.20	4.17	7.50	1.33	35.71
<i>T</i>	1	4.35	9.87	2.58	8.74	2.56	26.32
<i>I</i>	5	21.74	28.76	7.37	28.23	4.95	45.45
<i>C</i>	3	13.04	17.43	5.44	15.29	5.66	44.12

**Table 5.1 Comparison between DRASTIC-assigned and effective parameter weights and statistical analysis.**

The effective weight for each parameter throughout the entire model domain was computed using the following equation:

$$W_p = \frac{\sum_i W_{pi} \cdot nPix_i}{nPix} \quad (3)$$

where  $W_{pi}$  is the effective weight of parameter  $P$  over the unique condition subarea  $i$ ,  $nPix_i$  is the number of pixels (cells) comprising the subarea  $i$ , and  $nPix$  is the total number of cells throughout the model domain, in this case 51,838.

The unique condition subarea map was then reclassified based on the effective weight percentages of each parameter. Finally maps showing the spatial distribution of effective weight for each parameter were produced (see figures 5.9-5.15).

## **Results and discussion**

The common characteristic of the maps shown in figures 5.9 through 5.15 is the strong correlation between the effective weight distribution and the regional geology. This is because the ratings for aquifer media, hydraulic conductivity, and vadose zone were, for the most part, geology-based. The calculated effective weights in table 5.1 show significant departures from the DRASTIC-assigned theoretical weights.

The vadose zone configuration has the largest impact on the aquifer vulnerability index with an effective weight of 28.76 percent versus the theoretical 21.74 percent assigned by the method. This parameter's spatial distribution and magnitude (see figure 5.9) appear to be controlled by the depth to water in the northwestern half of the study area and by the types of overlying soils in the southeast. Greater depths to the water table in the highlands of Serranía del Burro and in the Edwards Plateau and the clayey and

loamy soils east of the Guerrero meridian yield effective weights for this parameter upwards of 40 percent in several areas.

The depth to water had an effective weight of 14.76 percent against the method-prescribed 21.74 percent, and shows larger impacts where unconfined conditions prevail (the Allende-Piedras Negras Valley aquifer, the area surrounding Amistad Reservoir near Del Rio). In contrast, figure 5.10 shows the depth to water is less important in confined or semiconfined aquifers, or in areas covered by less permeable soils. The closest match between the theoretical (8.70 percent) and effective (7.20 percent) weights (see table 5.1) was exhibited by the soils media. The effective weight distribution map (figure 5.11) is a rather faithful representation of the soil media rating map (figure 5.4), showing a 5 to 10 percent effective weight dispersed throughout most of the region. The presence of clayey, loamy soil types, such as the ones overlying the Uvalde – Sabinas aquifer, the terrigenous El Pico, Bigford, and Yegua formations, results in an effective weight of under 5 percent for this parameter. Both aquifer media and hydraulic conductivity had effective weights at least a third larger than the ones prescribed by DRASTIC (table 5.1). Although the conductivity weight distribution map (figure 5.12) displays some correlation with the regional geology, the factors governing the aquifer media effective weight distribution (figure 5.13) are unclear.

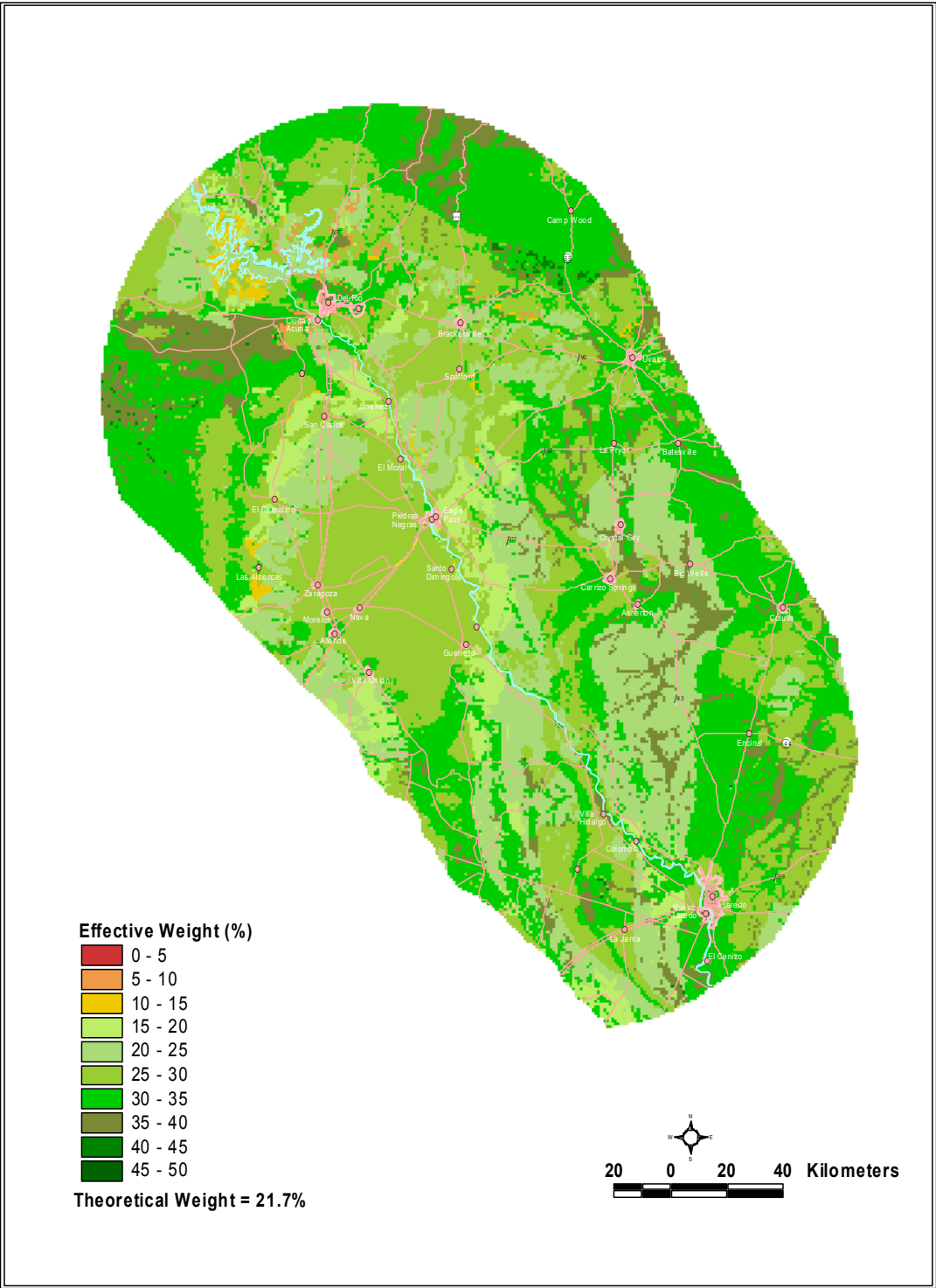


Figure 5.9 Effective weight distribution for the impact of the vadose zone DRASTIC layer

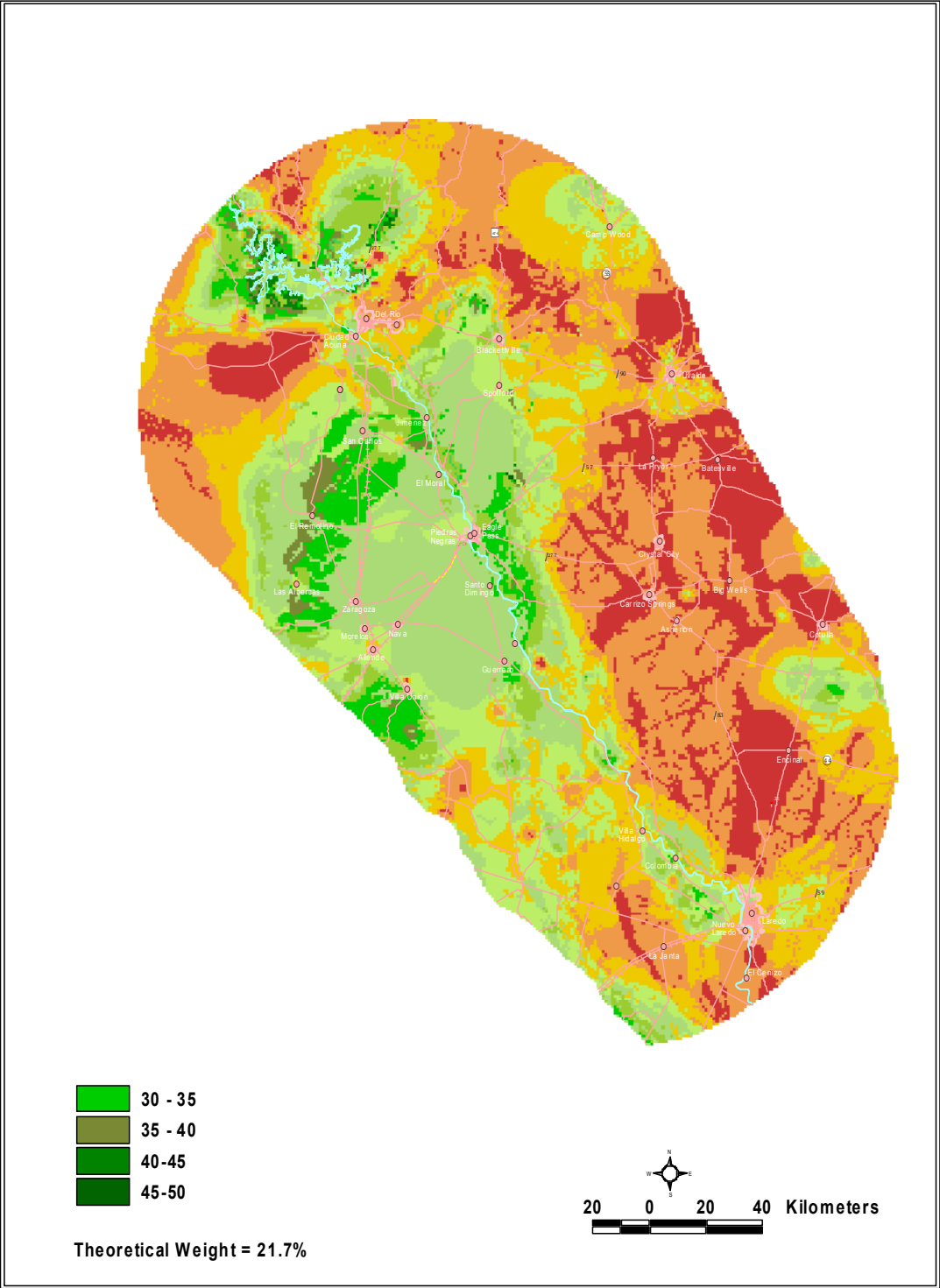


Figure 5.10 Effective weight distribution for the depth to water DRASTIC layer



The most unexpected result, shown in table 5.1, is that net recharge has the least influence over the vulnerability index, with an effective weight of only 4.05 percent against the theoretical weight of 17.39 percent. The only areas honoring method-prescribed weights are open bodies of water (Amistad Reservoir, and Lake Casablanca near Laredo, Texas) as shown in figure 5.14. The fact that the lowest possible DRASTIC rating (i.e., 1, see figure 5.2) for net recharge was assigned throughout the model domain - except above the lakes - could explain the lack of impact this parameter has on the final vulnerability index.

As surprising was the influence of topography over the vulnerability index, with an effective weight (9.87 percent) more than twice the theoretical weight (4.35 percent). The uniformly high (e.g., 10) rating assigned to the topographic slope parameter almost throughout the study area has enhanced the importance of this layer despite the minimal (e.g., 1), theoretical weight (see figure 5.15).

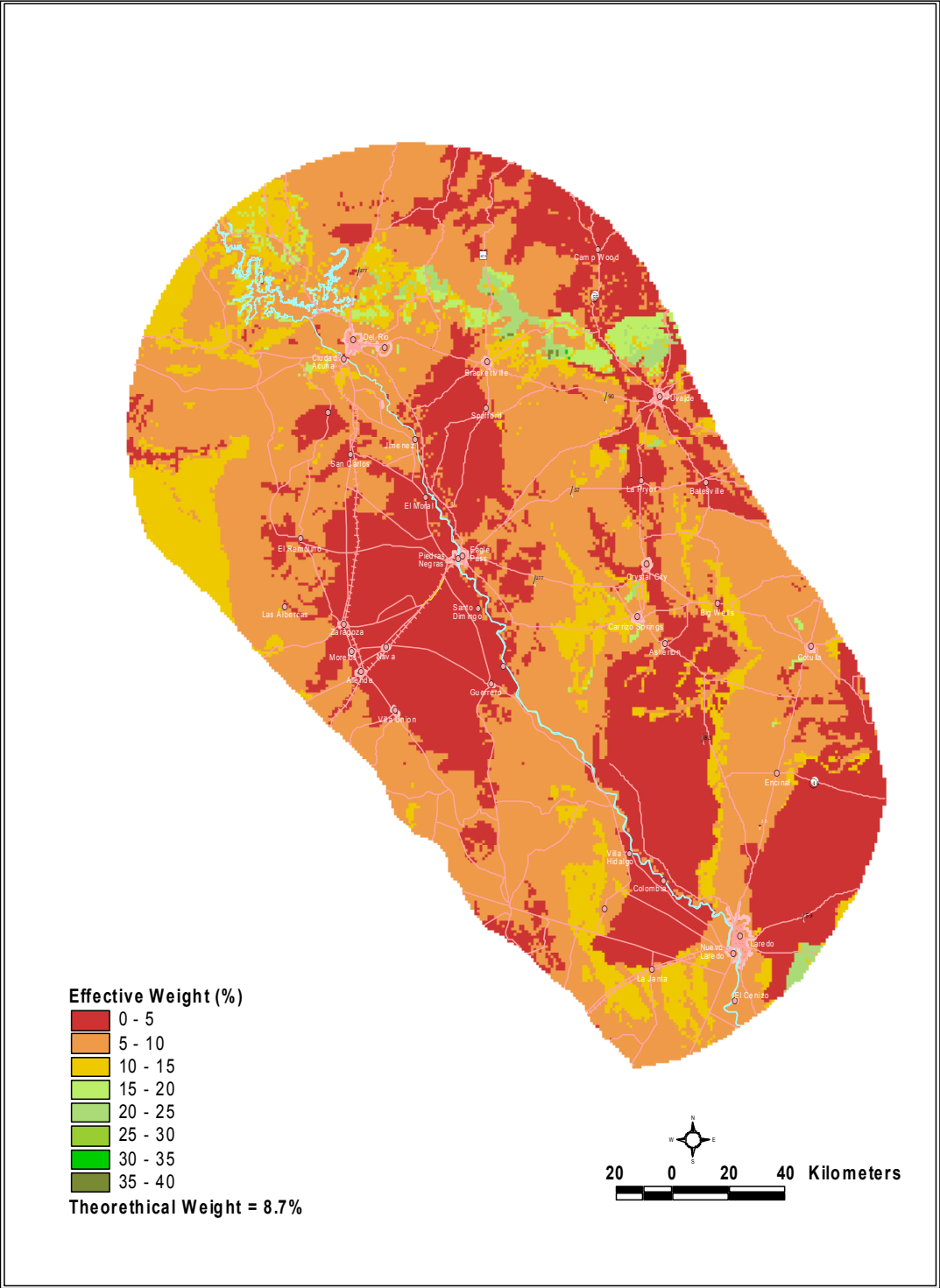


Figure 5.11 Effective weight distribution for the soil media DRASTIC layer

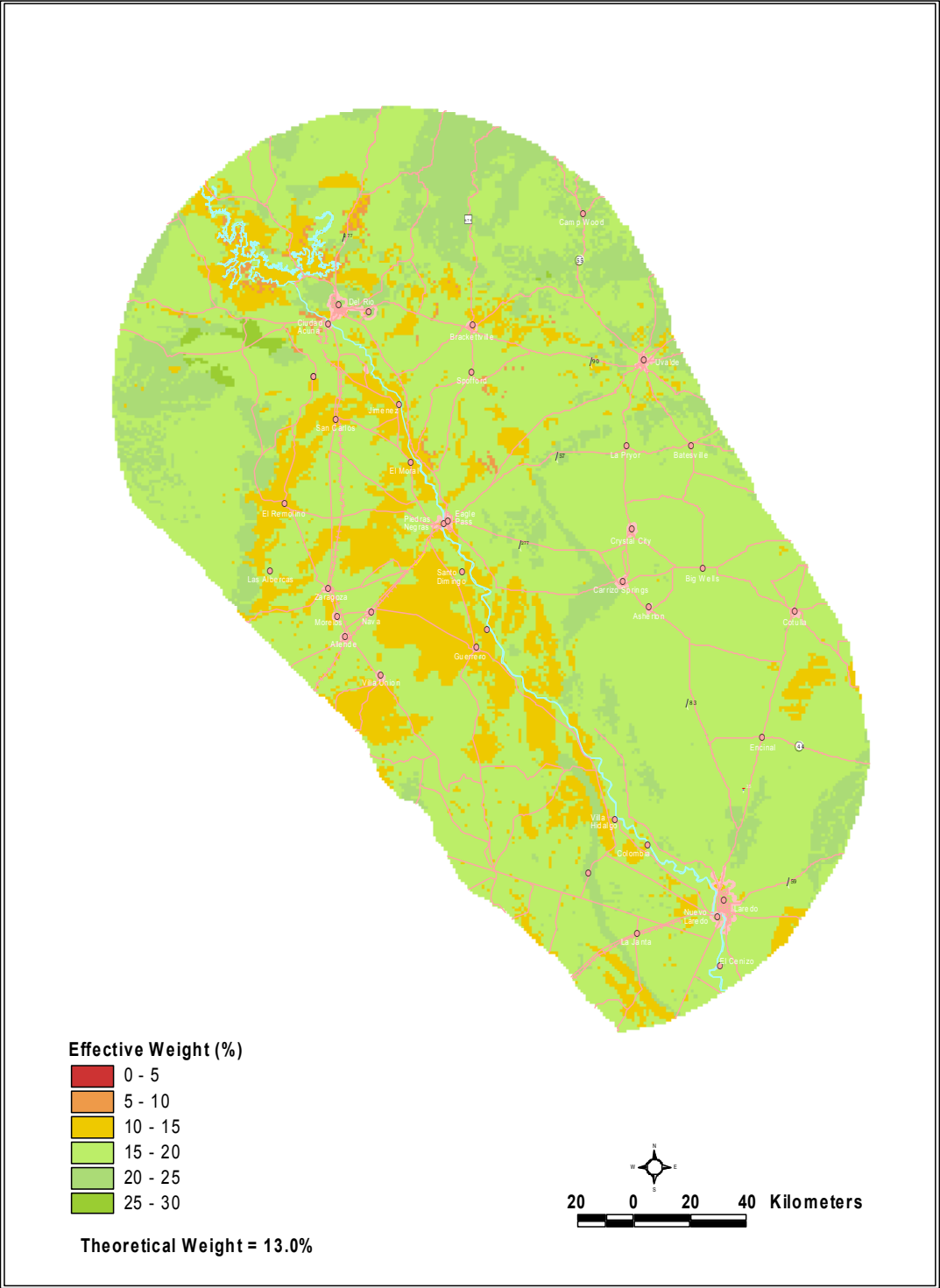


Figure 5.12 Effective weight distribution for the hydraulic conductivity DRASTIC layer

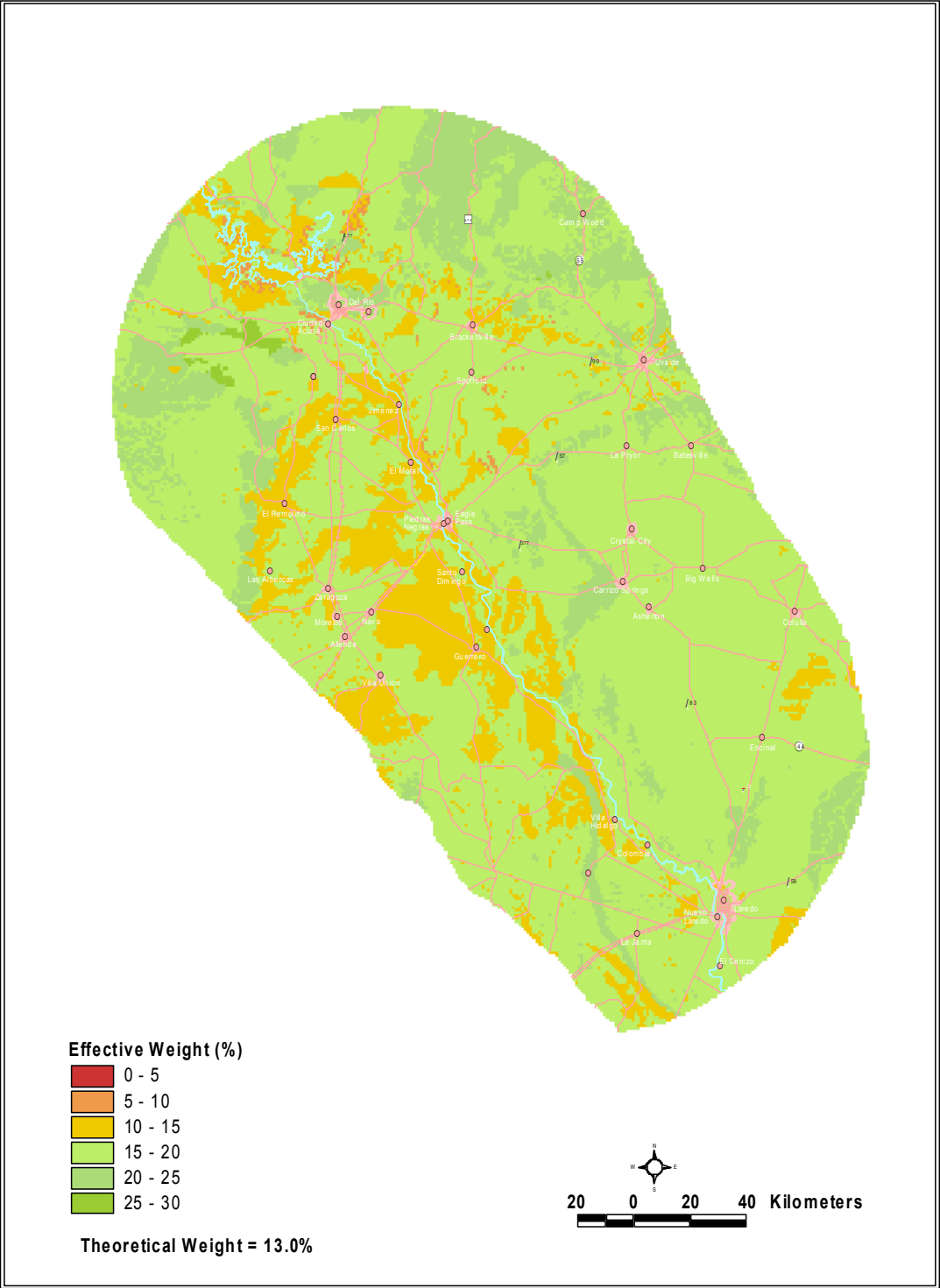


Figure 5.13 Effective weight distribution for the aquifer media DRASTIC layer

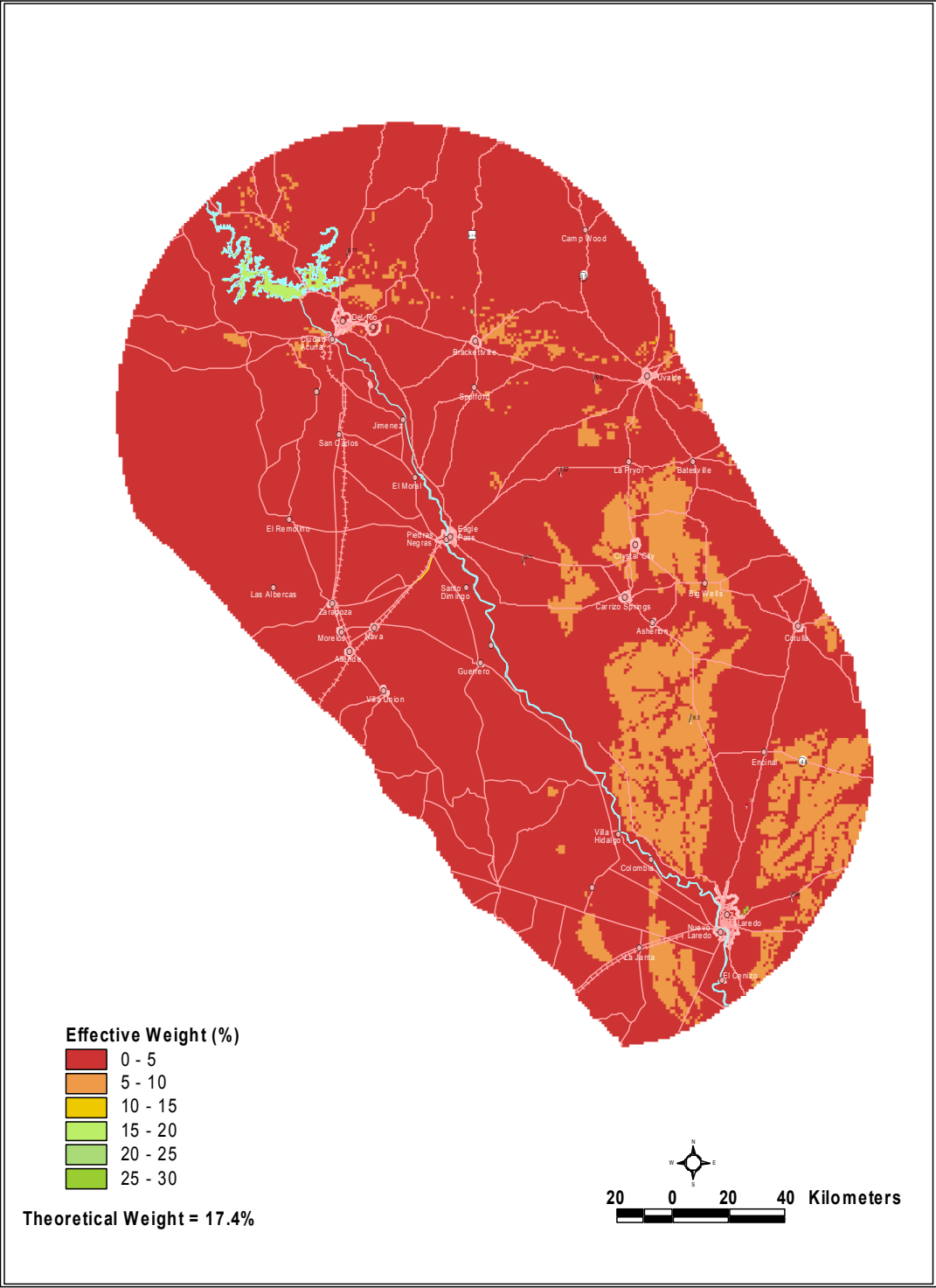
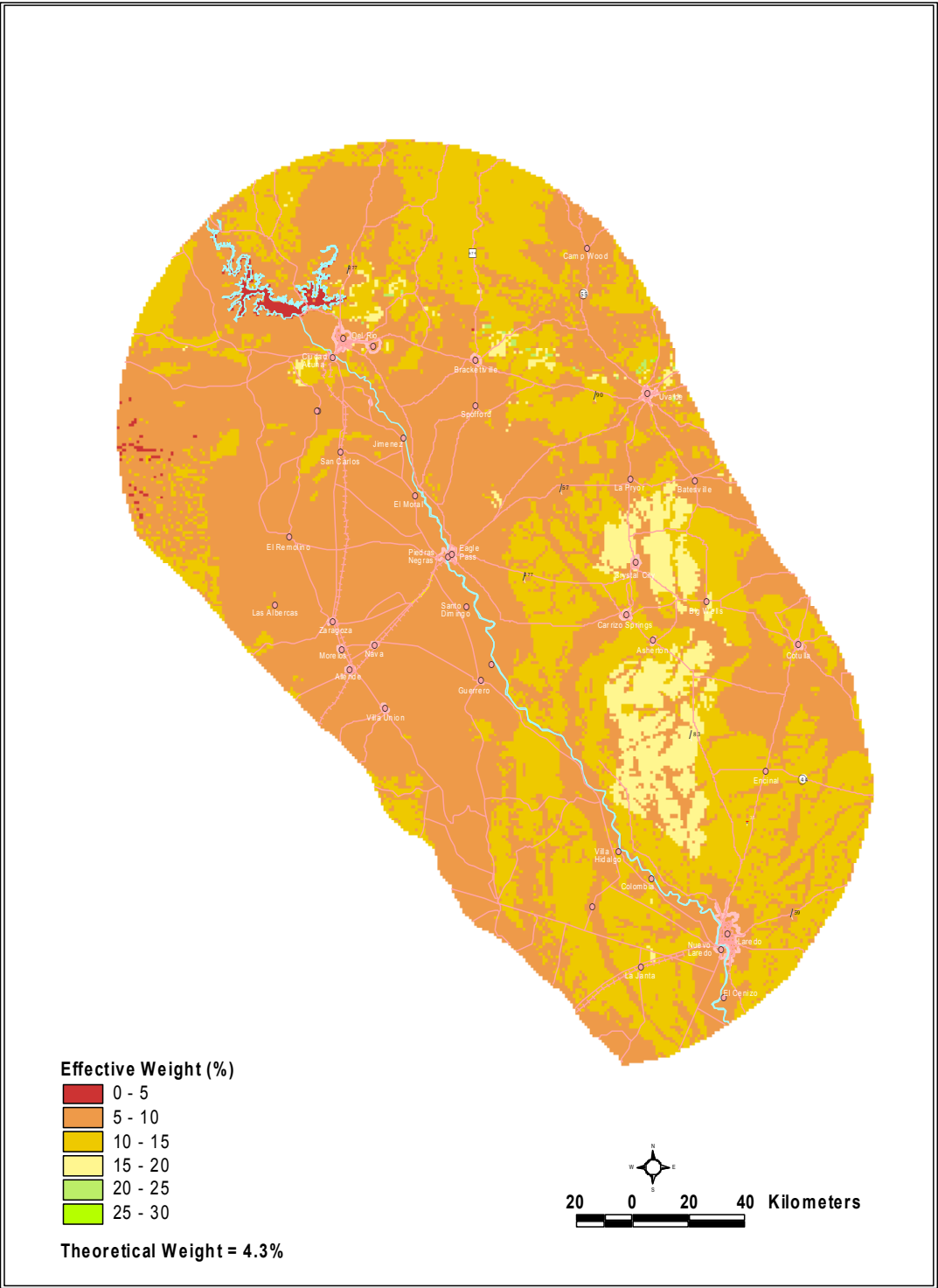


Figure 5.14 Effective weight distribution for the net recharge DRASTIC layer



**Figure 5.15 Effective weight distribution for the topography DRASTIC layer**

## **Conclusions**

The U.S. EPA DRASTIC method was employed to assess the vulnerability to pollution of aquifers shared between the United States of America and the United States of Mexico between Del Rio/Ciudad Acuña and Laredo/Nuevo Laredo. The results indicate that approximately two-thirds of the study area has low groundwater pollution potential. There are many method-related assumptions and limitations that need to be understood before attempting make planning decisions based on DRASTIC outputs. The single-parameter sensitivity analysis revealed that the weights for each input parameter can vary widely from place to place and did not follow the method-prescribed weights. The analysis can thus be useful for model fine-tuning and targeting of areas within the model domain that need more detailed information and accuracy.

## References

- Aller, L., Bennett, T., Lehr, J. H., Petty, R. J., and Hackett, G., 1987, DRASTIC: a standardized system for evaluating ground water pollution potential using hydrogeologic settings: U.S. Environmental Protection Agency publication EPA 600/2-87-035, 622 p.
- Napolitano, P. and Fabbri, A. G., 1996, Single-parameter sensitivity analysis using DRASTIC and SINTACS, *in* HydroGIS 96: Application of Geographic Information Systems in Hydrology and Water Resources Management, Proceedings of the Vienna Conference, IAHS Publication no. 235.
- Orr, B. W. and Risser, D. W., 1992, Geohydrology and potential effects of development of freshwater resources in the northern part of Hueco Bolson, Dona Ana and Otero Counties, New Mexico, and El Paso County, Texas: U.S. Geological Survey Water-Resources Investigations Report 91-4082, 92 p.
- Sharp, J. M., Jr., 1999, A Glossary of Hydrogeological Terms: Department of Geological Sciences, The University of Texas at Austin, 35 p.



## RECOMMENDATIONS

In establishing the transboundary aquifers GIS coverages and binational aquifer maps, a significant amount of data were acquired, verified, and evaluated. The value of any coverage or map is dependent on there being a sufficient amount of data to characterize the subject matter adequately and accurately. The following recommendations are intended to recognize specific data inadequacies and also to suggest future projects and activities that might enhance our understanding of the local aquifers.

- The most important problem faced by the author of this study was the absence of recent water-level and water-quality data for the Edwards-Trinity and Carrizo-Wilcox aquifers in Mexico. Groundwater information collected from 1979 to 1981 had to be used in these evaluations. The author recommends that water-level and water-quality monitoring activities be undertaken on the Mexican side of the study area for these aquifers.
- Similarly, the Allende – Piedras Negras Valley aquifer lacked recent water-level information on the Texas side. The TWDB should enhance their groundwater monitoring efforts in this area.
- A sizable number of wells on the Mexican side had to be excluded from analysis due to their unknown depth and completion data. Having that information would allow

for more wells to be included in the interpretations and would thus enhance the understanding of these aquifers' binational characteristics.

- Recharge to and contamination susceptibility of aquifers are significantly influenced by the aquifer geology. The geology of the Texas portion of the project area is currently being refined by the Bureau of Economic Geology (BEG). Revisions of existing maps should be digitized as replacements for the existing geology coverage. Mexico geology (figure 1.4) should be more accurately delineated and digitized to a level of detail comparable to Texas data. This would allow for more precise spatial parameter assignment for aquifer vulnerability determinations.
- The extent of the Carrizo-Wilcox aquifer in Mexico should be better delineated and digitized. Hydrogeologic data from the downdip portion of this aquifer are needed for refining its extent in Mexico.
- Wells in Mexico should be accurately located using GPS equipment. Well head elevations should be determined within an accuracy at least equal to those on the Texas side (U.S. based on five-foot topographic map contour intervals). This will allow for better regional mapping of groundwater movement.
- Effects of development on water quality should be monitored and evaluated for potential problems.

- Better estimates of groundwater pumpage volumes are needed for both countries. This could be achieved by equipping some of the wells with flow meters and by recording their groundwater pumpage.
- The geohydrology of the Laredo and Bigford formations in both Mexico and Texas should be studied in greater detail. These formations are water-producing and are used in both Mexico and Texas. They would make good candidates for future designation as binational aquifers. Specifically, the detailed geology, lateral and vertical extent of the Bigford and Laredo formations, their hydraulic properties, and the quantity and quality of groundwater on both sides are not well known and very difficult or impossible to estimate with available data.
- Computer groundwater flow models of the Edwards-Trinity and Carrizo-Wilcox aquifers are currently being developed by TWDB for the Texas side. A binational modeling effort should be undertaken at a later date for these aquifers. This would help bring about a better understanding of the aquifers' response to pumping stresses and, consequently, better groundwater management strategies would be devised.
- Stable and radiogenic isotope data are needed to determine groundwater sources, ages, and residence times, groundwater recharge areas, and areas of cross-formational flow. The quality of the groundwater flow models being developed by the TWDB may potentially improve if isotope data are available.

- Mexican well information generated prior to about 1990 was available only in hard copy. These data should be converted to electronic files.
- A formal procedure and timetable for binational groundwater data exchange should be reestablished and implemented if future binational groundwater research projects are envisioned. These data should be recognized for their authenticity by both Mexican and U.S. governments and should be in an electronic format suitable for GIS applications. It is important that these data be made easily accessible.
- The binational technical work group established for this project should extend this work to include more input on the hydrogeologic properties and processes operative in the Mexican portion of the transboundary aquifers and to seek technical solutions to common groundwater problems.
- A binational aquifer water-level and water-quality monitoring network should be established. Monitoring frequency and procedural protocol should be agreed upon, and subsequent data should be shared on a continuous real-time basis.

## **APPENDIX A**

### **List of water-related agencies and institutions**

Comisión de Cooperación Ecológica Fronteriza/ Border Environment Cooperation  
Commission

Blvd. Tomás Fernández 8069

Fracc. Los Parques

Cd. Juárez, Chihuahua

Mexico C.P. 32470

Phone: (52-16) 29-23-95; 29-23-95; Fax: 29-23-97; 29-23-97

Bureau of Economic Geology

University Station, Box X Austin, TX 78713-8924

Phone: (512) 471-1534; Fax: (512) 471-0140

Comisión Internacional de Límites y Aguas

Sección Mexicana

Av. Universidad 2180

Zona del Chamizal

Cd. Juárez, Chihuahua, 32310

Telefono: 13-99-42

Comisión Nacional del Agua

Texcoco 4860

Ciudad Juárez, Chihuahua 32310

Telefono: 13-77-16

International Boundary & Water Commission  
Mexican Section  
P.O. Box 10525  
El Paso, TX 79995

International Boundary & Water Commission  
United States Section  
4171 N. Mesa, C-310  
El Paso, TX 79902  
Phone: (915) 534-6700; Fax: 534-6680

Texas General Land Office  
Stephen F. Austin Building  
1700 N. Congress Avenue  
Austin, TX 78701-5001  
Phone: (512) 463-5001; Fax: 475-1415

Texas Natural Resource Conservation Commission  
Ground-Water Assessments Section  
P. O. Box 13087; MC 147  
Austin, TX 78711  
Phone: (512) 239-4514; Fax: 239-4450

Texas Parks & Wildlife Department  
Resource Protection Division  
4200 Smith School Road  
Austin, TX 78744  
Phone: (512) 389-8014; Fax: 389-4394

Texas Water Development Board  
Water Planning Division  
P. O. Box 13231 Capitol Station  
Austin, TX 78711  
Phone: (512) 936-0881; Fax: 936-0889

Texas Water Development Board  
Hydrologic and Environmental Monitoring Division  
P. O. Box 13231 Capitol Station  
Austin, TX 78711  
Phone: (512) 936-0841; Fax: 936-0889

Texas Natural Resources Information System  
Borderlands Data and Information Center  
Texas Water Development Board  
P. O. Box 13231 Capitol Station  
Austin, TX 78711  
Phone: (512) 463-8337; Fax: 463-7274

United States Department of Agriculture  
Natural Resources Conservation Service  
18 S Main St  
Temple, TX 76501-7652  
Phone: (254) 742 – 9800

United States Department of Interior  
Bureau of Reclamation  
Rio Grande Project Office  
700 E. San Antonio, Suite 318

El Paso, TX 79901

Phone: (915) 534-6324; Fax: 534-6299

United States Department of Interior

Geological Survey, Texas District Office

8027 Exchange Dr.

Austin, TX 78754

Phone: (512) 927-3500; Fax (512) 927-3590

United States Environmental Protection Agency

Region 6, Office of Ground Water

1445 Ross Avenue

Dallas, TX 75202-2733

Phone: (214) 665-7313



## **APPENDIX B**

### **Groundwater data sets and GIS coverages**

The groundwater databases included on the accompanying CD (see folder named “Data Sets”) have been provided by the participating agencies from the U.S. and Mexico as part of the binational data exchange conducted on February 24, 2000. The sources of the data are Texas Water Development Board for the Texas side and Comisión Nacional del Agua, Comisión Federal de Electricidad, and El Instituto Nacional de Estadística, Geografía e Informática for the Mexican side

The general types of information provided with the report are well data (construction, ownership, groundwater use, etc.), groundwater levels in wells, results of groundwater quality analyses, and pumping records. The information is organized by nation. Not all data types listed above are available for each country.

All the data exchanged by the U.S. and Mexico have been tabulated and saved as Microsoft Excel workbooks. Each workbook consists of spreadsheets named for the type of information they contain. An Allende-Piedras Negras Valley aquifer report produced by the Mexican side is included in the Mexico folder.

One of the project goals was to compile available groundwater information into a geographically referenced format. All the GIS data we generated during the project are distributed as ArcView™ shapefiles, and can be found in the folder named “GIS\_covs”. The shapefiles are organized by aquifer, and are accompanied by metadata sheets in XML format.